



# **The Role of Cyclic Strain on miRNA Mediated Human Aortic Smooth Muscle Cell (HAoSMC) Dynamics**

Brian Mac Donnell B.Sc,

Thesis Submitted to Dublin City University (DCU) for the Degree of  
Doctor of Philosophy (Ph.D)

Research was carried out in the School of Health and Human Performance, DCU  
under the supervision of Doctor Ronan P. Murphy.

School of Health and Human Performance,

Dublin City University

October 2013

## **Declaration**

I hereby certify that this material, which I now submit for assessment on the programme of study leading to the award of Doctor of Philosophy is entirely my own work, that I have exercised reasonable care to ensure that the work is original and does not to the best of my knowledge breach any law of copyright, and has not been taken from the work of others save and to the extent that such work has been cited and acknowledged within the text of my work.

**Signature:** \_\_\_\_\_

**I.D. 55673950**

**Date:** \_\_\_\_\_

## Acknowledgements

This is perhaps the most important section of my thesis, a chance to express my gratitude to everyone who supported me throughout the PhD.

Firstly I would like to thank Ronan for giving me the opportunity to do a PhD. From taking me on as a fourth year student many years ago to putting up with me over the four years of the project your irrefutable confidence and patience in Ciaran, Shan and myself helped us through some of the toughest moments of the work.

I would like to thank Phil for constantly offering up his experience and reassurance throughout my time in the lab. Your support during my transfer and viva was invaluable. I would like to mention and thank Ger who also shared her vast knowledge and sympathies during these times.

To the members of the lab before me; Paul, Mishan, Andrew and Tony were it not for you guys handing down your knowledge and skills I would have struggled to begin experimenting independently in the lab and I can assure you I was very nervous as each of you completed your time and began to leave. Thank you.

Anthony, we had the pleasure of hanging onto you for an extra few years. I don't believe I will ever again come across anyone more relaxed. In what, supposedly, were times of sheer stress on the run up to submission or the defence of your thesis you were able to find time to play that balloon popping game on the internet. I learned a lot from your approach and want to thank you for all the good fun and (periodically) advice you provided.

Fiona, Keith, Ciaran and Shan I couldn't have asked for a better group to share my time and the lab with over the course of the PhD. Fiona, your quick outbursts and even quicker apologies always kept things exciting. Keith you provided endless advice, brainstorming and a love of practical jokes...maybe the latter got out of hand from time to time. Ciaran, your practical jokes never seemed to work out but your attempts were funny. In four years I never seen you complain or be in anything other than a jolly mood. You kept me supplied with chewing gums and were a joy to sit beside. Shan....I love you.

Colin you were a latter addition to the lab but what an addition you were. Your ability to destroy a tissue culture facility in minutes while wearing sandals, a smile and playing awful music loudly will not be forgotten.

To the current members of the lab; Alisha, Hannah, Rob and Laura I hope your time in XB11/XB20 is as memorable as ours and that you take advantage of what's on offer.

Thank you too my lifelong friends and family Gary, Stephen, Niamh, Ciara, Des and Mark. When the last thing I wanted to do was talk or think science you guys were there. Our sporadic walks Gar, which inevitably ended up in the Two Sisters, would make everything simple and clear again.

I would like to give a special thanks to Laura your companionship and support over the last while has been immeasurable. I could not have gotten over the last hurdle(s) without you and I promise I will be there to support you through when your time comes. You were also the best distraction I could have asked for!!

Finally to my mam and dad you have supported me every step of the way and even kept me fed and watered. Thank you for providing everlasting encouragement and praise even when I didn't deserve it. Thank you for the endless times I have been difficult to put up with or destroyed the house as I was "studying" and you both would turn a blind eye.

I am forever in your debt.



## **Dedication**

To Family and Friends

## Abstract

Vascular smooth muscle cells (VSMCs) are major contributors to regulation of vascular tone through their contractile flexibility. Along with other stimulus, they are exposed to mechanical cyclic strain. It is thought such stimulus can be a major regulator of phenotypic modulation in smooth muscle cells. Differentiated SMCs are characteristically quiescent and adopt elongated spindle morphology. In this state the cell expresses an extensive range of contractile proteins such as SM  $\alpha$ -actin, Smoothelin and Calponin. SMCs in the synthetic end of the phenotype spectrum adopt a rhomboid morphology and display increased growth rate and higher migratory activity. Expression of the contractile proteins are significantly decreased and replaced with organelles involved in protein synthesis.

Studies have shown that several non coding micro RNA (miRNA), which negatively regulate gene expression, are differentially expressed in altered SMC phenotypes. However, work into the effect of mechanical stimulus such as shear stress or cyclic strain on miRNA expression is scarce with only a handful so far identified. This study hypothesizes that *“cyclic mechanical strain modulates vascular smooth muscle phenotype and ultimately function, mediated by miRNA regulation”*

This hypothesis was tested by exposing primary derived human aortic smooth muscle cells (HAoSMCs) to cyclic strain in an *in vitro* model. Results show cyclic strain at 5% and 10% levels of amplitude increases the abundance of contractile phenotype markers. A temporal study of the miRNA profile of SMCs exposed to 10% strain revealed a significant change in expression was evident after 24 hours of strain.

Novel chemotaxis experiments demonstrated cyclic strain reduced cell migration, the effect of which was most evident at 24 hours where migration of the cells was less than half that of the static culture. To implicate miRNA as key coordinators in the reduced cell migration observed after cyclic strain, siRNA were targeted against an essential miRNA biogenesis molecule, Argonaute2 (Ago2). Cells transfected with siRNA for Ago2 negated the physiological stimulus of strain and had a marked increase in migration even over the static control. These investigations highlight the physiological importance of cyclic strain on SMC phenotype and function how the cellular response to this stimulus is orchestrated via miRNA.

## Abbreviations

aa	Amino Acid
ABP	Actin Binding Protein
ADP	Adenosine Di-phosphate
Ago2	Argonaute 2
Ang	Angiotensin
APS	Ammonium Persulphate
ATP	Adenosine Tri-Phosphate
BCA	Bicinchoninic Acid
Ca	Calcium
BSA	Bovine Serum Albumin
CAM	Cell Adhesion Molecule
cDNA	Complimentary DNA
C/EBP $\alpha$	CCAAT Enhancer Binding Protein Alpha
C-Terminal	Carboxyl Terminal
CRBP	Cellular Retinol Binding Protein
DAVID	Database for Annotation, Visualisation and Integrated Discovery
DGCR8	Di George Syndrome Critical Region (Pasha)
DGPC	Dystrophin Glycoprotein Complex
CVD	Cardiovascular Disease
DMSO	Dimethylsulphoxide
DNA	Deoxyribonucleic Acid
dNTP	Deoxy nucleotide Tri-Phosphate
EC	Endothelial Cells
ECM	Extracellular Matrix
EDTA	Ethylenediaminetetraacetic Acid
FA	Focal Adhesion
F-actin	Filamentous – Actin
FAK	Focal Adhesion Kinase
FC	Focal Complex
FGF-2	Fibroblast Growth Factor-2
FITC	Fluorescein Isothiocyanate
FRNK	Focal Adhesion Non Receptor Kinase
G-Actin	Globular – Actin
GBD	Global Burden of Disease
GDP	Guanine Di-Phosphate
GFP	Green Fluorescent Protein
GO	Gene Ontology
HAEC	Human Aortic Endothelial Cell
HAoSMC	Human Aortic Smooth Muscle Cell
Hg	Mercury
ICAM	Intracellular Adhesion Molecule
KEGG	Kyoto Encyclopedia of Genes and Genomes
LASP	LIM and SH3 Protein
LB	Luria-Bertani
LSS	Laminar Shear Stress
MAPK	Mitogen Activated Protein Kinase
MHC	Myosin Heavy Chain

miRNA	Micro RNA
MLCK	Myosin Light Chain Kinase
Mg	Magnesium
MgCl <sup>2</sup>	Magnesium Chloride
Mn	Manganese
mRNA	Messenger RNA
NaCl	Sodium Chloride
NaOH	Sodium Hydroxide
NFκB	Nuclear Factor – κB
NO	Nitric Oxide
P	Significance
PAGE	Polyacrylamide Gel Electrophoresis
PBS	Phosphate Buffered Saline
PCR	Polymerase Chain Reaction
PDGF	Platelet Derived Growth Factor
PECAM	Platelet Endothelial Cell Adhesion Molecule
PI3K	Phosphatidylinositol-3-Kinase
PKC	Protein Kinase C
Pri miRNA	Primary miRNA
Pre miRNA	Premature miRNA
P/S	Penicillin/Streptomycin
qRT-PCR	Quantitative Real-Time – PCR
RGD	Arginine Glycine Serine
RIP-CHIP	RNA-Binding Protein Immunoprecipitation- Microarray (Chip) Profiling
RISC	RNA Induced Silencing Complex
RNA	Ribonucleic Acid
ROS	Reactive Oxidase Species
RPM	Rotations Per Minute
RT-PCR	Reverse Transcriptase – PCR
RT	Reverse Transcription
RTK	Receptor Tyrosine Kinase
SDS	Sodium Dodecyl Sulphate
SEM	Standard Error Mean
SH3	Src Homology region 3
SMC	Smooth Muscle Cell
SSB	Sample Solubilisation Buffer
ss	Single Stranded
siRNA	Small Interfering RNA
TAE	Tris Acetate EDTA
TE	Tris – EDTA
TEMED	Tetramethylethylenediamine
TGF-β	Transforming Growth Factor – β
TNF-α	Tumour Necrosis Factor Alpha
UTR	Un-Translating Region
VEGF	Vascular Endothelial Growth Factor
VEGFR	VEGF - Receptor
VSMC	Vascular Smooth Muscle Cells
VWF	Von Willebrand Factor
WHO	World Health Organisation

## Units

bp	Base Pairs
cm	Centimetre
C°	Degree Celsius
kDa	KiloDaltons
µg	Microgram
µl	Microlitre
µM	Micromolar
g	Grams
hr	Hours
kg	Kilogram
L	Litre
M	Molar
m	Meter
mA	Milliamperes
mg	Milligrams
min	Minutes
ml	Millilitres
mM	Millimolar
N	Newton
ng	Nanograms
nm	Nanometres
Pa	Pascal
pmol	Picomolar
sec	Seconds
w/v	Weight Per Volume
V	Volts

## **Presentations**

### **Oral Presentations**

*The Impact of Cyclic Strain on the miRNA Profile in Vascular Smooth Muscle Cells.*

Brian MacDonnell, Ciaran McGinn , Chunxu Shan , Philip Cummins , Ronan Murphy.

**8<sup>th</sup> International Symposium on biomechanics in vascular biology and  
Cardiovascular disease. Rotterdam, the Netherlands. (April 2013)**

*The Impact of Cyclic Strain on the miRNA Profile in Vascular Smooth Muscle Cells.*

Brian MacDonnell, Ciaran McGinn , Chunxu Shan , Philip Cummins , Ronan Murphy.

**Dublin City University, School of Biotechnology 5<sup>th</sup> Annual Research Day**

**Dublin, Ireland January 28<sup>th</sup>, 2013.**

**Posters**

***Role of Mechanosensitive miRNA (microRNA) in Focal Adhesion based dynamics in Vascular Smooth Muscle Cells.***

Brian MacDonnell, Ciaran McGinn , Chunxu Shan , Philip Cummins , Ronan Murphy.

**School of Biotechnology 3<sup>rd</sup> Annual Research Day**

**Dublin, Ireland January 28<sup>th</sup>, 2011.**

***The Impact of Cyclic Strain on Focal Adhesion Signalling and miRNA Expression in Vascular Smooth Muscle Cells.***

Brian MacDonnell, Ciaran McGinn , Chunxu Shan , Philip Cummins , Ronan Murphy.

**North American Vascular Biology Organisation (NAVBO)**

**Cape Cod, Massachusetts, USA. (16<sup>th</sup> -20<sup>th</sup> October 2011)**

***The Impact of Cyclic Strain on Focal Adhesion Signalling and miRNA Profile Expression in Vascular Smooth Muscle Cells.***

Brian MacDonnell, Ciaran McGinn , Chunxu Shan , Philip Cummins , Ronan Murphy.

**Atherosclerosis, Thrombosis and Vascular Biology (ATVB)**

**Chicago, USA. (18<sup>th</sup>-20<sup>th</sup> April 2012)**

## Contents

<b>Declaration</b> .....	<b>2</b>
<b>Acknowledgements</b> .....	<b>3</b>
<b>Dedication</b> .....	<b>5</b>
<b>Abstract</b> .....	<b>6</b>
<b>Abbreviations</b> .....	<b>7</b>
<b>Units</b> .....	<b>9</b>
<b>Presentations</b> .....	<b>10</b>
<b>Oral Presentations</b> .....	<b>10</b>
<b>Posters</b> .....	<b>11</b>
<b>CHAPTER ONE: Introduction</b> .....	<b>20</b>
<b>1.1 microRNA (miRNA)</b> .....	<b>20</b>
<b>1.2 Canonical miRNA Biogenesis</b> .....	<b>22</b>
<b>1.3 miRNA Clusters</b> .....	<b>24</b>
<b>1.4 miRNA Regulation of Cellular Networks</b> .....	<b>25</b>
<b>1.5 Level of Gene Suppression by miRNA</b> .....	<b>26</b>
<b>1.6 miRNA Isolation &amp; Analysis</b> .....	<b>27</b>
<b>1.6.1 Isolation</b> .....	<b>27</b>
<b>1.6.2 Data Analysis</b> .....	<b>29</b>
<b>1.6.3 Calculating Differential Expression</b> .....	<b>31</b>



<b>1.7 Bioinformatics</b> .....	<b>32</b>
<b>1.7.1 Target Prediction</b> .....	<b>32</b>
<b>1.7.2 Gene Annotation</b> .....	<b>33</b>
<i>1.7.2.1 Gene Ontology (GO)</i> .....	<i>33</i>
<i>1.7.2.2 The Kyoto Encyclopedia of Genes and Genomes</i> .....	<i>33</i>
<b>1.8 The Cardiovascular System</b> .....	<b>35</b>
<b>1.9 Cardiovascular Disease (CVD)</b> .....	<b>41</b>
<b>1.9.1 miRNA and Cardiovascular Disease</b> .....	<b>44</b>
<b>1.10 Vascular Smooth Muscle Cells</b> .....	<b>48</b>
<b>1.10.1 Contractile SMCs</b> .....	<b>48</b>
<b>1.10.2 Synthetic SMCs</b> .....	<b>50</b>
<b>1.11 Factors Influencing VSMC Phenotype</b> .....	<b>53</b>
<b>1.11.1 Biochemical factors</b> .....	<b>53</b>
<b>1.11.2 Extracellular Matrix Components</b> .....	<b>55</b>
<b>1.11.3 Haemodynamic Force</b> .....	<b>56</b>
<b>1.12 Mechano Sensors of VSMCs</b> .....	<b>60</b>
<b>1.12.1 Integrins</b> .....	<b>60</b>
<i>1.12.1.2 RGD Binding Integrins</i> .....	<i>63</i>
<b>1.12.2 Dystrophin-Glycoprotein Complex</b> .....	<b>64</b>
<b>1.12.3 Syndecans</b> .....	<b>65</b>
<b>1.12.4 Cell Adhesion Molecules (CAM)</b> .....	<b>66</b>
<b>1.12.5 Cadherins</b> .....	<b>66</b>
<b>1.12.6 Receptor Tyrosine Kinases</b> .....	<b>67</b>
<b>1.12.7 Ion Channels</b> .....	<b>69</b>
<b>1.13 The Cytoskeleton and Cell Migration</b> .....	<b>70</b>
<b>1.13.1 The Cytoskeleton</b> .....	<b>70</b>
<b>1.13.2 Cell Adhesion and Migration</b> .....	<b>71</b>

<b>Study Background, Hypothesis and Objectives .....</b>	<b>76</b>
<b>Study Background .....</b>	<b>76</b>
<b>Study Hypothesis.....</b>	<b>77</b>
<b>Study Objectives .....</b>	<b>77</b>
<b>CHAPTER TWO: Materials and Methods .....</b>	<b>78</b>
<b>2.1 Materials .....</b>	<b>78</b>
<b>2.1.1 Reagents, Chemicals and Cell Culture.....</b>	<b>78</b>
<b>2.1.2. Instrumentation .....</b>	<b>83</b>
<b>2.1.3 Consumables / Plastic ware.....</b>	<b>86</b>
<b>2.1.4 Preparation of stock solutions and buffers.....</b>	<b>88</b>
<i>2.1.4.1 Immuno-blotting.....</i>	<i>88</i>
<i>2.1.4.2 Molecular Biology Buffers and Medium.....</i>	<i>89</i>
<b>2.2 Methods.....</b>	<b>91</b>
<b>2.2.1 Cell Culture Technique .....</b>	<b>91</b>
<i>2.2.1.1 Human Aortic Smooth Muscle Cell (HAoSMC) Culture. ....</i>	<i>91</i>
<i>2.2.1.2 Human Aortic Endothelial Cell (HAEC) Culture. ....</i>	<i>91</i>
<i>2.2.1.3 Trypsinisation and Sub Culturing of Adherent Cells.....</i>	<i>92</i>
<i>2.2.1.4 Cell Counting. ....</i>	<i>93</i>
<i>2.2.1.4.1 Haemocytometer.....</i>	<i>93</i>
<i>2.2.1.4.2 Adam Counter .....</i>	<i>94</i>
<i>2.2.1.5 Cryo-Preservation of Cells.....</i>	<i>95</i>
<b>2.2.2 Molecular Biology .....</b>	<b>96</b>
<i>2.2.2.1 Reconstituting cDNA. ....</i>	<i>96</i>
<i>2.2.2.2 Transformation of Competent Cells.....</i>	<i>96</i>
<i>2.2.2.3 Overnight Culture and Glycerol Stock. ....</i>	<i>96</i>
<i>2.2.2.4 Midi – Preparation of Plasmid DNA.....</i>	<i>97</i>
<i>2.2.2.5 Spectrometric analysis of Plasmid DNA.....</i>	<i>97</i>
<i>2.2.2.6 Agarose Gel Electrophoresis.....</i>	<i>98</i>
<i>2.2.2.7 Plasmid Sequencing.....</i>	<i>99</i>
<b>2.2.3 Transfections.....</b>	<b>99</b>
<i>2.2.3.1 Electroporation.....</i>	<i>99</i>
<i>2.2.3.2 Amaxa/Lonza Nucleofector II.....</i>	<i>99</i>
<i>2.2.3.3 Invitrogen Microporator.....</i>	<i>100</i>
<i>2.2.3.4 siRNA.....</i>	<i>102</i>

<b>2.2.4 Immuno-Detection Techniques.....</b>	<b>103</b>
2.2.4.1 Immuno (Western) Blotting.....	103
2.2.4.1.1 Preparation of whole cell lysate.....	103
2.2.4.1.2 Bicinchoninic Acid Assay B.C.A. Assay.....	103
2.2.4.1.3 Preparing Samples.....	104
2.2.4.1.4 Polyacrylamide Gel Electrophoresis (SDS-PAGE).....	104
2.2.4.1.5 Electroblotting.....	106
2.2.4.1.6 PVDF versus Nitrocellulose.....	106
2.2.4.1.7 Blocking.....	107
2.2.4.1.8 Antibody Incubation.....	107
2.2.4.1.9 Detection with Substrate.....	108
2.2.4.1.10 Coomassie Gel Staining.....	108
2.2.4.1.11 Ponceau-S Membrane Staining.....	109
2.2.4.1.12 Membrane Stripping.....	109
2.2.4.2. Immunocytochemistry (ICC).....	109
2.2.4.3 Enzyme Linked Immuno Sorbent Assay (ELISA).....	110
2.2.4.3.1 Quantikine® ELISA.....	110
2.2.4.3.2 DuoSet ELISA.....	111
<b>2.2.5 Ribonucleic Acid (RNA) Work.....</b>	<b>112</b>
2.2.5.1 RNA Isolation.....	112
2.2.5.1.1 miRVANA Kit.....	112
2.2.5.1.2 RNA Extraction and Isolation using Trizol®.....	113
2.2.5.2 RNA/DNA Quantification Using NanoDrop® ND-1000 Spectrophotometer.....	114
2.2.5.3 RNA Purification.....	114
2.2.5.4 Polymerase Chain Reaction (PCR).....	115
2.2.5.5 Reverse Transcription (RT-PCR).....	115
2.2.5.6 PCR Primer Design.....	116
<b>2.2.6 Quantitative Real Time Polymerase Chain Reaction (QRT-PCR).....</b>	<b>116</b>
<b>2.2.7 miRNA Isolation and Amplification.....</b>	<b>118</b>
2.2.7.1 Isolation.....	118
2.2.7.2 Reverse Transcription of RNA for Taqman® Array Analysis.....	118
2.2.7.3 Preamplification of cDNA.....	119
2.2.7.4 Running the Taqman® microRNA Array.....	120
<b>2.2.8 miRNA Data Analysis.....</b>	<b>122</b>
2.2.8.1 Data Formatting.....	122
2.2.8.2 Target Prediction.....	123
2.2.8.3 Biological Processes and Pathway Analysis.....	123
<b>2.2.9 Pathophysiological Assays.....</b>	<b>124</b>
2.2.9.1 Cyclic Strain.....	124

<b>2.2.10 Cell Function Assays.....</b>	<b>126</b>
2.2.10.1 <i>xCELLigence Real Time Cell Analysis</i> .....	126
2.2.10.1.1 <i>Cell Adhesion/Proliferation Assay</i> .....	129
2.2.10.1.2 <i>Cell Migration/Proliferation Assay</i> .....	130
2.2.10.2 <i>Flow Cytometry</i> .....	131
2.2.10.2.1 <i>Apoptosis Study</i> .....	131
2.2.10.2.2 <i>Proliferation Study</i> .....	132
<b>2.2.11 Statistical analysis .....</b>	<b>133</b>
<b>CHAPTER THREE: Characterisation of the impact of cyclic strain on HAoSMCs</b>	
<b>.....</b>	<b>134</b>
<b>3.1 Introduction.....</b>	<b>134</b>
<b>3.1.1 Chapter Hypothesis .....</b>	<b>135</b>
<b>3.1.2 Specific aims and Experimental Approach: .....</b>	<b>135</b>
<b>3.2 Results .....</b>	<b>136</b>
<b>3.2.1 Characterisation of Human Aortic Smooth Muscle Cells (HAoSMCs).....</b>	<b>136</b>
3.2.1.1 <i>Investigation of SMC lineage through use of cell specific markers</i> .....	136
3.2.1.2 <i>Adhesion profiles of HAoSMCs</i> .....	137
3.2.1.3 <i>The effect of ECMs and coating factors on contractile gene expression</i> .....	139
<b>3.2.2 Injury Marker Expression .....</b>	<b>141</b>
3.2.2.1 <i>Secreted Fibroblast Growth Factor -2 (FGF-2)</i> .....	141
3.2.2.2 <i>Cellular Lysate Fibroblast Growth Factor -2 (FGF-2)</i> .....	143
3.2.2.3 <i>Secreted Thrombomodulin (TM)</i> .....	146
3.2.2.4 <i>Cellular Lysate Thrombomodulin (TM)</i> .....	147
<b>3.2.3 Investigation of phenotype modulation of HAoSMCs .....</b>	<b>150</b>
3.2.3.1 <i>Gene expression of contractile markers</i> .....	150
3.2.3.2 <i>Protein expression of contractile markers</i> .....	152
<b>3.3 Discussion .....</b>	<b>158</b>
<b>3.3.1 Cell Injury Caused by Cyclic Strain .....</b>	<b>162</b>
<b>3.3.2 Impact of Cyclic Strain on SMC Phenotype.....</b>	<b>167</b>
<b>3.4 Summary and Conclusion .....</b>	<b>169</b>

## CHAPTER FOUR: Impact of Cyclic Strain on the miRNA Profile of HAoSMCs 170

<b>4.1 Introduction</b> .....	<b>170</b>
<b>4.1.1 Chapter Hypothesis:</b> .....	<b>171</b>
<b>4.1.2 Specific aims and Experimental approach:</b> .....	<b>171</b>
<b>4.2 Results</b> .....	<b>172</b>
<b>4.2.1 Temporal 10% strain study on HAoSMC miRNA profile</b> .....	<b>172</b>
4.2.1.1 Hierarchial Cluster Analysis (HCA) .....	172
4.2.1.2 Two-way heat map miRNA from priority list.....	174
4.2.1.3 Correlated miRNA .....	176
4.2.1.4 Bioinformatic analysis on priority miRNA from temporal 10% strain study.....	179
<b>4.2.2 Investigation of strain amplitude on miRNA profile (biological replicates)</b> .....	<b>181</b>
4.2.2.1 Hierarchial Cluster Analysis (HCA) .....	181
4.2.2.2 Venn Diagram of commonly expressed miRNA across strain parameters .....	182
4.2.2.3 Bioinformatic analysis on priority miRNA from strain amplitude investigations.....	184
4.2.2.4 Cellular pathways analysis.....	189
4.2.2.4.1 Focal Adhesion.....	190
4.2.2.4.2 Regulation of Actin Cytoskeleton .....	192
4.2.2.4.3 Vascular Smooth Muscle Contraction.....	194
4.2.2.4.4 Cell Cycle .....	196
4.2.2.4.5 Adherens Junction.....	198
4.2.2.4.6 ECM-Receptor Interaction .....	200
<b>4.3 Discussion</b> .....	<b>202</b>
<b>4.3.1 Temporal 10% strain study on HAoSMC miRNA profile</b> .....	<b>203</b>
4.3.1.1 Data Analysis and Normalisation.....	203
<b>4.3.2 Investigation of strain amplitude on miRNA profile (biological replicates)</b> .....	<b>207</b>
4.3.2.1 Adjusted P Value .....	208
<b>4.4 Summary and Conclusion</b> .....	<b>211</b>

<b>CHAPTER FIVE: Functional Studies on HAoSMCs Exposed to Cyclic Strain...</b>	<b>214</b>
<b>5.1 Introduction.....</b>	<b>214</b>
<b>5.1.1 miRNA Regulation of Cell Function .....</b>	<b>215</b>
<b>Chapter Hypothesis: .....</b>	<b>217</b>
<b>Specific aims and Experimental approach .....</b>	<b>217</b>
<b>5.2 Results.....</b>	<b>218</b>
<b>5.2.1 Impact of cyclic strain on HAoSMC migration.....</b>	<b>218</b>
<b>5.2.2 Argonaute-2 (Ago2) Knock Down Study. ....</b>	<b>221</b>
<i>5.2.2.1 Optimisation of siRNA for Ago2.....</i>	<i>221</i>
<i>5.2.2.2 Quantification of Ago2 knock down efficiency with siRNA2 and Custom siRNA. ....</i>	<i>223</i>
<b>5.2.3 Impact of cyclic strain on migration of HAoSMCs with Ago2 knock down.....</b>	<b>224</b>
<b>5.2.4 Impact of cyclic strain on adhesion of HAoSMCs with Ago2 knock down .....</b>	<b>226</b>
<b>5.2.5 Effect of miRNA deficiency in HAoSMCs on Scratch Wound Closure.....</b>	<b>227</b>
<b>5.2.6 Impact of Ago2 knockdown in HAoSMCs on contractile phenotype.....</b>	<b>228</b>
<b>5.3 Discussion .....</b>	<b>229</b>
<b>5.3.1 Impact of Cyclic Strain on Cell Function .....</b>	<b>230</b>
<i>5.3.1.1 Migration.....</i>	<i>231</i>
<b>5.3.2 Argonaute 2 (Ago2) siRNA .....</b>	<b>233</b>
<b>5.3.3 Summary and Conclusion .....</b>	<b>237</b>

<b>Overall Summary and Conclusion .....</b>	<b>239</b>
<b>Future Work.....</b>	<b>243</b>
<b>Bibliography .....</b>	<b>245</b>
<b>Appendix .....</b>	<b>287</b>
<b>Chapter 3 .....</b>	<b>287</b>
<b>ECM Adhesion study.....</b>	<b>287</b>
<b>Chapter 4 .....</b>	<b>289</b>
<b>Complete priority list of miRNA .....</b>	<b>289</b>
<b>Chapter 5 .....</b>	<b>294</b>
<b>Apoptosis Study.....</b>	<b>295</b>
<i>Discussion .....</i>	<i>297</i>
<b>Integrin Study .....</b>	<b>298</b>
<i>Effect of RGD peptides (100µM &amp; 200µM concentrations) on HAoSMC adhesion. ....</i>	<i>300</i>
<i>Effect of RGD peptides (50µM concentration) on HAoSMC adhesion. ....</i>	<i>301</i>
<i>Discussion. ....</i>	<i>303</i>
<b>Over expression of FAK and FRNK plasmids in HAoSMCs.....</b>	<b>305</b>
<i>Discussion .....</i>	<i>310</i>

## CHAPTER ONE: Introduction

### 1.1 microRNA (miRNA)

Since their discovery in 1993 (Lee *et al.*, 1993) during experimentation on the nematode *Caenorhabditis elegans* (*C. elegans*) to present day genome wide studies, research into miRNA has grown exponentially. Opinion ranges from fine tuners of molecular systems (J. Chen *et al.*, 2012) to global regulators of every biological process in both plant and animal (M. S. Ebert *et al.*, 2012). Study into miRNA spans across all areas of research in biological science, as diverse as industrial bioprocessing (N.Barron, P. Kelly *et al.*, 2010) to cancer (A.G. Bader *et al.*, 2012) to cardiovascular disease (M. von Brandenstein *et al.*, 2012; E. Scalbert *et al.*, 2008; T. Thum *et al.*, 2012). Here they have been implemented in a range of biological functions from regulators of metabolic processes (B. Wilfried *et al.*, 2007) to diagnostic markers for disease (V Di Stefano *et al.*, 2011).

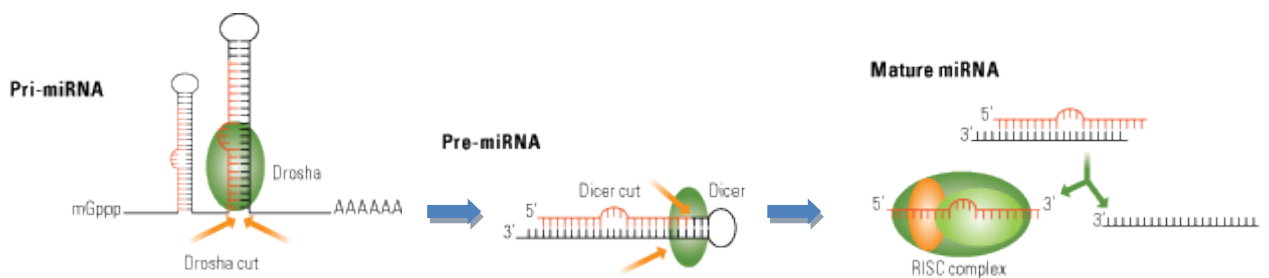


**Figure 1.1: Primary, Precursor and Mature miRNA:** Shows stages of miRNA biogenesis. Left - Primary miRNA as it exists in the nucleus following transcription by RNA Polymerase II. Middle – Precursor miRNA is generated following processing by Drosha which cleaves the 3' polyadenylated tail and 5' methylated cap. Right – Finally a mature miRNA is produced as a result of the stem loop has being cleaved by Dicer and strands separated to yield two single stranded templates, one a passenger miRNA and the other a mature miRNA which will be incorporated into RISC for gene repression. (<http://www.origene.com/MicroRNA/>)

#### What are they?

The current understanding of miRNA depicts them as short 18-24 nucleotide long non coding RNAs. Classically, they negatively control gene translation by binding to the 3' UTR (untranslating region) of their target mRNA. Here, depending on the complementarity, the miRNA promote either translational repression or degradation of their target mRNA. This results in silencing or suppression of many genes.

However, recent research has shown they may not solely bind to the 3'UTR. Fang *et al.*, (2011) has pertained that miRNA can also bind to both coding regions and the 5' UTR of mRNA targets. Several studies have also shown that negative miRNA regulation may not always be the case as some miRNA have up regulated or stimulated gene expression



as much as 100 fold (Vasudevan *et al.*, 2007, Cordes *et al.*, 2009, M Kozak *et al.*, 2008).

Collectively, more than 4000 miRNA sequences exist in a wide range of species of which up to a 1000 are encoded by the human genome, with considerable conservation across many of the species (S. van Dongen *et al.*, 2008).

Depending on the location of their encoding genes, miRNA can be categorised as intronic, exonic and intergenic miRNAs. As the name suggests, intronic and exonic miRNA are located within the intron and exon regions respectively and are typically co transcribed with their hosts (Wang *et al.*, 2009). Intronic miRNA account for ~ 50% of all miRNA and have been known to contain their own *cis* elements where they orchestrate transcription of the miRNA in the opposite direction of their host genes (Bartel *et al.*, 2004). When a miRNA is coded in a small intron it is deemed a “miRton,” and these small miRNA are able to bypass initial processing by Drosha/DGCR8 and be exported straight to the cytoplasm for maturation.

Intergenic miRNA are found between two protein-coding genes and employ their own promoters and regulatory molecules, they are the most widely characterized and studied of the miRNA families. These miRNA can be transcribed by either RNA PolymeraseII (RNAPII) or PolymeraseIII (RNAPIII). They can also exist either as monocistronic or polycistronic genes (Sarnow *et al.*, 2006).

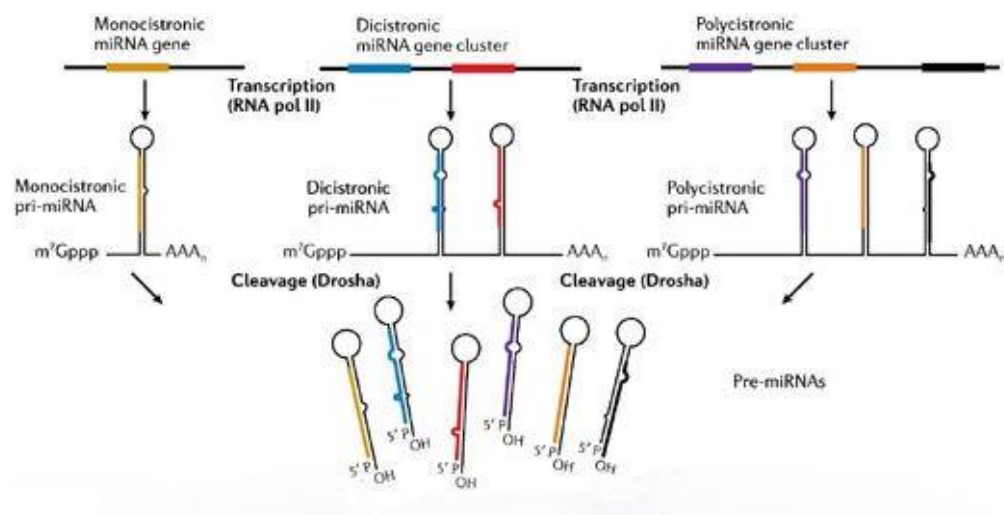


**Figure 1.2: Transcription of Monocistronic, Dicistronic and Polycistronic miRNA.**

Intergenic miRNA genes can exist as monocistronic, dicistronic or polycistronic units. These are then transcribed by either RNA Polymerase II or III into pri-miRNAs (Sarnow *et al.*, 2006).

## 1.2 Canonical miRNA Biogenesis

The micro RNA population in a given cell can be highly concentrated, with tens of thousands present per cell. They also possess a long half life and are very stable. A half life of over 1 week has been reported in some cells (VanRooji *et al.*, 2007).

Intragenetic miRNA are transcribed by RNA polymerase II from miRNA coding genes into long, hair pin stem looped, primary miRNA (pri-miRNA) hundreds of nucleotides long. They are 5' 7- methylguanosine capped and poly-adenylated at the 3' end (Han *et al.*, 2004). The poly-adenylated tail allows recognition by the microprocessor complex. This complex is made up of the ribonuclease III type protein, Drosha which is bound to the protein DGCR8 (Pasha). Interaction with this complex results in cleavage of both the 3' poly-A tail and the 5' cap. As well as cleavage Pasha (DGCR8) is also responsible for orientation of the pri-miRNA. This gives rise to a hair pin looped precursor miRNA or pre-miRNA of about 70bp in length (Ambros *et al.*, 2003) with a monophosphate at the 5' terminus and a 2-nucleotide overhang with a hydroxyl group at the 3' terminus (Sarnow *et al.*, 2006).

The pre-miRNA is then exported from the nucleus to the cytoplasm in a RAN-GTPase-dependant manner by the transport protein Exportin 5 (Bohnsack *et al.*, 2004). The binding of the pre-miRNA to this protein is facilitated by the 3' and 5' overhangs produced earlier by the Drosha/DGCR8 complex.

The next step to maturation is processing by the RNase III like protein, Dicer. This removes the hair pin loop and cleaves the pre-miRNA into a ~ 22 nucleotide duplex (Zhang *et al.*, 2002, Bartel *et al.*, 2004). This duplex is unwound by the Argonaute 2 complex producing a mature and passenger or star strand. Following unwinding the Argonaute 2 complex incorporates the mature strand into the RNA Induced Silencing Complex (RISC). The RISC then binds the miRNA to the 3' UTR of the target mRNA. This binding occurs on what is known as the "seed sequence" of the miRNA. This is typically 6-8 nucleotides long and starts at the second nucleotide. Typically, the star strand is rapidly degraded after incorporation of the mature strand into RISC, however, occasionally it is possible for both strands to be cleaved into mature, functional miRNA (M. K. Bhayani *et al.*, 2012).

Depending on the strand side incorporated, 3' or 5', the nomenclature follows as miRNA 3' or miRNA 5' (M. Von Brandenstein *et al.*, 2012).

The degree of complementarity between the target mRNA and miRNA deciphers whether the mRNA either undergoes translation repression or degradation (Miranda *et al.*, 2006, Van Rooij *et al.*, 2007). In most mammals miRNA induce mRNA degradation in 87% of the cases (H Guo *et al.*, 2010).

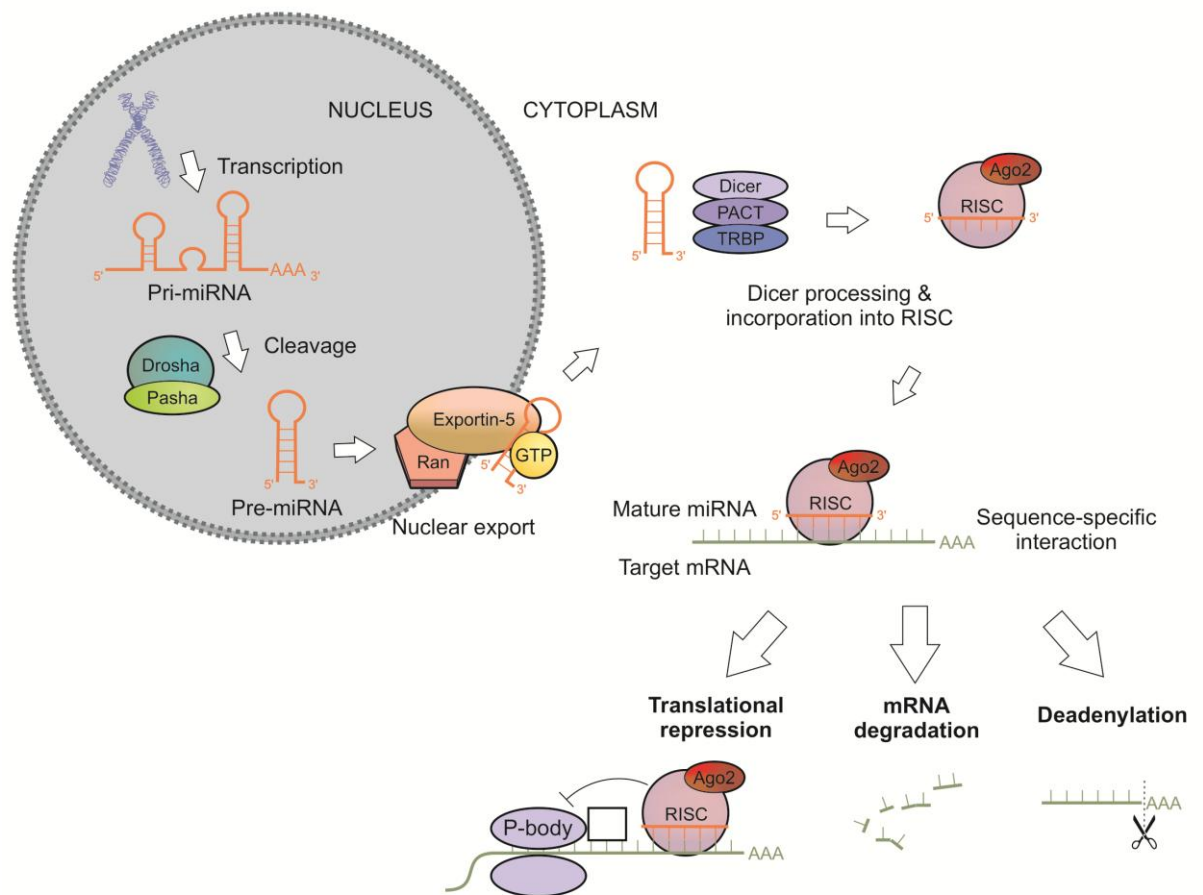


**Figure 1.3: Pathway of miRNA Biogenesis** - Transcription of miRNA is typically mediated by RNA polymerase II. This produces a stem looped primary miRNA with a 3' poly adenylated tail and a 5' 7-methylguanosine cap. The poly adenylated tail is recognized by the Drosha/DGCR8 (Pasha) ribonuclease partnership and cleaved to yield ~ 70 nucleotide “pre-miRNA”. This is then exported from the nucleus to the cytoplasm in RanGTPase manner by Exportin5. Here it undergoes further processing by Dicer in which the stem loop is cleaved yielding a ~ 22nt duplex. This is unwound and incorporated into RISC via the Argonaute 2 (Ago2) protein. From here, depending on sequence complementarity, the target mRNA either undergoes translational repression or degradation through cleavage or deadenylation. (Diagram adapted from Cordes *et al.*, 2009)

Regulation of miRNA maturation occurs at multiple stages throughout their biogenesis (Y. Junming *et al.*, 2012) including the following;

*miRNA editing*; which regulates the conversion of pri-miRNA to pre-miRNA by converting adenosine to inosine. This leads to an accumulation of edited pre miRNA which blocks processing by RISC and complete maturation of the miRNA.

*Hair pin loop binding*; a form of regulation in which a mutation of the loop reduces binding efficiency for processing.

*Epigenetic regulation*; where miRNA genes located near CpG islands in the genome is found to be hyper methylated by neighbouring chromatin.

*Self-regulation*; The components of the microprocessor complex, Drosha and DGCR8 can regulate expression of each other. The Drosha-DGCR8 complex can degrade the mRNA of DGCR8 itself, whereas DGCR8 stabilises Drosha in a feedback loop manner. Evidence of this regulatory feedback loop is shown when a miRNA binds to a 3'UTR of an mRNA that is in fact a transcription factor for regulating the miRNA itself. miRNA have also been shown to be heavily involved in supplying robustness to many diverse biological pathways via feed forward and feedback loop mechanisms in such a manner as this (M.S. Ebert *et al.*, 2012).

*Cross talk between other signalling pathways*; Pathways such as p53 have shown to assist in the cleavage of pri-miRNA to pre-miRNAs.

### **1.3 miRNA Clusters**

As previously stated miRNAs can be transcribed from a single polycistronic transcriptome, so that one polycistronic unit produces the sequence for multiple miRNA and functions where they function as a miRNA family. These contain the same seed sequence but different flanking bases which allow them to bind to the same mRNA (Lau *et al.*, 2001). These miRNA are deemed as clusters. A micro RNA cluster is a set of two or more miRNAs, which are transcribed from physically adjacent genes. To qualify as a cluster, each miRNA must be transcribed in the same orientation and must not be separated by a transcription unit or miRNA in the opposite direction. Typically miRNA clusters are composed of two or three miRNA such as the miR-143/miR-145 miR-221/miR-222 cluster, but larger clusters also exist, the miR-17-92 cluster is found on human chromosome 13 and is composed of six miRNAs.

#### 1.4 miRNA Regulation of Cellular Networks

Similar to transcriptional repressors, miRNA are most likely to be embedded in a large number of biological processes, pathways and regulatory networks. To ensure constant survival of a biological entity it is imperative that these systems run continuously and reliably. A view has emerged that a primary role for miRNA may have evolved to buffer and attenuate a diverse range of biological pathways and systems. This is the case in which a biological system or pathway is able to hold its function during alterations in environment and under stress conditions (Kitano *et al.*, 2004). For example, following a vascular injury a sub population of vascular cells may need to undergo differentiation allowing the cells to migrate and repair the wound. Here miRNA can modulate the phenotype of a cell to facilitate in wound repair while maintaining tissue specificity of the cells by ensuring a return to a quiescent differentiated state following repair of the wound (M. S. Ebert *et al.*, 2012). To reinforce this theory, genes with tissue-specific expression have displayed longer 3' UTR regions and more binding sites for miRNA (Stark *et al.*, 2005). miRNA expression has also shown to increase and diversify as the complexity of an organism and pathways within that organism increases (Lee *et al.*, 2007, Heimberg *et al.*, 2008).

Often biological pathways or processes will contain a failsafe or control which allows continued function even when conditions change or a component fails. One such example is the use of feed forward and feedback loops, which often implement miRNA (J. Tsang, 2007). In a coherent feed forward loop, component A inhibits (or activates) component C and respectively component B is activated (or inhibited) which also serves to inhibit (or activate) component C. In other words, components A and B both work to either inhibit or activate component C. If either component A or B is transiently lost the other will continue the inhibition or activation of component C. This not only incorporates a failsafe within a biological system during times of stress but also works to increase the fidelity of the action, in the case of miRNA enhancing gene suppression.

This is demonstrated in the production of granulocytes, a type of white blood cell. CCAAT enhancer binding protein alpha (C/EBP $\alpha$ ) inhibits transcription of the cell-cycle regulator E2F1 during granulopoiesis. C/EBP $\alpha$  also induces miR-223 which also inhibits E2F1.

As is often the case, this feed-forward loop is interlocked with a feedback loop in which E2F1 also inhibits production of miR-223. Combining these fail safes allows the cell to

distinguish between once off fluctuations which should be counteracted or evolutionary changes which should be enhanced (M.S. Ebert *et al.*, 2012, Pulikkan *et al.*, 2010). Another example of feedback loop is the interaction between miR-146a and Kruppel-life-factor-4 (KLF4). Here they regulate each other's expression while also regulating VSMC proliferation (Sun *et al.*, 2004).

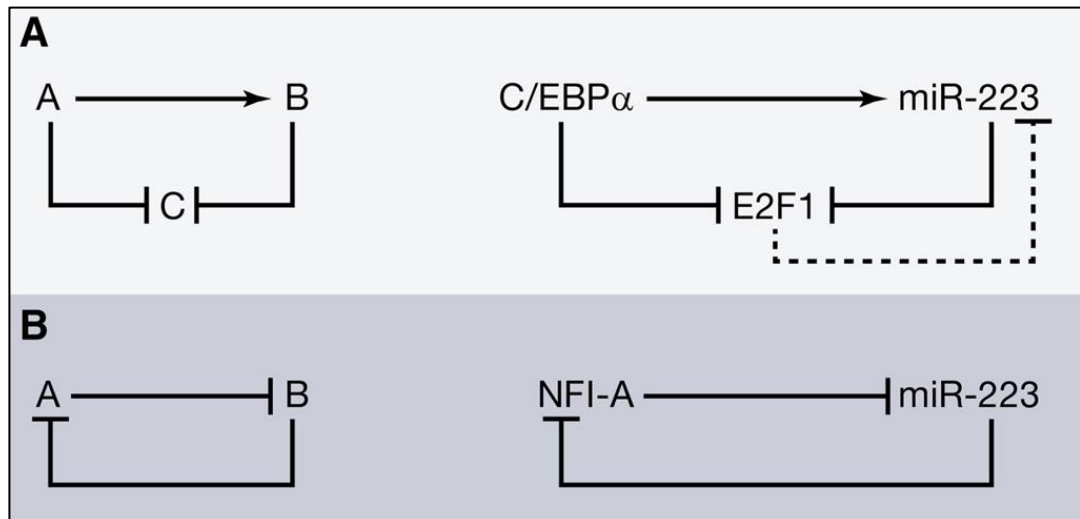


**Figure 1.4: (A) Feed Forward Loop (B) Feed Back Loop** – Diagram showing example of FF & FB loops involving miRNA. These are used in cellular networks to both attenuate and control signaling. Diagram modified from (M.S. Ebert *et al.*, 2012).

### 1.5 Level of Gene Suppression by miRNA

Although deeply conserved, many miRNA express a modest effect on their target mRNA often less than 2 fold and many miRNA can be deleted without any obvious effect on phenotype (Bartel *et al.* 2004). However, several miRNA often work together to co-target an mRNA. This is possible as many mRNA 3'UTRs have more than four highly conserved seed sequences, particularly transcripts involved in embryogenesis and tissue development. Combined with the previously described positive feed-forward and feedback loop systems, miRNA can exert enough change on the mRNA to constitute a large physiological effect (Mukherji *et al.*, 2011, Lliopoulos *et al.*, 2009, Friedman *et al.*, 2009, Baek *et al.*, 2008). miRNA can also amplify their potency by targeting mRNA contained in pathways (Linsley *et al.*, 2007).

For the reasons described, it is obvious why many *in vitro* and indeed, *in vivo* models using loss and gain function with individual miRNA have yielded disappointing results. To witness a considerable phenotype change it may be advantageous to target all

members of a seed family and non-seed family members who co target an mRNA (M.S. Ebert *et al.*, 2012).

It has also been outlined that mRNA 3' UTRs demonstrate considerable evolutionary degeneration with increased numbers of mutations. Therefore, potential 3'UTR target sequences that are conserved across species are thought to most likely represent genuine miRNA recognition motifs whose function confer an evolutionary advantage, targeting of these mRNA with miRNA could therefore yield the desired gene repression (B. R. Wilfred *et al.*, 2007)

## **1.6 miRNA Isolation & Analysis**

### 1.6.1 Isolation

Isolation of miRNA for analysis is now possible from a vast range of sources including, but not limited to, tissue, cell culture, body fluids such as blood plasma, semen ejaculate, urine, breast milk, menstruation blood, sweat, cerebrospinal fluid and serum (Etheridge *et al.*, 2011, *et al.*, Gilad 2008, *et al.*, Hanson 2009, *et al.*, Kosaka 2010, Mitchell *et al.*, 2008). The principles for isolating miRNA are generally the same for isolating total RNA, with the exception that some miRNA extraction methods enrich for the small RNA fraction. Widely used commercially available products typically rely on chemical extraction using chaotropic salts, such as guanidinium thiocyanate, followed by a solid phase extraction on silica columns (C.C. Pritchard *et al.*, 2012)

miRNA expression profiling- quantification and qualification- are carried out using several techniques with the most common being quantitative real time PCR, Northern Blot analysis or micro array analysis (Planell, Sauger and Rodicio *et al.*, 2011).

Quantitative Real Time PCR (qRT-PCR) remains the most frequently employed method for expression analysis and involves the reverse transcription (RT) of miRNA to cDNA followed by quantitative PCR (qPCR). However, many properties that are unique to miRNA pose challenges to their accurate detection and quantification while using qRT-PCR (A. Wark *et al.*, 2008). Their short length, ~ 22nucleotides, makes it difficult for traditional primers to anneal for the reverse transcriptase reaction. Also, unlike mRNA, miRNA lack a common structure or sequence, such as a poly adenylated tail which is typically used for enrichment or as a binding site for primers. This is cleaved by the Drosha/DGCR8 microprocessor complex during biogenesis. miRNA within a seed family also pose difficulties for qRT-PCR as they may only differ from one another by as little as one nucleotide making specificity of the primer particularly crucial.

To overcome these problems two different technologies can be used for preparing miRNA for RT. These include enzymatic addition of a poly adenylated tail on to the 3' end of the miRNA with consequent binding using universal linear primers.

The second method creates a RT binding primer site using a stem loop specific primer set binding to the 3' end of the miRNA. This is followed by individual reverse transcription and a TaqMan miRNA assay (Pritchard *et al.*, 2012).

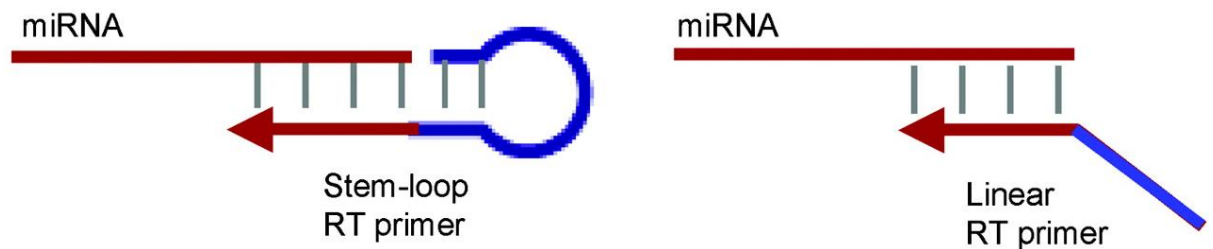


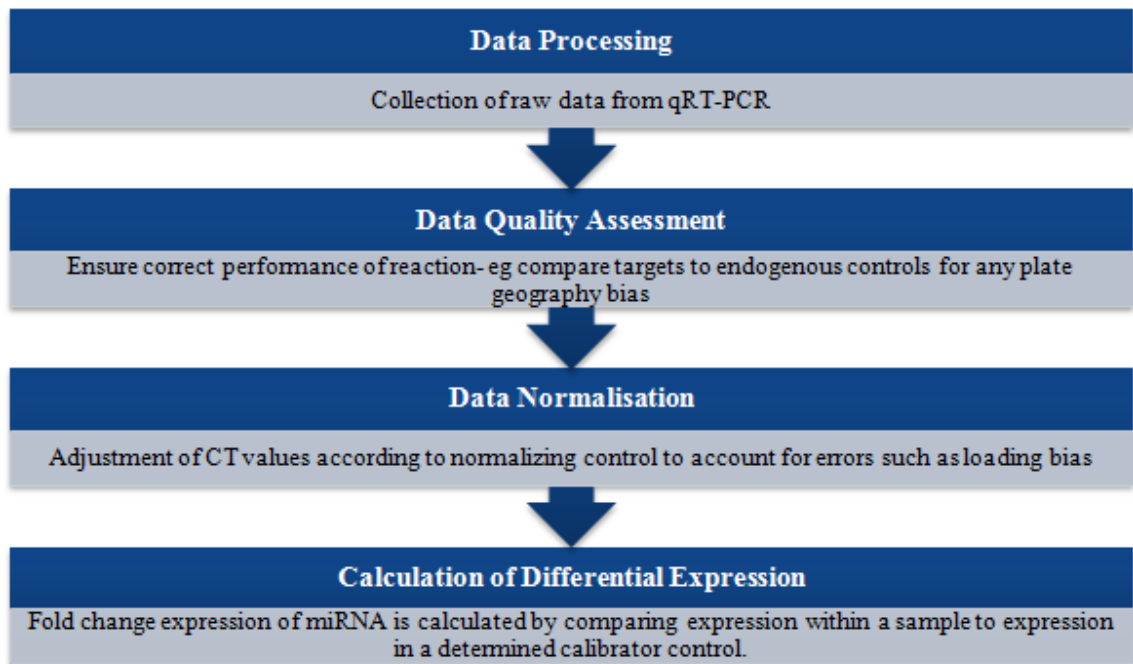
**Figure 1.5: Left – Stem Loop RT Primer, Right – Linear RT Primer** – Diagram of stem loop primer (left) binding to mature miRNA for cDNA synthesis and traditional linear primer (right) binding to mature miRNA for cDNA synthesis. Diagram modified from C. Chen *et al.*, (2005).

The use of stem loop primers has now become the more adopted approach for the majority of researchers. This method has shown to have a high specificity and dynamic range of at least 7 logs and is capable of detecting as few as 7 copies of product in a PCR reaction. Use of stem loop primers can also differentiate between mature and pre/pri miRNA as well as miRNA which differ by only a single nucleotide. The advantageous characteristics of stem loop primers over linear is attributed to the base stacking and spatial constraint of the stem-loop structure. This improves thermo stability and extends the effective footprint of the RT primer/RNA duplex, which is required for effective RT from shorter RT primers. The spatial constraint of the stem loop prevents binding of genomic double stranded DNA (C. Chen *et al.*, 2005).



## 1.6.2 Data Analysis

The workflow for miRNA profiling typically consists of;



For initial handling of the raw data, the software being used should be fully investigated to determine if there is any pre-processing of the data by the instrument software, for example automatic ROX dye normalisation used in TaqMan qRT-PCR. Following this, the output data is assessed for employability by investigating the performance of internal controls and analyzing replicates for bias, which could arise from such mitigating factors as plate geography (D. Sarka *et al.*, 2009)

Arguably the most important step is normalisation of the data, the goal at this point is to adjust the data to remove any bias or change in expression not arising from the biological conditions under examination.

Various approaches have been utilised; one of the most commonly employed is the use of one or a few endogenous controls on the micro-fluidic plate. These are typically small nuclear RNAs (U-24, U-26) or miRNAs (miR-191 & miR-103) which are found to be largely invariant in a given sample set (J.H. Peltier *et al.*, 2008). The methodological limitation of such an approach is that it relies on the assumption that the selected controls are completely independent to the biological variation being studied.

An alternative approach relies on the mean global expression of miRNA from a large scale study. This strategy is based on the assumption that although specific miRNAs may vary across biological samples owing to biological causes, the overall pattern of expression is expected to be invariable and therefore can be used as a normaliser (P. Mestdagh *et al.*, 2009). This was shown in several studies to outperform use of endogenous controls in terms of better reduction of technical variation and more accurate appreciation of biological changes and is the strategy adopted in the experimental design for this thesis (P. Mestdagh *et al.*, 2009, D. Wiley *et al.*, 2011).

### 1.6.3 Calculating Differential Expression

miRNA profiling experiments typically involve making comparisons between two or more groups, following normalisation the next stage of analysis is calculation of the differential expression of miRNA across the samples. Consideration needs to be taken however into the statistical significance of these changes and also the dynamic range and accuracy of the platform used in the quantification. Generally qRT-PCR has the widest dynamic range and highest accuracy. Never the less control of the false discovery rate should be considered when generating statistical significance for example using the Benjamini-Hochberg procedure, this uses an adjusted P value for significance.

The adjusted P value method allows for controlling the rate of false positives. To begin, an acceptable false discovery rate is selected, for example 10%. This means 10% of the significant miRNA will be false positives. This is acceptable in a large screening experiment like presented in this thesis as any false positives will be found in follow up experiments on short listed miRNA. Next P values of miRNA are placed in order from smallest to largest. The smallest P value has a rank of  $i=1$ , the next has  $i=2$ , etc. Each individual P value is then compared to

$$(i/m)Q$$

Where  $m$  is the total number being tested and  $Q$  is the chosen false discovery rate. The miRNA which has the largest P value but is  $\leq (i/m)Q$  is significant and all P values less than this are also significant (Y. Benjamini., Y. Hochberg *et al.*, 1995). This results in a shortlist being generated of statistically significant miRNA with an adjusted P value of a pre-determined level. This short list can then be utilised *in silico* for full bioinformatic profiling. Such as target prediction, biological processes and also involvement in cellular pathways.

## 1.7 Bioinformatics

### 1.7.1 Target Prediction

Following differential expression analysis, often the next stage in miRNA profiling is target prediction of the short listed miRNA. *In silico* target prediction is facilitated by an array of freely available on line algorithm suites.

Complementarity between the seed region of the miRNA and the 3'UTR of an mRNA is the underlying method used for *in silico* prediction of targets. However, there are many other parameters that can influence and facilitate binding which are used by the online resources. These include thermodynamic stability (decided via the Vienna RNA folding routines), free energy, AU content, conservation across species (typically at least two), size of the 3' UTR and the amount of binding sites or tandem repeats and site location, miRNA are more likely to bind if they are located at the beginning or end of the 3'UTR.

Each online resource has a unique selling point, for example, PicTar can provide co-expressed miRNA and mRNA targets if conservation across species is not evident. Consequently, overlapping of putative targets is small and a combination of different databases is often the best method in this initial step of target prediction.

Databases include:

- Target Scan <http://www.targetscan.org/>
- PicTar <http://pictar.mdc-berlin.de/>
- Micro Inspector <http://www.imbb.forth.gr/microinspector>
- miRNA.org <http://www.microrna.org/microrna/home.do>
- MicroCosm <http://www.ebi.ac.uk/enright-srv/microcosm/htdocs/targets/v5/>
- RNA hybrid <http://bibiserv.techfak.uni-bielefeld.de/rnahybrid/>
- RNA22 <http://cbcsrv.watson.ibm.com/rna22.html>
- PITA <http://genie.weizmann.ac.il/pubs/mir07/index.html>
- Diana <http://diana.cslab.ece.ntua.gr/microT/>
- GenMir <http://www.diana.pcbi.upenn.edu/miRGen.html>

These target prediction tools are an excellent resource and solid first step in deciphering the roles of specific miRNA, however they do not take into account individual cell types, availability of genes within that cell or if the miRNA is even expressed. In addition, as the name suggests they are just predictions and thus need to be experimentally validated in the lab. This can be carried out by a number of techniques

including western blot, luciferase assays, RIP-CHIP pull down assay, in which the RISC is co-immunoprecipitated and bound mRNAs are sequenced and identified. Another form of this is a technique in which miRNA are tagged with biotin and pulled down in a streptavidin-biotin pulldown system to see miRNA:mRNA interactions (UA Orom *et al.*, 2007).

### 1.7.2 Gene Annotation

Further bioinformatics may be carried on putative gene lists generated from target prediction software. For this thesis, enrichment of genes in biological processes and pathways were deduced using an online bioinformatics database, DAVID (Database for Annotation, Visualisation and Integrated Discovery). DAVID bioinformatics resources consist of an integrated biological knowledge base and analytical tools aimed at extracting meaning from large protein or gene lists. The first stage is to upload putative targets containing any number of gene identifiers i.e. official gene symbol or entrez gene ID. Following this, analysis is carried out taking advantage of the vast pathway miming tools such as Gene Ontology (GO) biological processes or KEGG biological pathways.

*1.7.2.1 Gene Ontology (GO)* is a major bioinformatics initiative which attempts to unify and standardise the representation of genes and their involvement in cellular processes across all species. The initiative was set up to aid scientists in the search for biological data and information on a myriad of research areas. It achieves this by maintaining and developing a controlled vocabulary and nomenclature of genes and gene products (RNA/protein). In addition, information pertaining to individual genes, such as involvement in cellular processes and functions is pooled to allow easy access for the user. The database is constructed of three controlled vocabularies (ontologies). Each of these ontologies describes gene products in terms of their associated *biological processes*, *cellular components* and *molecular functions* in a species-independent manner. The database, therefore aims to eliminate the hindrance of different terminology and nomenclature found across scientific disciplines, in addition to providing as much information as possible on the gene and gene products.

*1.7.2.2 The Kyoto Encyclopedia of Genes and Genomes (KEGG)* is a database resource for understanding high level gene functions. Developed as a result of the Japanese genome project, its developers believe it is a computer representation of a full biological

system. Unlike the GO database, KEGG, among other functions, can determine enrichment of genes within pathways and utilities of the biological system. This is available as a result of gene catalogues from completely sequenced genomes which being linked to higher level systemic functions such as the cell, the organism and the ecosystem. As with GO, by entering large data sets or gene lists, it is possible to access this information for that given data set or list. KEGG is comprised of 16 main databases which outputs into 3 categories; System information, Genomic information and Chemical information. Work for this project was concerned with the involvement of predicted miRNA targets in cellular pathways. The KEGG pathway database is found within the system information category. The full lists of databases are found in table 1.1.

**Table 1.1: KEGG Database** Table shows the 16 databases making up KEGG online resource which are divided across three categories System information, Genomic information and Chemical information

<b>Systems Information</b>	<b>KEGG Pathway</b>
	<b>KEGG Brite</b>
	<b>KEGG Module</b>
	<b>KEGG Disease</b>
	<b>KEGG Drug</b>
<b>Genetic Information</b>	<b>KEGG Environ</b>
	<b>KEGG Orthology</b>
	<b>KEGG Genome</b>
	<b>KEGG Genes</b>
<b>Chemical Information</b>	<b>KEGG SSDB</b>
	<b>KEGG Compound</b>
	<b>KEGG Glycan</b>
	<b>KEGG Reaction</b>
	<b>KEGG Rpair</b>
	<b>KEGG Rclass</b>
	<b>KEGG Enzyme</b>

By taking advantage of these vast data mining suites it is possible to gain an in-depth understanding of the biological themes in lists of genes enriched in large profiling studies such as the work carried out in this thesis.

## 1.8 The Cardiovascular System

The 16<sup>th</sup> century English Physician, William Harvey is credited with being the first person to describe in detail the existence of a blood circulatory system in vessels. Since then, our understanding of the vasculature system has increased exponentially, credited to the continual developments of cell and molecular biology methods and techniques.

With the exception of cells found in the cornea, the estimated 100 trillion cells which make up the human body rely on the blood in the circulatory system to provide oxygen and nutrients for survival as well as removing metabolic waste products. In addition, the circulatory system maintains an optimum cellular environment by regulating body temperature and pH (Gimbrone *et al.*, 1987). Humans have evolved an incredibly complex, closed and pressurized circulatory system in which the heart is responsible for pumping the 5 – 5.5 liters of blood throughout the entire network of blood vessels (Hahn & Schwartz *et al.*, 2009). During a human lifespan the heart will beat about 3 billion times and pump well over 200 million liters of blood. This circulatory system can essentially be subdivided into the vasculature and lymph system. In the broadest sense, the vascular system is composed of the heart, blood and blood vessels while the lymphatic circulatory system consists of lymphatic microvessels (capillaries) and larger lymph vessels (M.K. Pugsley *et al.*, 2000).

The blood vessels within the body are classified into three categories; arteries, veins and capillaries. Oxygenated blood returning from the lungs is ejected from the left ventricle into a large network of arteries. Arteries can be further categorised into two distinct types: elastic and muscular (Borysenko & Beringer *et al.*, 1984). Elastic arteries are found proximal to the heart as they are able to carry large volumes of blood and also “dampen” the oscillatory force of blood flow due to a beating heart. This is credited to their composition, consisting of many layers of perforated elastic membrane, this helps to create a more homogenous movement of blood as the artery bifurcates or divides into smaller vessels (Lusis *et al.*, 2000). The larger populations of arteries, muscular arteries, are responsible for the complete distribution of blood to all the organs and tissues within the body. The continual bifurcation of these arteries leads to the formation of smaller arterioles, which serve to reduce blood flow and therefore prevent damage to the fragile capillaries, of which there are over 40 billion in the human body.

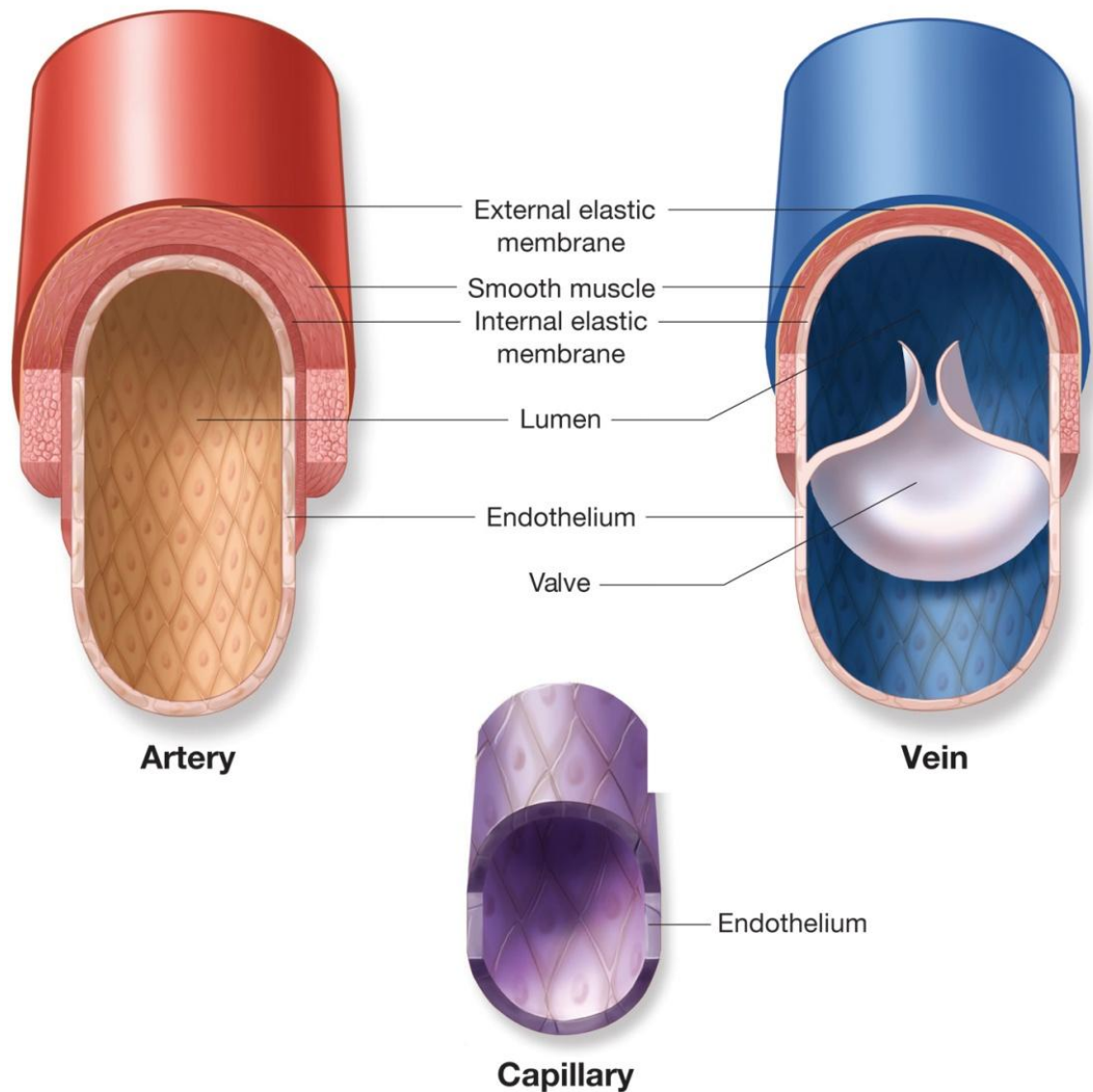


**Figure 1.6: Three Categories of Blood Vessels** - Shows cross sectional diagram of the three categories of blood vessels within the vasculature. From left to right; cross section of artery, capillary and vein. Main features highlighted in this figure include; thicker vessel wall in the artery compared to veins or capillaries. Valve is present in the lumen of the vein to prevent back flow of low pressure blood; this is not in the other blood vessel types. The capillary shows only an endothelial layer with no smooth muscle or elastic membranes, emphasizing the delicate nature of this vessel.

(<http://legacy.owensboro.kctcs.edu/gcaplan/anat2/notes/APIINotes5%20Circulatory%20Anatomy.htm>)



These capillaries, which lack smooth muscle, form fine vascular networks between tissues and cells allowing blood perfusion (Cines *et al.*, 1998). The total surface area of capillaries alone in the body equates to approximately 1000m<sup>2</sup> - roughly the size of a tennis court (M.K. Pugsley *et al.*, 2000). As a result of this large surface area of the capillary bed, water, solutes and nutrients from blood are able to diffuse into the surrounding tissue. Capillaries also connect the arterial vascular tree to the venous system allowing a return of deoxygenated blood to the right atrium of the heart via the superior vena cava. The transition from capillary to vein is marked by the gradual reappearance of smooth muscle.

Blood returned to the right atrium in turn flows through the tricuspid valve into the right ventricle then up to the lungs via the pulmonary artery. Through gaseous exchange, the lungs oxygenate the blood which then returns to the left atrium via the pulmonary vein. Circulation of deoxygenated blood flowing from the heart to the lungs and back to the heart is known as the pulmonary circulation. The oxygen rich blood now enters the left ventricle and is pumped into the aorta as the entire process begins again. The circulation of blood from the heart to the rest of the body is known as the systemic circulatory system.

The physical size and geometry of each blood vessel type differs considerably. Capillaries typically range between 5-8 µm in diameter, followed by veins, which vary between 1-10 mm which are also trumped by the motorways of the vasculature system, the arteries. At over 2.5cm in diameter and travelling the entire length of the torso, the aorta is the largest artery in the body.

## The Aorta

The aorta also has the thickest walls of any blood vessel and originates from the left ventricle of the heart. It arches over to the back of the heart and to the left, from here it descends inferior to the heart and anterior to the spinal column. The first section of the aorta is known as the ascending aorta. The ascending aorta branches into the left and right coronary arteries. The coronary arteries carry blood to the surface of the heart supplying it with oxygen and nutrients.

The second portion of the aorta, the aortic arch, branches into three major arteries:

- The brachiocephalic trunk
- The left common carotid artery
- The left subclavian artery

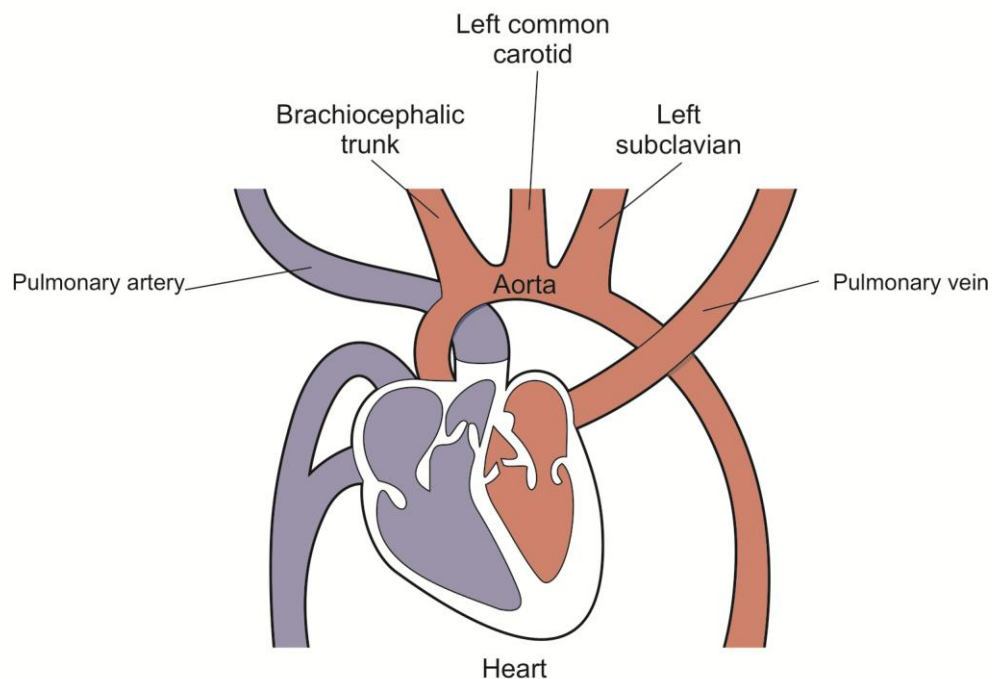


**Figure 1.7: Schematic of the heart and surrounding vessels.** Diagram shows the major veins and arteries which are proximal to the heart. The aortic arch branches into three major vessels the brachiocephalic trunk, the left common carotid and the left subclavian. The left and right coronary arteries, which branch from the ascending aorta, are not shown. The pulmonary system is shown in blue and the systemic system is shown in red.

The brachiocephalic trunk supplies blood to the right arm and right side of the head, including the brain. The left common carotid artery supplies blood to the left side of the head and brain. Finally the subclavian carries blood to the left arm.

The descending aorta carries blood through the thoracic and abdominal cavities of the body until it splits into the left and right common iliac arteries, which supply blood to the legs. The descending aorta is broken down into two sections – the thoracic aorta and abdominal aorta – named after the body cavities that it passes through. The abdominal aorta branches off into many smaller arteries that feed the major abdominal organs. The aorta carries all of the oxygenated blood exiting the heart in the systemic loop of the circulatory system. Thus, the aorta provides oxygenated blood flow to all the tissues of the body. The wall of the aorta is very thick and elastic; this allows it to withstand the high blood pressure produced by the heart and to stretch with every heartbeat to receive a large volume of blood. After filling with blood, the stretched aorta contracts to its original diameter and pushes blood into the arteries that branch off from it.

#### Blood Vessel Composition

In general, most blood vessels consist of three histologically distinct regions (Borysenko & Beringer *et al.*, 1984). Each region of a blood vessel is termed a “tunic” from the latin term meaning “a membrane”. Anatomically (from the lumen of the blood vessel out), these regions or layers are called the *tunica intima*, *tunica media*, and the *tunica adventitia* (Vita & Keaney *et al.*, 2002).

The *tunica intima* is the thinnest layer of just 0.2-4  $\mu\text{m}$ ; this consists of a single monolayer of endothelial cells mounted on the basement membrane. The endothelial cells are directly exposed to blood flow. Below this there is a sub-endothelial connective tissue layer composed of elastic fibres which provide flexibility and stability for endothelial cells. Also within close proximity are perivascular cells, or pericytes, which are multipotential stem cells capable of differentiating into an array of vascular cell types (Sims *et al.*, 1986; Hirschi & D’Amore *et al.*, 1996; Schor & Canfield *et al.*, 1995).

The *tunica media* contains predominantly smooth muscle cells and elastin fibres. This layer is primarily responsible for vascular tone and the movement of large volumes of blood throughout the circulatory system. Circumferential to this, we find an external elastic lamina that provides structural support. The *tunica adventitia* is the last and outermost layer of a blood vessel. This is mainly composed of connective fibrous tissue and fibroblasts along with various amounts of collagen. The collagen serves to anchor

the blood vessel to nearby organs giving it stability. The main focus of this thesis is on vascular smooth muscle cells, the principle component of the tunica media. Specifically human aortic smooth muscle cells (HAoSMCs) taken from the thoracic region of the aorta.

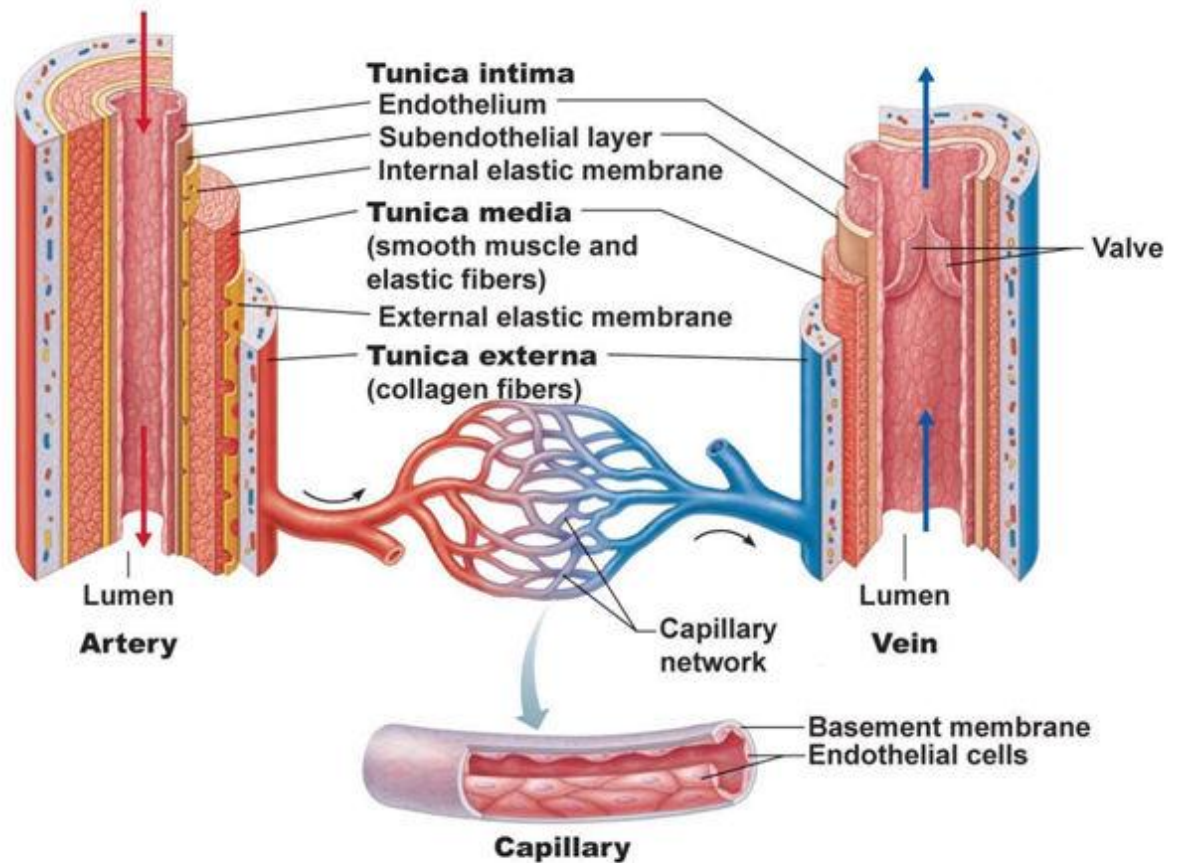


**Figure 1.8: Illustration of Layers which Compose Blood Vessels** – Artery: *Tunica Intima* Endothelium composed of endothelial cells, Subendothelial layer and internal elastic membrane, *Tunica Media* Composed of smooth muscle cells and elastic fibers exterior to this exists an elastic membrane, *Tunica Externa* Composed primarily of collagen fibers and fibroblasts. Vein: Similar composition to an artery without the internal and external elastic membrane in the tunica intima and tunica media which provide the elasticity needed in arteries to accommodate the haemodynamic forces of blood flow. Other differences include a thinner vessel wall due to the lower tensile pressure of deoxygenated blood and addition of valves to prohibit back flow of the lower velocity blood flow. Capillary: Smallest of the blood vessels composed of endothelial cells and a basement membrane, these vessels facilitate blood perfusion into surrounding tissue and cells.

(<http://legacy.owensboro.kctcs.edu/gcaplan/anat2/notes/APIINotes5%20Circulatory%20Anatomy.htm>)

### 1.9 Cardiovascular Disease (CVD)

Cardiovascular Disease (CVD) is a name given to a group of disorders of the heart and blood vessels. Although there are many conditions associated with this disease, the Global Burden of Disease Study (GBD) reported that ischemic heart disease is the leading cause of death worldwide, representing 63% of all deaths. It is also the prevailing cause of death in Ireland. The World Health Organisation (WHO) predicts that the number of people who die from CVDs, mainly from heart disease and stroke, will reach 23.3 million by 2030. As CVDs remain the leading cause of death they are projected to spread further and further into middle and low income countries. CVD often exists as an underlying complication; indeed the first foundation and initiation of CVD will appear well before any clinical threshold or horizon, for example before any acute conditions such as myocardial infarction or stroke.

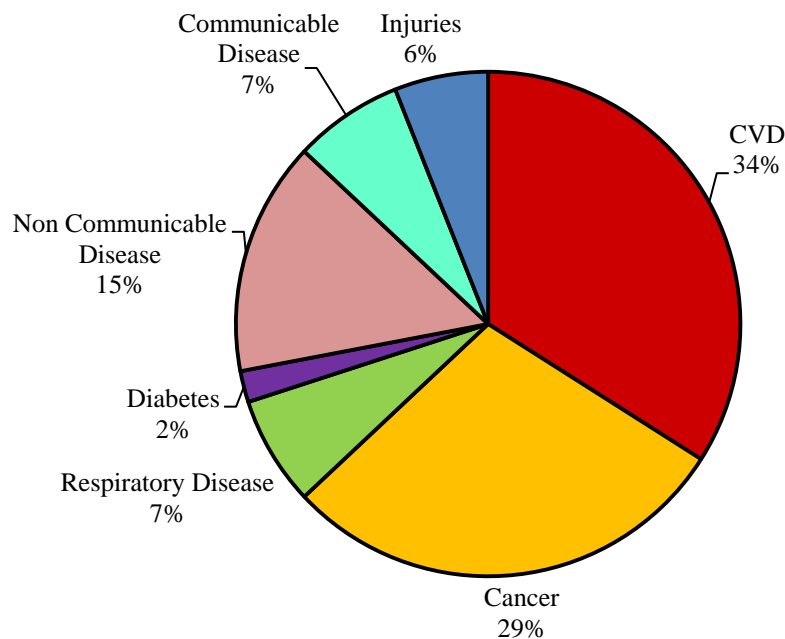


**Figure 1.9: Chart Representing Causes of Mortality in Ireland 2010.**World Health Organisation (WHO) statistics for 2010 of the causes of mortality in the Irish population.

There are many contributing factors to this disease. For example economic development, urbanisation and westernisation during the late 19<sup>th</sup> and early 20<sup>th</sup> century meant that people began to be exposed to tobacco smoking, high fat content diets and physical inactivity- all increasing the risk of CVD. Most CVDs can however be prevented by addressing these environmental risk factors. If left untreated, these risk factors can result in complications such as hypertension (high blood pressure).

9.4 million Deaths each year, or 16.5% of all deaths can be attributed to high blood pressure. This includes 51% of deaths due to strokes and 45% of deaths due to coronary heart disease. It is estimated that over 40% of the world's population has high blood pressure (S.S. Lim *et al.*, 2010).

High levels of vessel wall strain found in arterial hypertension can damage the endothelium and lead to the development of aneurysms or diseases such as atherosclerosis. Atherosclerosis refers to the development and progression of atherosclerotic plaques. This results in gradual narrowing of blood vessel lumens restricting blood flow. Obstructed blood flow can lead to a myriad of complications such as stroke, kidney failure, angina or a myocardial infarction. These plaques can be classified as either stable or unstable, depending on their composition. Stable plaques are predominantly composed of synthetic migrating SMCs which have transcended through the endothelium into the luminal space. The focus of the work undertaken in this thesis was to investigate the effect of varying strain conditions on the differentiation and migration of Human Aortic SMCs (HAoSMCs).

## Atherosclerosis

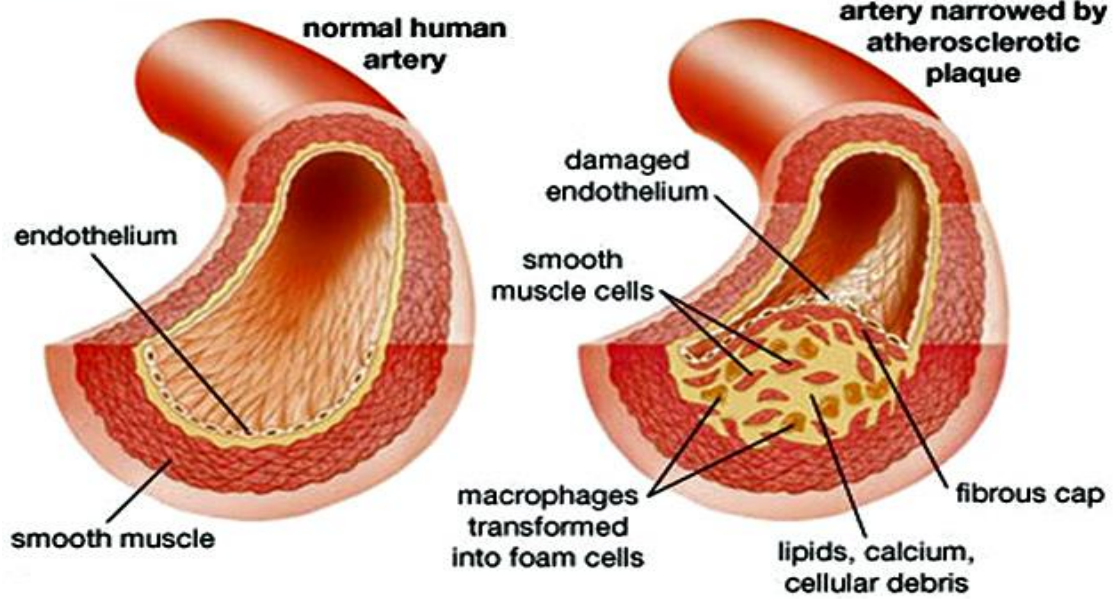


**Figure 1.10: Atherosclerosis.** Figure shows a schematic of a healthy blood vessel on the left with an unobstructed lumen. Blood vessel on the right shows a developed atherosclerotic plaque which is occluding the lumen resulting in restricted blood flow. Plaques are classified to be unstable or stable depending on their composition. Stable plaques are typically composed of migrated smooth muscle cells and a fibrous cap layed down by deposited ECM molecules. Unstable plaques consist of macrophages which have transformed into foam cells along with cellular debris, fats and calcium deposits. Plaque development can be brought on by conditions such as hypertension, damaging the endothelium and encouraging SMC migration. (<http://www.pharmaceutical-networking.com/merck-mk-0524b-treatment-of-atherosclerosis/>)

### 1.9.1 miRNA and Cardiovascular Disease

A plethora of studies now implicate miRNA deregulation and expression in cardiovascular diseases, such as hypertrophy, myocardial infarction angiogenesis and atherosclerosis. Of the 700 plus miRNA encoded by the human genome some 150-200 are expressed in the heart where they are dynamically regulated in response to disease (De-Li Dong *et al.*, 2011).

In the early stages of atherosclerosis the endothelium, made up of a monolayer of endothelial cells, is the first line of defense against harmful lesions and plaque formation. This becomes more apparent in the fact that endothelial dysfunction represents a common link among all known cardiovascular risk factors, including dyslipidemia, smoking, diabetes, obesity, mental stress and hypertension (Grover *et al.*, 2009). Endothelial dysfunction is characterised by a reduced bioavailability of nitric oxide, increased expression of adhesion molecules, increased levels of proinflammatory and prothrombotic factors, oxidative stress and abnormal modulation of vascular tone (Chen *et al.*, 2012).

Initial evidence that miRNA were involved in endothelial cell function surfaced when Keubacher *et al.*, (2007) silenced Dicer in endothelial cells *in vitro* to yield impaired angiogenesis on a matrigel substrate. Later endothelial cell specific Dicer knockout mice showed leaky vessel membranes and eventual lethality (Suarez *et al.*, 2008). Deregulation of several miRNA is now associated with endothelial dysfunction.

miR-21 has shown to be one of the most dynamically regulated miRNAs in various pathological processes, ranging from cancer to cardiovascular disease (Zhou *et al.*, 2011). This miRNA has shown to be significantly up regulated in atherosclerotic plaques compared to non-atherosclerotic arteries (Raitoharju *et al.*, 2011).

The most ubiquitously expressed miRNA in ECs is the endothelial specific miR-126. This miRNA regulates the influx of monocyte adhesion to areas of atherosclerotic lesions by directly targeting vascular cell adhesion molecule-1 (VCAM-1), thus controlling vascular inflammation (Harris *et al.*, 2008). Accordingly miR-126 may exert an antiatherosclerotic effect by reducing inflammation.

Endothelial cell senescence, often seen in aging, is also a major risk factor in progression of cardiovascular disease. miR-217 has been shown to be largely expressed in aged but not young endothelial cells (Menghini *et al.*, 2009). This suggests a negative role of miR-217 by promoting senescence in ECs.



As previously stated alterations in haemodynamic force, such as increase in magnitude as found in hypertension, can lead to development and progression of atherosclerosis. This is also seen in parts of the vessel which experience disturbed shear stress or blood flow. This typically happens at bifurcations of arteries where the blood flow is no longer laminar and ceases to have an atheroprotective stimulus on the endothelium (Passerini *et al.*, 2004). Fang *et al.*, (2010) found expression of miR-10a was lower in atherosusceptible region of the endothelium, such as the inner aortic arch. Knockdown of miR-10a in endothelial cells was also shown to induce inflammation mediated by nuclear factor kappa B (NF- $\kappa$ B) (Fang *et al.*, 2010).

Following endothelial dysfunction, the phenotypic modulation of VSMCs to a migratory synthetic state is at the forefront of neointima and plaque formation in atherosclerosis. There are several contributing factors which influence phenotype switching including; a wide variety of growth factors, such as platelet derived growth factor (PDGF) and insulin derived growth factor-1 (IDGF-1) (Wang *et al.*, 1994), extra cellular matrix components such as collagen type I and type IV (Orr *et al.*, 2010) and mechanical factors, including shear stress and cyclic strain resulting from the pulsatile nature of blood flow. Studies now suggest miRNA play a key role in facilitating this phenotype switch of VSMCs by targeting transcription factors and components of the cytoskeleton.

Perhaps the most characterised miRNA involved in SMC biology are miR-143 and miR-145. They exist as a clustered bicistronic primary transcript, which is located on chromosome 5. Their expression levels are now widely accepted as a marker of VSMC phenotype. The cluster has been shown to be highly expressed in VSMCs in the normal vascular wall while their expression is significantly reduced in proliferating VSMCs *in vivo* and *in vitro*. Like other VSMC markers their expression has shown to be influenced by the serum response factor (SRF) co-activator, myocardin (Sebastian *et al.*, 2010). miR-145 has also shown to function in a feed forward loop regulating both its own expression and miR-143. Here the miRNA cluster targets multiple transcription factors which are involved in VSMC differentiation, including KLF4, calmodulin kinase II  $\delta$  (CamKII $\delta$ ) and ELK1 (a member of the ETS oncogene family), this results in promotion of the SRF co activator, myocardin, consistent with a contractile phenotype (Cordes *et al.*, 2009). Studies of *in vitro* and *in vivo* down regulation of these miRNA in VSMCs resulted in the formation of actin rich membrane protrusions deemed

podosomes via a pathway involving Src and p53, these are indicative of a migratory synthetic VSMC (Quintavalle *et al.*, 2010).

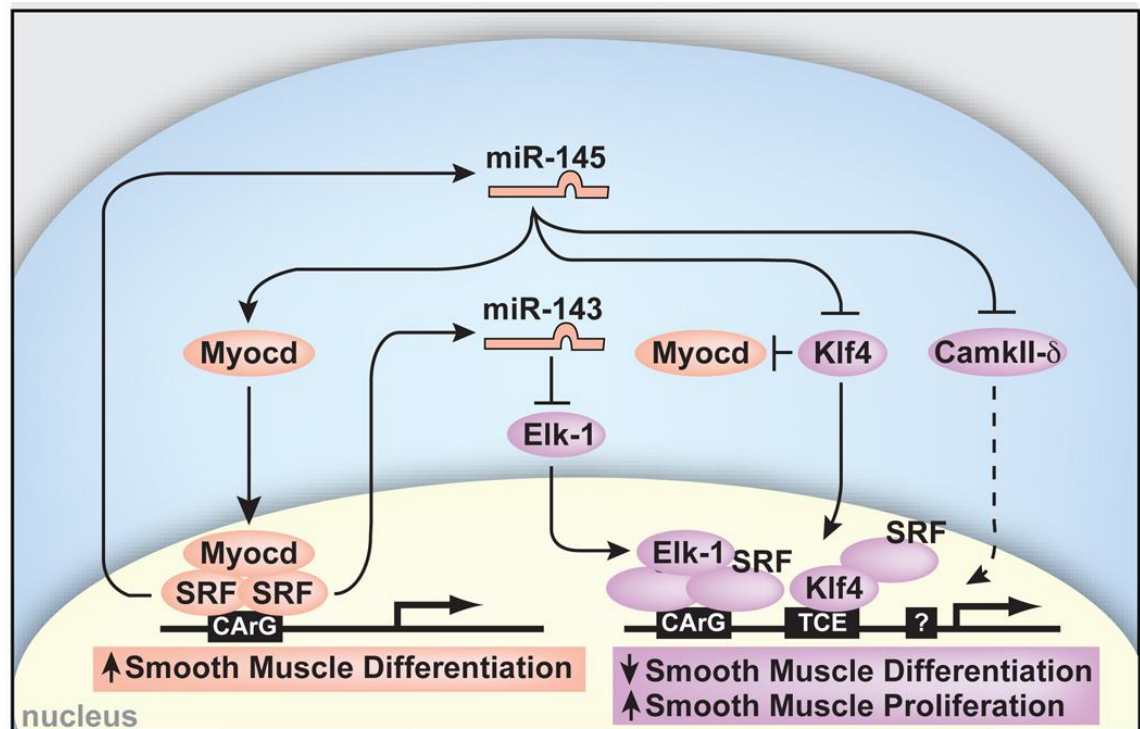


**Figure 1.11: Regulation of VSMC phenotype by miR- 143 and miR-145.** miR-143 and miR-145 are positively regulated by SRF and function to repress multiple factors that normally promote a synthetic phenotype (purple). These include Klf4, which also represses myocardin (“Myocd”). miR-145 has a positive effect on Myocd enhancing a contractile phenotype (pink), thereby also functioning to reinforce miR-143 and its own expression in a feed forward loop. Effects of miR-145 and miR-143 converge on SRF-dependent transcription by regulation of co-activators and co-repressors to dictate the proliferative or differentiated phenotype of VSMCs Diagram modified from Cordes *et al.*, (2009).

Despite having high expression in ECs in atherosclerotic lesions, miR-21 was actually shown to promote differentiation of VSMCs in response to transforming growth factor- $\beta$  (TGF- $\beta$ ) and bonemorphogenetic protein (BMP) stimulation via a decrease in programmed cell death protein 4 (PDCD4) expression (Sebastian *et al.*, 2010). TGF- $\beta$  activates transcription of the miR-143/145 gene cluster through the CArG box via myocardin expression, while BMP exerts a similar effect via nuclear translocation of myocardin-related transcription factor-A (Chen *et al.*, 2012). Interestingly miR-21 promotes both proliferation and differentiation of VSMCs as well as reducing apoptosis by down regulating phosphatase and tensin homolog (PTEN) and up regulating B-cell lymphoma 2 (Bcl-2) (Cheng *et al.*, 2007). While BMP and TGF- $\beta$  signaling pathways promote a contractile phenotype in VSMCs, the PDGF signaling pathway modulates

VSMCs to a synthetic state. Here miR-24 has shown to be up regulated in atherosclerotic lesions where it targets Tribbles like protein 3 (Trb3) in the PDGF pathway (Chan *et al.*, 2010).

Other cluster genes such as miR-1 and miR-133 have also shown to be involved in VSMC differentiation, over expression of this cluster was shown to inhibit proliferation by targeting KLF4 and SP1 (Chen *et al.*, 2011; Torella *et al.*, 2011). Conversely however Jiang *et al.*, (2010) suggested miR-1 reduced VSMC contractility by impairing the actin cytoskeleton, highlighting the complexity of regulation by miRNA.

Along with miR-24 there are also several other miRNA which have shown to promote a more synthetic phenotype. miR-221 and miR-222, also clustered, have shown to be up regulated in injured vascular walls and in areas of atherosclerotic plaques (Liu *et al.*, 2009). The cluster's expression was also increased in PDGF stimulated proliferating VSMCs. Over expression of miR-221/miR-222 was shown to reduce contractile markers by inhibition of c-Kit, which is a positive regulator of myocardin (Sebastian *et al.*, 2010). Another well characterised miRNA, miR-26a, was shown to promote a proliferative migrating VSMC phenotype by targeting transforming growth factor-  $\alpha$  (TGF- $\alpha$ ) (Leeper *et al.*, 2011). miR-26a was also shown to inhibit cell apoptosis by targeting expression of SMAD1 and SMAD4 genes (Chen *et al.*, 2012).

The myriad of studies involving specific miRNA in VSMC phenotype switching is perhaps not surprising as it is such a complex process. Therefore it should be noted the miRNA highlighted in this section must be looked at as a representation of the most characterised as opposed to a definitive list of miRNA involved in VSMC phenotypic modulation. To elucidate a clearer concept as to how miRNA facilitate phenotypic switching it is important to look at the complexity of a vascular smooth muscle cell and the factors which influence this phenotype plasticity.

## 1.10 Vascular Smooth Muscle Cells

As previously stated, smooth muscle cells (SMCs) predominantly make up the *tunica media* layer of arteries and veins. They are responsible for controlling vascular tone, which regulates blood pressure and also facilitates blood flow in the vessel. They can carry out these functions due to a unique plasticity where they can reversibly modulate their phenotype between that of a synthetic and a contractile state in a process known as phenotypic modulation (G.K. Owen *et al* .,2004). This results in relaxation or contraction of the cell, adjusting the vascular tone which in turn alters the diameter of the vessel lumen ultimately regulating blood pressure.

### 1.10.1 Contractile SMCs

The majority of SMCs making up the *tunica media* of a vessel wall exist primarily in a differentiated or contractile phenotype. Differentiated SMCs are characteristically quiescent and proliferate and migrate at an extremely slow rate. They also express a unique repertoire of contractile proteins, ion channels and signaling molecules which are required for contraction. Contractile SMCs adopt elongated spindle morphology. In this state the cell expresses an extensive range of contractile proteins which maintain the differentiated state. Some of the most commonly used to identify SMC phenotypes include; SM  $\alpha$ -actin, Smoothelin, Calponin and myosin heavy chain (MHC).

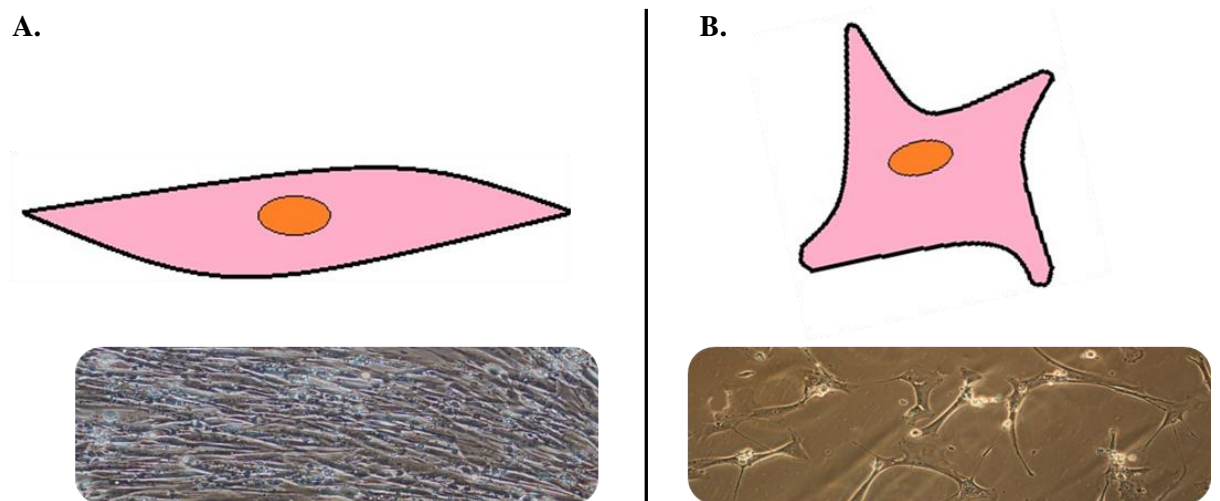


**Figure 1.12 A & B: SMC Phenotype Morphology** A shows diagram of a contractile SMC with slender spindle shaped morphology (top) and contractile HAoSMCs in culture (below). B shows diagram of a synthetic SMC with “cobble stone” shaped morphology (top) and synthetic, proliferating HAoSMCs in culture (below).

### Myosin Heavy Chain

Differentiated SMCs express cell specific isoforms of myosin such as myosin heavy chain (MHC). Myosin is an essential component of the contractile system that is present in all muscle and non-muscle cells. SMC specific variants of this protein termed, SM1 and SM2 are rigorous markers for SMC differentiation. Expression of SM1 and SM2 has never been detected in non SMCs *in vivo* and remains the only marker that is SMC specific during embryogenesis (J.M. Miano *et al.*, 1994).

### Alpha Actin

This is one of the 6 isoforms of actin found in mammalian cells (J. Vandekerckhove & K. Weber *et al.*, 1979). Mature, fully differentiated SMCs express four actin isoforms including smooth muscle  $\alpha$ -actin, non-muscle  $\beta$ -actin, non-muscle  $\gamma$ -actin and smooth muscle  $\gamma$ -actin (G.K. Owens & M. Schwartz *et al.*, 1986). The 42 kDa  $\alpha$ -actin is the most abundant, comprising up 70% of all SMC actin and over 40% of the total cell protein (V. Fatigati & R. A. Murphy *et al.*, 1984). This is essential for the cells high force generating capability. Originally thought to be solely expressed in SMCs, it is now known to be expressed in several other cell types. The protein is transiently expressed during development of cardiac and skeletal myocytes (J. Woodcock *et al.*, 1988). It can also be expressed by non-SMCs in culture such as endothelial and mesenchymal progenitor cells (R. M. Gordon *et al.*, 2007 & M. Cevallos *et al.*, 2006). Thus,  $\alpha$ -actin expression alone does not provide definitive evidence of smooth muscle cell lineage. However, its expression is highly specific in mature tissues and is the first known marker of differentiated SMCs that is expressed during vasculogenesis (J.E. Hungerford *et al.*, 1993; J.J. Mitchel *et al.*, 1990).

### Calponin

Calponin is a 28-34 kDa protein that interacts with F-actin and tropomyosin in a  $CA^{2+}$  independent manner. It also interacts with calmodulin in a  $CA^{2+}$  dependent manner. Furthermore, it has been shown to inhibit actin activated  $MG^{2+}$  ATPase activity of myosin *in vitro* (S.J. Winder *et al.* 1991). On this basis it is postulated to act as a SMC contractile regulator (G.K. Owens *et al.*, 1995).

## Smoothelin

Smoothelin is a cytoskeletal protein which is exclusively expressed in differentiated or contractile SMCs. Two isoforms have been detected termed smoothelin A and B. These are 59kDa and 100kDa respectively. Following vascular injury, Eys *et al.*, (2007) reported that smoothelin was the first smooth muscle marker to disappear. They also correlated smoothelin deficiency with considerable loss in contractile function suggesting it is an essential part of the contractile apparatus.

### 1.10.2 Synthetic SMCs

During vasculogenesis, however, SMCs are mostly synthetic where their principal function is proliferation, migration and production of matrix components of the vascular wall. The synthetic SMC state essentially boasts a contradictory phenotype to the contractile. They take on a more cobblestone appearance, which is referred to as epithelioid or rhomboid. Expression of the contractile proteins are significantly decreased and replaced with organelles involved in protein synthesis. They have increased growth rate and higher migratory activity. The contractile markers gradually decrease as SMC are cultured, and passage number increases (Fagar *et al.*, 1989). However expression of the different contractile markers, in SMCs undergoing modulation towards the synthetic phenotype, does not diminish uniformly and expression of some contractile proteins,  $\alpha$ -actin, calponin and SM22 $\alpha$  is still evident in fully synthetic SMCs. Expression of SM-MHC and smoothelins, however, is rapidly lost (S.M Rensen *et al.*, 2006). Unlike the contractile counterpart increase in synthetic proteins is difficult to characterise, quantify and qualify; instead a decrease in contractile markers is taken as an indicator of transition into a synthetic phenotype. Nevertheless expression of some proteins has shown to be increased in the synthetic state these include; Moesin, Osteopontin, Cellular Retinol Binding Protein 1 (CRBP1) and formation of Collagen I. Typically information on at least two contractile markers complemented with data on morphology, proliferation and migratory characteristics is sufficient for characterising a SMC population phenotype (S.M Rensen *et al.*, 2006). In addition, studies show that contractile SMC proteins are not the only indicators of SMC phenotype (S.S.M. Rensen *et al.*, 2007). Integrins such as  $\alpha$ 1 $\beta$ 1,  $\alpha$ 7 $\beta$ 1 and the dystrophin-glycoprotein complex (DGPC) have shown to be predominantly present on the surface of a contractile SMC, while ICAM-1 and VCAM-1 along with the  $\alpha$ 4 $\beta$ 1 integrin are found only on synthetic cells emphasizing the role of cell adhesion and cell membrane molecules in SMC differentiation.

It is important to note that SMCs should not be solely viewed as being in either one phenotypic state or the other, but rather at varying stages along a phenotypic spectrum. A fully contractile and synthetic SMC should be seen as representatives of the two ends of this phenotypic spectrum

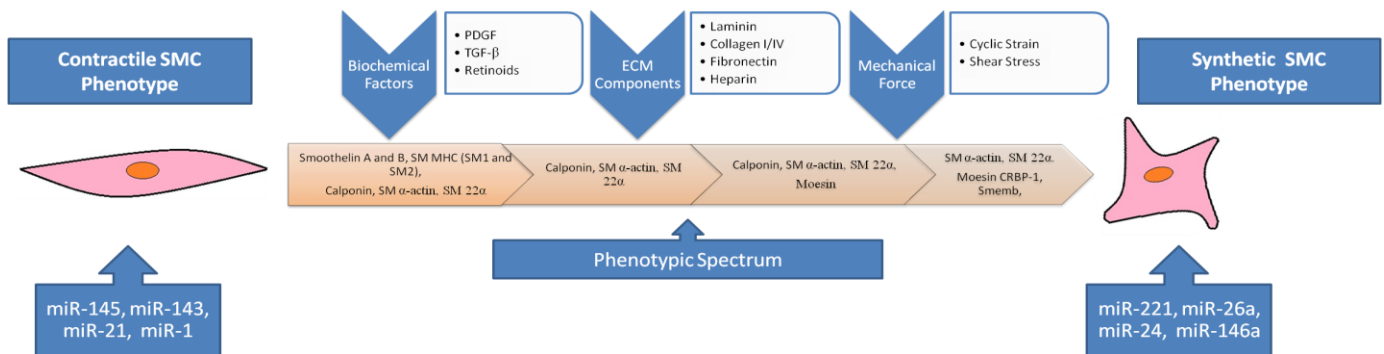


**Figure 1.13: Phenotypic Spectrum of VSMCs** Schematic highlights the phenotypic spectrum of VSMCs. Smooth muscle cells can reversibly modulate their phenotype to varying states across a spectrum flanked by a fully synthetic or fully contractile SMC. As the smooth muscle cell phenotype modulates towards either state change in expression of specific proteins is observed. In a fully contractile state (left) there is a high expression of contractile proteins such as; smoothelin A and B, smooth muscle Myosin Heavy Chain variants SM1 and SM2 (SM MHC SM1/SM2), Calponin, SM  $\alpha$ -actin and SM 22. A shift towards a synthetic state (right) is evident by loss of smoothelin A / B and SM 1/ SM2, along with reduced expression of Calponin, SM  $\alpha$ -actin and SM 22. SMCs which are further modulated towards a synthetic state will not show expression of calponin and have significantly diminished expression of SM  $\alpha$ -actin and SM 22 compared with more contractile counterparts. An increase in synthetic specific proteins may also be expressed such as moesin. Cells which are in a fully synthetic state will have higher expression of moesin, CRBP-1 and Smemb as well as significantly lower expressions of SM  $\alpha$ -actin and SM 22. Change in cell morphology is also observed between that of a slender elongated contractile cell to a cobblestoned synthetic phenotype. Along with a change in expression of specific proteins the miRNA profile within the cell is also altered in the different phenotype states. miR-145, miR-143, miR-21 and miR-1 are all up regulated in contractile SMCs whereas miR-221, miR-26a, miR-24 and miR-146a are up regulated in SMCs with a more synthetic phenotype. Factors which regulate SMC phenotype can be divided into three categories biochemical, ECM components and mechanical forces. Note this is not a conclusive list of SMC phenotype markers or factors which influence SMC phenotypic modulation rather a representation of the best characterised.

Studies have demonstrated that the population of SMCs which make up the *tunica media* of the vessel wall display considerable heterogeneous phenotypes. Even after *in vitro* culture of varying phenotype populations from the same artery, distinctions can still be made between the populations based on phenotype (M.G. Frid *et al.*, 1997; P. Bochaton *et al.*, 1996; H. Hao *et al.*, 2002 & Y.S. Ko *et al.*, 1999). A particularly illustrative example of these differences is evident in SMCs isolated from the thoracic artery (S. Li *et al.*, 2001). These phenotypic variations become even more attenuated following vascular injury (T. Christen *et al.*, 1999) and vessel remodeling. It is likely that a sub-population of synthetic migratory SMCs is required for vessel reorganization alongside a layer of contractile quiescent SMCs, which maintain vessel homeostasis.

S.S.M. Rensen *et al.*, (2007) postulated that although the full spectrum of phenotypic diversity is covered by the entire SMC population within a blood vessel, in a given population it may only be possible to cover a limited area of this spectrum. This indicates some populations of cells may not possess the epigenetic programming to move from a fully differentiated state to a fully contractile one or vice versa. Essentially, although each VSMC has the genetic make-up or DNA to cover the full phenotypic spectrum the cells environmental and hereditary influence such as, location in vessel e.g. thoracic or abdominal (in the case of SMCs from the aorta), surrounding cells, ECM composition haemodynamic force etc may be a limiting factor for full phenotypic modulation. Epigenetics is concerned with the post translational modification of genes. There are two main methods of epigenetic programming, DNA methylation and histone modification.

DNA methylation is a reversible modification of DNA in which a methyl group is added to a cytosine residue. The majority of methylation occurs at regions where a cytosine is directly followed by a guanine residue known as CpG sites. There are regions within the genome, termed CpG islands (CGIs), where there is an abundance of the C+G sequence. It is here that continued methylation of CpGs can result in specific gene silencing (Clifford *et al.*, 2012).

Histone modification, the nucleosome of chromatin is composed of an octamer of four core histones (H3, H4, H2A and H2B) around which 147 base pairs of DNA are wrapped. These core histones contain multiple residue sites which are susceptible to modification. At least eight types of post-translational histone modifications have been identified including acetylation, methylation, phosphorylation, ubiquitylation and



sumoylation. Histone acetylation and histone methylation are the best characterized, with the modifications being regulated by the enzymes; histone acetyltransferases (HATs), histone deacetylases (HDACs) and histone methyltransferases (HMTs), histone demethylases (HDMTs) respectively. These post translational modifications can influence gene silencing or gene expression within cells (Clifford *et al.*, 2012).

Although vast, transcription factors which regulate SMC phenotype are becoming more defined, the stimulants that can activate or inhibit these however continues to expand. Studies suggest a combination of both environmental cues and genetic hereditary are responsible for determining *in vivo* cell phenotype. As stated previously these represented by a diverse lineup of biochemical factors, ECM components and mechanical factors resulting from the pulsatile nature of blood flow.

## **1.11 Factors Influencing VSMC Phenotype**

### 1.11.1 Biochemical factors

Numerous elegant studies over the past few decades have identified and characterised an extensive repertoire of biocompounds that affect phenotypic modulation and expression of SMC phenotype markers. These include; PDGF, TGF- $\beta$ , activin A, retinoids, angiotensin II, TNF-  $\alpha$ , FGF-2, insulin growth factor (IGF)-I and -II, endothelin-I, Nitric Oxide (NO), Reactive Oxidase Species (ROS), peroxisome proliferator activated receptor-gamma (PPAR $\gamma$ ) ligands and complement 3 protein (Rensen *et al.*, 2007). These biocompounds have shown to be released during both pathophysiological growth states and through cell-cell interactions.

#### Release during pathophysiological growth states

Platelet-derived growth factor is a dimeric glycoprotein composed of two A (-AA) or two B (-BB) chains or a combination of the two (-AB). PDGF-A and -B were identified as important for initial stage SMC differentiation during vascular development in murine models. This was shown by recruitment of multipotent stem cells to endothelial tubes. Here in the presence of PDGF the cells differentiated towards a SMC lineage as shown by expression of SM  $\alpha$ -actin. In PDGF  $-/-$  embryos however there was no evidence of recruitment of multipotent stem cells to endothelial tubes and subsequent SMC differentiation (Hellstrom *et al.*, 1999, Schattmann *et al.*, 1996). Studies by Owens *et al.*, (1995) established that PDGF-BB caused a marked suppression of

contractile markers while inducing a synthetic proliferating phenotype in VSMCs *in vitro*. These results were also confirmed *in vivo* studies showing that inhibition of either PDGF A or B reduced SMC proliferation and migration following arterial injury in adults, reducing neointima formation (Kotani *et al.*, 2003). In contrast TGF- $\beta$  isoforms (TGF- $\beta$  1&2) were shown to induce a contractile phenotype by increasing  $\alpha$ -actin, SM-MHC and calponin in cultured VSMCs (Hao *et al.*, 2002; Hautmann *et al.*, 1997). Cultured neural crest cells were also shown to differentiate towards spindle-shaped SMCs when treated with TGF- $\beta$  (Shah *et al.*, 1996).

### Cell-Cell Interactions

As discussed earlier, the *tunica media* made up of SMCs is positioned just below the layer of endothelial cells making up the *tunica intima*. Cultured endothelial cells have been illustrated to secrete growth factors such as PDGF and FGF-2 (Collins *et al.*, 1987; Gajdusek *et al.*, 1982; Hannan *et al.*, 1988) as well as growth suppressors such as heparin and TGF $\beta$  (J.H. Campbell *et al.*, 1986; J.J. Castellot *et al.*, 1982). These can either stimulate or inhibit the growth of cultured SMCs. Conditioned media from confluent ECs placed on cultured SMCs was shown to either inhibit or delay the onset of SMC de-differentiation in culture (J.H. Campbell *et al.*, 1986). Heparin contained within the conditioned media was reported to be largely accountable for this response and it was further demonstrated to increase expression of  $\alpha$ -actin in cultured SMCs (A.L. Desmouliere *et al.*, 1991). In contrasting studies M.S. Schwartz *et al.*, (1987) and M.S. Vernon *et al.*, (1993) showed EC conditioned media stimulated growth of cultured rat SMCs along with almost complete suppression of  $\alpha$ -actin expression. These conflicting studies demonstrate that ECs can secrete biocompunds which can modulate SMC phenotype in either direction. Following secretion, these soluble growth factors can be trapped and stored within the ECM due to membrane bound glycoproteins. Changes in physiological conditions can trigger protease activities that cause a local release of these stored growth factors (Cheng *et al.*, 1997).

### 1.11.2 Extracellular Matrix Components

Research has shown that the ECM in which SMCs are seeded has as a profound impact on phenotype modulation. Most of the medial ECM is made up of collagen isoforms predominantly type I and III, elastin and proteoglycans such as heparin. Fibrillar collagen type I, IV and laminin have been shown to promote a contractile phenotype in VSMCs, however, monomeric collagen type I is known to activate SMC proliferation and induce a synthetic phenotype. Both of these forms of Collagen promote a different response by VSMCs to PDGF-B as well as altering gene pool expressions, highlighting the influential nature of the ECM in which VSMCs adhere (Raines *et al.*, 2000; Ichii *et al.*, 2001). Other ECMs which have shown to promote a synthetic phenotype include fibronectin and hyaluronan, a glycosaminoglycan (Hedin *et al.*, 1988; Evanko *et al.*, 1999).

Vascular SMCs cultured in a 3D matrix compared with the more common 2D have shown differential expression of contractile markers. This highlights the importance of ECM alignment as well as composition. Cells cultured in a 3D collagen matrix are less proliferative than those cultured in 2D and also express higher amounts of TGF- $\beta$ 1 (S. Li *et al.*, 2003). This would suggest the ECM could also be viewed as an intracellular reservoir of cytokines and growth factors, which bind to various cellular receptors and elicit specific signal transduction responses (S.S.M. Rensen *et al.*, 2007).

Orr *et al.*, (2010) demonstrated that SMCs plated on collagen IV expressed higher levels of contractile proteins compared with VSMCs coated on collagen I. In the same study collagen type IV stimulated binding of serum response factor (SRF) to CArG boxes in the promoter regions of  $\alpha$ -actin and smooth muscle myosin heavy chain (SM-MHC) as well as promoting the expression of the SRF coactivator, myocardin, all of which drive SMCs towards a contractile state. In contrast Orr *et al.*, (2010) found collagen I enhanced expression of the inflammatory protein, vascular cell adhesion molecule-1 (VCAM-1) again demonstrating the highly specific role of ECM ligands in modulating VSMC phenotype.

Another category of SMC phenotype stimulants are haemodynamic forces. Studies now show this mechanical parameter can hold an equal or greater command over VSMC fate as biochemical factors and extracellular matrix.

### 1.11.3 Haemodynamic Force

The mechanical or haemodynamic forces present in all blood vessels, as a direct result of blood flow, plays a pivotal role in vasculogenesis, vascular remodeling and SMC differentiation. Not only do haemodynamic forces aid in driving the physical changes seen in the developing embryo, they are also one of the major regulators of cell signaling, gene expression and cell function in adulthood (M. A. Schwartz *et al.*, 2009). Alteration in magnitude or any parameter of this force may have pathological consequences for vasculature homeostasis.

These forces are a permanent feature of the *in vivo* environment of all vascular cells. They can be categorized in to two forms, shear stress and cyclic strain. The former is as a result of the dragging frictional forces of blood flow and directly impacts on the endothelium. The magnitude of this force is directly proportional to the viscosity and velocity of the blood and is inversely proportional to luminal diameter. The latter, cyclic strain is a tensile force perpendicular to the lumen felt by both endothelial and smooth muscle cells (Lehoux *et al.*, 2006). This has a repeated temporary stretch effect on the vessel wall and is the stimulus used for work in this thesis.

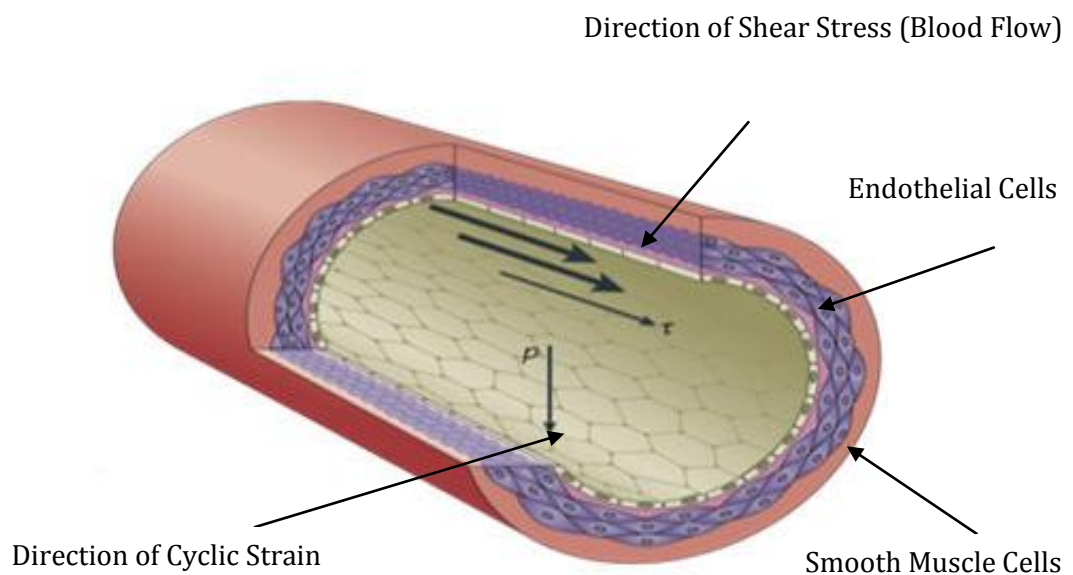


**Figure 1.14: Fluid Dynamics of Blood Flow** Illustration shows cross section of a blood vessel with cells most exposed to haemodynamics present (endothelial and smooth muscle). Direction of mechanical forces are also shown, Shear stress given as  $\tau$  and force by cyclic strain given as (P) pressure. Image taken from C. Hahn *et al.*, 2009.

## Shear Stress

The endothelium experiences friction shear stress as a result of blood flow across the endothelial layer. Unlike cyclic strain which affects both VSMCs and ECs, shear stress impacts predominantly on the endothelial cell layer. It is characterized as a longitudinal frictional force which runs parallel to the endothelium. Shear stress can be expressed in either units of force per unit of area Newton/meter squared ( $\text{N/m}^2$ ), Pascal (Pa) or Dynes/cm<sup>2</sup>.

$$1\text{N/m}^2 = 1\text{ Pa} = 10\text{ dynes/cm}^2$$

Under normal physiological conditions the shear stress in which the endothelium is exposed is in the range of 10-20 dynes/cm<sup>2</sup>. Laminar shear stress can be expressed as:

$$\tau = \frac{4\mu Q}{\pi r^3}$$

Where  $\tau$  =shear stress,  $\mu$  =blood viscosity, Q = blood flow rate and r = radius. Physiologically the flow rate is highest at the centre of the lumen and decrease closer to the vessel wall.

Laminar shear stress (LSS), found mostly in straight vessels, can be classified as an atheroprotective stimulus. This is characterized by reduced EC growth as evident through proliferation and DNA synthesis studies (Levesque *et al.*, 1990; Traub and Berk *et al.*, 1998). A reduction in apoptosis is evident by up regulation of nitric oxide (NO) production (Dimmeler *et al.*, 1997). Laminar shear stress also fortifies EC tight junctions, reducing the permeability of the endothelium (Colgan *et al.*, 2007).

Contrary to LSS is disturbed flow, this usually occurs in areas of bifurcations or branching points as well as arterial curvatures. At such sites, flow separation leads to transient vortex formations and even flow reversal, leading to a variety of different flow patterns such as oscillatory flow, low flow velocities and multi-frequency/multi directional secondary flows. Cells exposed to these areas of disturbed flow exhibit altered cell function such as proliferation, DNA synthesis and migration (Levesque *et al.*, 1990, Chiu *et al.*, 1998). Under these conditions, ECs lose their ability to maintain homeostasis and become dysfunctional, leading to the infiltration of lipids and leukocytes (monocytes and T-lymphocytes) into the sub-endothelial space. The resultant inflammatory response leads to formation of fatty streaks, the first stage in atherosclerotic plaque formation (Taniyam & Griendling *et al.*, 2003.)

## Cyclic Strain

Periodic contraction of the heart causes large pulsatile changes in blood pressure on the arterial side of the vascular network. Larger elastic arteries, particularly the aorta, expand at the peak of the systolic cardiac cycle and then gradually contract during the diastolic low pressure cycle which moves blood down into the muscular arteries. A healthy adult typically has a blood pressure of no lower than 90/60 mmHg and no higher than 120/80 mmHg. The first number represents the systolic pressure during contraction and the second is the residual diastolic pressure after the cardiac cycle, measured in millimeters of mercury (mmHg). A repeated stretch of 16% and relaxation back to 10% of cell length was demonstrated by J. O'Callaghan *et al.*, (2000) to represent a blood pressure of 120/80 mmHg.

Blood pressure causing cyclic stretching of vessel walls is determined by the lumen diameter in muscular arteries. VSMCs in these arteries and arterioles actively respond to acute changes in blood pressure through a mechanism known as the “myogenic tone” or “the Bayliss effect” (Hahn & Schwartz *et al.*, 2009). Stretch of the muscle membrane opens a mechano-sensitive activated ion channel. The cells then become depolarized resulting in a  $\text{Ca}^{2+}$  signal and trigger muscle contraction. This phenomenon was discovered by Sir William Bayliss in 1902. This contraction narrows the lumen of smaller arteries to keep blood flow constant and prevent damage to downstream capillaries. If the pressure remains elevated over long periods of time the vasculature undergoes remodeling, resulting in a thickened arterial wall to resist the higher blood pressure (Geng & Libby *et al.*, 2002; Hahn & Schwartz *et al.*, 2009).

According to the Law of Laplace the magnitude of cyclic strain is determined by the change of blood pressure. The tension (T) of the wall is proportional to the difference in pressure (P) across the vessel times the radius (r) of the vessel and is inversely proportional to the thickness (h) of the wall (Laplace *et al.*, 1899; H. Lamb *et al.*, 1928).

$$T = \frac{Pr}{h}$$

Thus a higher pressure difference and a larger radius results in high wall tension requiring the vessel to have a thickened wall to become mechanically stable.

This mechanical cyclic strain regulates a myriad of vascular cell biological processes including proliferation, apoptosis and migration along with the synthesis, degradation and reorganization of the ECM (J.H. Haga *et al.*, 2006).

Over chronic periods of high blood pressure, vessel remodeling will eventually compromise the elasticity of the artery resulting in an inability to regulate blood flow during acute phases of altered blood pressure (Folkow *et al.*, 1993). This vascular dysfunction can lead to disease such as atherosclerosis in which the higher pathological strain results in proliferation and migration of VSMCs through the now permeable endothelium into the lumen. This becomes the basis of stable plaque initiation and formation.

Due to the staggering complexity of the *in vivo* environment, the majority of studies of cellular responses to biomechanical stimulus have relied on *in vitro* systems. Pioneering work from Glucksmann *et al.*, (1939) using hanging drop cultures to study tensile pressure has evolved to present day vacuum deformation of flexible membrane substrates over fixed loading posts (T.D. Brown *et al.*, 2000). Modern apparatus make it possible to simulate a range of strain parameters including steady equibiaxial strain, cyclic equibiaxial strain, cyclic uniaxial strain, amplitude or magnitude of the strain and also frequency and duration of the cyclic strain (Lee *et al.*, 1996; Sotoudeh *et al.*, 1998; Kaunas *et al.*, 2005; Wang *et al.*, 2000 & 2001). These stimuli can be used as models for pressure-induced cardiac hypertrophy and vascular hypertension (A. Katsumi & W. Orr *et al.*, 2004). Studies have shown that a range of vascular cells including fibroblasts, SMCs and cardiac myocytes re-locate and orientate in response to cyclic strain. However, direction of alignment can be either parallel or perpendicular, depending on cell type and nature of the strain (S. Lehoux *et al.*, 2003 J. Sadoshima *et al.*, 1997). Recent studies using *in vitro* models have elucidated the importance of strain parameters, showing that variance in frequency, amplitude, direction and duration can elicit different molecular and cellular responses. This includes regulation of the expression or activation of numerous second messenger molecules such as PI3K/Akt, PKC, NFκB, Rho family of GTPases and MAPKs (J.H. Haga *et al.*, 2007).

Although this thesis focuses on HAoSMCs it should be noted that cyclic strain also impacts on ECs and many other vascular cells, activating and regulating similar pathways within them.

## 1.12 Mechano Sensors of VSMCs

Mechanotransduction is the process by which cells convert the mechanical forces discussed earlier into biochemical signals. These signals are necessary to maintain homeostasis within the vessel. (A. Katsumi & W. Orr *et al.*, 2004; P.A. Jammey *et al.*, 2004; H. Huang *et al.*, 2004; K.S. Ko *et al.*, 2001). This section will focus primarily on membrane bound mechano-sensors of VSMCs, which respond to haemodynamic force, in particular cyclic strain (J. H. Haga *et al.*, 2006). It should be noted there are many similarities between these and the EC mechano-sensors of shear stress. Several membrane proteins have been found to be mechano-sensitive to strain including integrins, receptor tyrosine kinases (RTKs), ion channels, cadherins, cell adhesion molecules, syndecans and  $\alpha$ -dystroglycan.

### 1.12.1 Integrins

Integrins are one of the major families of cell adhesion receptors (Hynes *et al.*, 2000). Integrin mediated cell adhesions are intrinsically mechano-sensitive as they are the main receptor that connect the cell cytoskeleton to the extracellular matrix (ECM) (A. Katsumi & W. Orr *et al.*, 2004). The interaction of VSMC integrins with the ECM plays a significant role in the initiation of mechanotransduction by strain (Wang *et al.*, 1993; Wilson *et al.*, 1995). Integrins are non-covalently linked heterodimeric molecules and are made up of either an alpha ( $\alpha$ ) or beta ( $\beta$ ) glycoprotein sub unit; to date there have been 18 alpha and 8 beta subunits identified. This allows for a total of 24 different  $\alpha$ - $\beta$  integrin compositions, based on various combinations and permutations of both  $\alpha$  and  $\beta$  subunits. They are a type I transmembrane molecule consisting of a short intracellular and larger extra cellular domain (Wang *et al.*, 2004; Arnaout *et al.*, 2005).

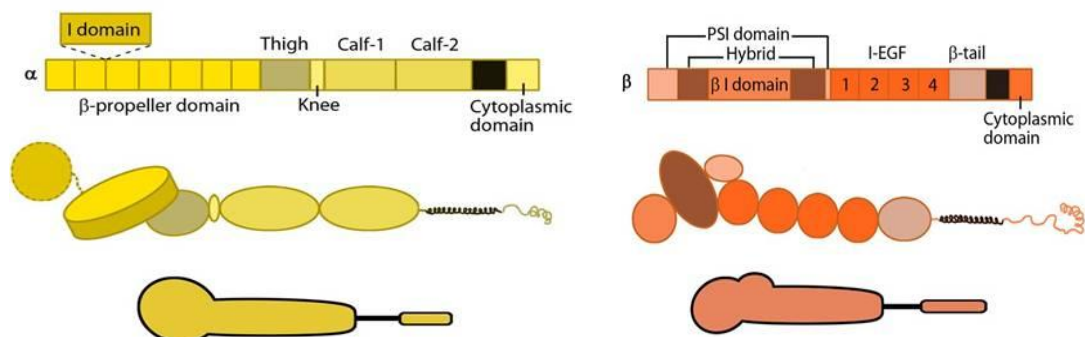


**Figure 1.15: Illustration of  $\alpha$  sub unit (left) and  $\beta$  subunit (right).** Integrins are cell membrane bound glycoproteins made of a  $\alpha$  (left) and  $\beta$  (right) sub unit. (<http://www.mechanobio.info/Home/glossary-of-terms/proteins/integrin>)



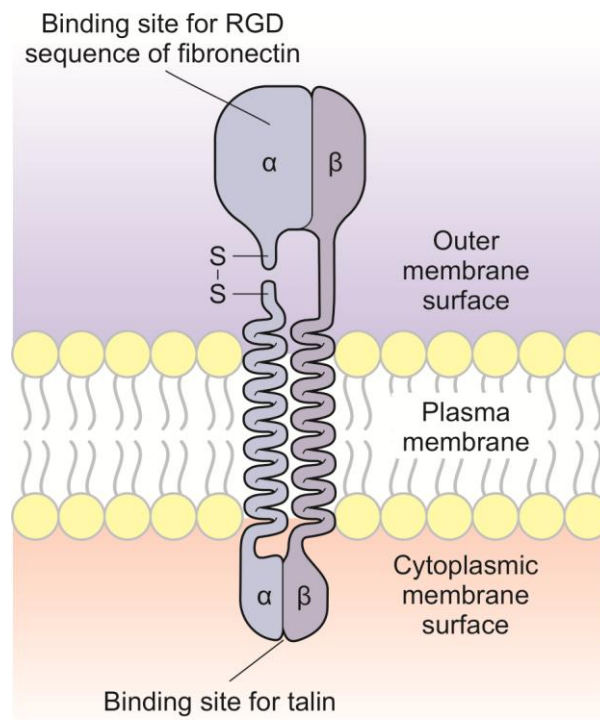


**Figure 1.16: Illustration of Integrin Heterodimer Structure.** Shows integrin as found on cell surface with two non-covalently linked  $\alpha$  and  $\beta$  sub units. Extracellular surface domain shows binding site for ligands such as the RGD motif found in many ECM proteins. Intracellular domain shows binding site for recruitment of effector proteins such as talin. When an integrin becomes activated, these effector proteins bind to initiate a signaling cascade within the cell. Image taken from “Becker’s World of the Cell” Hardin, Bertoni & Kleinsmith *et al.*, 2012

Integrins are capable of both “inside-out” and “outside-in” signaling. For example, tractional forces generated in the cytoskeleton during migration are transmitted across the plasma membrane to the ECM to allow re-organisation. Simultaneously, the external cyclic strain stimulus due to pulsatile blood flow applied to cells is transmitted intracellularly via integrins, resulting in biochemical signals and activation of signaling pathways (A. Katsumi & W. Orr *et al.*, 2004; S. Huang *et al.*, 1999; M. A. Schwartz *et al.*, 2001). Although not fully elucidated, integrins are the best studied transducer of mechanical force into a cellular response by cells.

On the cytoplasmic face of the plasma membrane, integrins organise and coordinate the assembly of cytoskeletal polymers and signaling complexes. On the extracellular side, integrins bind with high affinity to either ECM ligands or counter receptors on adjacent cell surfaces (J.D. Humphries *et al.*, 2006). A characteristic feature of most integrin receptors is their ability to bind a wide variety of ligands from both the ECM and other cell surface receptors (Plow *et al.*, 2001; Van der Flier & Sonnenberg *et al.*, 2001). Despite their wide variety and diversification, it is possible to class integrin/ligand combinations into four main classes; LDV binding integrins which bind to an acidic LDV motif that is functionally similar to RGD,  $\alpha$  domain  $\beta$ 1 integrins which bind to laminin and collagen, Non  $\alpha$  A domain containing laminin binding integrins which are laminin selective and finally RGD Binding integrins.

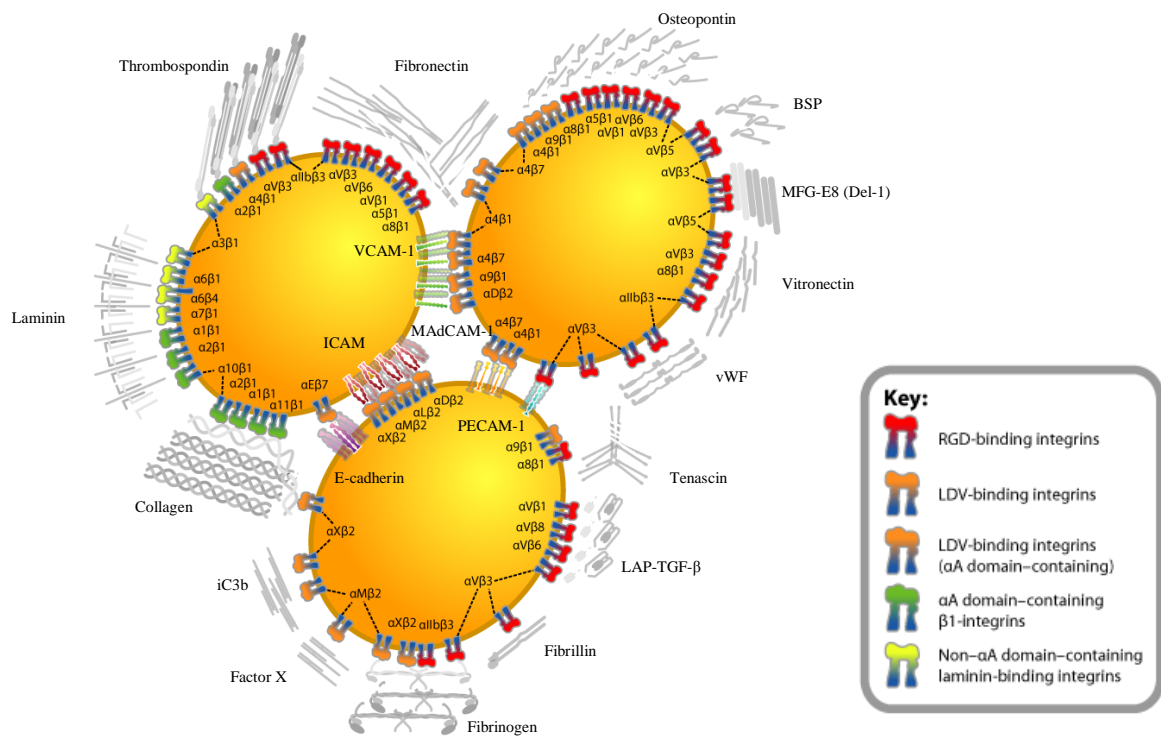


**Figure 1.17: Schematic of the four main classes of ligand binding integrins.** Schematic of the four main classes of integrin/ligand combinations found on the cell membrane. The RGD and LDV binding integrins interact with the largest number of ligands. Ligands for the RGD binding integrins include; Thrombospondin, Fibronectin, Osteopontin, BSP, MFG-ES (Del-1), Vitronectin, vWF, Tenascin, LAP-TGF- $\beta$ , Fibrillin, Fibrinogen and PECAM-1. LDV binding integrins find ligands with MadCAM-1, VCAM-1, Fibronectin, Tenascin, Fibrinogen, Factor X, iC3b, Collagen, ICAM, Thrombospondin, E-Cadherin and Osteopontin. The  $\alpha$  A domain containing  $\beta$ 1 and non  $\alpha$  A domain containing laminin binding integrins interact with far fewer ligands. These include Collagen, Laminin, Thrombospondin and Laminin, Thrombospondin respectively (J.D. Humphries *et al.*, 2006).

### 1.12.1.2 RGD Binding Integrins

The arginine-glycine-aspartic acid (RGD) sequence was discovered as a cell attachment site in fibronectin over 20 years ago. Unexpected at the time, this 3 amino acid sequence motif proved to be a fundamental recognition site for cells and proteins (Pierschbacher & Ruoslahti *et al.*, 1984; Ruoslahti *et al.*, 2003). Since then, RGD-recognition sites were reported in a host of other ECM proteins (Grant *et al.*, 1989; Lawler *et al.*, 1988; Miyachi *et al.*, 1991; Pytela *et al.*, 1988).

All five  $\alpha$ V integrins, two  $\beta$ 1 integrins ( $\alpha$ 5,  $\alpha$ 8) and  $\alpha$ IIb $\beta$ 3 are capable of binding ligands containing the RGD sequence motif. The RGD motif binds at an interface between the  $\alpha$  and  $\beta$  subunits, the R residue fitting into a cleft in a  $\beta$ -propeller module in the  $\alpha$  subunit and the D coordinating a cation bond in a von Willerbrand factor A domain in the  $\beta$  subunit.

The RGD binding integrins can bind a vast array of ligands however; there exists a rank order of affinity depending on the complementarity of the fit. Blocking integrins by using specific antibodies or synthetic RGD peptides can significantly affect strain induced integrin activation, negating any strain induced effects on cell function (Wernig *et al.*, 2003; Wilson *et al.*, 1995).

Initial interactions between integrins and their ligands occur irrespective of mechanical stimulus. Following initial ligation, integrins attach to the actin cytoskeleton, inducing a 2-pN(pico Newton) talin dependent increase in adhesion strength. These early adhesions initiate signals that include activation of Rac and Cdc42, which in turn induce formation of lamellipodia and filopodia which drives the progression of early focal contacts (FC) (A. Katsumi & W. Orr *et al.*, 2004; C. Galbraith *et al.*, 2002; J. Giang *et al.*, 2003; M. A. Schwartz *et al.*, 2000). Progression of early focal contacts is marked by recruitment of paxillin, various phospho-proteins and vinculin (C. Galbraith *et al.*, 2002).

When integrins are activated by a stimulus such as strain they undergo a conformational change which results in a higher affinity for their ligand. This can have a direct impact on SMC function such as adhesion and migration (E. P. Moiseeva *et al.*, 2001). Activation of the integrin families is also mediated by contact with specific ECM components such as fibronectin and collagen which lead to the formation of focal adhesion structures. These focal adhesions contain anchorage points for the cell where the cytoplasmic tail of the integrin is physically tethered to the actin microfilaments of the cytoskeleton. They also contain signaling molecules, which become activated in an

adhesion dependent manner (K. Burridge *et al.*, 1996). Recruitment of the protein Focal Adhesion tyrosine kinase, FAK, to the integrin rich sites appears to be central to focal adhesion formation. Vascular injury is known to deactivate integrins to allow cell motility and facilitate in repair (N Koyama *et al.*, 1996; J. Seki *et al.*, 1996).

#### 1.12.2 Dystrophin-Glycoprotein Complex

The dystrophin-glycoprotein complex (DGPC) is expressed in all types of muscle and is critical for correct muscle function as it serves as a structural tether between the cell and the ECM (E. P. Moiseeva *et al.*, 2001). The dystrophin gene is one of the longest human genes known covering over 2.2 mega base pairs (C.N. Tennyson *et al.*, 1995). Disruptions in this gene can lead to forms of muscle dystrophy and cardiomyopathy (J.A. Towbin *et al.*, 1998; R. Baressi *et al.*, 2000). Its function is to provide mechanical stability to the cell membrane during contraction and also to prevent over stretching (B.J. Petrof *et al.*, 1993). The DPGC serves as a link between the basement membrane around muscle cells and the actin filaments. The glycoprotein,  $\alpha$ -dystroglycan, serves as the cell surface receptor for DGPC on SMCs. It connects other components of the DPGC with the ECM laminin and perlecan (E. P. Moiseeva *et al.*, 2001).

### 1.12.3 Syndecans

Studies now suggest that syndecans, members of the proteoglycan family of adhesion transmembrane receptors, may also be involved in cell signaling (A.C. Rapraeger *et al.*, 1998 & 2000). There are four known mammalian syndecans. These adhesion molecules bind to an array of ligands including ECM proteins, cell adhesion molecules, growth factors, lipoproteins, lipases and components of the blood coagulation cascade (E. P. Moiseeva *et al.*, 2001). They interact with their ligands via polysaccharide chains which are covalently bonded to the extracellular domain of the receptor. These receptors facilitate cell-cell and cell-ECM based adhesion and migration. They also bind to PDZ (PSD-95, DlgA, and ZO1) containing proteins, linking syndecans to the cytoskeleton, thus they are potential mechano- sensors. They provide additional binding sites for ECM ligands which strengthens cell adhesion. Although more research is required around the area of Syndecans in VSMC, all four are present on the cell membrane and undoubtedly play apart in mechanotransduction.

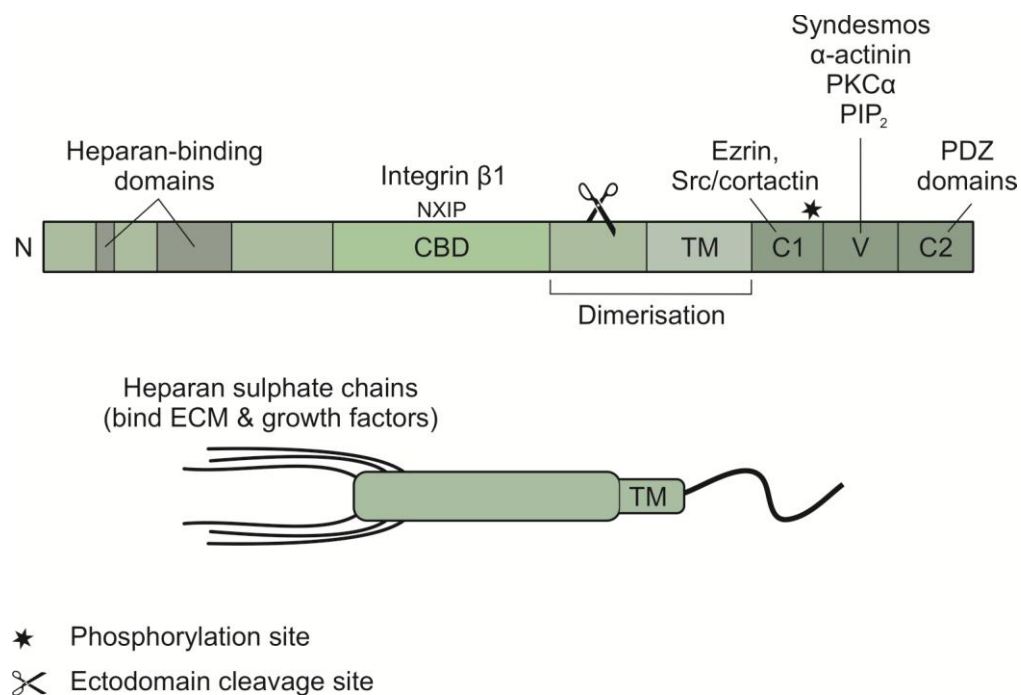


**Figure 1.18: Schematic of Syndecan Structure.** Structural domains of transmembrane syndecan are highlighted in this figure as well as polysaccharide strands which bind to syndecan ligands. The core protein domains are similar in all 4 members except for the length. The ectodomain contains heparan sulphate (HS) binding domains and regions that directly or indirectly interact with integrins. The transmembrane spanning region is responsible for oligomerization along with residues in the ectodomain and is enhanced by C2 interactions. The cytoplasmic domain C1 mainly binds with proteins that link to the actin cytoskeleton. The V domain interacts with signaling proteins such as PKC $\alpha$  (Multahupt *et al.*, 2009).

#### 1.12.4 Cell Adhesion Molecules (CAM)

CAMs belong to the immunoglobulin family of cell-cell adhesion receptors. So far the adhesion molecules VCAM-1 (Vascular Adhesion Molecule-1) and ICAM-1 (Intracellular Adhesion Molecule-1) have been detected in VSMCs. ICAM-1 is known to interact with cytoskeletal proteins  $\alpha$ -actinin and ezrin (O. Carpen *et al.*, 1992). It binds to fibrinogen allowing interaction between cell and ECM, thus facilitating mechanotransduction (L.R Languino *et al.*, 1993). VCAM-1 is a counter receptor for  $\alpha 4\beta 1$ ,  $\alpha 9\beta 1$ ,  $\alpha 4\beta 7$  and  $\alpha D\beta 2$  integrins present on monocytes and lymphocytes highlighting and emphasizing its role in inflammatory response (I. Stuiver *et al.*, 1995). Both of these adhesion molecules are only present in synthetic SMCs, especially following vascular injury.

#### 1.12.5 Cadherins

With the exception of T-cadherin (Cadherin 13), all other cadherin's belong to a family of transmembrane  $Ca^{2+}$  dependent homophilic cell-cell adhesion receptors. T-Cadherin is anchored to the cell membrane via glycosylphosphatidylinositol (GPI), lacking an intracellular domain. Cadherin homodimers form a "zipper" structure at the intercellular contact zone on the cell surface (B.M. Gumbiner *et al.*, 1996). These receptors bind to the cytoplasmic plaque proteins catenins which provide a link with vinculin and the actin cytoskeleton. However, as contractile SMCs in the normal vasculature are predominantly linked to the ECM, adhesion via cadherins is mostly evident during vascular remodeling or following vascular injury where the basement membrane is degraded exposing ECs (E. P. Moiseeva *et al.*, 2001).

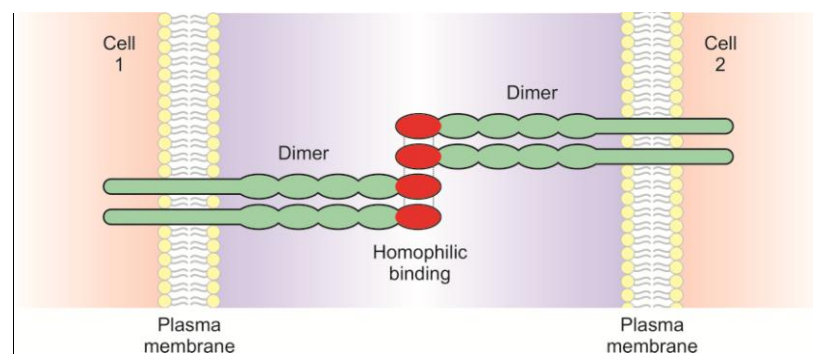


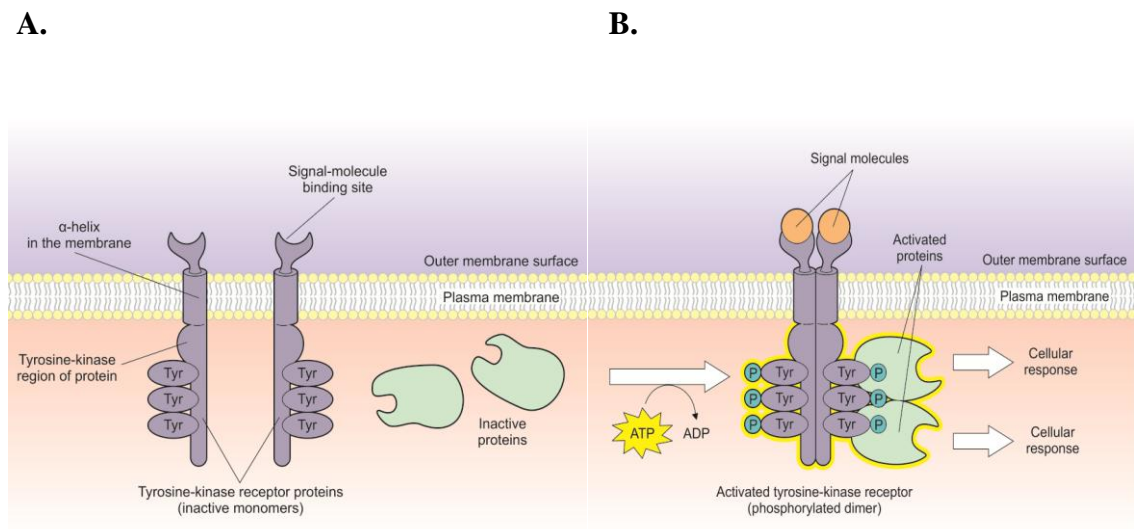
**Figure 1.19: Schematic of Cadherin** Each cadherin has a small cytoplasmic component, a transmembrane component, and the remaining bulk of the protein is extra-cellular. This mediates the cell-cell binding of calcium dependent cadherins. Image taken from “Becker’s World of the Cell” Hardin, Bertoni & Kleinsmith *et al.*, (2012)

### 1.12.6 Receptor Tyrosine Kinases

Receptor Tyrosine Kinases are membrane bound cell surface receptors. They have a high affinity for many polypeptide growth factors, cytokines and hormones. RTKs are typically monomeric subunits but many exist in multimeric complexes (J. Sadoshima *et al.*, 1993). Each RTK has a single hydrophobic transmembrane spanning domain composed of 25-38 amino-acids, an extracellular N-terminal region and an intracellular C-terminal region.

The principal functions of the tyrosine kinase family include cell-cell signalling, adhesion and motility. In order to elicit a response, the monomeric subunits must bind to a ligand which causes a conformation change in the receptors. The monomeric subunits join to form an unphosphorylated dimer. At this point the tyrosine kinases are activated and each subsequently recruits a phosphate group from an ATP molecule, giving rise to an ADP molecule. A fully active, phosphorylated tyrosine kinase is now formed which can elicit multiple cell signalling cascades by recruitment of a relay protein to the now phosphorylated tyrosine docking site. Such proteins include Src and Shc which can activate the intracellular transduction pathways like phosphatidylinositol 3-kinase (PI3K)/Akt, mitogen activated protein kinase (MAP) kinase and Protein kinase C (PKC) (D.R. Robinson *et al.*, 2000; Blume Jesnsen & Hunter *et al.*, 2000; Cantley & Cantley 1995).

Cyclic straining of VSMCs was shown to induce a rapid phosphorylation of PDGF receptor  $\alpha$  (PDGFR $\alpha$ ) in a magnitude dependant manner (Hu *et al.*, 1998). Strain also induces the phosphorylation of EGF receptor (EGFR) and it recruitment of relay protein Shc and Grb2, which in turn lead to ERK activation (Iwasaki *et al.*, 2000). These results highlight the role RTKs play in mechanotransduction.



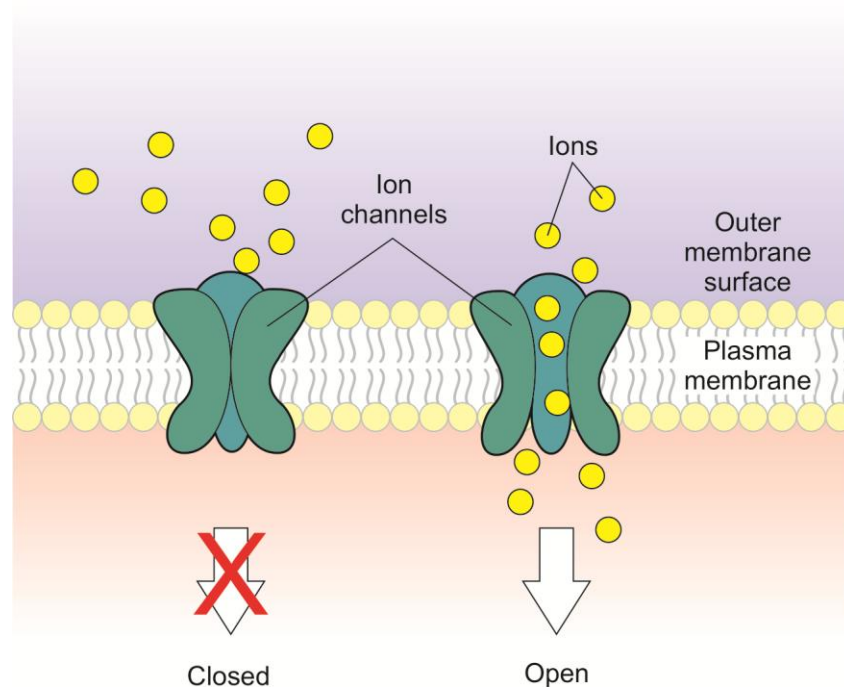
**Figure 1.20 A&B: Inactive and activated states of Receptor Tyrosine Kinases.** (A) inactive monomeric subunits of RTKs. Tyrosine sites are un-phosphorylated and sub units are not linked. (B) activated form of RTKs from binding a signal molecule ligand. Monomeric subunits have relocated together and phosphorylation of tyrosine binding sites from the molecule ATP occurs. This ultimately elicits a cellular response.

Image taken from “Becker’s World of the Cell” Hardin, Bertoni & Kleinsmith *et al.*, (2012)



### 1.12.7 Ion Channels

Ion channels have also been identified as sensors of mechanical stimulus. They create an open channel in response to stretching of the plasma membrane. They are cell surface membrane complexes that enable transport of ions across biological membranes and in doing so establish and control voltage gradients. The passage of large fluxes of cations non-specifically allows the cell to accommodate swelling as a result of being stretched. Due to their diversity of functions, numerous ion channels are involved in cardiac, skeletal, and smooth muscle contraction along with epithelial nutrient and ion transport (Hahn and Schwartz, 2009; Lehoux and Tedgui, 2003; Martinac, 2004). Straining of VSMCs activates a non-selective cation channel that is permeable to  $K^+$ ,  $Na^+$  and  $Ca^{2+}$  (Davis *et al* 1992). More recent experiments have shown that the strain induced increase of cytosolic  $Ca^{2+}$  concentration in SMCs results from the release of intracellular  $Ca^{2+}$  stores via a stretch activated  $Ca^{2+}$  channel (Mohanty & Li *et al.*, 2002).



**Figure 1.21: Transport of Ions through cell membrane** Ion channels control voltage gradients across cells by allowing the influx of ions through the cell membrane. They maintain a resting membrane potential and have shown to open upon stretch or cyclic strain. Image taken from “Becker’s World of the Cell” Hardin, Bertoni & Kleinsmith *et al.*, (2012)

From the literature, it is clear that the manners in which cells, particularly smooth muscle cells, adhere to and sense their substratum is a complex process which involves an orchestra of cell signaling and cell adhesion molecules. To maintain homeostasis cells also need to be able to functionally respond to external stimuli, this often requires motility of the cell. This is facilitated by an array of traction proteins which interact with a scaffolding type structure within the cell deemed the cytoskeleton.

### **1.13 The Cytoskeleton and Cell Migration**

A cell can change from a stationary to a mobile phase depending on signals received by the microenvironment in which it lies. These signals which evoke cell motility include ECM molecules, growth factors or chemokines and haemodynamic force (B. Wehrle-Haller *et al.*, 2003). Actual traction of the cell is achieved by the cytoskeleton.

#### 1.13.1 The Cytoskeleton

The cytoskeleton is made up of three types of protein filaments, large microtubules, medium sized intermediate filaments and thin microfilaments. The cell relies on the cytoskeleton for an array of functions including structural scaffolding, signalling, motility and cell division. All three proteins structures are interconnected and cross-linked with actin binding proteins such as lasp-1 and palladin (Lee and Gotlieb *et al.*, 2003).

Microfilaments or actin filaments, with a diameter of approximately 7nm, are flexible and easily cross-linked into bundles that absorb external forces acting on the cell along with the internally exerted contractile myosin based forces (Higgs and Pollard *et al.*, 2001). Microtubules are the largest of the three systems with a diameter of approximately 25nm. They act as rigid, hallow reinforcing rods that sustain both compression and tension and made up of readily available tubulin. It is the ability of microfilaments along with microtubules to resist deformation and to transmit forces that allow the cytoskeleton to determine cell shape and ultimately the structure of both tissues and organisms.

Intermediate filaments have a diameter between that of actin filaments and microtubules of approximately 10 nm (Desai and Mitchison *et al.*, 1997). The main function of intermediate filaments is to prevent excessive stretching of cells by external forces. If intermediate filaments are defective, tissues become mechanically fragile. They also fixate the cell nucleus within the cytoplasm.

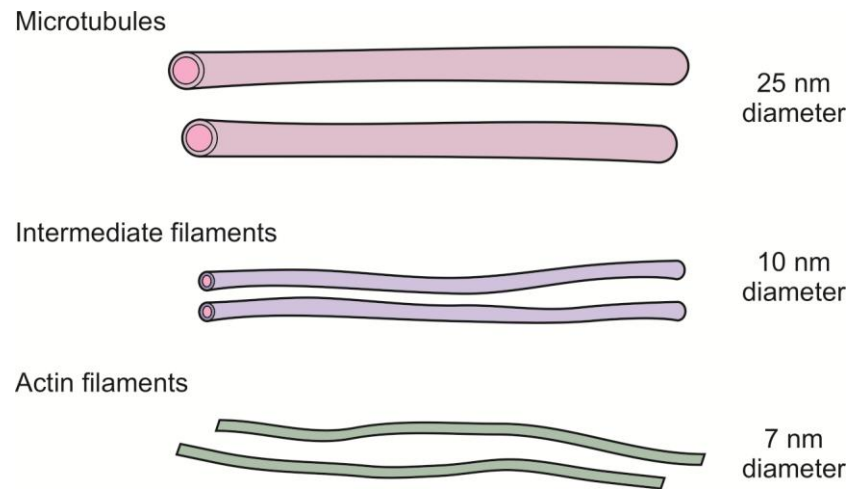


**Figure 1.22: Classes of Cytoskeleton protein fibers.** Diagram demonstrates the relative scale of each protein filament.

Image adapted from (<http://library.thinkquest.org/C004535/cytoskeleton.html>)

To add perspective, if microtubules were enlarged one million fold to a diameter of 25mm, they would have mechanical properties similar to a steel pipe: quite stiff locally but flexible over distances. On the same scale, actin filaments would be similar to 8-mm steel wires and intermediate filaments would be likened to braided steel cables (Goldman *et al.*, 1999).

### 1.13.2 Cell Adhesion and Migration

Cell migration is a complex and highly orchestrated process between a cell and the substratum on which it is attached and over which it migrates. Cell migration can range from single cell movement to collective cell migration, where intercellular interactions are retained and groups of cells move coordinately Friedl and Wolf *et al.*, 2010. Cell surface adhesion molecules are central to the migratory process as they bind interactions with the substratum to the interior cell cytoskeleton. There are several families of adhesive receptors on the cell surface as discussed earlier however the most characterised and paramount to cell motility is the integrin family of receptors. The dynamic polarized ability of integrin adhesions to form and turn over is essential to facilitate cell migration and directional persistence Huttenlocher and Horwitz *et al.*, 2011.

Integrins attach to the actin cytoskeleton, inducing a 2 pico Newton (2pN) talin dependent increase in cell adhesion strength (A. Katsumi & W. Orr *et al.*, 2004). These early adhesions initiate signals from the *rho* subfamily of small GTP-binding proteins. These are a sub family of the Ras super family of GTP-binding proteins. Members of the *rho* family include rho, rac and cdc42.

It is the activation of cdc42 and Rac, following these early integrin adhesions, that induces formation of protruding cellular structures that form the leading edge of the cell. These include filopodia and lamellipodia (J.V. Small *et al.*, 2002). The directional protrusion of these structures, composed of numerous actin filaments, marks the initiation of cell locomotion. Their protrusion and movement are as a result of actin polymerization. Orientation of actin filaments during polymerisation can be detected by the cleaved myosin heads which bind laterally to the F-actin filament giving a “barbed” impression at one end, and an arrow or pointed appearance at the other.

Monomeric G-actin polymerises F-actin at their “barbed end”. G-actin is then liberated from the pointed end by de-polymerisation via an actin depolymerising factor (ADF) (C. Pantaloni *et al.*, 2001). This process is referred to as treadmilling and, in a lamellipodium it operates towards the interior of the cell where actin molecules are added at the periphery and then released towards the cell centre. In general, the orientation of treadmilling indicates the polarity of each actin filament (B. Wehrle-Haller *et al.*, 2003).

In order to transform the treadmilling action into cell movement the actin filaments must also be anchored at their pointed end to sites called focal complexes at which point the cell can pull or push itself forward (K. Rottner *et al.*, 1999, B. Geiger *et al.*, 2001). The transition from early adhesions (focal contacts) to focal complexes is marked by the recruitment of paxillin, phosphor-proteins and vinculin (C. Galbraith *et al.*, 2002). Expression of vinculin in cell adhesions is proportional to the level of tractional force by the cell. This adhesion must be sufficient enough to allow the cell generate traction and the force required for migration.

Focal Complexes are a precursor to focal adhesions. These are longer, elongated structures which form in response to Rho activation. They require an increase in cellular contractility mediated by the Rho effector, Rho kinase; this in turn induces increased phosphorylation of the myosin light chain. This increased force at adhesion sites results in an increase in the density of activated integrins (avidity regulation), the recruitment of adhesion structural proteins and the elongation of the adhesion site. (Katsumi & W. Orr *et al.*, 2004). When focal complexes mature into focal adhesions at the leading edge of the cell, they become stationary relative to the ECM. This provides an anchor from which the cell can pull itself over the ECM.

Parallel to the extension of a lamellipodium and formation of stable adhesions for traction, migration also requires mechanisms that regulate the release of adhesions especially at the cell rear to allow detachment and facilitate movement of the cell in the direction of migration. These adhesions are inherently weaker. There appears to be two fates offered to integrins tracking at the rear of the cell. A substantial population of them will remain associated with the substratum. Cytoskeleton associated adhesive proteins such as vincullin are not present in these suggesting a severing of integrin cytoskeleton linkages. The other fate, the integrin is disassembled and carried forward to the front of the advancing cell to participate in newly formed focal adhesions Huttenlocher *et al.*, 1995.

As the cell progresses along its chosen path, a given focal adhesion moves closer and closer to the trailing edge of the cell. Once at the trailing edge, the focal adhesion must be dissolved to facilitate continued cell migration. All rear assemblies retract and slide towards the protruding lamellipodia and filopodia where new adhesions are formed. As the process is repeated it has the effect of pulling the cell forward, similar to the way tank tracks work.

Cells which are typically slow to migrate such as fibroblasts and contractile SMCs exhibit actin filaments which are bundled into stress fibers. These are anchored within focal contacts located at the cell periphery. These stress fibers are often found orientated along lines of tension, strapping the cell to the substrate. In comparison to the actin filaments in lamellipodia of migrating cells, actin stress fibers have a reversed orientation in that they are anchored to focal contacts by their barbed ends and not the pointed end. This also means the monomeric G actin is incorporated at the opposite end of the filament.

In order to switch from a stationary stress fibre rich state, to a migratory, lamellipodia rich state, the actin cytoskeleton must reorganise by recruiting G-actin. The monomeric protein can be recruited by depolymerisation of F-actin, however, the actin pool within in a cell is limited and migration is most likely constrained by the G actin: F actin ratio.

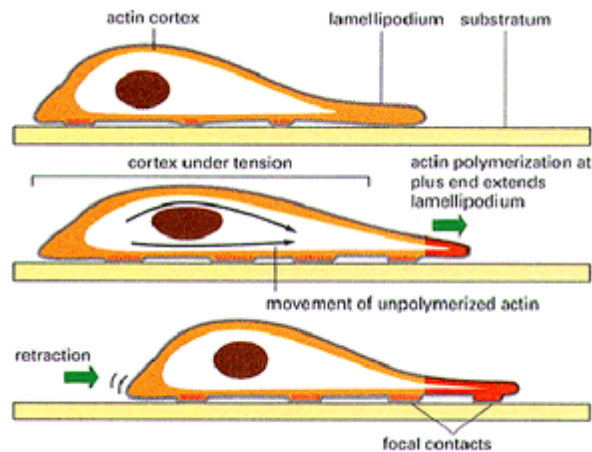


**Figure 1.23: Dynamics of cell migration.** As actin polymerises it extends lamellipodium in the direction of migration. Along with this integrins bind to the polymerised actin and form focal contacts which work as a molecular clutch. These provide an anchorage point from which the cell can gain traction and pull itself forward. Simultaneously to this adhesion points at the rear of the cell disengage and retract to allow cell motility. Image taken from ([http://www.cytochemistry.net/Cell-biology/actin\\_filaments.htm](http://www.cytochemistry.net/Cell-biology/actin_filaments.htm))

In 2D culture systems rate of cell migration is maximum at intermediate levels of cell-substratum adhesion where both adhesion formation and release are efficient DiMilla *et al.*, 1993. Too low an adhesive strength and the cell can not generate the sufficient traction for migration in contrast at higher adhesive strength the rear assembly of the cell is not released inhibiting movement. In 3D *in vivo* other factors such as the release of matrix metalloproteinases (MMPs) facilitate migration by breaking down the ECM barrier. The concentration of substrate and ligand receptors on the cell surface also dictates the magnitude of adhesion. In environments of low ligand concentration smooth muscle cells and do not migrate on fibronectin. Whereas a high fibronectin environment causes cell spreading, focal adhesion formation and inhibition of cell movement Huttenlocher *et al.*, 1995. Indicating that balanced concentrations of ligand substrate and cell receptor is required for cell movement.

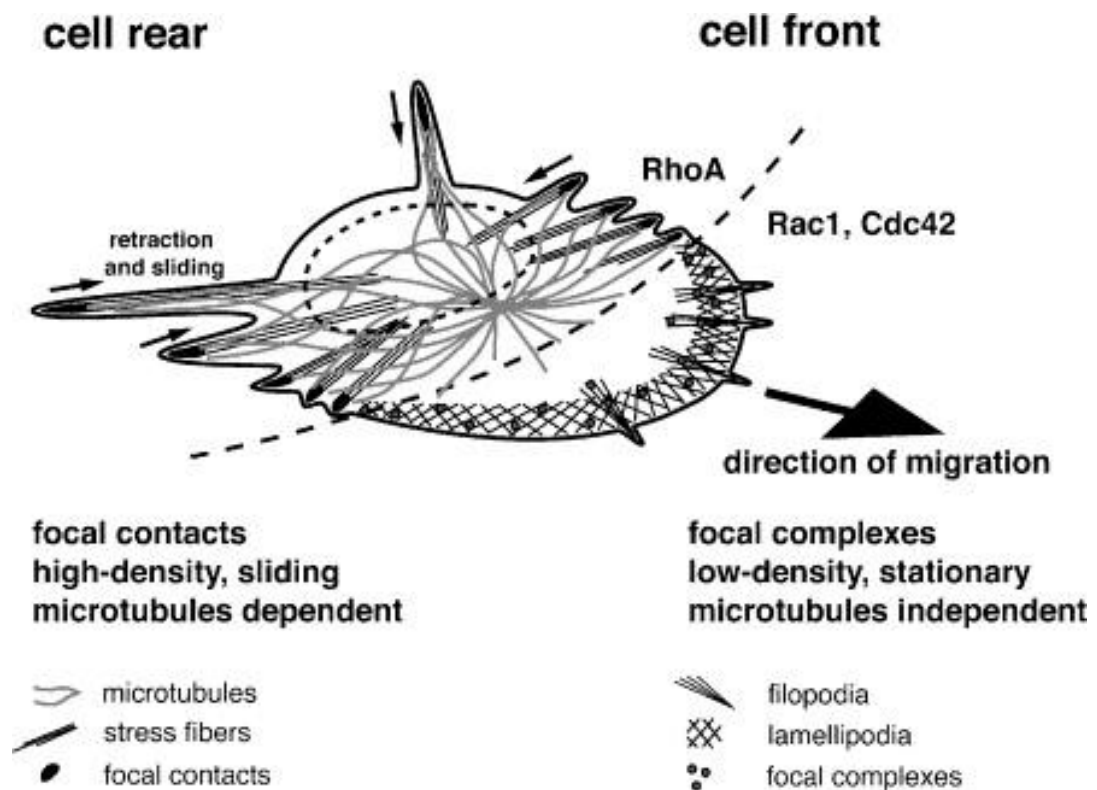


**Figure 1.24: Diagram of Cell Migration** - Actin driven cell migration in the front and microtubule controlled retraction in the rear. A schematic view of a migrating cell is shown that illustrates the main features of the actin and microtubule cytoskeleton. At the cell front, Cdc42/Rac1 induced actin polymerization results in the formation of filopodia and lamellipodia that drive the cell edge forward. The advancing lamellipodia is anchored to the substrate by stationary focal complexes. While the cell moves forward, low-density focal complexes located at the lateral edges of the lamellipodium transform into high-density focal contacts that are linked to actin stress fibers in a RhoA dependent manner. When the focal contacts localize to the rear of the cell, a microtubule controlled inward sliding, release and retraction takes place (arrows), which allows the cell to move forward (B. Wehrle-Haller *et al.*, 2003).

## Study Background, Hypothesis and Objectives

### Study Background

Vascular smooth muscle cells (VSMCs) are primarily responsible for regulating vascular tone and blood pressure. They achieve this through a unique plasticity which allows them to reversibly differentiate between a synthetic and contractile phenotype. This is known as phenotypic modulation. Differentiated SMCs are characteristically quiescent and adopt elongated spindle morphology. In this state the cell expresses an extensive range of contractile proteins such as SM  $\alpha$ -actin, Smoothelin and Calponin. SMCs in the synthetic end of the phenotype spectrum adopt a rhomboid morphology and their expression of contractile proteins is significantly decreased and replaced with organelles involved in protein synthesis. Synthetic SMCs also display increased migration and cell motility, a precursor to many cardiovascular diseases and complications such as atherosclerosis and restenosis.

Cell migration is a complex and highly orchestrated process between a cell and the substratum on which it is attached and over which it migrates. Cell migration can range from single cell movement to collective cell migration, where intercellular interactions are retained and groups of cells move coordinately Friedl and Wolf *et al.*, 2010.

In brief cell migration is characterised by a multistep cycle initiating with protrusion, adhesion formation and stabilization at the leading edge. This is achieved by integrins attaching to the actin cytoskeleton, which stimulates the formation of filopodia and lamellipodia. These are composed of actin containing cytoskeletal filaments, primarily microfilaments. This is followed by translocation of the cell body where by the actin filaments polymerise and present the membrane to the leading edge of the cell. From here focal adhesions are formed which establish a site of traction from which the cell can anchor and pull itself forward. At this point, a combination of actin treadmilling and release of adhesions at the cell rear, allowing for detachment, facilitate cell motility in the direction of migration Abercrombie *et al.*, (1971).



The phenomenon of SMC phenotype switching appears to be as a result of both innate genetic pathways and environmental cues, such as haemodynamic pressure (Owens *et al.*, 1995). Haemodynamic force is a permanent feature of the *in vivo* environment of all vascular cells as a result of the dynamic nature of blood flow. This pressure can be categorized in to two forms, shear stress and cyclic strain. The latter, cyclic strain is a tensile force perpendicular to the lumen felt by both endothelial and smooth muscle cells (Lehoux *et al.*, 2006). This has a repeated temporary stretch effect on the vessel wall and is the stimulus used for work in this thesis.

Studies have shown that several non coding micro RNA (miRNA) ,which negatively regulate gene expression, are differentially expressed in these altered SMC phenotypes (W. Sessa *et al.*, 2010, N. J. Leeper *et al.*, 2010, X. Lin *et al.*, 2010). However, work into the effect of mechanical stimulus such as shear stress or cyclic strain on miRNA expression is scarce and only a handful have been identified (Y.J. Guan *et al.*, 2011, J. Shaik *et al.*, 2010).

### **Study Hypothesis**

This study hypothesizes that “*cyclic mechanical strain, mediated by miRNA regulation, modulates vascular smooth muscle phenotype and ultimately function,*”

### **Study Objectives**

The objectives for this project were to:

- Establish if cyclic mechanical strain and its properties, namely duration and amplitude, influenced HAoSMC phenotype.
- Determine a miRNA signature or “miRNOME” for HAoSMCs and test if this alters with application of cyclic strain.
- Monitor the rate of migration of HAoSMCs in culture vs cells exposed to cyclic strain.
- Implement miRNA as mediators of any alteration observed in HAoSMC phenotype or migration as a result of cyclic strain.

## CHAPTER TWO: Materials and Methods

### 2.1 Materials

#### 2.1.1 Reagents, Chemicals and Cell Culture

The listed companies provided the following chemicals, reagents and cell culture material:

#### **Applied Biosystems / Ambion (Life Technologies), CA, USA:**

##### miRNA Isolation and Analysis;

mirVana™ miRNA isolation kit (40 Isolations)	Product# AM1560
TaqMan® miRNA Reverse Transcription Kit (200 reactions)	Product# 4366596
Megaplex™ RT Primers Human Set (A & B) v2.0 10X (50 reactions)	Product# 4400928
Megaplex™ PreAmp Primers, Human Se (Pool A & B)v2.0	Product # 4400927
TaqMan® Pre Amp Master Mix 2X (40 reactions)	Product# 4391128
TaqMan® Array Human miRNA Cards Set v2.0 (A & B)	Product# 4400238
Taqman® Universal Master Mix II, no UNG 5- Pack (5 X 5ml)	Product # 4440048
DNA ZAP™	Product # 9892G

##### Real Time qPCR

High Capacity cDNA Reverse Transcription Kit (200 Reactions)	Product # 4368814
--	-------------------

##### Argonaute 2 siRNA:

1) siRNA ID s25931	Cat#4392420 (5nm)
2) siRNA ID s25932	Cat# 4392420 (5nm)
3) Custom siRNA	ID # ADAAYKB
Scrambled Negative Control	Product#4390843(5nm)
Positive Control, GAPDH siRNA	Product#4390849(5nm)

#### **BDH Limited:**

Tween® 20	Product# 66368
-----------	----------------

**Bio-Rad, Hercules, CA, USA:**

Ammonium Persulfate

Product#161-0700

2-mercaptoethanol

Product#161-0710

10X TGS (Tris/Glycine/SDS)

Product#161-0772

TEMED

Product#161-0800

**DAKO, CA, USA:**

Fluorescent Mounting Media

Product# S3023

**Eurofins MWG Operon, Ebersberg, Germany:**

Gene Specific Primers:

$\alpha$ -Actin	Sense: TTCAATGTCCCAGCCATGTA Anti Sense: GAAGGAATAGCCACGCTCAG
Calponin	Sense: AGGCTCCGTGAA GAAGATCA Anti Sense: CCACGTTACCTTGTTTCCT
Smoothelin	Sense: TGGAGGAATTGACTGCACTG Anti Sense:GAAACCTCTGCCTGCTGTTC
FAK	Sense: NA Anti Sense: NA
FRNK	Sense: NA Anti Sense: NA
GAPDH	Sense: NA Anti Sense: NA
18S	Sense: NA Anti Sense: NA
Exportin 5	Sense: GTTGCCATCGTCAGACATT Anti Sense: CCACTACAATTCGAGACAGAG
Drosha	Sense: CTAATAACAGCAGTAGTCCTCATT Anti Sense: GCCTGTGGTCATCATAGTG
Dicer	Sense: GACTGTCGTGCCGTATTG Anti Sense: GTAGTTCTCTTACCATCATTCCA
Argonaute 2	Sense: CTAATAACAGCAGTAGTCCTCATT Anti Sense: TTCTGCCACTGCTCCTTA

**Fermentas, York, UK (Thermo Fisher):**

Dream Taq Green Buffer10X	Product# B71
Gene Ruler 100bp Plus DNA Ladder	Product# SM0321
Page Ruler Plus-	
Prestained Protein Ladder	Product# SM1811
Spectra Multicolour High Range Protein Ladder	Product# PN26625
Taq DNA Ppolymerase	Product# EP0402

**GE-Healthcare, Buckinghamshire, UK:**

Goat monoclonal to Mouse IgG (HRP) secondary antibody

**Invitrogen, CA, USA (Life Technologies):**

AlexaFluor® 488 goat anti mouse	Product# A-10667
DAPI Nuclear Stain	Product# D357
DEPCTreatedWater	
Pyrogen Free, Certified DNase/RNase Free	Product# 46-2224
DH5α E-coli Max Efficiency Competent Cells	Product# 12034013
Propidium Iodide	Product# P3566
Rhodamine Phalloidin	Product#R415
SYBR® Safe Solution	Product# S33102
Trizol® Reagent	Product# 15596018

**Lennox Laboratory Supplies LTD, Dublin, Ireland:**

100% Industrial	
Methylated Spirits (IMS)	Product# CRTSI0330716

**Medical Supply Company / Pierce (Thermo Scientific):**

BCA Protein Assay Kit	Product# 23227
Restore™ Western Blot Stripping Buffer	Product# 21059
Super Signal® West Pico Chemiluminescent Substrate	Product# 34080

**Merck Millipore CA, USA:**

Antibodies:

Activated form of β1	
Integrin	Product# MAB2079Z
Argonaute2 (Ago2) 200µg	Product# 07-590

Dicer, MSX 5D12.2 100µg	Product# 04-721
Focal Adhesion Kinase (FAK) Pc 12-305	Product# 06-543
GAPDH	Product# ABS16
Smoothelin MSX 100µg	Product# MAB3242
Goat anti Mouse HRP Secondary	Product#AP308P
EasyCheck™ Kit for HT Systems	Product# 4500-0025
Immobilon-P (PVDF Transfer Membrane)	Product# IPVH00010
Luminata™ Forte HRP Substrate 100ml	Product# WBLUF0100

**Promocell, Heidelberg, Germany:**

Human Aortic Smooth Muscle Cells (HAoSMC);	
-500,000 Cryopreserved Cells	Product# C-12533
-500,000 Proliferating Cells	Product# C-12532
Cryo-SFM serum free medium for cryopreservation;	
-30ml	Product# C-29910
-50ml	Product# C-29912
HAoSMC Growth Medium2 Kit	Product# C-22162
HAoSMCCell Growth Medium2 Supplement Mix;	Product# C-39262
-Fetal Calf Serum 0.05ml/ml	
-Epidermal Growth Factor (recombinant human) 0.5ng/ml	
-Basic Fibroblast Growth Factor (recombinant human) 2ng/ml	
-Insulin (recombinant human) 5µg/ml.	
Detach Kit;	
-30ml	Product# C-41200
-125ml	Product# C-41210

**Qiagen, West Sussex, UK:**

HiSpeed Plasmid Midi-prep kit	Product# 12643
-------------------------------	----------------

### **R & D Systems**

Quantikine® ELISA Human FGF-2	Product# DFB50
Duo Set ELISA Thrombomodulin	Product#DY3947

### **Roche Diagnostics, Basal, Switzerland:**

Complete (EDTA – Free), Protease Inhibitor	
Cocktail Tablets	Product# 11873580001
Fast Start Universal SYBR Green	
Master (ROX)	Product# 04913914001

### **Sigma Aldrich Chemical Company Ltd, Dorset, UK:**

Acetone	Product# 34850-2.5L
Agarose (500g)	Product# A5093-500g
Ammonium Persulfate (100g)	Product# A9164-100g
Ampicillin	Product# A0166-5g
Bovine Serum Albumin (BSA)	Product# A2153-50g
Chloroform	Product# C2432
Ethanol (for miRNA work)	Product# E7023-500ml
Glycerol	Product# G6279-1L
Glycine;	
-500g	Product# G8898-500g
-1kg	Product# G7126-1KG
Kanamycin Sulphate (5g)	Product# K4000-5g
37% Formaldehyde	Product# F8775-500ml
Phosphate Buffered Sulphate (PBS) Tablets	Product# P4417-100TAB
Penicillin/Streptomycin 10X (100ml)	Product# P4333-100
Ponceau S solution	Product# P7170-1L
Trypsin-EDTA (10X)	Product# T4174-100ml
Triton X- 100 (500ml)	Product# 9002-93-1
Sodium Chloride	Product# s3014-5kg
Sodium Deoxycholate	Product# D6750-100g
Sodium Dodecyl Sulfate	Product# L3771-500g
Sodium Orthovanadate (250g)	Product# s-6508
Sodium Phosphate	Product# S3264-1KG

**Thermo Fisher Scientific, Leicestershire, UK:**

Methanol	Product#34860-2.5L
10X PBS Solution	Product# 10649743
Trizma Base	Product# BP152-2
Isopropanol	Product# P/7490/15
Hydrochloric Acid	Product# H/1100/PB17
Acetic Acid	Product# A/03601/PB17

2.1.2. Instrumentation

**Applied Biosystems, CA, USA:**

Applied Biosystems 7900HT Fast Real Time PCR Machine with Sequence Detection Software (SDS)

**Bennett Scientific Ltd., Devon, UK:**

Clifton Duo Water Bath

**Becton Dickinson**

FACS Aria

**Bio-Rad, Hercules, CA, USA:**

MJ-Mini Gradient Thermocycler

Mini-PROTEAN Tetra Cell System

-(4-Gel System Includes: Electrode Assembly, Electrophoresis PowerPak® Basic, Companion Running Module, Tank, Lid With Power Cables, Mini Cell Buffer Dam, Gel Casting Stands, 10 well combs, Gel Casting Frames, 5Short Plates,5Spacer Plates and Transfer Electrode Rig)

**BioTEK, VT, USA:**

Microplate Reader ELX800

**Eppendorf, Cambridge, UK:**

Centrifuge 5702

Centrifuge 5430R

Centrifuge 5810R

Centrifuge 5415D

**Flexcell International Corp, NC, USA:**

Flexercell® tension plus™ FX-4000T system

**Heraeus Frankfurt, Germany:**

HERA Safe Laminar Air Cabinet

**Invitrogen (Life Technologies):**

Neon Transfection System

Product# MPK5000

**Labtech (East Sussex, UK):**

ADAM™ Counter

Nikon® Eclipse TS100 phase-contrast microscope

**Mason tech (Dublin, Ireland):**

Nanodrop 1000™ system

**Medical Supply Company (Dublin, Ireland):**

Horizontal Agarose Gel Electrophoresis Rig

Liebherr 4°C Refrigerator

Liebherr Profiline -20°C Freezer

**Memmert (Distributed by Mason Technology):**

Cell Culture Incubator INC 246



**Merck Millipore CA, USA:**

Guava® Easy Cyte™ 8HT Bench Top Flow Cytometer

Product# 0500-4008

**Nalgene, Rochester, NY, USA:**

Cryo-freezing container

**Roche/ Acea Diagnostics, Basal, Switzerland:**

RTCA DP Analyzer

**Stuart Scientific Ltd, Staffordshire, UK:**

Block Heater

Product# SBH130D

Orbital Shakers

Product#SSL1/SSM1

Rotator

Product# SB3

See-Saw Rocker

Product# SSL4

Vortex

Product# SA8

**Syngene, Cambridge, UK:**

G-Box Fluorescence and Chemi-Luminescence Gel Documentation and Analysis System

**Taylor-Wharton, USA:**

Liquid Nitrogen Cryo-Freezer Unit (VHC-35 ®)

**Thermo Fisher Scientific, Leicestershire, UK:**

Holten LaminAir laminar flow cabinet

-80 Freezer

HERA Cell 150 Cell Culture Incubator

**VWR International Ltd. (West Sussex, UK)**

Nalgene Mr Frosty® Freezing Container

Haemocytometer

### 2.1.3 Consumables / Plastic ware

#### **Applied Biosystems, CA, USA:**

Fast Optical 96 Well Reaction Plate with barcode (0.1ml) Product # 4346906

MicroAmp Optical Adhesive Film-

PCR Compatible, DNA/RNA/RNase free Product# 4311971

#### **Dunn Labortechnik GmbH, Asbach, Germany:**

6-well Bioflex plate

AminoCoated Product#BF-3001A/10

#### **DigitalBio Technology, Boston MA, USA:**

4 channel Accuchip kit with Accustain Solution Product# AD4K-200

#### **Eppendorf, Cambridge, UK:**

Safelock Tubes 2.0ml PCR Clean Product# 123.344

#### **GE-Healthcare, Buckinghamshire, UK:**

Whatman Filter Paper Product# 3001919

#### **Invitrogen, CA, USA:**

Neon Transfection System 100µl Kit (192 Reactions) Product#

MPK10096

#### **Pall Life Science, NY, USA:**

Nitrocellulose Transfer Membrane Product# 66485

Acrodisc 32 mm Syringe Filter with 0.2 µm Supor Membrane Product# 4651

#### **Roche/ Acea Diagnostics, Basal, Switzerland:**

xCELLigence E-Plate 16 Product#05 469 830 001

xCELLigence CIM-Plate 16 Product# 05 665 817 001

**Sarstedt AG & Co Numbrecht, Germany:**

Individually Wrapped and Plugged Sterile Serological Pipettes:

- 2ml	Product# 86.1252.001
- 5ml	Product# 86.1253.025
- 10ml	Product# 86.1254.025
- 25ml	Product# 86.1685.001
Aspiration Blow- Out Pipette	Product# 86.1252.011
100mm x 20mm Tissue Culture Dishes	Product# 83.1802.002
6 Well Tissue Culture Dish	Product# 83.1839
24 Well Tissue Culture Dish	Product# 83.1836
96 Well Tissue Culture Dish	Product# 83.1835
15ml Polypropylene Reagent & Centrifuge Tubes	Product# 62.554.001
50ml Polypropylene Reagent & Centrifuge Tubes	Product# 62.559
Cryotubes	Product# 73.380.992
2ml Safe Lock Tubes	Product# 72.695.500

**StarLab, Hamburg, Germany:**

1000 µl Graduated Filter Tips	Product# S1120-8810 200
200 µl Graduated Filter Tips	Product# S1122-1830
20 µl Graduated Filter Tips	Product# S1120-1810
10 µl Graduated Filter Tips	Product# S1121-3810

**VWR International Ltd. (West Sussex, UK)**

Cover slips	Product# 631-0124
Super Frost Glass Slides	Product# 631-0104

## 2.1.4 Preparation of stock solutions and buffers.

### 2.1.4.1 Immuno-blotting.

#### **RIPA Cell Lysis Buffer Stock (1.28X)500ml**

HEPES, pH7.5	64mM
NaCl	192mM
Triton X-100	1.28% (v/v)
Sodium Deoxycholate	0.64% (v/v)
SDS	0.128% (w/v)
dH <sub>2</sub> O to final volume	500ml

#### **RIPA Cell Lysis Buffer (1X)**

1.28X RIPA Stock	1X
Sodium Fluoride	10mM
EDTA, pH8.0	5mM
Sodium Phosphate	10mM
Sodium Orthovanadate	1mM
Protease Inhibitors	1X

#### **Sample Solubilisation Buffer (4X)**

Tris-HCl, pH6.8	250mM
SDS	8% (w/v)
Glycerol	40% (v/v)
β-Mercaptoethanol	4% (v/v)
Bromophenol Blue	0.008% (w/v)

#### **Transfer Buffer (1X)**

Tris-HCl	25mM
Glycine	192mM
SDS	0.1%
Methanol	20%

### **TBS wash Buffer**

Tris-HCl, pH7.4	50mM
NaCl	150mM

### **Coomassie Stain**

Coomassie Brilliant Blue R250	0.2%
Methanol	45%
Glacial Acetic acid	10%
dH <sub>2</sub> O	44.8%

Filter the Coomassie stain using a 0.25µm filter.

### **Coomassie Destain Solution**

Methanol	20%
Glacial Acetic acid	10%
dH <sub>2</sub> O	70%

### *2.1.4.2 Molecular Biology Buffers and Medium.*

#### **SOC Media**

Tryptone	2% (w/v)
Yeast Extract	0.5% (w/v)
NaCl	10mM
KCl	2.5mM
MgCl <sub>2</sub>	10mM
MgSO <sub>4</sub>	10mM
Glucose	20mM

#### **Luria-Bertani (L.B) Media**

Tryptone	1% (w/v)
Yeast Extract	0.5% (w/v)
NaCl	171mM

#### **Luria-Bertani (L.B) Agar (1L)**

Agar	15g
Made up to 1L with L.B. media	

### **Antibiotics**

Ampicillin 100 µg/µl

Kanamycin 50 µg/µl

Antibiotics were dissolved with dH<sub>2</sub>O and subsequently sterilised using a 0.25µm filter. Aliquots may be stored at -20C, but must be kept wrapped in tin foil to avoid degradation through exposure to natural light.

### **TE Buffer**

Tris 10mM

EDTA (pH8.0) 1mM

### **DNA Loading Buffer**

Sucrose 40% (w/v)

Bromophenol Blue 0.25% (w/v)

## 2.2 Methods

### 2.2.1 Cell Culture Technique

For the entirety of this study, the cell types used were as follows: Human Aortic Smooth Muscle Cells (HAoSMC) and Human Aortic Endothelial Cells (HAEC). Both cell types were maintained in a 37°C humidified atmosphere containing 5% CO<sub>2</sub>. (Freshney *et al.*, 2011).

#### 2.2.1.1 Human Aortic Smooth Muscle Cell (HAoSMC) Culture.

HAoSMC obtained from Promocell®, Germany. Lot # 1012003.2. Cells were isolated from a 19 year old, male, Caucasian, non-smoker with a population doubling time estimated at 40.6 h derived from the thoracic region. The cells were maintained in HAoSMC specific growth medium, containing basal media, 5% fetal calf serum (FCS), human endothelial growth factor (hEGF), human basic fibroblast growth factor (hbFGF) and Insulin. Primocin® antibiotic was also added at a final concentration of 100µg/ml to protect against fungal and bacterial infection. The cells were primarily cultured and sub cultured on 78cm<sup>2</sup> tissue culture dishes from Starstedt®. For experimental purposes cells were typically seeded on 6, 24 and 96 well plates. For use in cyclic strain experiments the cells were seeded onto an amino coated flexible membrane Bioflex® 6 well plate. (<http://www.promocell.com/fileadmin/promocell/PDF/C-12532.pdf>)

#### 2.2.1.2 Human Aortic Endothelial Cell (HAEC) Culture.

HAECs (Promocell®) were derived from the thoracic aorta of a 21 year old male, non-smoker. The isolated endothelial cells were maintained in a cell growth medium MV supplemented with a separate Supplement Mix ® of growth factors containing; endothelial cell growth supplement/ heparin (ECGS/H) 0.4% (v/v), fetal calf serum (FCS) 5.0% (v/v), endothelial growth factor (EGF) 10ng/ml and Hydrocortison 1µg/ml. The antibiotic/antifungal Primocin was also added to a final concentration of 100µg/ml to protect against fungal and bacterial infection. The cells were primarily cultured and sub cultured on 78cm<sup>2</sup> tissue culture dishes from Starstedt®. For experimental purposes cells were typically seeded on 6, 24 and 96 well plates. (<http://www.promocell.com/fileadmin/promocell/PDF/C-12271.pdf>)

### *2.2.1.3 Trypsinisation and Sub Culturing of Adherent Cells.*

Adherent cells were lifted from culture dishes using the pancreas derived enzyme trypsin in a process known as trypsinisation. This is required for sub culturing or seeding cells for experimental purposes. Cells were grown to a confluence of 70-90%. To passage a confluent dish, all required solutions are brought to 37°C including, trypsin, PBS and cell culture media. New cell culture dishes were filled with 7mls of media and allowed equilibrate in a 37°C humidified incubator with 5% CO<sub>2</sub> (v/v) for at least 30 minutes prior to sub culturing.

Using a sterile disposable aspiration pipette, growth media from the confluent dish was removed. The cells were then gently washed 3 times with 2mls of PBS to remove trypsin inhibiting compounds such as  $\alpha$ -macroglobulin present in serum. Any solutions added to cell culture dishes was done so by allowing them to run down the wall of the dish to reduce shear stress on cells and prevent lifting by applying directly to the cell layer. Following washing with PBS 2ml of 0.25% (v/v) trypsin was added to a 78cm<sup>2</sup> dish or 1ml for a single well of a 6 well plate. The cells were incubated at room temperature for approximately 3 minutes then viewed under a microscope at 4X and 10X magnification. When approximately 50% of cells were lifted the remaining, which were rounded in morphology, were dislodged by gently tapping on the side of the dish. An equal volume of full culture medium to that of trypsin was then added to neutralise and prevent further trypsinisation. Cell suspension was then added to a sterile 15ml tube and centrifuged at 700 RPM (50g) for 5 minutes at room temperature. The supernatant was carefully aspirated off and the pellet gently re-suspended in 500 $\mu$ l of media by careful pipetting up and down. The cells were then counted and seeded as required for sub culturing or experimental use. (<http://www.promocell.com/fileadmin/promocell/PDF/C-12532.pdf>)



#### 2.2.1.4 Cell Counting.

To ensure precise seeding densities of cells, for culturing and experimental reasons, cells were counted using both a Neubauer chamber haemocytometer and an automated ADAM cell counter. ([http://scienceservices.eu/media/pdf/User\\_manual\\_ADAM-MC\\_V3\\_0.pdf](http://scienceservices.eu/media/pdf/User_manual_ADAM-MC_V3_0.pdf))

##### 2.2.1.4.1 Haemocytometer

The haemocytometer was covered with a precision ground cover slip. 20µl of trypan blue was added to 100µl of cell suspension and the haemocytometer chamber filled by capillary action.

Cells were visualised by phase contrast microscopy under a 10X objective. Viable cells excluded the trypan blue stain whereas dead cells stained blue. The outer four corners of the haemocytometer are used for counting purposes where cells touching the bottom and left lines of the corner were excluded.

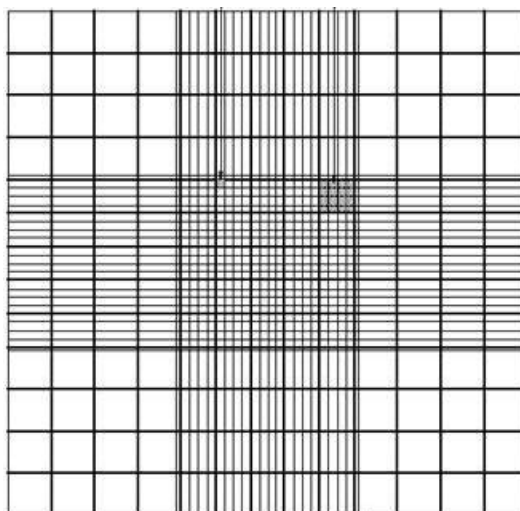


**Figure 2.1 The Haemocytometer:** Four outer squares of 4x4 boxes with a centre grid of 5x5 boxes. Outer four corners are counted omitting cells touching bottom and left side lines. Image taken from ([www.microbehunter.com](http://www.microbehunter.com))

Cell number from each four corners were added then divided by four to give an average count per  $1\text{mm}^2$ . The volume under the coverslip is  $0.1\text{mm}^3 = (0.0001\text{cm}^3 = 0.0001\text{ml}$  or  $10^{-4}$ )

Hence, total viable cell number = average cell number x dilution factor (if any) x  $1 \times 10^{-4}$  (conversion factor) = viable cells/ml

(<http://www.abcam.com/index.html?pageconfig=resource&rid=11454>)

#### 2.2.1.4.2 Adam Counter

Digital Bio ADAM (Advanced Detection and Measurement) Counter is an automated viable cell counter that uses a laser based fluorescent microscope and CCD detection system. Two 20µl aliquots of cell suspension were added, respectively, to a 20µl sample of Accustain solution T ® and Accustain solution N ®. Solution T contains a lysing solution and propidium iodide (PI) stain to give a total cell count. Solution N contains only PI stain to give a non-viable cell count. Viability percentage is calculated as follows:

$$Viability\% = \frac{(T - N)}{T} \times 100$$

The cell/dye suspension is then added to the microfluidic card and read in the ADAM counter. Cell counts are given as total cell per ml and viable cells per ml.

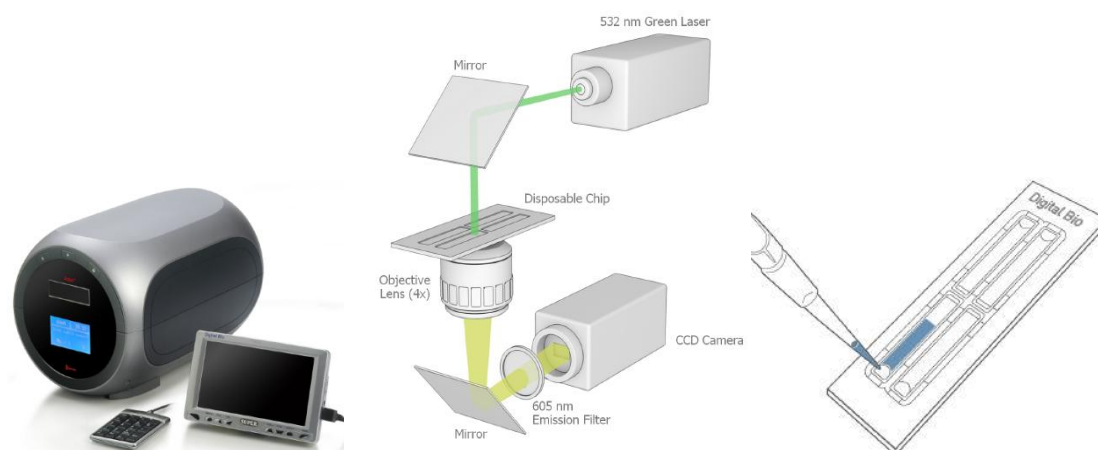


**Figure 2.2 ADAM Counter:** Left- ADAM Counter unit, Middle – 562nm green laser excitation of PI stain, detected using 605nm excitation filter and CCD camera, Right – Microfluidic chip on which cell/dye suspension is loaded. Images taken from (<http://www.digital-bio.com/>).

#### *2.2.1.5 Cryo-Preservation of Cells.*

For long-term storage, cells were stored at -196°C in a Taylor – Wharton VHC-35 ® liquid nitrogen containing dewar. Following trypsinisation the cells were centrifuged at 700RPM (50g) for 5 minutes. The supernatant was aspirated off and the cells resuspended, by gently pipetting up and down, in 1ml of serum free CRYO-SFM™ medium from Promocell. The 1ml cell suspension was then aliquotted into sterile 1ml cryovials and quickly placed into a Mr-Freeze ® cryo-freezing container. The cryovial container was then placed into a -80°C freezer. This freezes the cells at a rate of -1°C per minute. The following day the cells were transferred to the liquid nitrogen cryo unit.

For cell recovery, the cryovials were heated rapidly in a 37°C water bath. The cell suspension was added to a 58cm<sup>2</sup> culture dish containing 7mls of pre equilibrated growth medium to dilute the DMSO. Medium was changed 24 hours later.

(<http://www.promocell.com/fileadmin/promocell/PDF/C-29910.pdf>)

## 2.2.2 Molecular Biology

### 2.2.2.1 Reconstituting cDNA.

DNA plasmids arriving dried on filter paper were reconstituted in the following manner. Using flame sterilised scissors and forceps, a 1cm<sup>2</sup> area of filter paper containing the plasmid of interest was cut out and added to a sterile 1.5ml micro-centrifuge tube.

100µl of endotoxin free TE buffer (10mM TRIS base, 1mM EDTA, pH 8.0) was added to the micro-centrifuge tube against the filter paper and the mixture was vortexed briefly. The reconstituted DNA was then incubated for 5 minutes at room temperature and the vortex was repeated. The tube was then centrifuged at 10,000 RPM for 15 seconds. 1-2µl was used in the transformation of competent cells.

### 2.2.2.2 Transformation of Competent Cells.

For transformation of FAK and FRNK plasmids, JM109 and DH5α strains of *E. Coli* competent cells were used respectively. 1-2µl of reconstituted plasmid DNA was added to a vial of 50 µl competent cells. They were mixed by gentle tapping on the side of the tube, and then incubated on ice for 30 minutes. Following this the tube was heat shocked for 30 seconds in a 42°C water bath. This makes the bacterial cell membrane porous to allow the transformation of the plasmid DNA. The cells were then immediately transferred to ice for 2 minutes, following this 500µl of nutrient SOC media was added at room temperature. Cells were then incubated at 150RPM in an orbital shaker at 37°C for 30 minutes then placed on ice. Transformants were then spread on two *L.B.* agar plates containing the appropriate selective antibiotic in volumes of 40µl and 400µl. They were then incubated for 10 minutes at room temperature and placed inverted at 37 °C overnight.

### 2.2.2.3 Overnight Culture and Glycerol Stock.

Single colonies were selected from the inoculated spread plate if possible; otherwise colonies were diluted using a streak plate, to inoculate sterilised baffled culture flasks containing 150ml of *LB* broth containing the appropriate antibiotic. These were incubated at 150RPM in an orbital shaker at 37°C overnight. Glycerol stocks of the overnight culture were made to eliminate the need to go back to the reconstituted DNA and transform into competent cells again. These were made by taking 250µl of glycerol, 250µl of de-ionised water and 500µl of the overnight culture into a 2ml microcentrifuge tube. The tube was then stored in a -80°C freezer.

#### 2.2.2.4 *Midi – Preparation of Plasmid DNA.*

DNA purification was carried out using a Qiagen plasmid midi-prep kit as per the manufactures instructions.

In brief, the bacterial cells were pelleted at 6000 x g for 15 minutes at 4°C in a sterile 50ml tube. The supernatant was removed by inverting. The pellet was resuspended using 6ml of chilled P1 buffer. 6ml of P2 buffer was then added and mixed vigorously for 30 seconds to lyse the bacterial cells then incubated at room temperature for 5 minutes. 6ml of P3 buffer was then added, to neutralise the lysing effect of the P2 buffer, and solution was mixed vigorously again for 30 seconds. The cell lysate was then poured into the barrel of a QIA midi-cartridge and incubated at room temperature for 10 minutes to allow cell debris settle. Using the QIA filter the cell lysate was filtered into a previously equilibrated hi speed midi-prep tip where the DNA was allowed bind to the resin column. Bacterial cell proteins were removed by washing the column with 20ml of QC buffer and then precipitated with 3.5ml room temperature isopropanol and the tube was gently mixed by inversion. The DNA was then allowed precipitate by incubation at room temperature for 5 minutes. The isopropanol mixture was then added to the QIA-precipitator and filtered through. Plasmid bound to the precipitator was then washed with 2ml, 70% (v/v) ethanol, air dried and eluted finally into a 1.5ml micro-centrifuge tube using 700µl sterile TE buffer. Lastly the eluted DNA was flushed through the precipitator once again to remove any unbound DNA and quantified by spectrometric analysis. (<http://www.qiagen.com/knowledge-and-support/resource-center/resource-download.aspx?id=0bc0a0fe-480e-4e5e-b6e2-e75a654dd791&lang=en>)

#### 2.2.2.5 *Spectrometric analysis of Plasmid DNA.*

The concentration and purity of the recovered DNA was measured using an automated Nano Drop® system (detailed below). The purity of the DNA was determined by measuring the ratio of absorbance at 260nm and 280nm. Pure DNA which has no bound protein impurities should have an  $A_{260}/A_{280}$  ratio of 1.8-1.9. (<http://www.nanodrop.com/library/nd-1000-v3.7-users-manual-8.5x11.pdf>)

### 2.2.2.6 Agarose Gel Electrophoresis.

Agarose gel electrophoresis was used to visualise and quantify size of plasmid DNA and bench top PCR products from gene specific oligonucleotides. It was also used, along with dissociation curves, to quality control qRT-PCR products post amplification.

The agarose solution is prepared by adding 2g of ultra-pure agarose to 200ml of TAE buffer or 1g to 100ml of TAE for a smaller sized rig; this gives a 1% gel. This solution was swirled gently in a conical flask then boiled to dissolve the agarose until clear. It was allowed cool briefly then 20 $\mu$ l of Sybr Safe® was added to the 200ml or 10 $\mu$ l for the 100ml. This allows for visualization of the DNA. The agarose solution was then poured into a sealed gel cassette with the comb set in place and covered with tin foil to prevent photo bleaching and allowed to set for approximately 30 minutes.

The apparatus consists of a horizontal rig which houses the gel cassette and comb; this was then filled with TAE buffer and samples loaded into the wells created by the comb. (Meyers *et al.*, 1976).



**Figure 2.3: DNA Gel rig** Shows gel rig containing empty cassette. Combs (green) for creating the wells are inset at the bottom. Image taken from (<http://www.thermoscientific.com/>)

The gel was electrophoresed at 80V until the loading dye ran approximately three quarters of the way down the rig. The gel was then visualised using a G- Box fluorescence gel documentation and analysis system (Syngene, UK). (<http://www.bio-rad.com/webroot/web/pdf/lsr/literature/M1704400B.PDF>)

#### *2.2.2.7 Plasmid Sequencing.*

Both FAK and FRNK plasmids were sent for sequencing to Source BioScience - AUTOGEN™ & Geneservice™. The plasmids were eluted in 50 µl of ultrapure RNAase, DNAase free water at a concentration of 100ng/ µl.

The sequence was then confirmed using Finch TV software.

#### *2.2.3 Transfections.*

##### *2.2.3.1 Electroporation.*

Nucleofection by electroporation is a novel transfection technique in which the DNA/siRNA is transported directly into the nucleus to yield high transfection efficiency and cell viability. The transfection is non-viral based using a unique set of cell specific electric parameters and solutions.

##### *2.2.3.2 Amaxa/Lonza Nucleofector II*

Cells to be transfected were grown to 60% confluence on 58cm<sup>2</sup> culture dishes prior to transfection. All cell culture solutions trypsin, growth medium etc along with HAoSMC specific transfection solutions, were pre warmed to 37°C. 2.5ml of full culture medium was added to each of well of the six well plate and allowed equilibrate in the 37°C incubator. HAoSMC were trypsinised and counted. The required numbers of cells were aliquotted and pelleted at 700RPM (50g) for 5 minutes.

Media was aspirated off the pelleted cells which were then resuspended in 100µl of the supplemented Nucleofector solution. For one transfection 18µl of supplement 1 was added to 82µl of nucelofector solution to make the supplemented nucleofector solution, this included allowance for pipetting error. 3µg of plasmid DNA was then added to the cell suspension.

The DNA/cell suspension was then transferred to the supplied cuvette, ensuring no air bubbles were present. The cuvette was then capped and placed in the nucleofector device, programme U-025 for HAoSMC was selected and ran. Immediately after, 500µl of prewarmed full growth medium containing no antibiotic was added to the cuvette. The transfected cell suspension was then carefully transferred to a pre warmed well of the 6 well using the supplied soft plastic pipette. This pipette reduced shear force on the cells during transfer. The plate was incubated over night at 37°C in a tissue culture

incubator and the medium was replaced the following day. ([http://bio.lonza.com/fileadmin/groups/marketing/Downloads/Protocols/Generated/Optimized\\_Protocol\\_227.pdf](http://bio.lonza.com/fileadmin/groups/marketing/Downloads/Protocols/Generated/Optimized_Protocol_227.pdf))



**Figure 2.4:** left- Nucleofector II device, right- cell type specific solution kit with cuvettes. Image taken from ([www.lonza.com](http://www.lonza.com))

### 2.2.3.3 *Invitrogen Microporator*

The Microporation device is a unique method of transfection which uses a gold plated tip to electroporate plasmid DNA/siRNA into cells. This allows a more uniform electric field to be generated with minimal heat generation, metal ion dissolution, pH variation and oxide formation, which can present difficulties in alternative electroporation methods. Microporation was carried out according to the manufacturer's instructions.

In brief, Cells to be transfected were grown to 60% confluence on 58cm<sup>2</sup> culture dishes prior to transfection. Cell culture solutions, trypsin, growth medium etc. were pre warmed to 37°C. Transfection solutions, including resuspension R buffer and electrolyte E buffer were allowed come to room temperature. Cells were trypsinised and counted to give a final density of 7x10<sup>5</sup> cells/100µl. For each well of a 6 well to be used, 2.5ml of full culture medium ,without antibiotics, was added and allowed equilibrate in the 37°C incubator. Counted cells were pelleted at 700RPM (50g) for 5 minutes then resuspended with 110µl of R buffer and transferred to a 1.5ml micro-



centrifuge tube. 3 $\mu$ g or 20-100nM of siRNA was added. Upon the addition of 3mls of E buffer the microporation tube was inserted to the microporator device. 100 $\mu$ l of cell/DNA suspension was taken up in the gold tip, ensuring no air bubbles formed, and placed into the microporation tube gently.

For HAoSMC, the desired electrical parameters were a pulse voltage of 1350, pulse width of 20ms and a pulse number of 2. After transfection the cell suspension was transferred to the pre equilibrated growth medium containing 6 well. Cells were allowed to recover overnight and medium changed the next day.

(<http://www.lifetechnologies.com/content/dam/LifeTech/migration/en/filelibrary/cell-culture/neon-protocols.par.11634.file.dat/smooth-muscle-cells-cascade-biologics.pdf>)



**Figure 2.5: Invitrogen Microporator.** Left - Microporation tube and pipette which holds gold tip, Centre- Microporator device for setting electric parameters and delivering the charge, Right – Electrolyte (E) & Resuspension (R) buffers, gold plated tips & microporation tubes which hold the E buffer. Image taken from (<http://www.lifetechnologies.com/>)

#### 2.2.3.4 siRNA.

For gene knock down experiments small interfering RNA (siRNA) were used. These were purchased from both Sigma Aldrich ® and Ambion silencer ® select pre-designed siRNA from Invitrogen Life Sciences.

siRNA were designed and purchased for Drosha, Exportin 5, Argonaute 2 and Dicer. A positive GAPDH control and negative scrambled were also implemented in gene knock down experiments. The sequences of these siRNA are found in table 2.1.

**Table 2.1:** List of siRNA used, genes they target and the gene accession number.

Gene	siRNA code	Gene
Drosha	SASI_Hs02_00321994	NM_013235
	SASI_Hs02_00321995	NM_013235
	SASI_Hs02_00321996	NM_013235
Dicer	SASI-Hs01-00160748	NM_030621
	SASI-Hs01-00160749	NM_030621
	SASI-Hs01-00358175	NM_030621
Argonaute 2	s259321	NM_012154
	s25932	NM_012154

## 2.2.4 Immuno-Detection Techniques.

### 2.2.4.1 Immuno (Western) Blotting.

#### 2.2.4.1.1 Preparation of whole cell lysate.

For western blot assays, cells were harvested in the following manner. Cells to be lysed were placed on ice or at 4 °C, cell culture media was removed and the cells were washed 3 times with PBS. The cells were then lysed with 1X radioimmunoprecipitation assay (RIPA) buffer (30 µl per well of a 6 well and 60µl for a 58cm<sup>2</sup> dish) and collected using a cell scraper. The lysate was collected in a sterile 1.5 ml micro-centrifuge tube and rotated at 4 °C for 45 minutes to ensure full lysis of cells. The lysate was then centrifuged at 10,000g for 20 minutes at 4 °C to ensure the sedimentation of triton insoluble material to a compact pellet. The protein containing supernatant was then carefully lifted off into 30µl aliquots and frozen at -80 °C. Alternatively the lysate was used straight away in a BCA assay and ultimately a western blot. (Tobin *et al.*, 1979)

#### 2.2.4.1.2 Bicinchoninic Acid Assay B.C.A. Assay.

To ensure that samples are in the proper range for detection of the assay, and so they can be compared on an equivalent basis, it is important to know the concentration of total protein in each sample. This was achieved using a BCA or Smith assay. The assay depends on two reactions, firstly the ability of peptide bonds to reduce Copper (Cu<sup>2+</sup>) ions to Cu<sup>1+</sup> and secondly, on the ability of bicinchoninic acid (green) to chelate with each Cu<sup>+</sup> to form a complex (purple) that strongly absorbs light at 562nm.

The assay consists of each sample being read in triplicate, this includes protein standards (0-2mg/ml) along with each lysate sample and the 1XRIPA buffer used to lyse the cells, to exclude background measurement. The reagents used were from Pierce Biotechnology that comes as two solutions; (A) an alkaline bicarbonate solution and (B) a copper sulphate solution. These were mixed in a ratio of 50 parts A to 1 part B. 200µl of this mixture was then added to each well to be assayed on the 96 well plate. The plate was then covered to protect from light and incubated for 30 minutes at 37 °C, then ran on a plate reader at an absorbance of 562nm. (Smith *et al.*, 1985)

### 2.2.4.1.3 Preparing Samples

Samples were prepared in a solution of 4 X Laemmli, this buffer contains glycerol which enables the sample to sink to the bottom of the well and bromophenol blue which allows separation to be tracked as it migrates through the gel. SDS and  $\beta$  Mercaptoethanol are added to fully reduce and denature the protein and remove any higher order structure. Samples are then heated to 95°C for 5 minutes to further aid in denaturing.

### 2.2.4.1.4 Polyacrylamide Gel Electrophoresis (SDS-PAGE).

After the samples have been prepared, they are separated by size using sodium dodecyl sulphate polyacrylamide gel electrophoresis (SDS-PAGE). The SDS containing loading buffer applied a uniform negative charge to the samples which migrate in an electrical field towards the positive electrode. The proteins are separated primarily by size as a result of the mass to charge ratio following binding of the SDS.

10 x 100mm glass plates (one short one long containing 1mm spacers) were cleaned with 70% v/v (ethanol) and dried completely. They were assembled and sealed tight using the casting frame and stand. Resolving gels of 7.5 and 10% were prepared as described in table 2.2 below. 7-8 ml of the resolving gel was poured between the glass plates, avoiding air bubbles, this was then topped with a layer of 70% v/v ethanol to remove any surface air bubbles and give an even surface to the gel. The gel was allowed polymerise for 30-40 minutes at room temperature. Following this the ethanol was carefully poured off and the stacking gel was prepared as described in table 2.2. The stacking gel was added on top of the polymerized resolving gel and a 1.0mm comb was gently inserted to create the loading wells. (Tobin *et al.*, 1979)

**Table 2.2:** Recipe for SDS-PAGE resolving gel.

<b><u>Solutions</u></b>	<b><u>7.5%</u></b>	<b><u>10%</u></b>	<b><u>12%</u></b>
Distilled Water	4.85ml	4.00ml	3.35ml
1.5M Tris-HCL,pH 8.8	2.5ml	2.5ml	2.5ml
Bis Acrylamide (30%)	2.5ml	3.33ml	4.0ml
10% SDS	100 $\mu$ l	100 $\mu$ l	100 $\mu$ l
10% Ammonium persulfate	50 $\mu$ l	50 $\mu$ l	50 $\mu$ l
TEMED	5 $\mu$ l	5 $\mu$ l	5 $\mu$ l
Total Volume	10ml	10ml	10ml

A 4% v/v polyacrylamide stacking gel was used throughout all experiments and was prepared according to table 2.3 below.

**Table 2.3:** Recipe for SDS-PAGE Stacking gel.

<b><u>Solutions</u></b>	<b><u>4%</u></b>
Disitlled Water	6.1ml
0.5M Tris –HCL, Ph6.8	2.5ml
Bis- Acrylamide (30%)	1.3ml
10% SDS	100µl
10% Ammonium Persulfate	100µl
TEMED	5µl
Total Volume	10ml

Upon polymerization, the comb was carefully removed and the gel was inserted into the cassette and loaded into the electrophoresis tank. The chamber between the gel and buffer dam is filled with running buffer and any loose acrylamide is flushed from the wells using a pipette. The tank was filled to the mark with the remaining running buffer.

The wells were loaded with 30µl of prepared sample in SSB buffer as well as 5µl of the molecular weight marker. The samples and marker then underwent electrophoresis at 80V for 20 minutes then the voltage was increased to 100V for ~ 80 minutes.

#### 2.2.4.1.5 Electroblotting

Following electrophoresis, the gel containing the separated proteins was transferred to a solid support for further analysis. The electric field used for the transfer is orientated perpendicular to the surface of the gel causing proteins to move out of the gel and onto the blotting membrane. This membrane sits between the gel surface and the positive electrode. The blotting membrane used was either nitrocellulose or PVDF (polyvinylidene fluoride), the latter had to be activated by soaking in methanol for 5 minutes prior to use. The gel and blotting membrane are assembled into a sandwich along with several sheets of filter paper which protect the gel and membrane and ensure close contact between their surfaces. The sandwich was then pressed with a roller wetted in transfer buffer to eliminate any possible air bubbles. It is imperative that the membrane is placed between the gel and the positive electrode so that the negatively charged proteins migrate from the gel to the membrane. The transfer buffer used for electroblotting is similar to that used for running the gel with the addition of methanol which helps proteins bind to the membrane.

Electrophoretic transfer can be accomplished under wet or semi-dry conditions. In a wet transfer the gel/membrane sandwich is placed inside a cassette and then submersed in a tank filled with transfer buffer and subjected to an electrical field. In semi-dry the gel/sandwich is assembled on large electrode plates which generate the electrical field and transfer buffer is confined to the stack of wet filter papers.

Wet tank transfers were typically performed overnight at 4°C. Transfer buffer was agitated using a magnetic stirring bar and voltage set to 50V or at room temperature for 2 hours at 100V. (Tobin *et al.*, 1979)

#### 2.2.4.1.6 PVDF versus Nitrocellulose

Nitrocellulose was preferred for its protein binding capabilities. However, it is brittle and can be difficult to reuse. For blots that needed to be re-probed PVDF was used due to its higher strength however care needed to be taken with washing as it can produce higher background signal. It also needs to be activated prior to use with methanol and not allowed to dry out.

#### 2.2.4.1.7 Blocking

To reduce non-specific binding of the antibody, the membrane was blocked by incubating with either 5% non-fat dried milk in 0.05 % Tween PBS or 5% BSA in 0.05% Tween PBS at room temperature for 40 minutes on a see-saw rocker. Following blocking the membrane was washed for 5 minutes on a see-saw rocker with 0.05% PBS Tween. (<http://www.abcam.com/ps/pdf/protocols/wb-beginner.pdf>)

#### 2.2.4.1.8 Antibody Incubation

After blocking and washing, the blot was incubated, usually overnight at 4°C and gentle rocking, with the appropriate primary antibody. The antibody was made up in a solution of 1-5% BSA 0.05% PBS Tween or TBS Tween. See table below for specific antibody solutions and dilution factor.

Bernette *et al.*, 2009. (<http://www.abcam.com/ps/pdf/protocols/wb-beginner.pdf>)

**Table 2.4:** List of antibodies used for Immunodetection including: species, dilution factor (primary and secondary) and diluent make up.

<i>Antibody</i>	<i>PBS/TBS BSA/Milk</i>	<i>Tween %</i>	<i>Species</i>	<i>Dilution Factor</i>	<i>2° Antibody</i>
<b>Smooth muscle <math>\alpha</math>-actin</b>	PBS/BSA	0.05	Rabbit	1:600	1:3000
<b>Calponin</b>	PBS/BSA	0.05	Rabbit	1:1000	1:3000
<b>Smoothelin</b>	PBS/BSA	0.05	Mouse	1:250	1:3000
<b>FAK</b>	PBS/BSA	0.05	Rabbit	1:200	1:3000
<b>Phospho FAK</b>	TBS/BSA	0.05	Rabbit	1:200	1:3000
<b>Phospho FRNK</b>	TBS/BSA	0.05	Rabbit	1:200	1:3000
<b>Argonaute2</b>	PBS/BSA	0.05	Rabbit	2 $\mu$ g/ml	1:3000
<b>Dicer</b>	PBS/BSA	0.05	Mouse	1:200	1:3000
<b>FGF-2</b>	PBS/BSA	0.05	Rabbit	2 $\mu$ g/ml	1:3000
<b>VWF</b>	PBS/Milk	0.1	Rabbit	1:500	1:3000
<b><math>\beta</math>-actin</b>	PBS/BSA	0.05	Rabbit	1:3000	1:5000
<b>GAPDH</b>	PBS/BSA	0.05	Rabbit	1:3000	1:5000

After incubation with the primary antibody the blot was washed 3 times with 0.05% TBS/PBS tween for 5 minutes with gentle rocking. Following this the blot was incubated with the appropriate species of secondary antibody conjugated with HRP (horse radish peroxidase) in 1-5% BSA 0.05% TBS/PBS Tween for 2 hours at room temperature. HRP is a small stable enzyme with high specificity and rapid turnover. See table 2.5 for appropriate secondary species and the dilution factor for each protein.

Finally, the membrane was washed 3 times in TBS/PBS Tween 0.05% for 5 minutes each time with gentle rocking.

#### *2.2.4.1.9 Detection with Substrate*

Detection of target proteins was possible once they were specifically tagged with the appropriately labeled antibody. This was achieved through use of either Millipore; Luminata ® Enhanced Chemiluminescent (ECL) substrate or Thermo Scientific SuperSignal® West Pico Chemiluminescent Substrate. When probing for an abundant cellular protein with a reliable antibody, the less sensitive SuperSignal® West Pico Chemiluminescent Substrate was used. The peroxide solution and luminal enhancer solution were mixed in equal parts and approximately 1ml of this mixture was added for an entire 10 well blot. When probing for minimally expressed proteins or using weak antibodies the Millipore, Luminata ® was used, capable of detecting (pg) amounts. Approximately 500µl was added to a full 10 well membrane. In both cases detection imaging was carried out immediately. The light emission was captured using either X-Ray film or a Syngene G-Box, CCD camera. Exposure times ranged from 30 seconds to 10 minutes depending on the signal strength. Image J software was used for densitometry and relative band comparison. (<http://www.abcam.com/ps/pdf/protocols/wb-beginner.pdf>)

#### *2.2.4.1.10 Coomassie Gel Staining*

Coomassie gel staining was used to visualise proteins on the SDS-PAGE gel, which was useful to ensure an efficient transfer by showing protein left behind. In brief, the SDS-PAGE gel was covered with filtered coomassie solution and agitated by gentle rocking for up to 4 hours. The solution was then poured off and the gel de-stained using a mixture of methanol and acetic acid (50:50) until the protein bands appeared clear with no background. (<http://www.abcam.com/ps/pdf/protocols/wb-beginner.pdf>)



#### 2.2.4.1.11 Ponceau-S Membrane Staining

Ponceau S is a red stain applied in an acidic solution which reversibly stains all protein present on the membrane prior to any immuno blotting. This was used to confirm the transfer and help to show equal transfer of protein from the gel. The stain was subsequently removed by washing in distilled water. (<http://www.abcam.com/ps/pdf/protocols/wb-beginner.pdf>)

#### 2.2.4.1.12 Membrane Stripping

To allow for re-probing of the membrane with different antibodies or to optimize antibody concentration, the membrane was stripped with RESTORE® stripping buffer. This was used as per the manufacturer's instruction. In brief, the blot was washed in wash buffer to remove any previous ECL substrate then covered with stripping buffer and agitated by rocking gently for 15 minute. Removal of both primary and secondary antibody was confirmed by first incubating the membrane with the appropriate secondary and subsequent detection with ECL substrate. If no bands were detected the blot had been successfully stripped. It was then washed again to remove ECL substrate and re probed with alternative antibodies as previously described. (Zhang *et al.*, 2003)

#### 2.2.4.2. Immunocytochemistry (ICC)

ICC was performed to show the presence and location of specific proteins within the cell. This was carried out on glass coverslips. Coverslips were immersed in 70% v/v ethanol and flame sterilised before being placed in the well of a sterile 6 well plate. Cells were lifted using EDTA, counted and seeded onto the coverslips overnight. The following day cells were washed with PBS and fixed using 3.7% formaldehyde pH 7.4 at room temperature for 20minutes. The cells were then washed twice with PBS and permeabilised with 0.2% Triton X-100 solution in PBS for 5 minutes at room temperature. Cells were again washed with PBS and then blocked for 1 hour with 5% BSA in TBS 0.05% Tween while being gently rocked. Cells were then incubated with primary antibody over night at 4°C. Following incubation the primary antibody was taken off. Cells were then washed with PBS and incubated with the appropriate secondary fluorophore antibody for 2 hours at room temperature.

Following this, cells were washed and incubated with a 1:40 dilution of Rhodamine Phalloidin (Invitrogen) for 20 minutes at room temperature to visualise actin. Cells were washed one final time then inverted and mounted on a flame sterilised microscope slides using DAKO mounting medium. The slides were allowed to set for two hours and then placed in the fridge and protected from light. (<http://www.invitrogen.com/site/us/en/home/brands/Molecular-Probes.html>)

#### *2.2.4.3 Enzyme Linked Immuno Sorbent Assay (ELISA)*

##### *2.2.4.3.1 Quantikine® ELISA*

The Quantikine Human Fibroblast Growth Factor-2 (FGF-2) immunoassay kit is a solid phase ELISA designed to measure (FGF-2) in cell media and lysate. It contains *E. Coli* expressed recombinant human FGF-2 and antibodies raised against the recombinant factor.

##### *Principle of the Assay*

This assay employs the quantitative sandwich enzyme immunoassay technique. A monoclonal antibody specific for FGF-2 is pre coated on a 96 well plate. Standards and samples are pipetted into the wells and any FGF-2 present is bound by the immobilized antibody.

After washing away any unbound substances, a horse radish peroxidase linked monoclonal antibody specific for FGF-2 is added to the wells. Following a wash to remove any unbound antibody-enzyme reagent, a substrate solution is added. A colour then develops the intensity of which is proportional to the amount of FGF-2 present. The colour development is stopped and the intensity measured using a plate reader.

The protocol was followed as per the manufacturers' guideline;

In brief, 20 ml of wash buffer (0.05% Tween in PBS) was diluted in distilled water to prepare 500ml of wash buffer. Substrate solution was made 15 minutes prior to use by mixing equal volumes of reagents A (H<sub>2</sub>O<sub>2</sub>) and B (tetramethylbenzidine) protected from light. The FGF-2 standard was reconstituted with calibrator diluents (1% BSA in PBS) to give a 640 pg/ml stock. This stock was serial diluted 1:2 down to 10pg/ml to give 7 standards.

100µl of assay diluent (1% BSA in PBS with blue dye) was added to each well using a multichannel pipette. Following this 100µl of standard or sample were added to each well and the plate was sealed and incubated at room temperature for 2 hours. After incubation the wells were aspirated and the plate was washed 4 times by submerging it in wash buffer ensuring complete removal of wash buffer from each well by blotting against paper towels at each stage.

200µl of FGF-2 conjugate (HRP Ab) was then added to each well and the plate was sealed and incubated at room temperature for 2 hours once more. Following this, the plate was washed as previously described. 200µl of substrate solution was then added and the plate was protected from light and incubated for 30 minutes. The colour reaction was stopped by adding 50µl of stop solution (2N H<sub>2</sub>SO<sub>4</sub>) to each well, changing the colour from blue to yellow. If the colour was green the plate was gently tapped to ensure proper mixing. The optical density (OD) of each well using a plate reader set to 450nm. Wavelength correction was calculated by removing readings at 540nm. This removed optical inaccuracies within the plate itself.

The results were calculated on a spreadsheet using equation of the line incorporating readings from the standards. (Wide *et al* 1966)

#### 2.2.4.3.2 DuoSet ELISA

The DuoSet ELISA for human Thrombomodulin from R&D systems is a sandwich ELISA similar to that described previously for human FGF-2. The principle of the assay is identical. The DuoSet differs from the Quantikine® ELISA in that the capture antibody is added to the 96 well plate by the user. In brief, Wash buffer was made with 0.05% Tween in PBS. The capture antibody was reconstituted in 1ml of PBS to a stock concentration of 360 µg/ml. This was further diluted in PBS to a working concentration of 2µg/ml. 100µl of this working concentration was added to each well and the plate was incubated overnight. The plate was then washed as previously described. The plate was then blocked for 1 hour by adding 300µl of reagent diluent (1% BSA in PBS) to each well. Following this the plate was washed. 100µl of sample or standard was then added to the plate and incubated for 2 hours. The plate was subsequently aspirated/washed. The protocol after sample addition is identical to that of the Quantikine® ELISA kit following sample addition stage. (Wide *et al* 1966)

### 2.2.5 Ribonucleic Acid (RNA) Work

As RNA is easily damaged and degraded by ubiquitous ribonuclease (RNase), all RNA work was carried out according to the protocol outlined in Sambrook, Fritsch and Maniatis' "Molecular Cloning, A Laboratory Manual". To prevent genomic DNA contamination, prior to any RNA work, surfaces and equipment were cleaned down with DNA Zap (Invitrogen). This consists of two solutions that are innocuous when used alone, but become a potent nucleic acid degrading solution when mixed. This mixture is able to instantaneously degrade high levels of contaminating DNA and RNA from surfaces. Gloves were also used and changed frequently. (Chomczynski *et al.*, 2006).

#### 2.2.5.1 RNA Isolation

Two methods were used for isolation and purification of total RNA from cell culture samples. The miRVANA® RNA extraction kit and isolation by Trizol® reagent. RNA isolation was developed by (Chomczynski & Sacchi *et al.*, 1987).

##### 2.2.5.1.1 miRVANA Kit

The miRVANA® kit uses an organic extraction method followed by immobilisation of RNA on glass-fibre filters to purify total RNA.

For (1-2x10<sup>6</sup>) HAoSMC the culture medium was aspirated off and the cells washed twice with PBS. 600µl of total lysis binding solution was added to the cells (in the case of a 6 well plate 100µl into each well). The cells were then scraped and collected, using a rubber cell scraper, into a 1.5ml RNase free micro centrifuge tube. The sample was vortexed for 30-60 seconds to obtain a homogenous lysate. The volume of the lysate was recorded and 1/10 of this volume of miRNA homogenate additive was added to the lysate. This solution was well mixed by vortexing for 30-60 seconds. The solution was then incubated on ice for ten minutes after which the volume prior to addition of the miRNA homogenate additive was the volume added of acid-phenol chloroform and ensured it was taken from the bottom phase of the acid phenol chloroform. The lysate solution was again vortexed for 30-60 seconds before being centrifuged for 5 minutes at 10,000g at room temperature to separate the aqueous and organic phases.

Following centrifugation, the lysate solution was checked for a compact interphase and if this was not evident the centrifugation step was repeated. The upper aqueous phase

was transferred to a fresh tube taking care not to disturb or carryover any of the bottom organic phase. The volume of upper aqueous phase recovered was noted and 1.25X of this volume of room temperature 100% high grade ethanol was added to the fresh tube. A maximum of 700 µl of this lysate/ethanol mixture was pipetted onto a glass-fibre filter cartridge, which was placed in a fresh tube. This was centrifuged at 10,000g for 15 second to pass the mixture through the filter. This step was repeated until all of the lysate/ethanol had been passed through the filter and the flow through was discarded each time. 700µl of wash buffer 1 was then added to the filter column and passed through by centrifugation at 10,000g for 15 second. This was repeated using 500µl of wash buffer 2/3 again with the flow through being discarded each time. After the third wash the filter column was centrifuged at 10,000g for 1 minute to dry off the filter column and prevent ethanol carry over to the new tube in which filter column was placed. The total RNA was then eluted into a fresh collection tube by centrifugation at 10,000g for 30 seconds using 100µl of elution buffer which was pre-heated to 95°C. The RNA was quantified and qualified on a NanoDrop® Spectrophotometer. The sample was then stored at -80°C. ([http://tools.lifetechnologies.com/content/sfs/manuals/cms\\_055423.pdf](http://tools.lifetechnologies.com/content/sfs/manuals/cms_055423.pdf))

#### *2.2.5.1.2 RNA Extraction and Isolation using Trizol®*

Trizol® is a ready to use reagent for the isolation of total RNA, DNA and/or protein from cultured cells and tissue. Trizol® reagent maintains integrity of total RNA while disrupting cell membranes and dissolving cellular components.

Media was aspirated from cultured cells and they were washed 3 times with PBS. Cells were then lysed by addition of 1ml chilled Trizol® reagent. The final volume of Trizol® per sample was always made to 1ml, for example if 3 wells of a 6 well are of the same sample 333µl was used in each and pooled. The plate was then left on ice for 10 minutes to allow complete dissociation of nucleoprotein complexes. The cell lysate was scraped from culture dishes and collected in a sterile RNase free micro-centrifuge tube. 20% volume of Chloroform was added (i.e. 0.2ml of Chloroform for each 1ml of Trizol® used.) The sample was then vortexed for 20 seconds and incubated at room temperature for 15 minutes. The lysate was then centrifuged at 13,000g for 20 minutes at 4°C. Following this the upper aqueous phase was transferred to a new micro-centrifuge tube taking care not disturb or carry over any of the lower organic phase or interphase. To precipitate the RNA out of solution, 0.5 ml of isopropanol per 1ml of Trizol® used was added to the aqueous phase and the new tube was mixed by inverting

several times. The solution was then placed at -20 °C overnight. The next day the sample was taken from the -20 °C and incubated at room temperature for 15 minutes. The tube was then centrifuged at 13,000g for 15 minutes at 4°C. The supernatant was removed taking care not to disturb the small opaque pellet of RNA. The pellet was washed by gently knocking it off the wall of the tube with 75% v/v room temperature ethanol. The re-suspended pellet was then centrifuged at 13,000g for 10 minutes at 4 °C. The ethanol was then aspirated off, again being careful not to disturb the small opaque pellet of RNA. The pellet was air dried in a laminar air cabinet. Finally the Pellet was then re-suspended in 50µl nuclease free water and incubated at 55°C for 10 minutes to homogenise the sample prior to quantification. The RNA was quantified and qualified on a NanoDrop® Spectrophotometer. The sample was then stored at -80°C. ([http://tools.lifetechnologies.com/content/sfs/manuals/trizol\\_reagent.pdf](http://tools.lifetechnologies.com/content/sfs/manuals/trizol_reagent.pdf))

#### *2.2.5.2 RNA/DNA Quantification Using NanoDrop® ND-1000 Spectrophotometer*

The NanoDrop® ND-1000 Spectrophotometer was used to determine nucleic acid sample concentrations and integrity. An undiluted 1.2 µl sample was pipetted onto the end of a fiber optic cable (the receiving fiber). A second fiber optic cable (the source fiber) was then brought into contact with the liquid sample causing the liquid to bridge the gap between the fiber optic ends. A pulsed xenon flash lamp provides the light source and a spectrometer is used to analyse the light after passing through the sample. The instrument is controlled through use of specific PC based software.

The NanoDrop® automatically calculates the purity of the nucleic acid samples by reading the absorbance at 260 nm and the absorbance at 280 nm and then determining the ratio between the two (Abs.260/Abs.280) . Pure DNA which has no protein impurities has a ratio of 1.8 whereas pure RNA has a ratio of 2.0. Lower ratios indicate the presence of protein; higher ratios imply the presence of organic reagents. (Sambrook *et al.*, 2001)

#### *2.2.5.3 RNA Purification.*

RNA for use in Reverse Transcription-PCR (RT-PCR) was pre treated with amplification grade DNase1 to remove any RNase activity and DNA from sample RNA. In brief, 8µl of RNA suspended in water along with 1µl of 10X reaction buffer and 1µl of DNase1(1unit/µl) were added to a PCR tube. The solution was mixed gently and incubated for 15 minutes at room temperature. Following this 1µl of stop solution was

added and the tube was heated at 70°C for 10 minutes. This heating step also removed any hair pin structures within the RNA. RNA was then chilled on ice ready to be synthesized into cDNA. (Sambrook *et al.*, 2001)

#### 2.2.5.4 Polymerase Chain Reaction (PCR)

PCR is a process used to amplify specific sequences of DNA at an exponential rate for use in a variety of applications. Standard PCR, coined bench top PCR, was used for making of cDNA and as a cost effective method to analyse and optimise newly synthesized primers before committing them to quantitative real time PCR (QRT-PCR). (Bartlett, J. M. S.; Stirling, D. *et al* 2003).

#### 2.2.5.5 Reverse Transcription (RT-PCR)

RT-PCR is a variant on PCR, used to reverse transcribe the RNA strand into its DNA complement. This is achieved by utilising an enzyme called reverse transcriptase as outlined in (Roth *et al.*, 1985; Sambrook *et al.*, 1989). This was accomplished by using a high capacity cDNA reverse transcription kit (Applied Biosystems, CA, USA) In brief, 20µl reactions were made up as shown in table 2.4.

**Table 2.5:** Recipe for single sample reverse transcription Master Mix.

RT Buffer	2ul
Random Primer	2ul
dNTP	0.8ul
Multiscribe	1ul
Pure H <sub>2</sub> O	4.2ul
<b>Master Mix</b>	
<b>Final Volume</b>	10ul

RNA was made up to 1000ng in 10µl of nuclease free water and added to an RNase free 0.2ml PCR tube, to this 10µl of master mix was added for each RNA sample. The tubes were spun down briefly and placed in aMiniJ bench top PCR thermocycler (BioRad). The programme included 25°C for 10 minutes, 37°C 120 minutes and finally 85°C for 5 minutes. cDNA products were then quantified on the NanoDrop® spectrophotometer as previously described.

#### 2.2.5.6 PCR Primer Design

For PCR, DNA primers were designed using the online website <http://frodo.wi.mit.edu/primer3/> in accordance with the standard rules of primer design. Each primer was designed to anneal to exon-exon border regions so as to only amplify reverse transcribed cDNA and not genomic DNA. The generated primers were then run through BLAST to verify their sequence homology and ensure there would be no primer dimer formation or risk of the primer folding on itself. All primers and optimum temperatures used can be found in table 2.7. For all mRNA QRT-PCR endogenous controls used were 18s and GAPDH.

#### 2.2.6 Quantitative Real Time Polymerase Chain Reaction (QRT-PCR)

Quantitative real time polymerase chain reaction follows the standardized principles of PCR. It is used to amplify target DNA with the addition of simultaneously quantifying the targeted DNA sequence as it accumulates during the reaction. Two types of chemistries were used in this project for detection of PCR products. For mRNA work SYBR® Green was incorporated. This dye does not inhibit PCR and increases fluorescence upon binding to double stranded DNA. As the reaction progresses more PCR product is created. SYBR® Green binds to all double stranded DNA, so the result is an increase in fluorescence proportional to the amount of PCR product produced. Endogenous controls 18S or GAPDH were monitored in tandem with the target gene to correct for loading bias.

For miRNA profiling a Taqman® probe was used. This chemistry, also known as “fluorogenic 5'” nuclease chemistry uses a fluorogenic labeled 5' probe. This relies on the nuclease activity of Taq DNA polymerase.

An oligonucleotide probe contains a reporter fluorescent dye on the 5' end and a quencher dye on the 3' end. While the probe is intact, the proximity of the quencher dye greatly reduces the fluorescence emitted by the reporter dye by fluorescence resonance energy transfer (FRET).

If the target sequence is present, the probe anneals downstream from one of the primer sites and is cleaved by the 5' nuclease activity of *Taq* DNA polymerase as this primer is extended.

This cleavage of the probe:

- Separates the reporter dye from the quencher dye, increasing the reporter dye signal.
- Removes the probe from the target strand, allowing primer extension to continue to



the end of the template strand. Thus, inclusion of the probe does not inhibit the overall PCR process.

Additional reporter dye molecules are cleaved from their respective probes with each cycle, resulting in an increase in fluorescence intensity proportional to the amount of PCR product produced.

The QRT-PCR was carried out using an Applied Biosystems 7900 HT real time thermo cycler.

When using SYBR® Green for mRNA gene analysis a master mix containing enough volume for sample triplicates and pipetting error was made up as shown in table 2.5.

**Table 2.5:** Recipe for single sample triplicate in qRT-PCR.

<b>Component</b>	<b>Volume (µl)</b>
SYBR Green MM	39.13
Forward Primer	3.2
Reverse Primer	3.2
cDNA (500ng/µl)	6.5
Nuclease Free H <sub>2</sub> O	29.42
Total Volume	81.45

Samples were loaded on to a 96 well optical PCR plate sealed and centrifuged to eliminate any air bubbles and ensure the entire sample was pulled to the bottom of each well.

$\Delta\Delta$ CT programme was used for comparative analysis and the samples were subjected to an initial denaturing step of 95°C for 10 minutes followed by 40 cycles of 95° for 15 seconds and 50°C for 1 minute and 72 ° for 30 seconds before a final extension step of 72°C for 5 minutes.

Following amplification dissociation /melt curve analysis was carried out. This was to ensure single product production and rule out possible contaminant from foreign DNA and possible primer dimerisation.

### 2.2.7 miRNA Isolation and Amplification.

miRNA profiling was carried out using the Applied Biosystems® Taqman® Low Density Array (TLDA) Human miRNA Cards Set (v2.0)

#### 2.2.7.1 Isolation

For analysis on the TLDA cards, total RNA was extracted from HAoSMC using the Ambion™ mirVANA miRNA® isolation kit as previously described.

#### 2.2.7.2 Reverse Transcription of RNA for Taqman® Array Analysis.

Single stranded cDNA was synthesised from the total RNA using the Applied Biosystems TaqMan® microRNA Reverse Transcription (RT) Kit. For a full miRNA profile two RT reactions were needed incorporating primers for both pool A and B miRNA panels. This kit creates cDNA from only mature miRNA and not precursors.

The RT reaction has a final volume of 7.5µl and contains:

- 3µl (1-350ng) total RNA
- 4.5µl of RT master mix

The master mix was made up as shown in table 2.6 in a 2ml RNase free tube.

**Table 2.6:** Recipe for reverse transcription of miRNA to cDNA (pool A and B).

<b>RT Reaction Mix Components</b>	<b>Volume for one samples (µl)</b>	<b>Volume for ten samples (µl)*</b>
Megaplex RT Primers (Pool A & B) 10x	.8	9.00
dNTPs (100mM)	0.2	2.25
Multiscribe Reverse Transcriptase (50 U / µL)	1.5	16.88
10 X RT Buffer	.8	9.00
MgCl	.9	10.12
RNase Inhibitor (20 U / µL)	0.1	1.12
Nuclease Free Water	0.2	2.25
Total	4.5	50.62

\* includes 12.5% excess for volume loss from pipetting.

The samples are mixed by gentle pipetting and incubated on ice for 5 minutes. The samples are then run on the bench top PCR thermo cycler under the conditions found in table 2.7.

**Table 2.7:** Thermocycler conditions for miRNA specific reverse transcription.

Stage	Temp °C	Time
Cycle (40 cycles)	16	2 min
	42	1 min
	50	1 min
Hold	85	5 min
Hold	4	∞

### 2.2.7.3 Preamplification of cDNA

If total RNA from sample is less than 350ng a preamplification step is carried out prior to committing the cDNA to the TaqMan microRNA arrays. This uniformly pre amplifies desired cDNA prior to quantification with the TLDA cards. The preamplification reaction has a final volume of 25 µl containing:

- 2.5 µl RT product
- 22.5 µl Preamp reaction mix

The master mix is made up as shown in table 2.8 in a 2ml RNase free tube.

**Table 2.8:** Recipe for Pre-Amplification master mix.

PreAmp Reaction Mix Components	Volume for one sample (µl)	Volume for ten samples (µl)
TaqMan PreAmp Master Mix (2X)	12.5	140.62
Megaplex PreAmp Primers (10X)	2.5	28.13
Nuclease Free Water	7.5	84.37
Total	22.5	253.12

The sample is then mixed by gentle pipetting and run on a bench top PCR thermocycler under the conditions found in table 2.9.

**Table 2.9:** Thermocycler conditions for miRNA cDNA Pre-Amplification.

Stage	Temp °C	Time
Hold	95	10 min
Hold	55	2 min
Hold	72	2 min
Cycle (12 cycles)	95	15 sec
	60	4 min
Hold (for enzyme inactivation)	99.9	10 min
Hold	4	∞

Following PCR the sample is diluted with 75 µl of 0.1x TE buffer (pH8) and used for array analysis immediately or stored for up to one week at -20°C.

#### 2.2.7.4 Running the Taqman® microRNA Array

DNA polymerase from the TaqMan® Universal PCR Master Mix amplifies the target cDNA using sequence specific primers and a probe on the TaqMan microRNA array. The presence of the target is detected in real time through cleavage of the TaqMan probe by the polymerase 5'-3' activity.

The master mix for the cards is made up as shown in table 2.10 for preamplified cDNA.

**Table 2.10:** Recipe for miRNA array sample when using a Pre-Amplified product.

Component	Volume for One Array (µl)
TaqMan Universal PCR MasterMix	450
Diluted PreAmp Product	9
Nuclease-Free Water	441
Total	900

For non preamplified cDNA the master mix changes are as shown in table 2.11.

**Table 2.11:** Recipe for miRNA array sample which has not been Pre-Amplified.

<b>Component</b>	<b>Volume for one array (µl)</b>
TaqMan Universal PCR MasterMix	450
Diluted PreAmp Product	6
Nuclease-Free Water	444
Total	900

The sample is mixed by gentle pipetting and centrifuged briefly. The arrays are allowed to come to room temperature then 100µl of the mix is dispensed into each chamber of the array and the card is centrifuged twice for 1 minute at 1000 RPM to fill each of the 384 wells of the card. The card is then sealed and the loading chambers are cut off.

The card is then run on the Applied Biosystems® 7900 HT thermo cycler using the parameters contained within the SDS setup file on the supplied CD as shown in table 2.12.

**Table 2.12:** Real time thermocycler parameters for miRNA array.

<b>Temperature(°C)</b>	<b>Time (min)</b>	<b>Cycles</b>
50	2	40
94.5	10	40
97	30(seconds)	40
59.7	1	40

## 2.2.8 miRNA Data Analysis

### 2.2.8.1 Data Formatting

Following qRT-PCR, the SDS files were opened in RQ manager and a manual threshold of 0.1 was set to ensure CT determination consistency across each miRNA target. The amplification data was then exported as TXT.files. The files were finally imported into R statistical analysis software for initial bioinformatics including generation of P values and establishing a short list of the most differentially expressed miRNA. Data from the temporal study and biological replicates was processed as follows:

#### 0-48 hour Temporal Study

- All endogenous controls were removed to allow for mean normalisation (Pieter Mestdagh *et al* 2009).
- Calculation of Pearson Correlation Coefficient (PCC).
- P-values generated for PCC.
- Only miRNA with strong correlation were retained  $\geq 0.9$  or  $\leq -0.9$  with a P value of  $\leq 0.05$ .
- Hierarchical Cluster Analysis was performed to validate the experiment.
- Two way heat map plotted of priority miRNA.
- dCT was multiplied by -1 to correlate increasing value with increasing expression when plotted.

#### Biological Replicates of 24hour time point

- All endogenous controls were removed to allow for mean normalization (Pieter Mestdagh 2009).
- Priority miRNA short lists were made up of miRNA whose adjusted P value was  $\leq 0.05$  using the Benjamini Hochberg approach.
- Hierarchical Cluster Analysis was performed to validate the experiment.
- Venn diagrams generated for a 3 way comparison of Static Vs 3%, Static Vs 10% and 3% Vs 10% to elucidate commonality of miRNA across the strains.

#### 2.2.8.2 Target Prediction

To determine which genes may be affected by the priority miRNA the putative targets were downloaded using the on line database TargetScan (version 6.2).

TargetScan predicts biological targets of miRNAs by searching for the presence of conserved 8mer and 7mer sites that match the seed region of each miRNA (Lewis *et al.*, 2005). As an option, nonconserved sites are also predicted. Also identified are sites with mismatches in the seed region that are compensated by conserved 3' pairing (Friedman *et al.*, 2009). In mammals, predictions are ranked based on the predicted efficacy of targeting as calculated using the context and scores of the sites (Grimson *et al.*, 2007).

#### 2.2.8.3 Biological Processes and Pathway Analysis

The gene list generated from Target Scan, for a miRNA of interest, was entered into the online bioinformatics database DAVID (Database for Annotation, Visualisation and Integrated Discovery) (version 6.7)

DAVID tools were used to determine enrichment for biological themes such as GO (Gene Ontology) biological processes. They were also used to visualise genes on KEGG (Kyoto Encyclopedia of Genes and Genomes) pathway maps for analysis. (Huang *et al.*, 2009; Sherman *et al.*, 2009)

## 2.2.9 Pathophysiological Assays

### 2.2.9.1 Cyclic Strain

In order to assess the impact of haemodynamic force on the cell it was necessary to replicate it. This was achieved using a Flexcell® FX-4000T™ Tension Plus™ system which utilises a micro-processor controlled vacuum (Banes *et al* 1985). This allows for cyclic deformation of cells cultured on flexible-bottomed culture plates. The Flexcell® system can reproduce several waveforms found in the body. These include those found in an electrocardiogram (ECM), a heart P wave which mimics the pressure experienced by vessels from the heart beat, a static wave for constant pressure and a sine, triangle and square wave which show increasing rates from minimum elongation to maximum respectively. For the purpose of this project the heart P wave form was used.

HAoSMC were seeded to an amino, Poly- D – Lysine, coated 6 well Bioflex® plate at a density of  $3 \times 10^5$  per well. Once the cells had completely adhered (~ 7 hours) they were exposed to either a physiological (5%) or pathological (10%) strain from 2 – 72 hours. Following the experiment cells were harvested for total RNA for miRNA/mRNA analysis, lysed for protein quantification by western blot or used in cell function assays including, migration, adhesion, apoptosis and cell cycle/ proliferation.



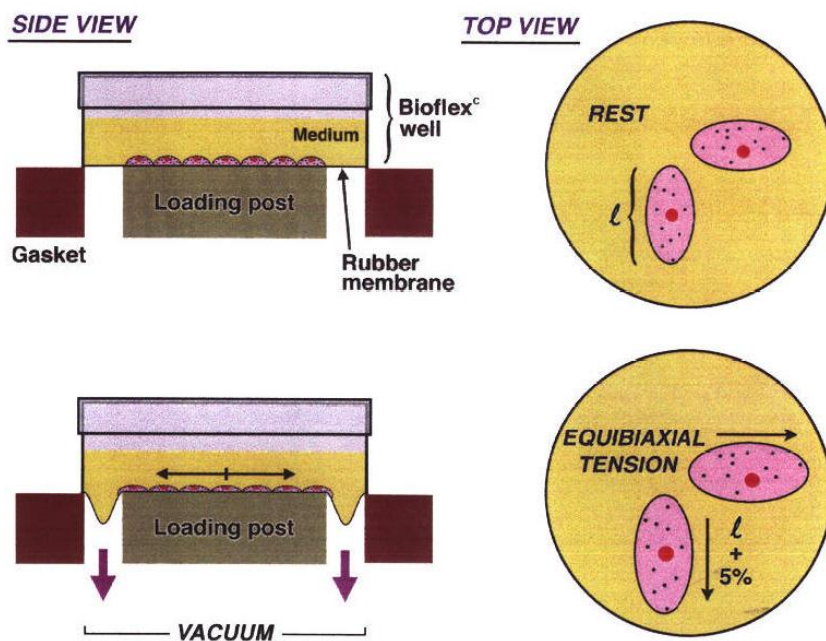
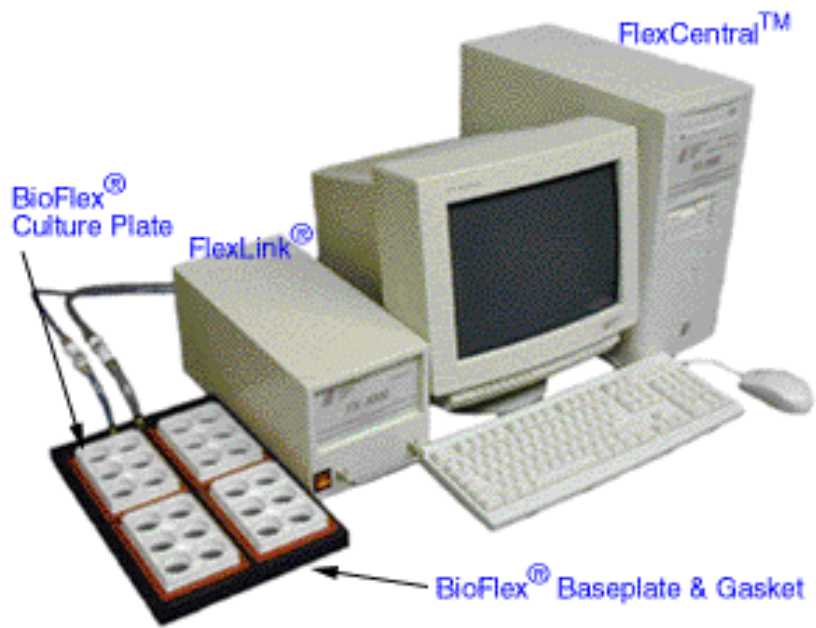


**Figure 2.6:** Top: Image of Flexcell® FX-4000T™ Tension Plus™ system. Includes vacuum base plate on far left, to the right is the Flex Link® housing the valves and to the far right is the Flex Central® PC containing the software to run the system. Bottom: Schematic diagram showing a side view (left) of cells under strain from the applied vacuum as they are pulled over the loading post. Right: top view of cells on BioFlex® plate highlighting the equibiaxial strain when under vacuum. Image taken from (<http://www.flexcellint.com/>)

## 2.2.10 Cell Function Assays

### 2.2.10.1 xCELLigence Real Time Cell Analysis

The xCELLigence system monitors cellular events in real time without the incorporation of labels. The system measures electrical impedance across integrated micro-electrodes on the bottom of tissue culture E and CIM plates. The impedance measurement provides quantitative information about the biological status of the cells, including cell number, viability and morphology. The system was used to measure cell adhesion and migration using the E-plate and CIM plate respectively. Presence of cells on the electrodes alters the local ionic environment at the electrode/solution interface leading to increased electrode impedance. The more cells attached or the stronger the attachment the higher the impedance.

The impedance is measured using a dimensionless parameter termed Cell Index (CI) which is derived from the relative change in electrical impedance.

Characteristics of this parameter include:

- When cells are not present or are not well-adhered on the electrodes, the CI is zero.
- Under the same physiological conditions, when more cells are attached on the electrodes, the CI values are larger. Thus, CI is a quantitative measure of cell number present in a well.
- Additionally, change in a cell status, such as cell morphology, cell adhesion, or cell viability will lead to a change in CI. Ke N *et al.*, (2011).

([http://www.aceabio.com/UserFiles/doc/literature/20131108\\_xCELLigence\\_Publication\\_List.pdf](http://www.aceabio.com/UserFiles/doc/literature/20131108_xCELLigence_Publication_List.pdf))

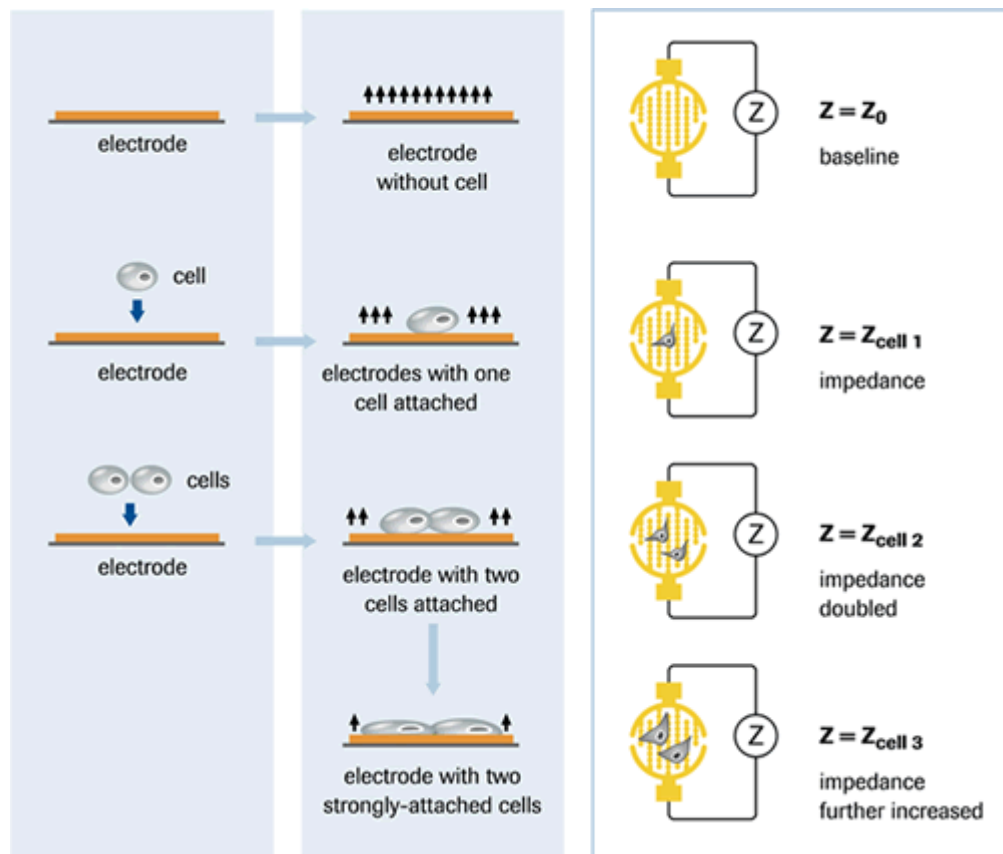


**Figure 2.7:** Schematic diagram explaining Cell Index (CI). Diagram taken from ([www.roche-applied-science.com](http://www.roche-applied-science.com))



**Figure 2.8:** Image of E-Plate (left) and cover (right)

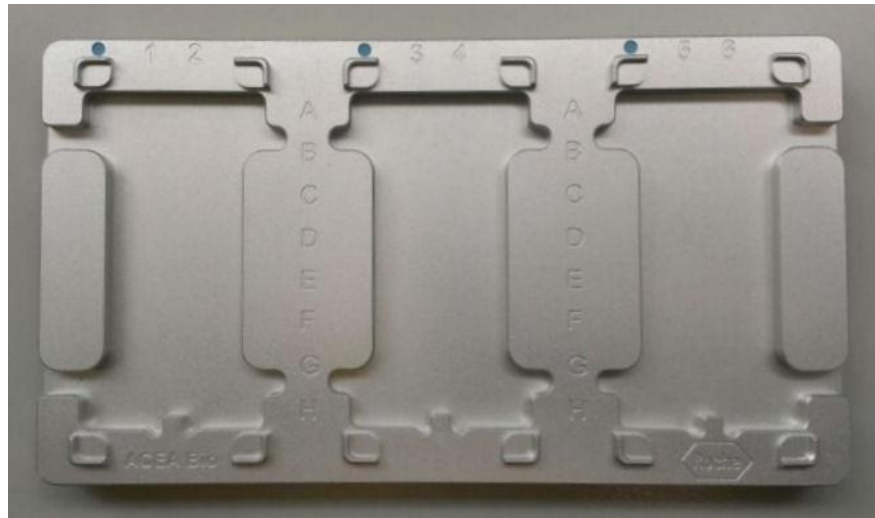


**Figure 2.9:** Image of assembly plate for CIM migration plates.

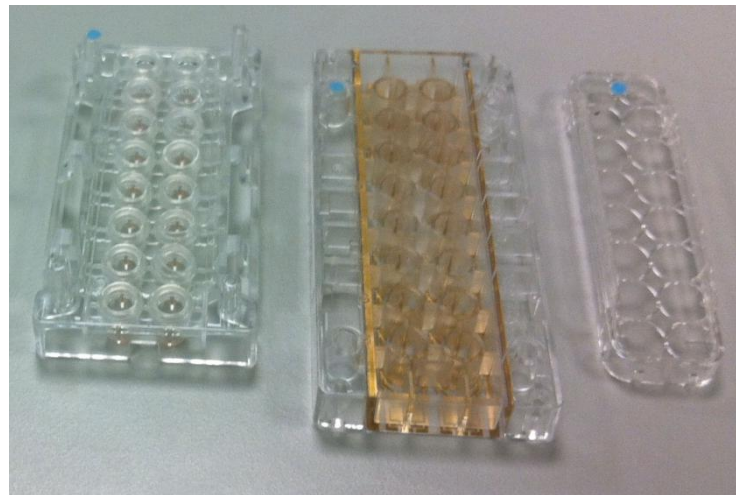


**Figure 2.10:** Image of CIM migration plate. Left: Lower chamber plate containing the chemoattractant. Middle: Upper, electrode containing, chamber plate to which the cell suspension is added. Right: Cover.

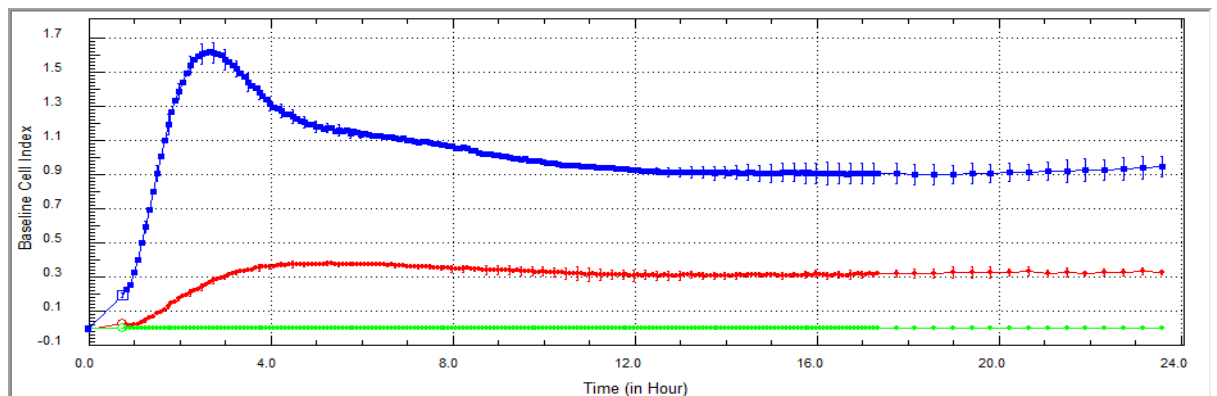


**Figure 2.11:** Typical xCelligence graph depicting CI values (y axis) Vs time in hours (x axis).

### 2.2.10.1.1 Cell Adhesion/Proliferation Assay

E-Plates are single-use, disposable devices used for performing cell-based assays on the xCELLigence system. Each individual well on an E-Plate incorporates a sensor electrode array that allows cells in the well to be monitored and assayed.

- 1) Using a multi-channel pipette, 100  $\mu$ l of full culture media was added to each well of the E-Plate 16. It was important to ensure no air bubbles were introduced and also be careful not to touch the electrodes on the bottom of the well with the tips. Approximately 300  $\mu$ l of de-ionized water was then added to the troughs surrounding the wells. This helped humidify the plate. The plate was then left to equilibrate in the laminar for 30 minutes.
- 2) While the plate was incubating experimental parameters were set up on the RTCA software as follows.
  - Exp Notes tab: Experimental information, purpose, name etc. were entered.
  - Layout tab: Here, wells are highlighted to enter information on the cell number, type, treatment etc. within that well. This is what will decide whether you are doing duplicates or individual well analysis. It is best to set up for a minimum of duplicates.
  - Schedule tab: This is what determines the length of the experiment and timing of intervals between sweeps. Right click on page and choose add step for initial back ground reading. Next right click and add a second step, for a typical adhesion/proliferation experiment 48 sweeps at 15min intervals were selected. This gives monitoring of adhesion over a 12 hour period. A sub step was then added which runs automatically after step 2. In this sub step reading intervals were set at 30 minutes and 192 sweeps giving proliferation monitoring over a 4 day period.
- 3) The equilibrated E-Plate is then inserted into the dock cradle ensuring it was aligned correctly. The background reading was taken by starting step 1.
- 4) The plate was removed and a 100 $\mu$ l of cell suspension was added or a 100 $\mu$ l of media for the no cell controls. The plate was left for 30 minutes in the laminar for cells to settle, with the plate gently tapped to help with even distribution of the cells.
- 5) Following incubation the plate was reinserted to the cradle for a final time and step 2 was started.

### *2.2.10.1.2 Cell Migration/Proliferation Assay*

CIM-Plates are single use, disposable devices used for performing cell invasion and cell migration assays on the instrument. The CIM-Plate 16 comprises a plate cover (lid), an upper chamber and a lower chamber. The upper chamber has 16 wells that are sealed at the bottom with a microporous polyethylene terephthalate (PET) membrane containing microfabricated gold electrode arrays on the bottom side of the membrane. The median pore size of this membrane is 8  $\mu\text{m}$ . The lower chamber has 16 wells, each of which serves as a reservoir for media and any chemo attractant for the cells in corresponding upper chamber wells.

- 1) The metal plate holder was placed in the laminar with the blue alignment dots facing away. The lower chamber of the CIM-Plate was then placed on to the holder. Using a multichannel pipette 160  $\mu\text{l}$  of full serum media was added to the sample wells. For a negative control 160  $\mu\text{l}$  of serum free medium was used in 2 of the 16 wells. No air bubbles were allowed to form.
- 2) The upper (electrode containing) chamber was then clicked in place on top of the lower chamber.
- 3) 50  $\mu\text{l}$  of serum free media was added to each well of the upper chamber; again ensuring no bubbles formed.
- 4) The completed CIM-Plate was then loaded into the xCELLigence system cradle and allowed to equilibrate for one hour.
- 5) During the incubation time the experiment was set up on the RTCA software as described for the cell adhesion/proliferation experiment.
- 6) Following one hour equilibration the one minute background check was conducted.
- 7) 100 $\mu\text{l}$  of cell suspension was then added to each well and 100  $\mu\text{l}$  of media for the no cell control. The plate was left for 30 minutes in the laminar cabinet following addition of cells. After the 30 minute incubation the plate was again loaded into the cradle and step 2 was started.

### 2.2.10.2 Flow Cytometry

Flow cytometry is a sensitive technology which can give a quantitative and qualitative measurement on the size, complexity and condition of a cell. As the name suggests, it involves flowing single cells through a capillary past a point of detection. Detection is typically achieved through use of lasers and detectors. The technology enables studies of a multitude of cell functions such as proliferation, cell cycle and apoptosis. Forward scatter is a measure of the size of the cell, whereas side scatter denotes the granularity of the cell. Fluorescence is the property of a molecule to absorb light and re-emit it at a different wavelength. (Fulwyler *et al.*, 1965; van Engeland *et al.*, 1996).

#### 2.2.10.2.1 Apoptosis Study

Apoptosis is a carefully regulated process of cell death that occurs as part of normal development. In normal live cells, phosphatidylserine (PS) is located on the cytoplasmic surface of the cell membrane. However in apoptotic cells, PS is translocated from the inner to the outer leaflet of the plasma membrane, thus exposing PS to the external cellular environment. The human anticoagulant, annexin V, is a 35-36kDa  $\text{Ca}^{2+}$  dependent phospholipid-binding protein that has a high affinity for PS. Thus annexin V labelled with a fluorophore can identify apoptotic cells by binding to the exposed PS on the outer membrane. In conjunction, red-fluorescent propidium iodide (PI) nucleic acid binding dye is incorporated to the cell population. PI is impermeable to live or apoptotic cells. Thus, after staining a cell population with Alexafluor®488 annexin V and PI, dead cells will show red and green fluorescence, apoptotic cells will show green only and live healthy cells should show little or no fluorescence.

Cells were trypsinised and counted to give a final concentration of  $1 \times 10^6$  /ml. As a positive control apoptosis was introduced by incubating cells with 3.7% para-formaldehyde at room temperature for 15 minutes. PI was used at a concentration of 100µg/ml.

Cells were pelleted at 700RPM for 5 minutes, washed with PBS and re-suspended in 1 x annexin V binding buffer, 100µl per assay. Samples were then incubated with 5µl of Alex Fluor 488 and 1µl of 100µg/ml PI for 15 minutes at room temperature. Following incubation 400µl of 1x annexin V binding buffer was added and samples analysed on a BD FACS Aria.

(<http://tools.lifetechnologies.com/content/sfs/manuals/mp13199.pdf>)

For initial experiments to set gates and flow parameters 5 samples were prepared, 4 of which were controls, as shown in table 2.13.

**Table 2.13:** Staining parameters of samples for optimization.

Live Cells	Dead Cells
Unstained	Stained with PI and Alexa Fluor 488
Stained with PI and Alexa Fluor 488	Stained with PI only
-----	Stained with Alexa Fluor 488 only

#### 2.2.10.2.2 Proliferation Study

Measuring a cell's ability to proliferate is a fundamental method for assessing cell health and investigating diseases such as atherosclerosis. The most accurate way is to measure newly synthesised DNA.

#### **Clik-iT® EdU**

The Clik-iT EdU flow cytometry assay kit is a novel alternative to BrdU incorporation. It uses a 5-ethynyl-2' – deoxyuridine nucleoside analog to thymidine. This is incorporated into the DNA during active DNA synthesis. Detection is based on a click reaction, a copper catalyzed covalent reaction between an azide and an alkyne. In this assay the alkyne is found in the ethynyl moiety of EdU, while the azide is coupled to Alexa Fluor 488 dye.

(<http://tools.lifetechnologies.com/content/sfs/manuals/mp10338.pdf>)

Cells were trypsinised and counted then placed in suspension with 4ml of full growth medium. A final concentration of 10 µM EdU was added to the cell suspensions which were then incubated for two hours at 37°C, 5%CO<sup>2</sup>. Cells were then pelleted and washed with 1% BSA PBS. Pellet was re-suspended in 100µl Clik-iT fixative, 4% formaldehyde, at room temperature protected from the light for 15 minutes. Cells were again pelleted and washed with 1% BSA PBS. The pellet was then re-suspended in



100µl 1x saponin based permeabilisation and wash reagent and incubated at room temperature for 15 minutes.

During this incubation the “Click-iT® reaction cocktail” was prepared as shown in table 2.14.

**Table 2.14:** Recipe for Click-iT® reaction cocktail

Reaction Component	Number of reactions
	1
PBS	438µl
CuSo <sub>4</sub>	10 µl
Fluorescent Dye Azide 488	2.5 µl
Reaction Buffer	50 µl
Total Reaction Volume	500 µl

0.5ml of this reaction cocktail was added per sample and protected from the light. The sample was incubated at room temperature for 30 minutes. Cells were then pelleted and washed with 3mls of 1% BSA PBS and the supernatant was removed. Cells were pelleted one last time and re-suspended in 600 µl of 1x saponin based permeabilisation and wash reagent. The samples were then analysed on the BD FACS Aria.

#### 2.2.11 Statistical analysis

Results are expressed as mean  $\pm$ sem. Experimental points were performed in triplicate with a minimum of three independent experiments (n=3). Statistical comparisons between controls versus treated groups were performed using One-way Anova and by Student’s unpaired t-test. A value of \*P $\leq$ 0.05 or  $\delta$ P $\leq$ 0.05 was considered significant.

## CHAPTER THREE: Characterisation of the impact of cyclic strain on HAoSMCs

### 3.1 Introduction

Vessels, particularly arterial vessels, experience mechanical or haemodynamic force as a direct result of the pulsatile nature of blood flow *in vivo*. Physiological intraluminal pressure is essential to ensure homeostasis within the vessel (Lehoux *et al.*, 2006; Birukov *et al.*, 1998).

Change in any parameter of haemodynamic force can have a pathological consequence for the blood vessel. For example, persons suffering from prolonged hypertension are at greater risk of developing atherosclerotic plaques resulting from migrating smooth muscle cells (Timmins *et al.*, 2011). Atherosclerosis results from the development and progression of atherosclerotic plaques. These plaques can be classified as either stable or unstable, depending on their composition. Stable plaques are predominantly composed of synthetic migrating SMCs which have transcended through the endothelium into the luminal space.

Vascular smooth muscle cells (VSMCs) are primarily responsible for regulating vascular tone and blood pressure. They possess a unique plasticity which allows them to reversibly differentiate between a synthetic and contractile phenotype. This is known as phenotypic modulation. The synthetic form is characterised by a proliferating migratory phenotype, while cells in the contractile state are predominantly quiescent. This phenomenon appears to be as a result of both environmental cues, such as haemodynamic pressure and innate genetic pathways (Owens *et al.*, 1995). Expression of specific contractile cell markers such as SM  $\alpha$ -actin, Smoothelin, Calponin and myosin heavy chain (MHC) can be used to determine SMC phenotype.

Ironically, the procedures used to reopen occluded atherosclerotic vessels such as stenting or balloon angioplasty, often result in damaging surrounding vascular cells and an increase in the pressure on the vessel wall. This heightened force on the VSMCs can result in a synthetic migratory phenotype ultimately leading to restenosis (Taylor *et al.*, 2000).

As a result, a myriad of *in vitro* investigations into the mechanical sensitivity of VSMCs has been performed using deformable substrates (Brown *et al.*, 2000). These have attempted to elucidate both the molecular mechanisms in which SMCs convert mechanical stimulation into a cell response and also the direct impact of cyclic strain on SMC phenotype (Haga *et al.*, 2006). The results have demonstrated that cyclic strain undoubtedly regulates SMC growth, however, to what extent and direction remains ambiguous. This is due to conflicting data, exemplified by both an increase and decrease in VSMC proliferation following exposure to cyclic strain (Hipper *et al.*, 2000; Birukov *et al.*, 1995).

Coincidentally, a definitive extent of mechanical parameters which elicit a specific reproducible cell response and function remains to be fully elucidated. Therefore, work carried out in this chapter was designed to assess the specific impact of cyclic strain and deformation on VSMC injury and phenotype.

### **3.1.1 Chapter Hypothesis**

Mechanical cyclic strain regulates VSMC health as well as expression of VSMC contractile genes, specifically SM  $\alpha$ -actin, Smoothelin and Calponin in human aortic smooth muscle cells (HAoSMCs).

### **3.1.2 Specific aims and Experimental Approach:**

To test this hypothesis, experiments included in this chapter were designed to:

- Characterise and confirm the HAoSMC lineage through use of cell specific markers.
- Determine which extracellular matrix (ECM) facilitated the longest adhesion of HAoSMCs on the silicone membrane flex plates which are required for application of cyclic strain.
- Explore the impact of cyclic strain on HAoMSC phenotype and assess its pathophysiological properties on the cell by quantifying expression of injury and contractile markers.

Cyclic strain was applied by adhering cells to a flexible silicone membrane to which a vacuum is applied stretching the membrane over a fixed loading post. Injury markers quantified were Fibroblast Growth Factor-2 (FGF-2) and Thrombomodulin (TM). HAoSMC phenotype was determined by quantification of expression of the contractile markers SM  $\alpha$ -actin, Smoothelin and Calponin at both mRNA and protein level.

## 3.2 Results

### 3.2.1 Characterisation of Human Aortic Smooth Muscle Cells (HAoSMCs)

#### 3.2.1.1 Investigation of SMC lineage through use of cell specific markers

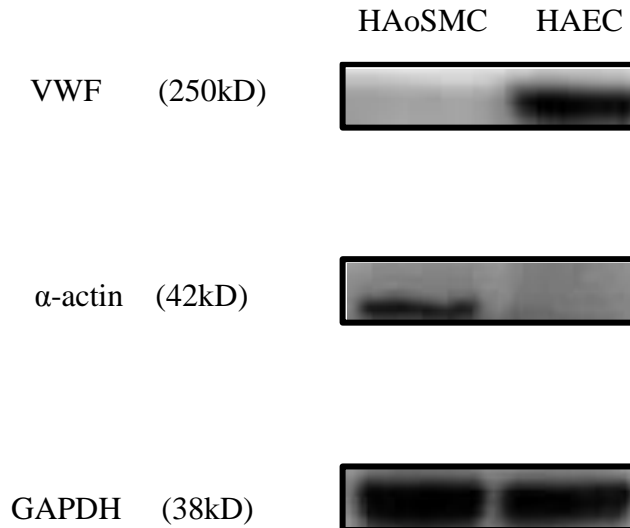


**Figure 3.1: Western Blot for Cell Specific Markers.** **Top:** shows presence of Von Willebrand Factor (VWF) in Human Aortic Endothelial Cells (HAEC) and absence in Human Aortic Smooth Muscle Cells (HAoSMC). **Centre:** shows presence of smooth muscle specific  $\alpha$ -actin in HAoSMC and absence in HAEC. **Bottom:** Shows GAPDH positive control.

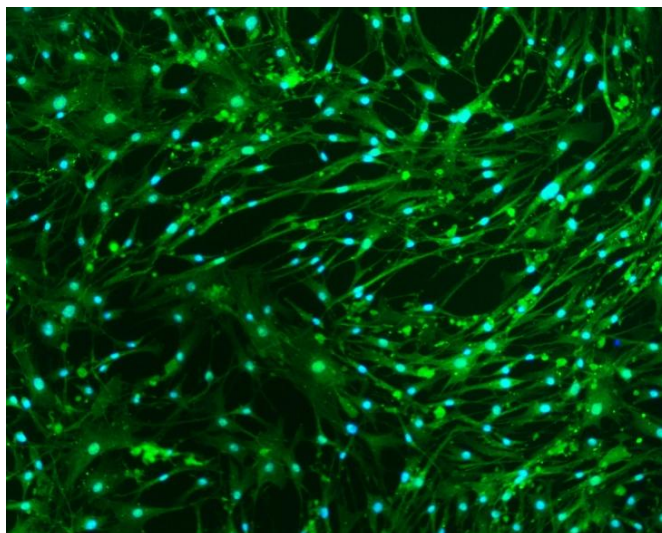


**Figure 3.2: Immunohistochemistry of  $\alpha$ -actin (10X Magnification).** HAoSMC were fixed to a glass slide using 3.7% paraformaldehyde. Cells were then incubated with AlexFluor 488 conjugate secondary Ab to bind to the smooth muscle specific  $\alpha$ -actin Ab. The nucleus was also imaged using nuclear stain DAPI (blue).

### 3.2.1.2 Adhesion profiles of HAoSMCs

In order to subject the HAoSMCs to cyclic strain, they were seeded on to the flexible silicone membrane of the Flexcell® plates. The silicone membrane, however, has a hydrophobic property making prolonged adhesion (>24hr) of HAoSMCs difficult. To overcome this, adhesion profiles were created on the xCELLigence real time impedance system for a range of extracellular matrices (ECMs) and coating factors. This enabled an ECM or coating factor, which would provide optimal adhesion and attachment to be selected.

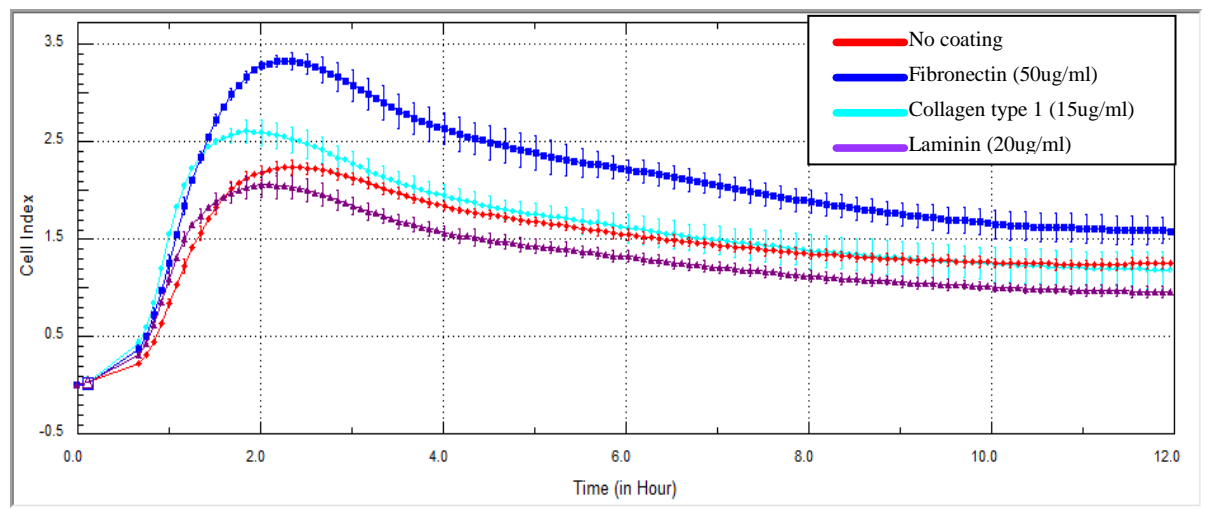


**Figure 3.3: xCELLigence plot of HAoSMC adhesion.** Adhesion profile of HAoSMC on several ECM and coating factors. Experiment was conducted over a 12 hour time point. Red - No Coating, Blue – Fibronectin (50µg/ml), Light Blue – Collagen Type I (15 µg/ml), Purple - Laminin (20 µg/ml) n=3.

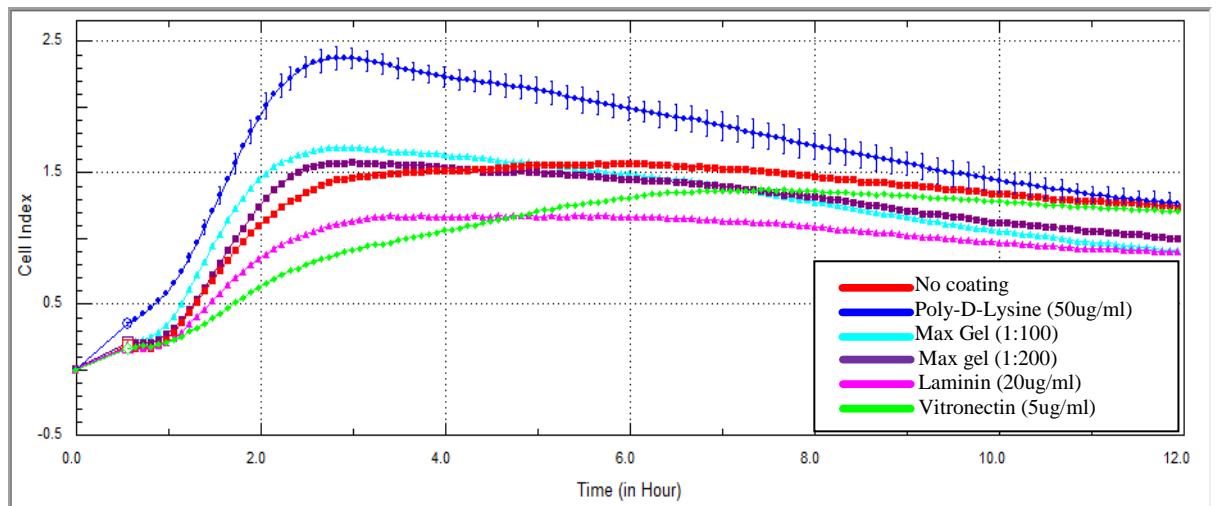
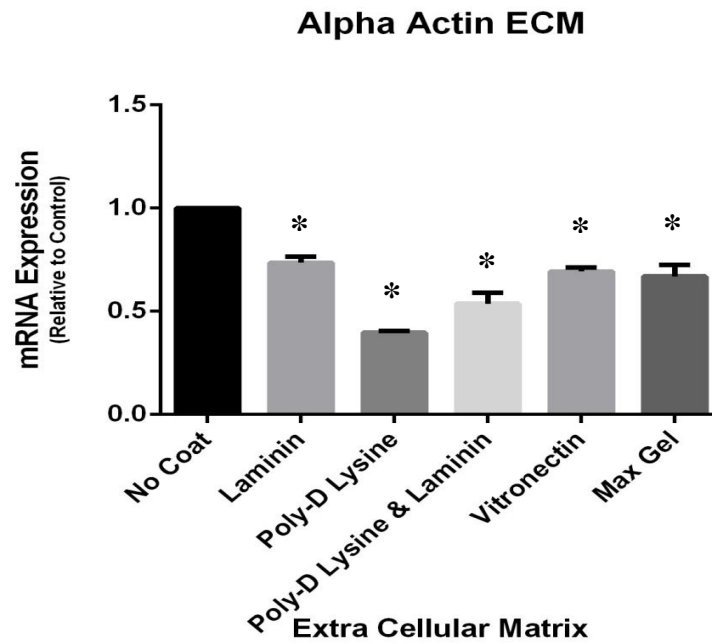


**Figure 3.4: xCELLigence plot of HAoSMC adhesion.** Adhesion profile of HAoSMC on several ECM and coating factors. Experiment was conducted over a 12 hour time point. Red – No Coating, Blue – Poly – D – Lysine (50 $\mu$ g/ml), Light Blue -1:100 dilution of Max Gel, Purple – 1:200 dilution of Max Gel, Pink – Laminin (20  $\mu$ g/ml), Green Vitronectin (5  $\mu$ g/ml) n=3.

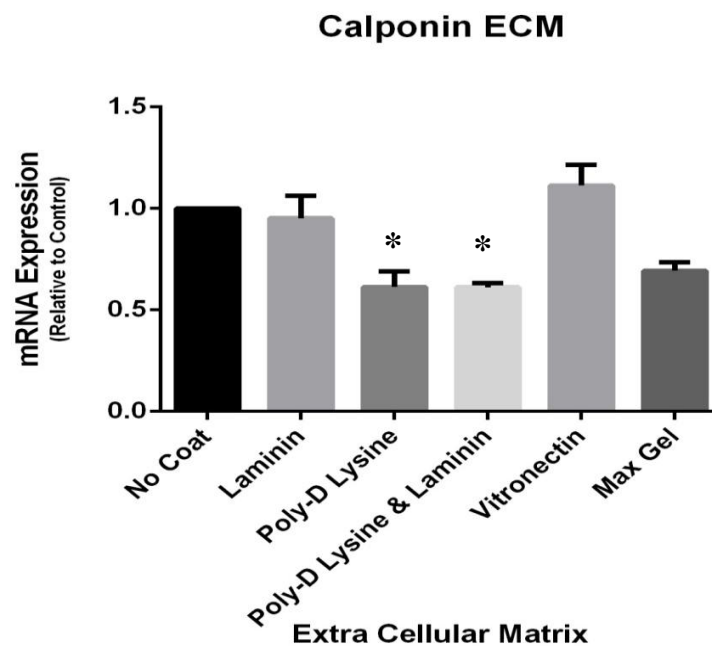
### 3.2.1.3 The effect of ECMs and coating factors on contractile gene expression

To assess if the ECMs and coating factors had an impact on HAoSMC phenotype, transcript expressions of SM  $\alpha$ -actin, Smoothelin and Calponin were quantified in total RNA extracted from the cells.

**A**



**B**



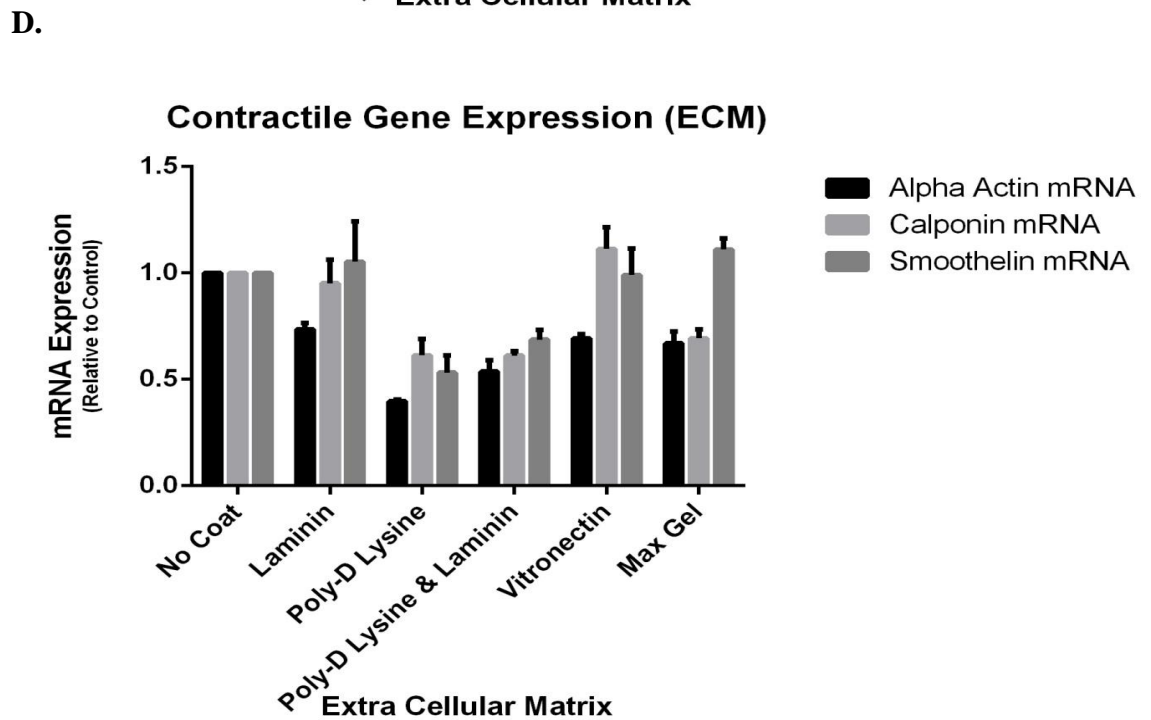
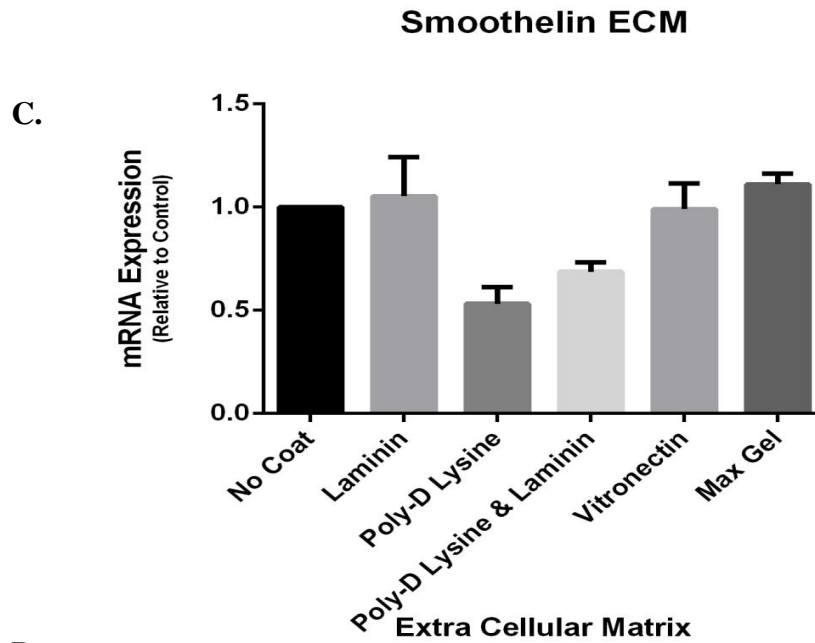


**Figure 3.5: mRNA Expression of Contractile Genes.** **A** – Alpha Actin mRNA expression from HAoSMC coated on various extra cellular matrices. n=3,  $*P \leq 0.05$  vs. no coating; one-way Anova. **B** - Calponin mRNA expression from HAoSMC coated on various extra cellular matrices. n=3  $*P \leq 0.05$  vs. no coating; one-way Anova. **C** - Smoothelin mRNA expression from HAoSMC coated on various extra cellular matrices. n=3, data just outside statistical significance. **D** – Comparative analysis of contractile genes expression on several ECM and coating factors. n=3.



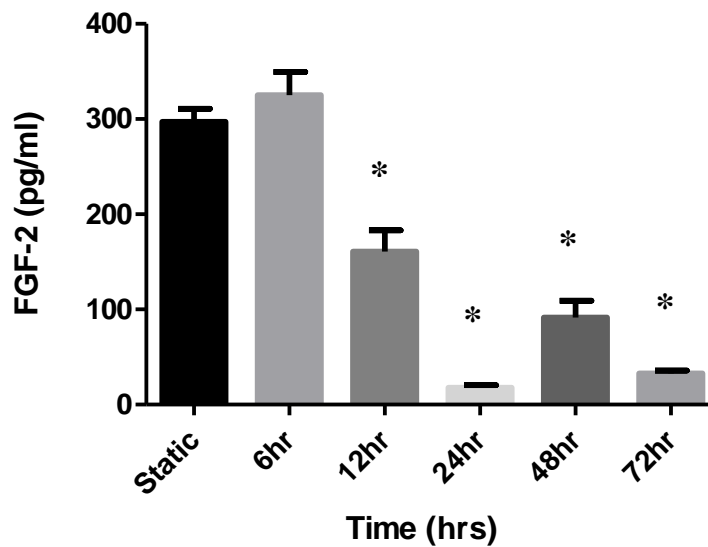
### 3.2.2 Injury Marker Expression

Expression of *in vitro* SMC injury markers Fibroblast Growth Factor -2 (FGF-2) and Thrombomodulin were quantified to assess any HAoSMC injury resulting from cyclic deformation at 5% and 10% amplification. Expression levels of these proteins were quantified in both culture medium and cell lysate using ELISA and western blot.

#### 3.2.2.1 Secreted Fibroblast Growth Factor -2 (FGF-2)

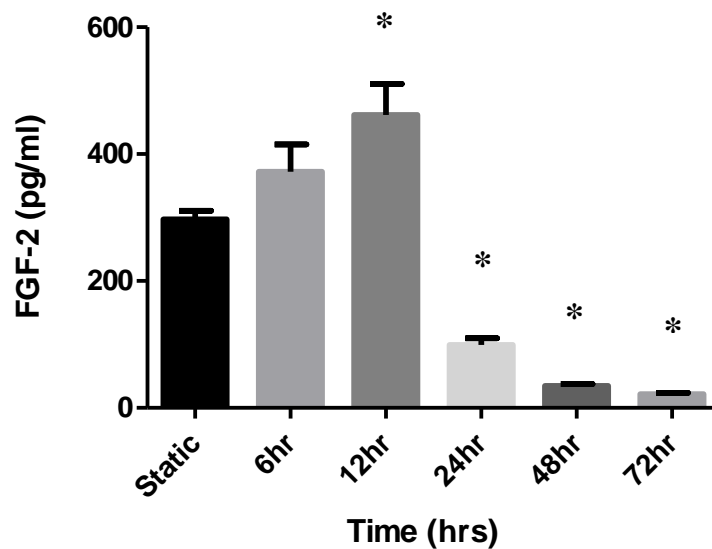
A.

#### Cell Media FGF-2 10% Cyclic Strain



B.

#### Cell Media FGF-2 5% Cyclic Strain



C.

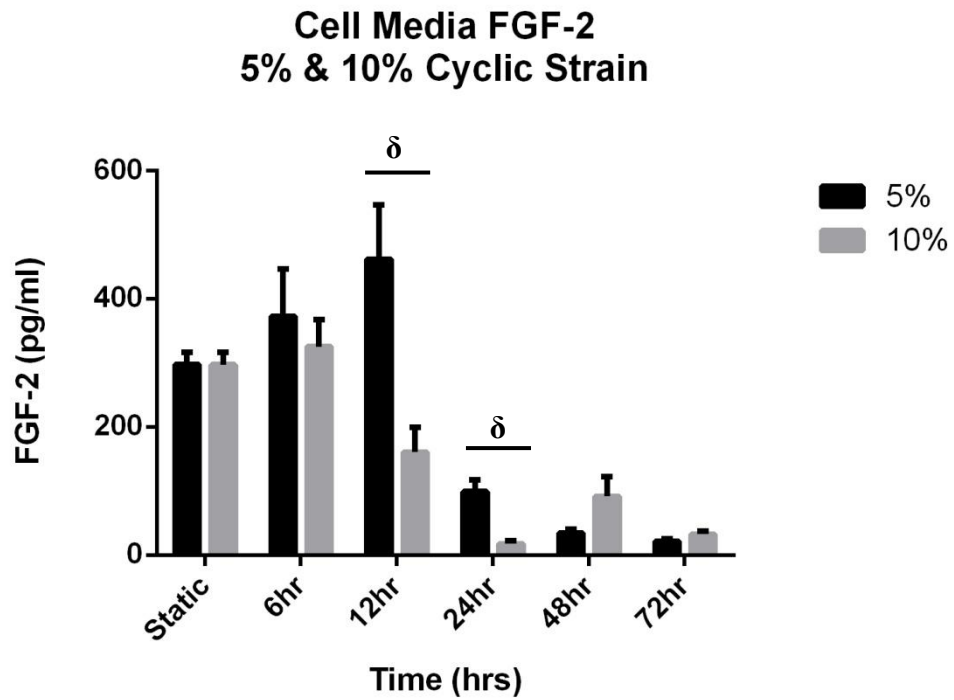


**Figure 3.6: ELISA analysis of secreted Fibroblast Growth Factor- 2 (FGF-2).** A – FGF-2 levels quantified in HAoSMC media, cells were exposed to 10% cyclic strain over a time course of 72 hours. n=3, \* $P \leq 0.05$  vs. static adhesion; one-way Anova **B** - FGF-2 levels quantified in HAoSMC media, cells were exposed to 5% cyclic strain over a time course of 72hours. n=3, \* $P \leq 0.05$  vs. static adhesion; one-way Anova **C** – Comparative analysis of levels of FGF-2 in HAoSMC media, cells were exposed to 5% and 10% cyclic strain over 72 hours. n=3,  $\delta P \leq 0.05$  pairwise; t-test.

### 3.2.2.2 Cellular Lysate Fibroblast Growth Factor -2 (FGF-2)

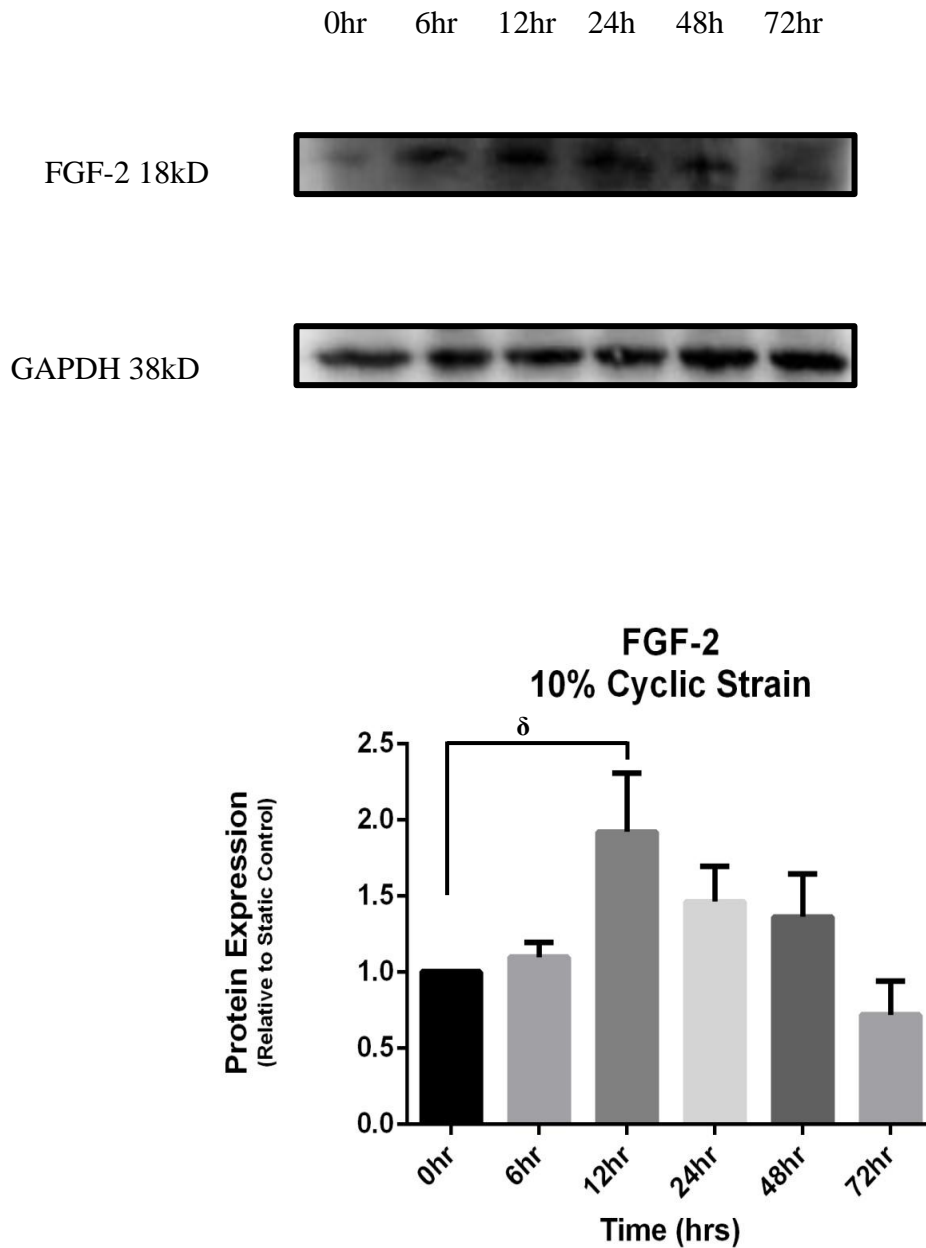


**Figure 3.7: Western Blot of HAoSMC Lysate.** Blots are for SMC injury marker Fibroblast Growth Factor -2 (FGF-2) and endogenous loading control GAPDH. HAoSMC were exposed to 10% cyclic strain over a time course of 72 hours. FGF-2 was quantified from cell lysate. Values are normalized for loading bias using GAPDH endogenous control and calibrated against 0hr. n=3,  $\delta P \leq 0.05$ ; pairwise t-test.

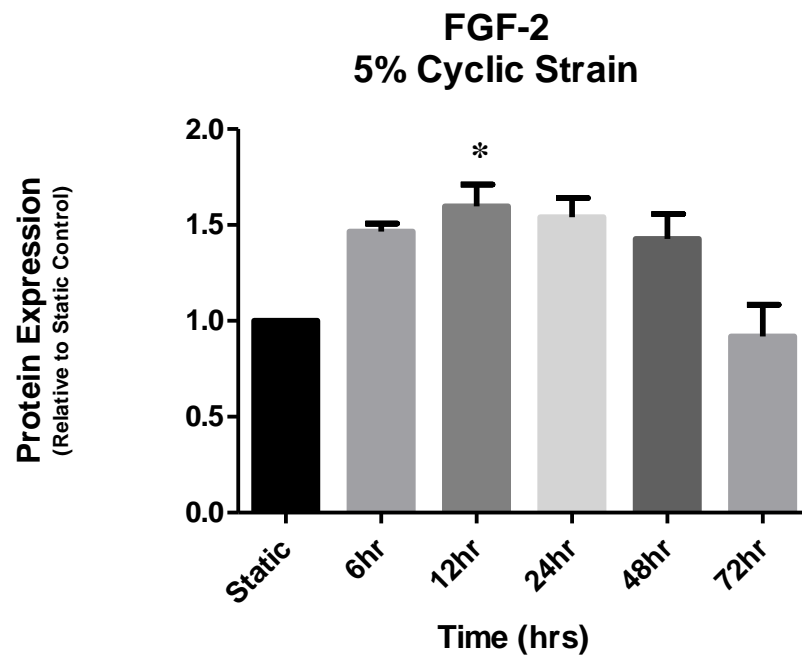
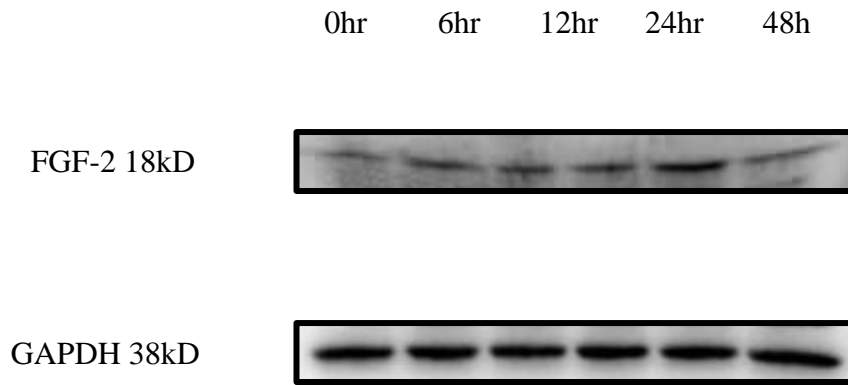


**Figure 3.8: Western Blot of HAoSMC Lysate.** Blots are for SMC injury marker Fibroblast Growth Factor -2 (FGF-2) and endogenous loading control GAPDH. HAoSMC were exposed to 5% cyclic strain over a time course of 72 hours. FGF-2 was quantified from cell lysate. Values are normalized for loading bias using GAPDH endogenous control and calibrated against 0hr. n=3, \* $P \leq 0.05$  vs. static adhesion; One-way Anova.

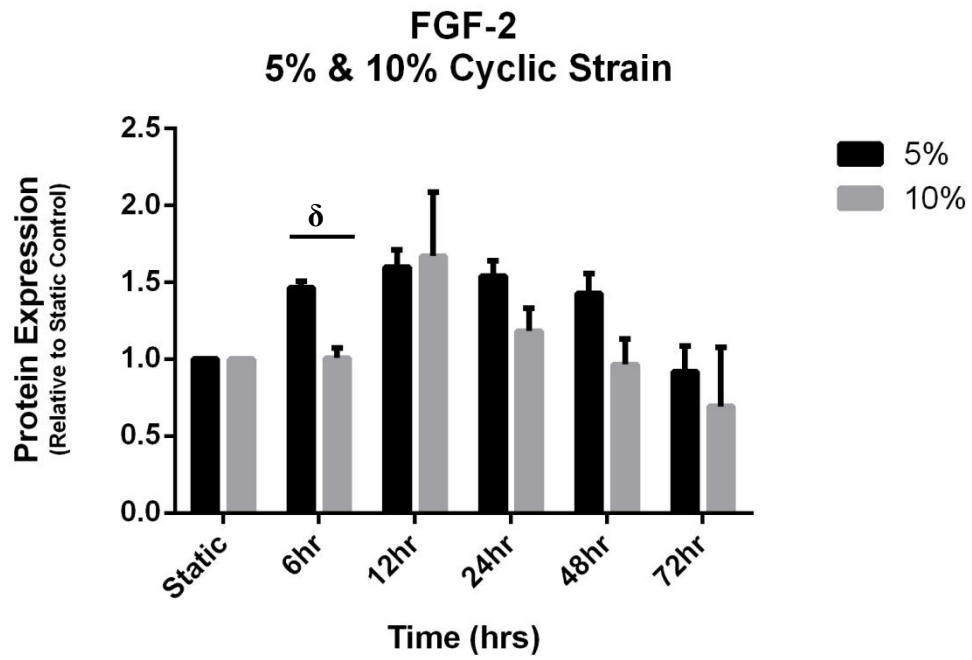


**Figure 3.9:** Grouped data from figures 3.7 & 3.8. Comparative analysis of FGF-2 expression in lysate from HAoSMCs exposed to 5% and 10% cyclic strain over 72 hours.  $n=3$ ,  $\delta P \leq 0.05$ ; pairwise t-test.

### 3.2.2.3 Secreted Thrombomodulin (TM)

The second injury marker utilised was Thrombomodulin (TM), a robust endothelial cell marker which is also known to be expressed by SMC in culture. Levels of TM in HAoSMC lysate and media was quantified using a sandwich ELISA.

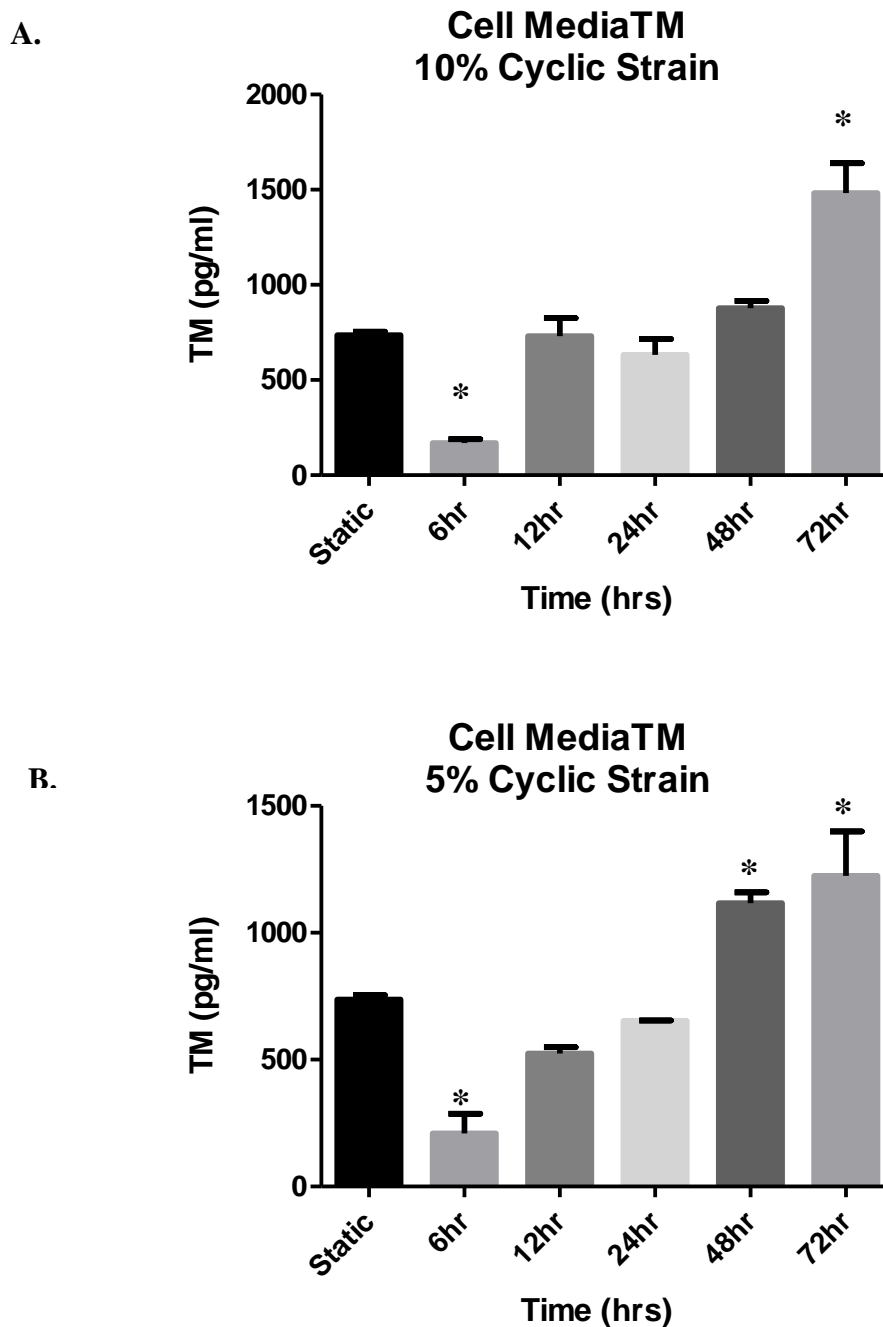
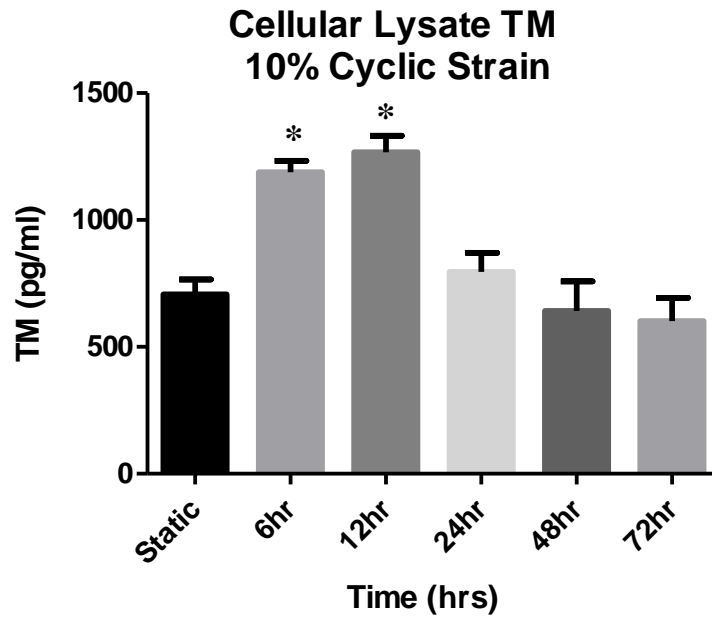


**Figure 3.10: ELISA analysis of secreted Thrombomodulin (TM).** Levels of Thrombomodulin were quantified in media from HAoSMCs exposed to strain. **A** – HAoSMC exposed to 10% cyclic strain over a time course of 72 hours. n=3, \* $P \leq 0.05$  vs. static adhesion; one-way Anova **B** - HAoSMC exposed to 5% cyclic strain over a time course of 72 hours. n=3, \* $P \leq 0.05$  vs. static adhesion; one-way Anova.

3.2.2.4 Cellular Lysate Thrombomodulin (TM)

A.



B.

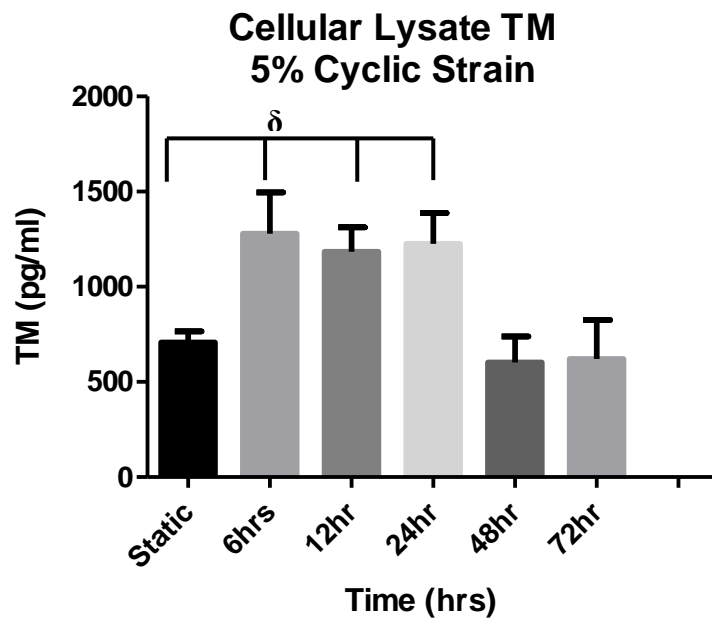


**Figure 3.11: ELISA analysis of total cellular Thrombomodulin (TM).** Levels of total cellular Thrombomodulin were quantified in lysates of HAoSMCs exposed to strain. **A** – HAoSMC exposed to 10% cyclic strain over a time course of 72hours.  $n=3$ ,  $*P\leq 0.05$  vs. static adhesion; one-way Anova. **B** - HAoSMC exposed to 5% cyclic strain over a time course of 72 hours.  $n=3$ ,  $\delta P\leq 0.05$ ; pairwise t-test.

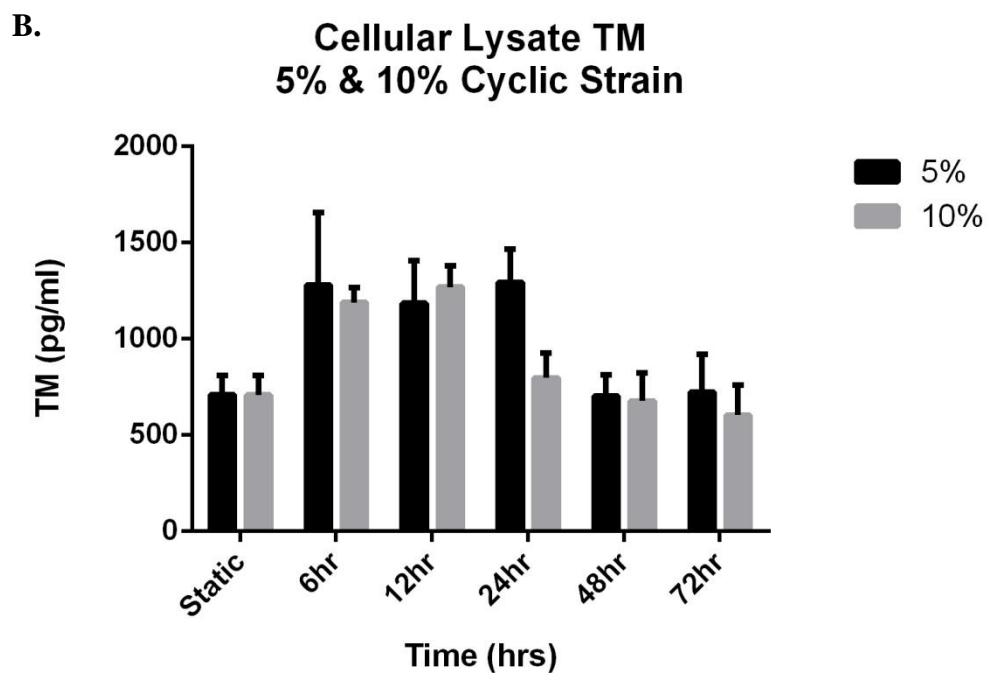
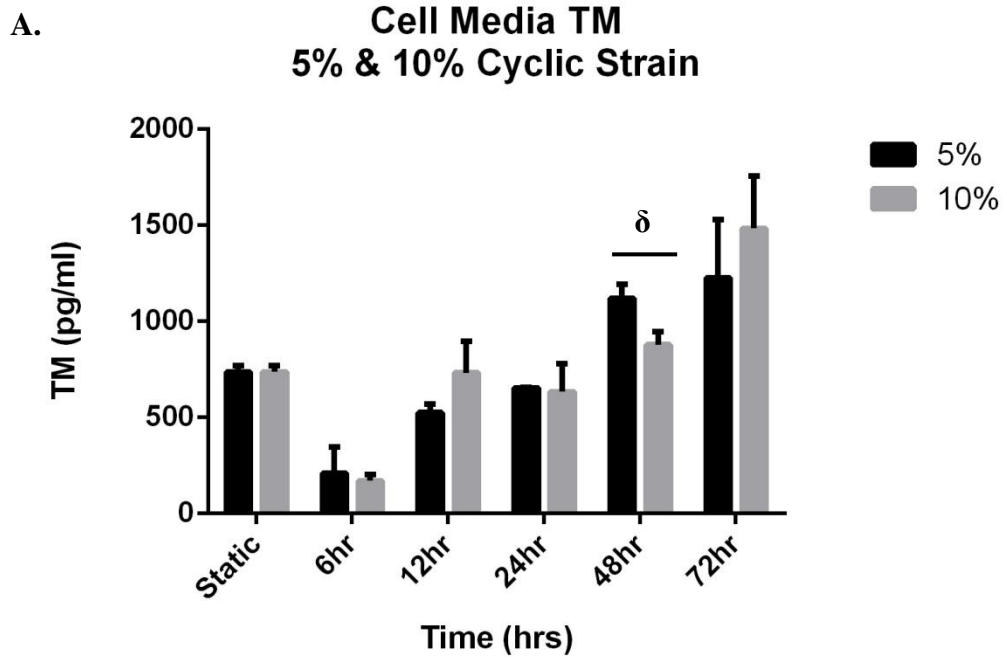
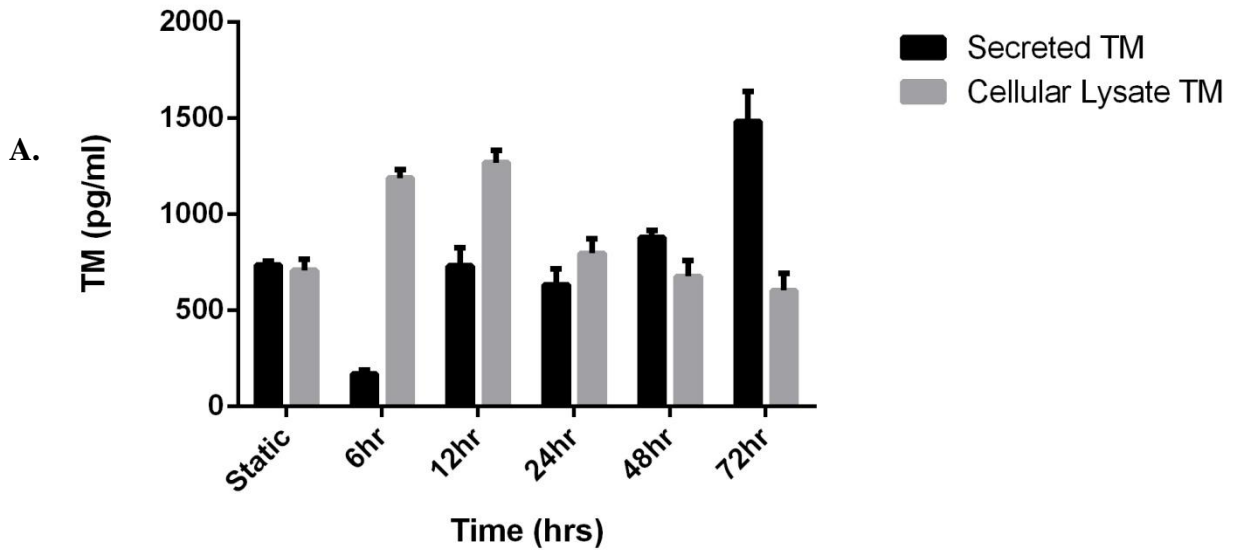


**Figure 3.12:** **A** – Comparative analysis of TM expression in culture media of HAoSMCs exposed to 5% and 10% cyclic strain.  $n=3$ ,  $\delta P \leq 0.05$ ; pairwise t-test. **B** – Comparative analysis of TM expression in total cell lysate of HAoSMCs exposed to 5% and 10% cyclic strain.



### Cellular Lysate and Media TM Expression 10% Cyclic Strain



### Cellular Lysate and Media TM Expression 5% Cyclic Strain

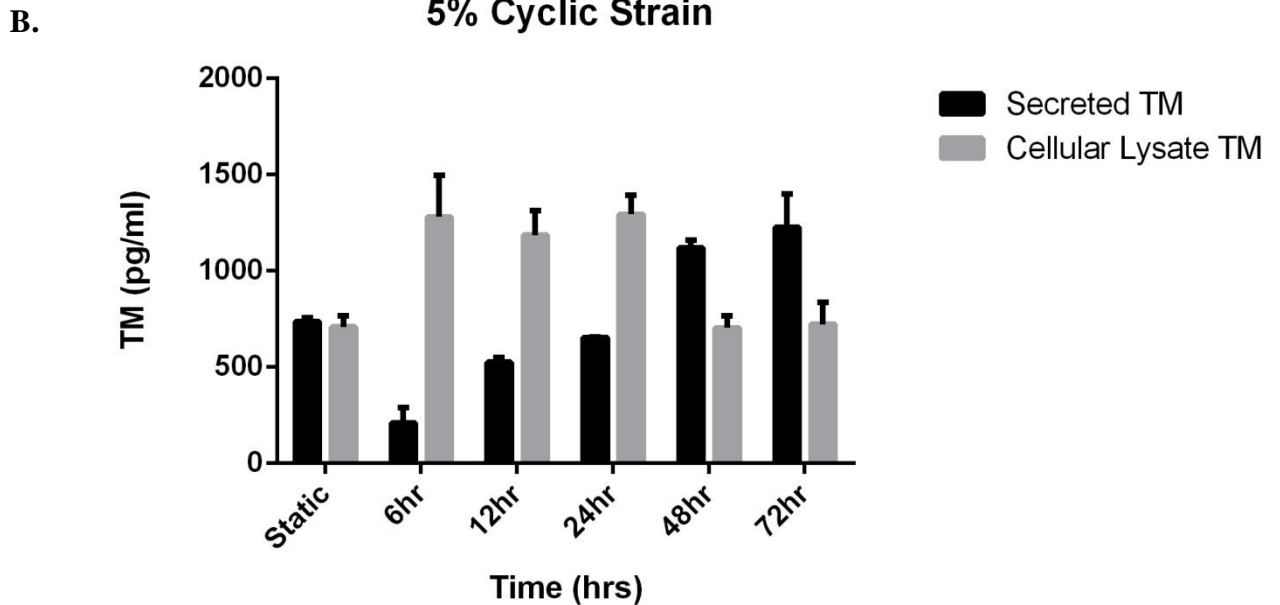


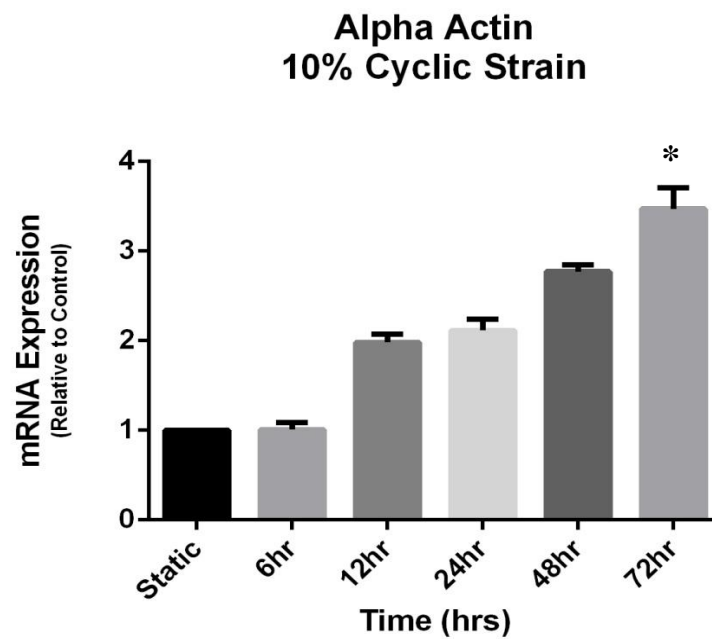
**Figure 3.13 A** - Comparative analysis of TM expression in HAoSMC media and cell lysate of cells exposed to 10% strain over 72 hours. **B** - Comparative analysis of TM expression in HAoSMC media and cell lysate of cells exposed to 5% strain over 72 hours.

### 3.2.3 Investigation of phenotype modulation of HAoSMCs

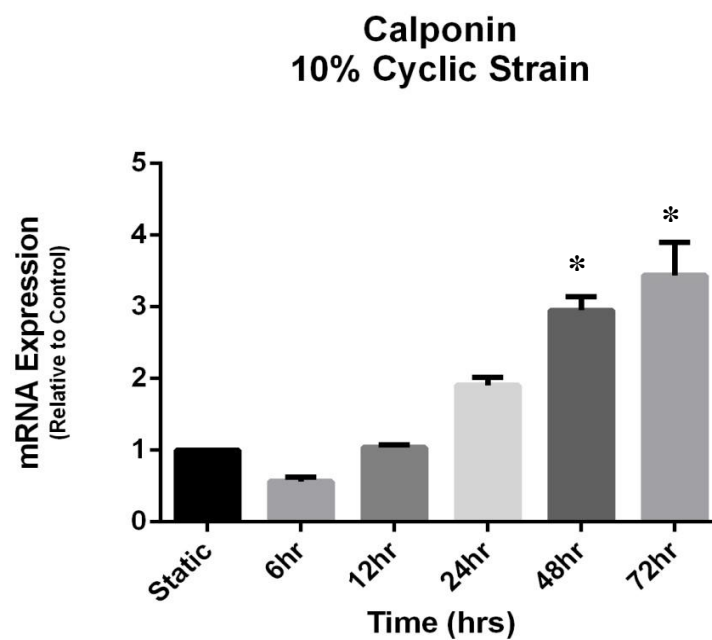
To assess the effect of cyclic strain on HAoSMC phenotype, the expression of three contractile markers was quantified. These were; Smooth Muscle Alpha Actin, Calponin and Smoothelin. Following strain, both gene and protein expression were quantified through the use of specific primers and antibodies for SM  $\alpha$ -actin and calponin, while only gene expression was quantified for smoothelin as the protein detection in cell lysate was unreliable.

#### 3.2.3.1 Gene expression of contractile markers

A.



B.



C.

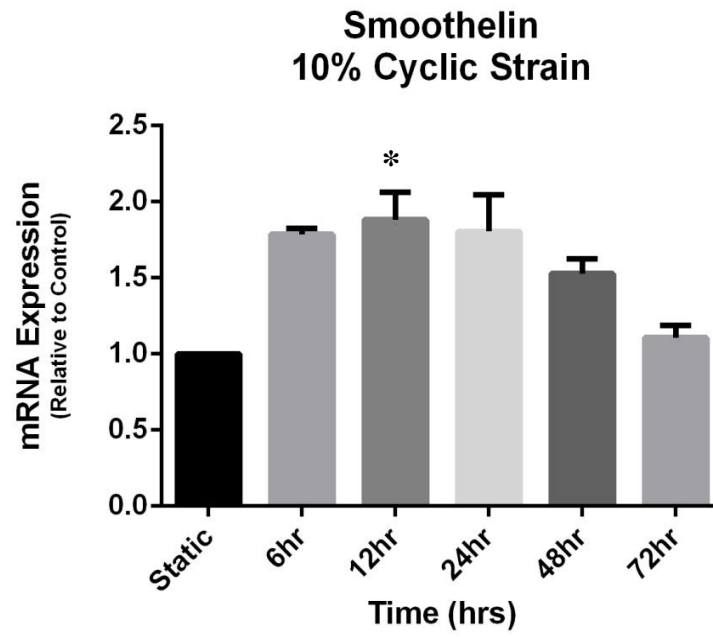


**Figure 3.14: Expression of contractile genes in total HAoSMC RNA. A, B & C** Alpha Actin, Calponin and Smoothelin mRNA expression from HAoSMC exposed to 10% cyclic strain over a 72 hour time course, respectively. n=3, \* $P \leq 0.05$  vs. static adhesion ; one-way Anova.

### 3.2.3.2 Protein expression of contractile markers

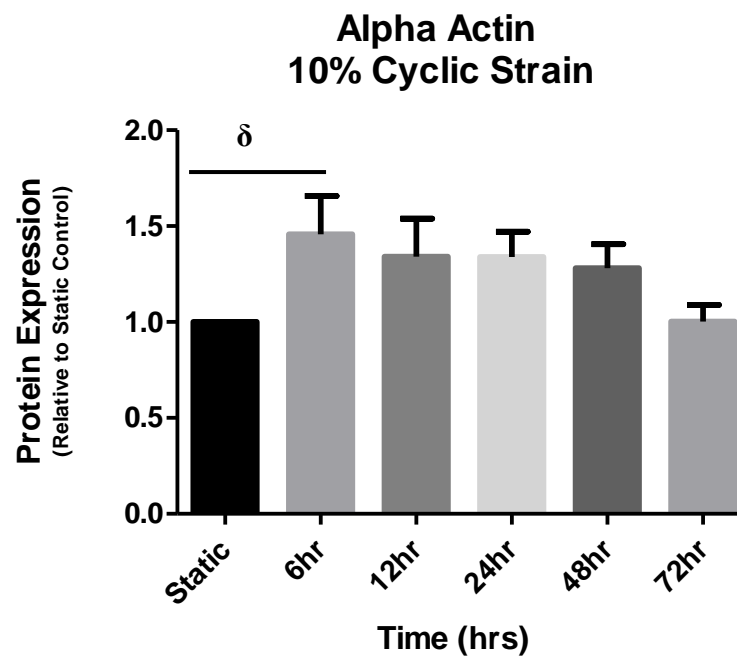
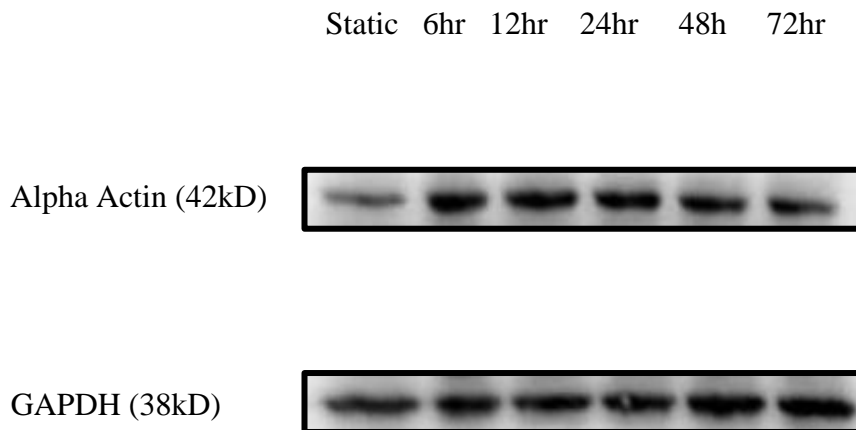


**Figure 3.15: Western Blot of HAoSMC Lysate.** Blots for SMC contractile marker Alpha Actin and endogenous loading control GAPDH. HAoSMC were exposed to 10% cyclic strain over a time course of 72 hours. Values are normalized for loading bias using GAPDH endogenous control and calibrated against 0hr.  $n=3$ ,  $\delta P \leq 0.05$ ; pairwise t-test.

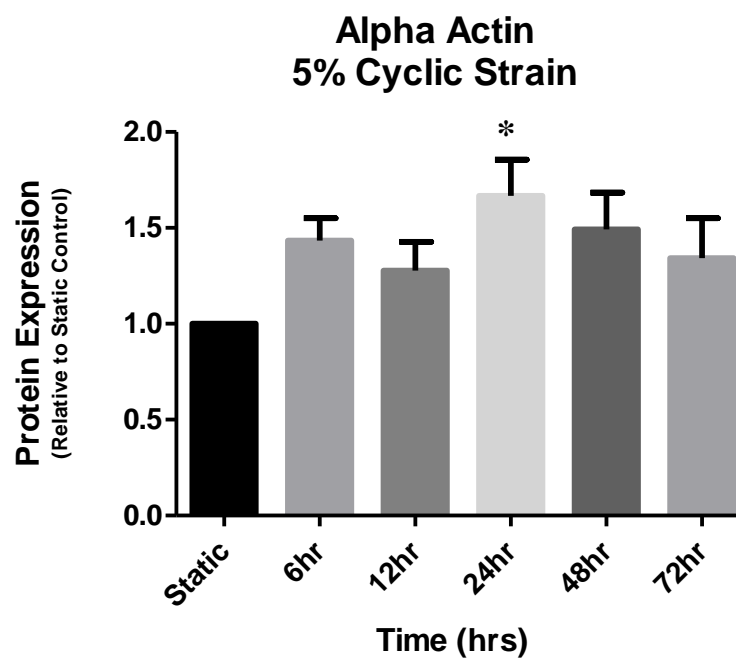
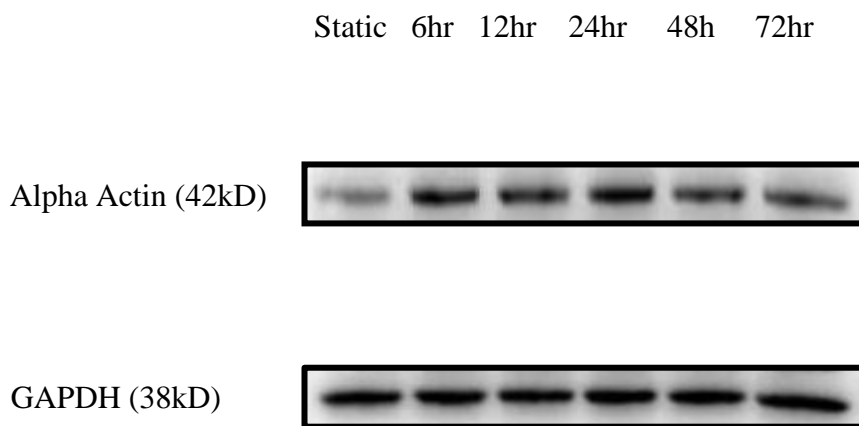


**Figure 3.16: Western Blot of HAoSMC Lysate.** Blots for SMC contractile marker Alpha Actin and endogenous loading control GAPDH. HAoSMC were exposed to 5% cyclic strain over a time course of 72 hours. Values are normalized for loading bias using GAPDH endogenous control and calibrated against 0hr.  $n=3$ ,  $*P \leq 0.05$  vs. static adhesion; one-way Anova.

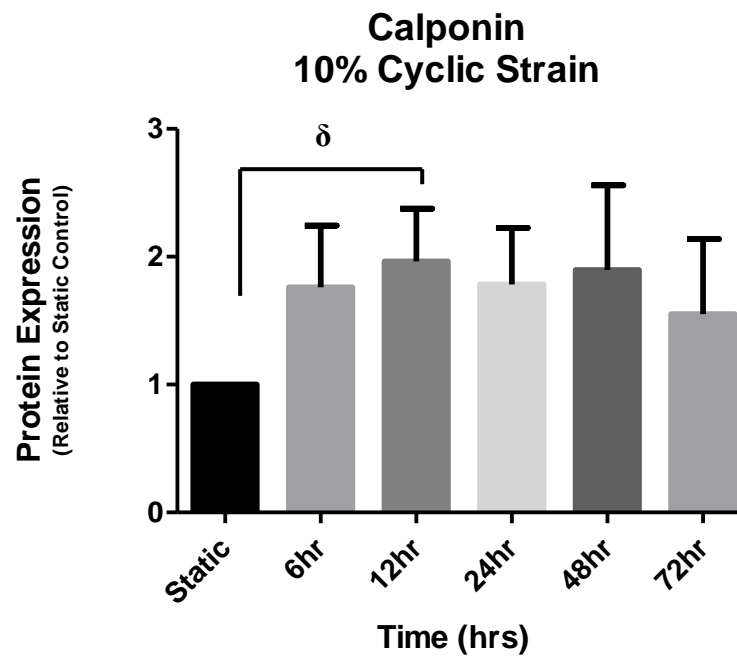
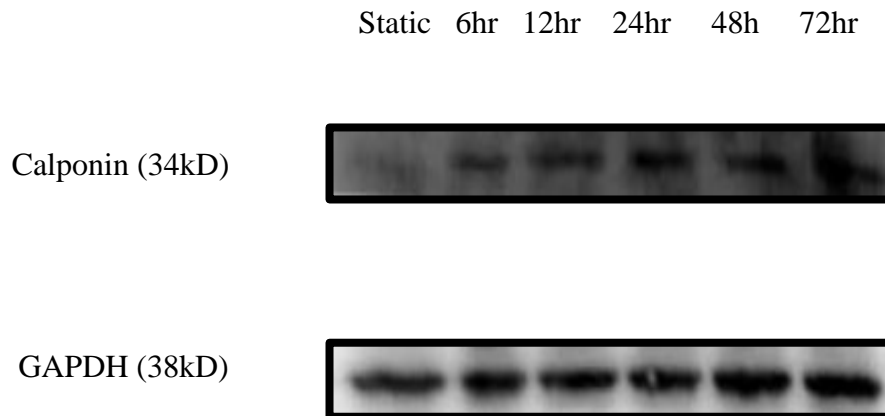


**Figure 3.17: Western Blot of HAoSMC Lysate.** Blots for SMC contractile marker Calponin and endogenous loading control GAPDH. HAoSMC were exposed to 10% cyclic strain over a time course of 72 hours. Values are normalized for loading bias using GAPDH endogenous control and calibrated against 0hr.  $n=3$ ,  $\delta P \leq 0.05$ ; pairwise t-test.

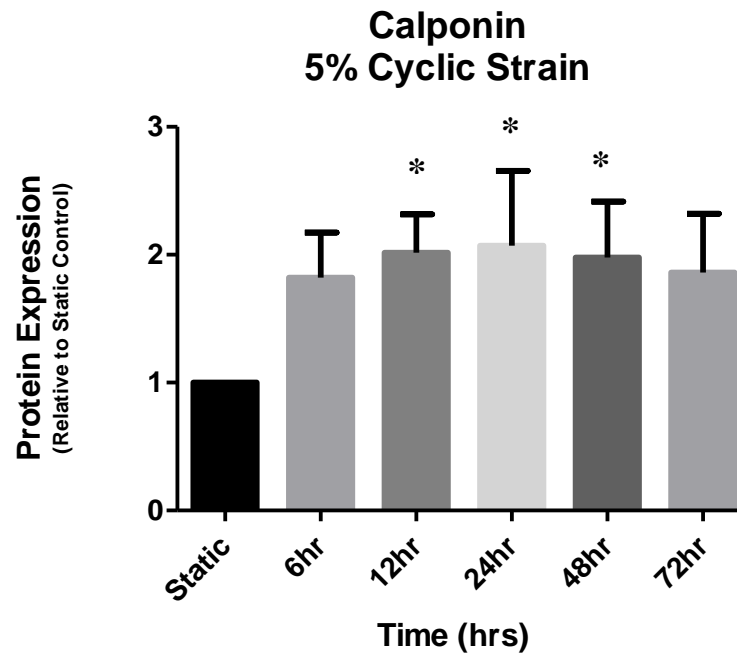
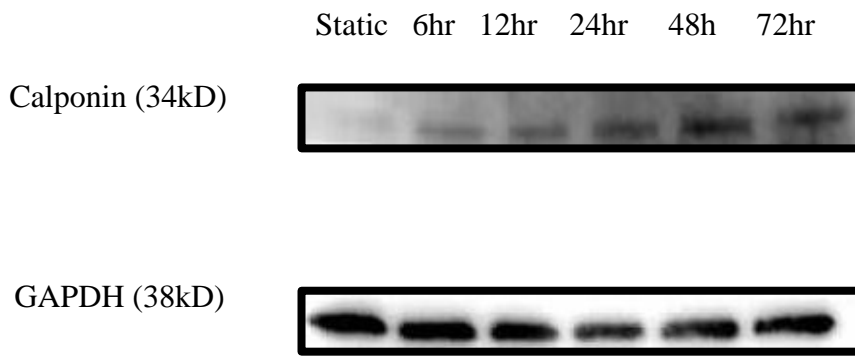
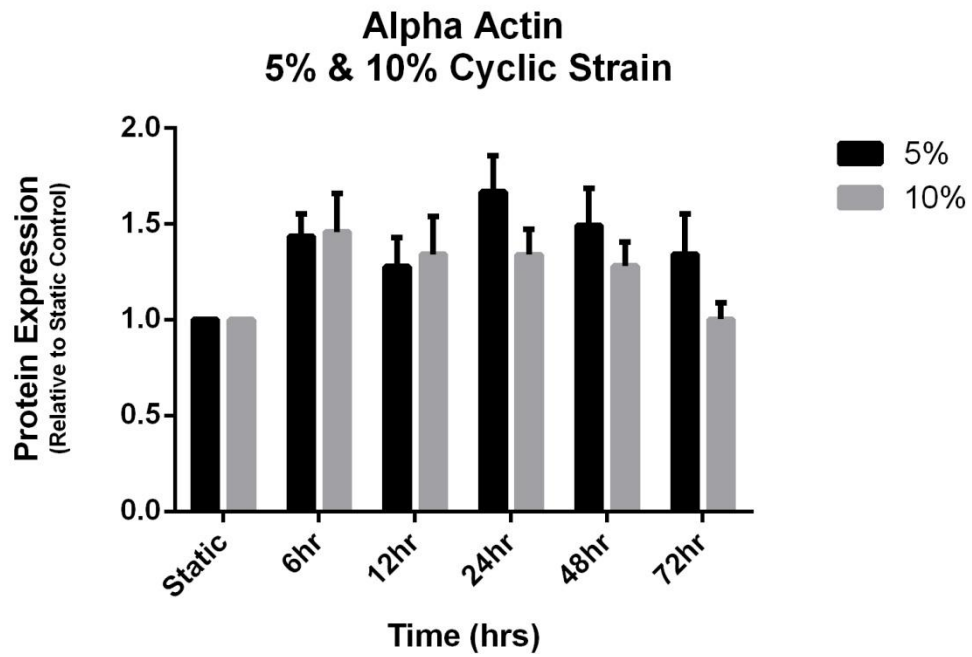


**Figure 3.18: Western Blot of HAoSMC Lysate.** Blots for SMC contractile marker Calponin and endogenous loading control GAPDH. HAoSMC were exposed to 5% cyclic strain over a time course of 72 hours. Values are normalized for loading bias using GAPDH endogenous control and calibrated against 0hr. n=3, \*P<0.05 vs. static adhesion; one-way Anova.

A.



B.

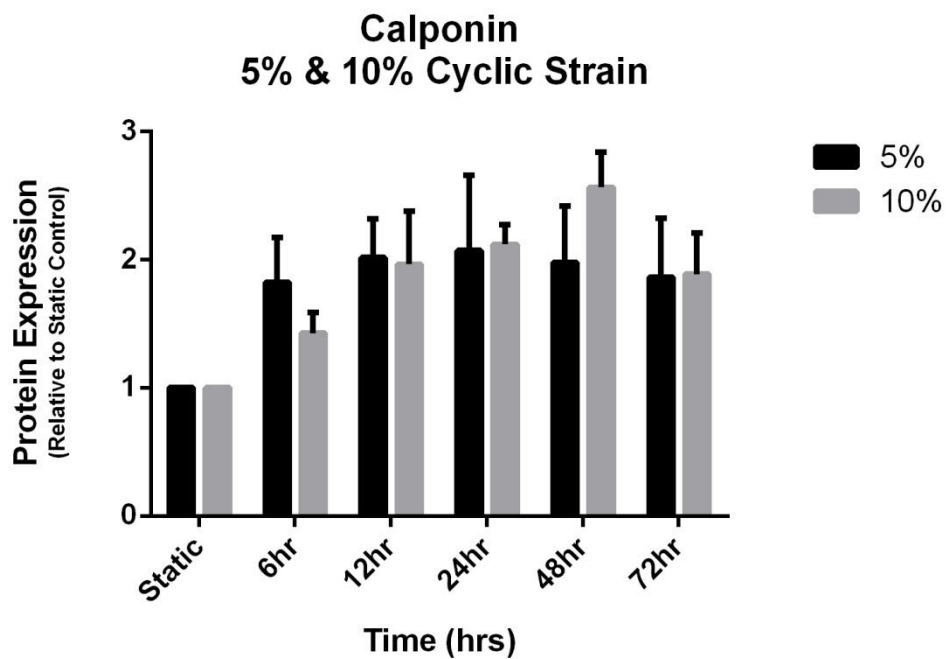
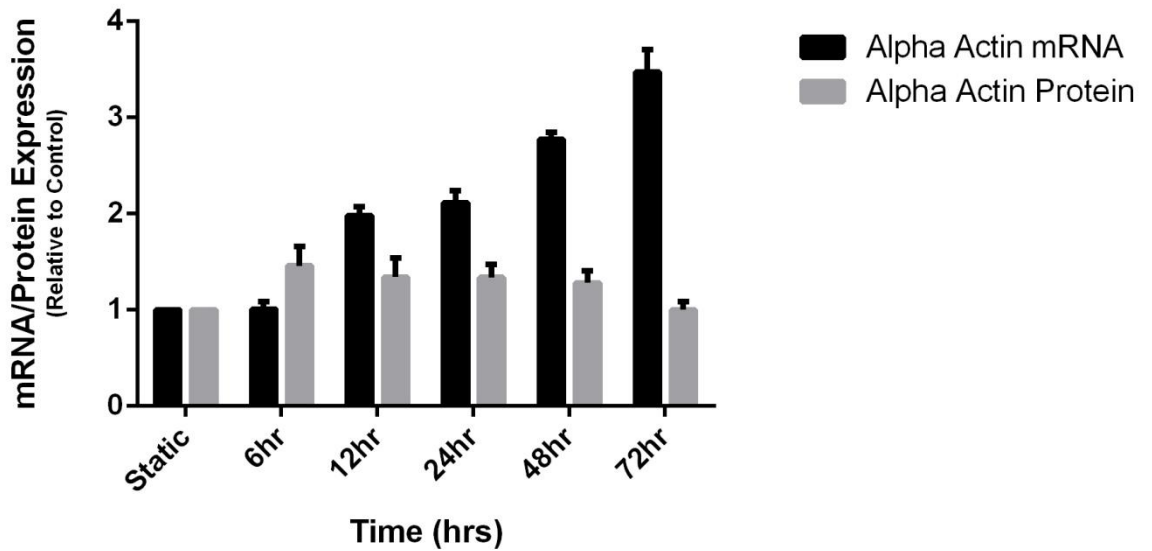


**Figure 3.19: Effect of strain amplitude on Calponin expression.** HAOsMC were exposed to both 5% and 10% cyclic strain over a time course of 72 hours. Expression of Alpha Actin (A) and Calponin (B) were quantified for both strains and each time point using densitometry analysis of western blots.



A.

### Alpha Actin mRNA/Protein Expression 10% Cyclic Strain



B.

### Calponin mRNA/Protein Expression 10% Cyclic Strain

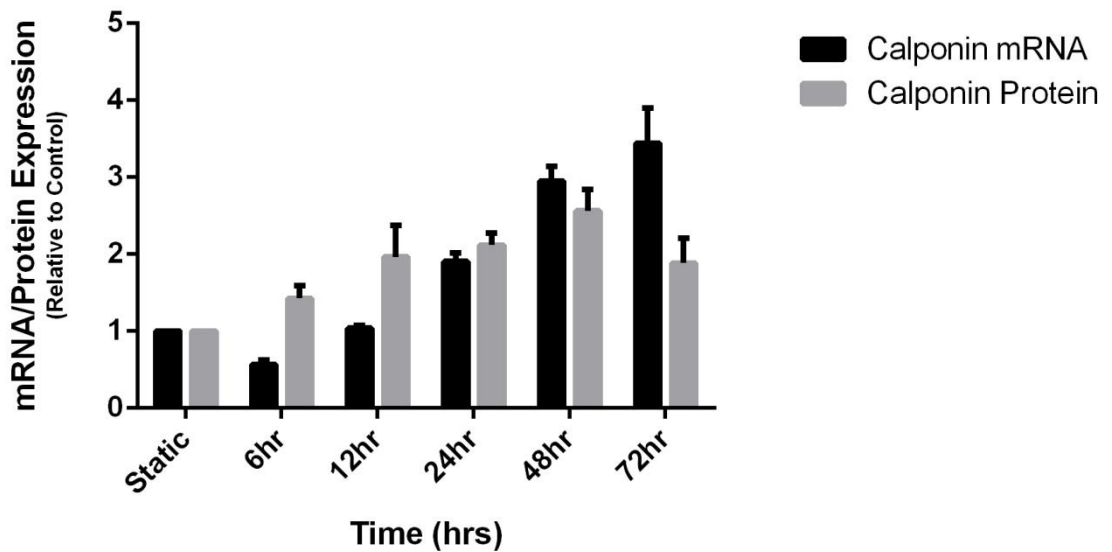


**Figure 3.20: Correlation between gene and protein expression.** A - Alpha Actin mRNA and protein levels were quantified from total RNA and cell lysate, respectively, from HAoSMC exposed to 5% cyclic strain over 72 hours. Calponin mRNA and protein levels were quantified from total RNA and cell lysate, respectively, from HAoSMC exposed to 10% cyclic strain over 72 hours.

### 3.3 Discussion

As previously stated, haemodynamic stresses are innate to the *in vivo* environment of the vascular smooth muscle cell. One of these mechanical forces is cyclic strain, this has been characterised as a tensile stress which is perpendicular to the lumen and cyclic due to the pulsatile nature of blood flow (Cevallos *et al.*, 2006; Lehoux and Tedgui *et al.*, 2003). *In vivo*, each cardiac cycle causes an arterial stretch of anything between 5 and 10%. During some physiological conditions a stretch of up to 25% is possible (Gotlieb *et al.*, 1996; Osol *et al.*, 1995). Vascular smooth muscle cells exposed to this deformation experience higher local strains in the actin rich pseudopods than in the cell body (Barbee KA *et al* 1994). The strain experienced by the cell may also depend on its particular cytoskeletal arrangement and focal adhesion organization and distribution.

Chronic changes to this mechanical force *in vivo*, particularly in the setting of hypertension, is often accompanied by vessel remodeling such as a thickened arterial wall and decreased luminal diameter (Geng & Libby *et al.*, 2002; Hahn & Schwartz *et al.*, 2009). Hypertension also increases the risk of pathological disease states such as atherosclerosis. Typically, the underlying driving force of vessel remodeling and progression of atherosclerosis is synthetic, pro proliferative and pro migratory SMCs. The altered luminal pressure can modulate VSMC phenotype between a contractile and synthetic phenotype (Rensen *et al.*, 2007). However, the exact properties of the mechanical force and its associated biological consequence remain to be fully detailed. As such investigations into the significance of amplitude of strain, frequency of cardiac cycle and duration of the force in modulating cellular dynamics and selecting for a particular SMC phenotype over another is at the centre of much debate amongst groups. Work carried out in this chapter aims to address some of these questions.

Experiments were designed to elucidate the impact of cyclic strain on HAoSMCs in culture, in particular its effect on cell injury and phenotype. To achieve this, the expression of both injury and contractile markers, found within the cell and secreted into the growth media, were quantified. The injury markers investigated were FGF-2 and Thrombomodulin while the contractile markers were SM  $\alpha$ -actin, Calponin and Smoothelin.

The HAoSMCs used throughout experiments were routinely characterised for cell specific markers to ensure genuine lineage. Qualitative western blot analysis was carried out for the presence of smooth muscle specific  $\alpha$ -actin (figure 3.1), and as a negative control Human Aortic Endothelial Cell (HAEC) lysate was used. Von Willebrand Factor was also probed for, as a follow up negative control showing presence in HAEC lysate and absence in HAoSMC, (figure 3.1).

Immunohistochemistry of smooth muscle specific  $\alpha$ -actin was also carried out on HAoSMCs. The SM  $\alpha$ -actin specific Ab was bound with a secondary antibody, conjugated with AlexaFluor 488. This decorated SM  $\alpha$ -actin in green; the nuclei of the cells were also stained blue using DAPI (figure 3.2, 10X magnification).

In order to subject the SMC to cyclic strain, they were seeded on to the flexible silicone membrane of the Flexcell® plates as described in chapter 2.2. The silicone membrane, however, is slightly hydrophobic making prolonged adhesion (>24hr) of HAoSMC difficult. To overcome this, adhesion profiles were created on the xCELLigence real time impedance system for a range of extracellular matrices (ECMs) and coating factors. This enabled an ECM or coating factor, which would provide optimal adhesion and attachment to be selected. It should also be noted that VSMCs will deposit their own ECM over the duration of the experiment particularly when mechanically stimulated with strain (O'Callaghan *et al.*, 2000).

Figure 3.4 and 3.5 show adhesion plots of SMCs on several different ECMs and coating factors. The data shown is for 12 hours and rate of adhesion is given as the dimensionless figure CI or cell index. This denotes the amount of resistance created by the cells for that particular sample, the full adhesion time course plots (~ 60-72 hours) can be found in the appendix. Resistance can be directly correlated for ~ the first five hours, to the strength of adhesion.

In figure 3.4, cells seeded on un-coated wells (red plot) show a basal adhesion of ~ 2.2. Fibronectin 50 $\mu$ g/ml (blue plot) shows the highest adhesion at ~ 3.3 CI followed by Collagen type I 15 $\mu$ g/ml (blue plot) ~2.6 CI. Finally a decrease in adhesion was seen in the well coated with 20 $\mu$ g/ml of Laminin (pink plot) with a CI of 2.0.

Figure 3.5 also shows a plot of adhesion profiles of HAoSMCs on additional ECM as well as various coating factors. Cells seeded onto un-coated wells showed a CI of 1.5 (red plot). The highest adhering sample was Poly-D-Lysine 50 $\mu$ g/ml (blue plot) ~ 2.9

CI. This was followed by 1:100 (light blue) and 1:200 (purple) dilutions of MaxGel® CIs of 1.6 and 1.5 respectively. MaxGel® ECM is a commercial coating factor containing extracellular matrix components including collagens, laminin, fibronectin, tenascin, elastin, a number of proteoglycans and glycosaminoglycans. It is designed to aid in adhesion and proliferation of many cell types. The two remaining ECMs, Laminin 20 µg/ml (pink) and Vitronectin 15µg/ml (green), showed decreased adhesion at 1.1 and 1.2 CI respectively.

From this experiment it was concluded that the amino acid Poly-D-Lysine showed strongest adhesion over the first 5 hours with minimal effect on cell growth over the following 72 hours. Poly-lysine is a polycation which binds negatively charged ions of the cell membrane and the culture surface. When adsorbed to the culture surface, poly-lysine increases the number of positively charged sites available for cell binding. Both the D- and L- form of the poly-lysine can be used as a coating substrate since poly-lysine is a nonspecific attachment factor for cells; however, certain cells can digest poly-L-lysine. For this reason, poly-D-lysine was used so that the HAoSMCs were not disrupted by excessive uptake of L-lysine (Jacobson *et al.*, 1977; Bottenstein *et al.*, 1977).

Although cells coated on Fibronectin showed strong adhesion for the first 5 hours, an increase in cell death was observed over the remaining 72 hours of the experiment, see appendix figure A2. The strong adhesion can be attributed to the fact integrins  $\alpha V\beta 3$  and  $\alpha 5\beta 1$ , which are abundant on the smooth muscle cell surface, are receptors for fibronectin. The increased cell death was possibly due to an inflammatory response by the cells to this ECM as fibronectin is known to be involved in wound repair. Following injury plasma fibronectin along with fibrin are deposited at the damaged site to form an initial clot, here macrophages and fibroblasts are recruited to further aid in repair (Grinnel *et al.*, 1984). For this reason Poly-D-Lysine (PDL) was preferable to fibronectin as it has not known to evoke an inflammatory response in HAoSMCs. As PDL are synthetic molecules, they do not stimulate biological activity in the cells cultured on them, and they do not introduce impurities carried by natural polymers.

The lower adhesion of cells coated on laminin was possibly due to the fact the integrins  $\alpha V\beta 3$  and  $\alpha 5\beta 1$ , do not find ligands with this ECM. Interestingly though cells seeded onto vitronectin also demonstrated lower adhesion despite the fact  $\alpha V\beta 3$  is a receptor for this ECM. An explanation may be found in the fact the 2D environment of cell

culture will not necessarily stimulate activation of the same integrins as are present *in vivo* (Haga *et al.*, 2007). A second theory is that the HAoSMCs may have adhered, spread and then retracted so strongly as to pull the Vitronectin ECM back off the E-plate. This would rationalize the low CI value and yet the cells may have been tightly bound in solution to the ECM.

The fact Max Gel® coated plates did not provide the strongest adhesion despite having a combination of most ECMs would highlight how certain ECM proteins provide stronger adhesion than others. When they are pooled together competition between each ECM for the receptors may reduce cell binding to a high adhesion substrate, such as fibronectin. Collagen type I has shown to promote a synthetic phenotype within SMCs (Orr *et al.*, 2009). To allow motility in this synthetic state, cells must release adhesions to the substrate to facilitate traction, this could explain the lower adhesion of HAoSMCs coated on Collagen type I. Variation in CI values across both experiments for the uncoated wells can be attributed to a difference in cell number.

Results from this experiment encouraged the choice of the amino coated plates from Flexcell®. Using these plates it was possible to achieve strong adhesion from the HAoSMC and an extended experimental time course using the strain unit.

Seeding any cell on a specific ECM will evoke, to a lesser or greater extent, a biological response. To investigate the HAoSMC response, at molecular level, to being seeded onto the ECMs and coating factors used in figure 3.3 & 3.4, expression of mRNA of three contractile genes was quantified. These were smooth muscle  $\alpha$ -actin, calponin and smoothelin, figure 3.5 A, B & C respectively. There was a marked decrease in each of the transcripts of these genes when cells were seeded onto the different matrices. This highlights a change towards a more synthetic SMC. In particular, the coating factor chosen, Poly-D-Lysine, showed a significant reduction in gene expression for these markers.  $\alpha$ -actin showed the most significant drop, down to 0.5 fold that of the uncoated control. Although these are significant findings, the core investigation of this chapter was to elucidate the impact cyclic strain has on SMC dynamics. Predisposing the SMCs to a synthetic state should not alter this work. In addition, extracellular matrix is synthesized and released by the cell during culture, which will ultimately negate the effect of the chosen coating factor as the experiment extends. On top of this the static adhesion of the culture itself promotes an unhealthy phenotype, giving confidence that

cells used in the experiments of this thesis were predominantly in a synthetic state at the start of each study.

### 3.3.1 Cell Injury Caused by Cyclic Strain

With the HAoSMCs now strongly adhered and able to undergo deformation for up to 72 hours, it was subsequently important to discern if cyclic strain was exerting either a pathological or physiological effect. This was achieved through quantification of two injury markers, Fibroblast Growth Factor-2 (FGF-2) and Thrombomodulin.

The initial injury marker looked at was FGF-2, this growth factor participates in the response to vascular injury. FGF-2 is ubiquitously found throughout most vascular cells. It has been well documented that FGF-2 is released from vascular cell cytoplasm following cellular injury, particularly in SMCs (Reidy *et al.*, 1992; Linder *et al.*, 1993; Crowley *et al.*, 1995; George *et al.*, 1997). FGF-2 contributes to growth responses of SMC by exerting an auto or paracrine mitogenic effect on the cell (Mason *et al.*, 1994; Clowes *et al.*, 1983). It occurs in many forms and is distributed differentially in subcellular compartments in the cytoplasm and nucleus (Renko *et al.*, 1990). FGF-2 has also been shown to be released from cells *in vitro* by cytosolic leakage through an injured membrane (S.T. Crowley *et al.*, 1995). For this study FGF-2 released into cell media was quantified using a Quantikine® human FGF basic immunoassay (ELISA) by R&D Systems®.

Figure 3.6 (A) shows quantified levels of FGF-2 released from HAoSMC that have been subjected to 10% cyclic strain at 1Hz. Samples were taken over a time course of 72 hours at 0hr, 6hr, 12hr, 24hr, 48hr and 72hr. The time course reveals that during the first 6 hours of strain there is an increase of ~ 30 pg/ml of FGF-2 compared with the static control, from ~300pg/ml to ~330pg/ml. This may be viewed as an initial adaptive response of the cells to the acute strain. As the strain becomes more chronic, a significant reduction in secreted FGF-2 is seen throughout the remaining time points down to ~ 20pg/ml at 24 hr. The reduced levels of injury marker would suggest a physiological response of the cells is evoked by the 10% strain after the initial 12 hours. The modest peak at 48 hr to ~ 90pg/ml may be indicative of some cell detachment or cell injury caused by the extended culture time, whereas another theory is that the intracellular pool of FGF-2 is regenerated and a further release is seen. At 72 hours, levels of FGF-2 in the media are down to ~ 30pg/ml.

To establish the relevance of strain amplitude on FGF-2 release, SMCs were also subjected to a lower 5% strain for the same time course (figure 3.6 B). Some literature suggests this may be a more physiological representation of *in vivo* haemodynamics (Qi *et al.*, 2010).

The increase of FGF-2 secretion at both the 6 and 12 hours to ~ 370 and 460pg/ml respectively compared with 300pg/ml of the static control would suggest the acute response of the cells to the lower amplitude strain is extended compared to that of the higher strain which dropped after 6 hours to below that of the static control. However, similar to the 10% experiment, as the strain becomes more chronic the level of FGF-2 in the media is significantly reduced, and by 72 hr it has dropped to ~ 20pg/ml.

The grouped graph in figure 3.6 (C) shows a clearer comparison of FGF-2 release by HAoSMCs subjected to 5% and 10% strain. The higher release of the protein over the first 24 hours by cells subjected to 5% cyclic deformation would suggest the cells are being understrained and in a more pathological state. At the longer chronic time points of 48 and 72 hours, the higher 10% strain conversely shows a greater expression of FGF-2 in the media compared to cells strained at 5%, yet this is still markedly lower than the static adhesion control. Although distinct profiles are evident the trend in both experiments is comparable, that is the initial hours of strain cause a large release of FGF-2 into the culture media. By 24 hours, however, levels of secreted FGF-2 in both experiments are significantly less than that of the static adhesion control and remain lower for the duration of the experiment. First observations would conclude cyclic strain at both 5% and 10% has an acute effect on the cells signalling vascular injury and therefore stimulating FGF-2 release but as the strain becomes more chronic an adaptive response is seen where the cells are secreting far less amounts of FGF-2 and have entered into a more physiological phenotype. The protein that is initially released over the acute time points may be sequestered back into the ECM or broken down by matrix enzymes such as MMPs (Pintucci *et al.*, 2003).

To strengthen this theory and observe a more global expression change of the protein in the cell, levels of FGF-2 from total cell lysate was also quantified (Figures 3.7 & 3.8). The comparative graph of both strain amplitudes in figure 3.9 shows the expression of the protein seems to peak in both strain conditions at 12hours to ~ 1.5 fold that of the static culture and then gradually drops back to basal level over the remaining time

points. It should be noted, however, that levels of the protein remain higher in cells exposed to 5% compared to 10% strain.

This expression profile was surprising following quantification of the secreted protein in the culture media. The high level of FGF-2 found in the media at the earlier time points would have suggested a lower level quantified in the cellular lysate due to a depletion of the cellular pools instead of the peak in expression which was actually observed. Similarly low levels of secreted FGF-2 did not correspond to a higher cellular content. One possible interpretation is down to the way FGF-2 is compartmentalised in the cells. The FGF-2 secreted into the cell media may not have originated from cytoplasmic reservoirs but instead pools of FGF-2 located in extracellular matrices. These reservoirs have shown to be released rapidly and easily requiring neither cell death nor injury (Presta *et al.*, 1989). The lower amounts of secreted protein in the longer time points may also be consequence to the fact unbound FGF-2 which was secreted over the time course was potentially sequestered by extracellular low affinity receptors such as heparin sulphate proteoglycans and other pericellular matrix components (Aviezer *et al.*, 1994; Bashkin *et al.*, 1989). Taking this into account and the fact cellular levels are not replenished at the later time points when such low levels of FGF-2 are secreted in the culture media would suggest a finite resource of the protein within the cell.

Similarly, work carried out by G. C. Cheng *et al.*, (1997) showed FGF-2 release from SMCs was tightly regulated by mechanical strain and is amplitude, frequency and duration dependent. However, past 90 cycles of strain there was no further release even when tested up to 90,000 cycles. Their interpretation was that the rapid and limited nature of FGF-2 release in response to cellular strain was consistent with a cell injury-mediated mechanism. They also highlighted that under long term oscillatory strain the cell synthesizes and maintains a cellular pool of FGF-2. This is only released following cell deformation which exceeds an amplitude threshold, as found in cases such as balloon angioplasty. Below that, release may be from a sub population of injured cells. This would give reasoning to the relatively low amounts released during the longer strain time points as seen in figure 3.6 (A-C). It has been shown that healthy cells under little or no mechanical stimulus may also release FGF-2. This is also the case for cells undergoing normal physiological activities such as migration and contraction (Clarke *et al.*, 1993; Clarke *et al.*, 1995).



This said, it appears that both extensive trauma and mild mechanical stimulation may induce FGF-2 release suggesting it plays a role both pathologically and physiologically. Consequently, it is impossible to say for certain that results shown in figures 3.6 – 3.9 are as a result of strain alone. For this reason a second injury marker, Thrombomodulin, was also investigated. This was hoped to show a more stable secretion and therefore be a better representative model for cellular injury resulting from strain.

Thrombomodulin (TM) is an integral membrane bound glycoprotein, which binds thrombin, the final enzyme in the coagulant pathway (Sadler *et al.*, 1997). It is primarily used as an injury marker for endothelial cells *in vitro* (Wolfgang *et al.*, 2003). However, it has also shown to be expressed in SMC in culture (Soff *et al.*, 1991; Grinnel *et al.*, 1991). Work by Feng *et al.*, (1999) show it is also mechanically regulated by cyclic strain within SMCs. To assay this protein a Duo Set® ELISA from R&D Systems® was used. The samples quantified were the same as those used for the FGF-2 ELISA assaying both total cellular TM and secreted TM at the same time points and strain regimes.

In figure 3.10 (A) HAoSMCs subjected to 10% strain at 1Hz for 6 hours showed a marked reduction in the levels of secreted TM in the cell culture media compared with the static adhesion control. Here, a drop from ~730 pg/ml to ~ 160pg/ml was seen. The level goes back to ~ 630 pg/ml at 12 hr, but still remains below that of the static past 24 hours. It is not until the 48hr time point that the level goes over that of the control, with a marked increase seen at 72 hours, 877 pg/ml & 1400 pg/ml respectively. The 72 hour strain time point is up nearly two fold that of the static control. To correlate secreted TM expression with total cell expression of the protein cell lysates were also analysed from the same samples.

Figure 3.11 (A) shows an increased level of total cellular TM over the first 12 hours from ~ 700pg/ml for the static culture to ~ 1200pg/ml at 12 hours of 10% strain. By 24 hours of strain the cellular level of TM drops by~ 400pg/ml to ~ 800pg/ml. Levels of the protein decrease further at the longer time points of 48hr and 72hr to ~640pg/ml and ~600pg/ml respectively, dropping just below that of the static adhesion control.

The higher expression in cellular TM at the 6hr and 12hr time points, matched by a reduced level in the culture media, would suggest the cells are switching to a healthier phenotype in comparison to cells in static culture. As the strain continues into longer time points this expression drops off and levels of TM in the culture media also

increase. Chronic exposure of HAoSMCs to 10% strain seems to transition the cell back to an unhealthy phenotype as cellular levels of TM are depleted. HAoSMCs strained at the lower amplitude of 5%, showed a similar expression profile of TM over the 72 hours. Secreted levels of TM, figure 3.10 (B), were lower in the first 24 hours than the static adhesion control, with the lowest expression again shown following 6 hours strain. It is only at the chronic strain time points of 48 and 72 hours that secreted levels of TM are higher than those in the static adhesion control. Again TM expression in cell lysates had a corresponding profile, with cell reserves of the protein increasing by ~ 750pg/ml over the first 24 hours to that of the static control. The later chronic strain time points show a drop of TM to ~600pg/ml for the 48hr and 620pg/ml for the 72hr. This is still an increase on the static sample of ~ 150pg/ml.

The comparative graphs of 5% and 10%, (figure 3.12 A&B) show an extended physiological response is evident in cells subjected to 5% strain, with total cellular levels of TM remaining high up until the 24hr time point, after which a drop back to static level is seen. The higher levels of cellular TM at 24hr for the 5% strain when compared with those of the 10% may suggest the lower strain being closer to the physiological pressure found in the arterial system. This is reinforced by the lower levels of secreted TM at the 72 hour time point. Correlation between the increases in TM secreted into the media and the drop in cellular lysate levels are outlined in figure 3.13 A&B.

Thrombomodulin was useful as a secondary injury marker as it is not as readily secreted in resting or static cells as compared with FGF-2 which provided a more accurate analysis of SMC response to strain. It has also been proven to be a marker of both late and early stages of cell injury and necrosis induced by neutrophil derived proteases and oxygen radicals (Boehme *et al.*, 2002). What should be noted is the experiment was run without a media change. Therefore as the cells are cultured and strained, there is a buildup of metabolites in a confined culture well which may have adverse/potent effects on the cells themselves, and their response to this may potentiate the effect seen by the strain.

### 3.3.2 Impact of Cyclic Strain on SMC Phenotype.

To investigate if cyclic strain altered VSMC phenotype, three SMC contractile markers were selected for analysis of expression. These included smooth muscle  $\alpha$ -actin, smoothelin and calponin. Both gene and protein expression were assayed for  $\alpha$ -actin and calponin, only the gene transcript was assayed for smoothelin. The reason for this is that smoothelin is almost solely expressed in contractile SMCs and therefore protein detection was difficult and unreliable in a cell culture of mixed phenotype.

As detailed in the introduction, smooth muscle  $\alpha$ -actin is ubiquitously expressed in SMCs, making up over 40 % of the total cellular protein and is an integral part of the SMC cytoskeleton (Fatigati *et al.*, 1984). As the cell moves towards a contractile state, expression of this protein increases. SM  $\alpha$ -actin is responsible in providing the cell with its force generating capabilities. Smoothelin, another constituent of the smooth muscle cell cytoskeleton is exclusively expressed in fully differentiated SMC. Smoothelin co-localises with actin stress fibers and is detected at two isoforms on a western blot including 59kD and 100 kD. The third contractile protein used in this study, Calponin, is a thin filament-associated protein, also implicated in the regulation and modulation of smooth muscle contraction. It is capable of binding to actin, calmodulin, troponin C and tropomyosin. The interaction of calponin with actin inhibits the actomyosin Mg-ATPase activity.

As before with the injury markers HAoSMCs were exposed to 5% and 10% cyclic strain over a time course of 72 hours. Both total RNA and cell lysate for protein were extracted from samples at each time point for analysis. Each time point was compared relative to control. Initial quantification of mRNA expression of Calponin and  $\alpha$ -actin show a steady increase with time when exposed to 10% cyclic strain as shown in figure 3.14 A&B. The Smoothelin transcript shows an increase up to ~24 hours after which point a drop in mRNA of this gene is seen, figure 3.14 C. The drop in expression may be consequence of this gene's selective association in only the contractile phenotype. As shown with the injury marker, TM, 10% strain at chronic time points appears to cause cell injury, therefore this may also revert the cells back to the synthetic phenotype.

To get a better representation of the cells' phenotype protein expression of SM  $\alpha$ -actin and Calponin was also quantified. The protein expression of  $\alpha$ -actin shows to be increased with both 5% and 10% strain over 72 hours, figures 3.25 & 3.16. However, the expression is higher throughout nearly all the time points in HAoSMC exposed to 5% clearly shown in the comparative graph, figure 3.19 A. Expression of the Calponin protein follows a similar profile under the same conditions when exposed to 5% and 10% strain, figures 3.17 & 3.18. When the effect of 5% and 10% strains are compared, figure 3.19 B, the levels of Calponin at 5% strain increase rapidly within 6 hours and remain relatively constant throughout the experiment. In comparison, the 10% strain shows a more gradual increase in expression of the protein up to 48 hours and then a drop at 72 hours.

It is evident from these contractile markers that cyclic strain at either strain amplitude induces a more contractile phenotype within HAoSMCs. At mRNA level both  $\alpha$ -actin and calponin are increased throughout all the time points with 10% strain compared to the static. Smoothelin shows increasing expression up to 12 hours at which point it begins to drop back, importantly though even at 72 hours it still remains above the static control. As stated the protein expression of  $\alpha$ -actin and calponin are also increased at both 5% and 10%. However cells exposed to 5% show both a higher and longer expression of SM  $\alpha$ - actin when compared with the 10% counterpart, figure 3.19A. The poor correlation between the mRNA expression and protein expression of  $\alpha$ -actin and calponin in figure 3.20 (A&B) is not surprising as there are many processes between transcription and translation. An excellent review by Vogel and Marcotte *et al.*, (2012) highlights the causes of this and also shows as little as 40% correlation can be observed in some genes. Factors include; protein stability, the half-life of different proteins can vary from minutes to days - whereas the degradation rate of mRNA would be far tighter regulated, 2-7hrs for mammalian mRNAs, lower rate of mRNA transcription compared to protein translation in mammalian cells, alternative splicing and post translational modification. What is important is that the correlation of increased expression in both mRNA and protein of the contractile markers, when exposed to strain, is evident.

Many stimulants such as vasoconstrictors, polypeptide growth factors and extracellular matrix have been shown to regulate expression of contractile markers, specifically SM  $\alpha$ -actin. (Tock *et al.*, 2003). Results in this chapter, however, demonstrate that cyclic mechanical strain is a critical regulator of HAoSMC contractile expression.

The mechanism by which the contractile protein expression is regulated has been associated with numerous pathways including the mitogen activated kinases (MAPK) such as c-Jun NH<sub>2</sub>-terminal kinase (JNK), p38 (Tock *et al.*, 2003) and the extracellular signal-regulated kinase (ERK) (Wang *et al.*, 2003).

### 3.4 Summary and Conclusion

To summarise this chapter, HAoSMC lineage was confirmed through the use of cell specific markers. ECM and coating factor experiments on the xCELLigence revealed that the use of poly-d-lysine amino flex plates allowed a strong cell adhesion which enabled prolonged cyclic strain time points. However, coating on this amino acid results in a push towards the synthetic state of the HAoSMCs as assayed by mRNA expression of the contractile markers. As the experiment was to characterise the impact of cyclic strain on SMC injury and phenotype, having the cells in a uniform synthetic state at the beginning of the study did not bias the results. After quantifying the mRNA and protein expression levels, it is clear cyclic strain increases the abundance of these contractile phenotype markers. This holds for both 5% and 10% levels of amplitude. However, the higher strain, although encouraging a more physiological state initially, appears to create a higher degree of cell injury. This is evidenced through the use of injury markers FGF-2 and TM. Expression of  $\alpha$ -actin is also higher in SMCs exposed to 5% compared with 10%.

Works carried out in this chapter show HAoSMC phenotype may be modulated by cyclic strain as assayed by contractile markers. It is also evident that the mechanical properties of the strain as well as duration play a pivotal role in cell adaption and response to this stimulus. Studies in this chapter looked at amplitude and duration of strain only whereas frequency is certainly a key contributor. Greater strain amplitude than 10% is also most likely needed to represent a pathological hypertensive model as although cell injury was evident through use of TM, the contractile markers still remained elevated in cells exposed to 10%. A higher, more pathological 15% was attempted using the *in vitro* model discussed here but resulted in cell rounding and detachment. To conclude, haemodynamic force by way of cyclic strain is essential to maintain homeostasis within the vasculature yet variation in parameter of this force can have pathophysiological consequences.

## CHAPTER FOUR: Impact of Cyclic Strain on the miRNA Profile of HAoSMCs

### 4.1 Introduction

Experimental results outlined and discussed in chapter 3 have demonstrated that cyclic strain has a direct impact on cultured SMC phenotype and health. This was revealed through quantification of injury markers and changes in expression of both contractile marker mRNA and protein. To further understand the significance of mechanotransduction in the regulation of SMC fate and function, and the molecular mechanisms which underpin and ‘fine-tune’ the phenotypic switching phenomena, we hypothesised that micro RNA (miRNA) are haemodynamically regulated and are responsible for cell fate decisions and function.

In brief, miRNA are canonically generated into short (18-24) nucleotide long non coding RNA molecules. They regulate gene expression by hybridising to the 3’ UTR of mRNA. This results in either mRNA degradation or translational inhibition depending on the complementarity between the strands (V. Ambros *et al.*, 2001).

There exists a miRNA profile or “miRNome” characteristic or specific for individual cell types. To determine if the miRNome for HAoSMC is altered by cyclic strain, we extracted highly pure total RNA from strained lysates and determined the miRNA profile with qRT-PCR using Applied Biosystems® Taqman LowDensity Array® cards.

For a complete profile of miRNA, two microfluidic cards containing a total of 384 TaqMan® MicroRNA Assays per card were used. In total, this allows accurate quantification of 754 human microRNAs. These are deemed the A and B card. The A card contains miRNA which have been well documented tending to be functionally defined, and are broadly and/or highly expressed. The miRNAs in card B are narrowly expressed and/or expressed at low levels and are usually not as well functionally defined.

The data was analysed using both SDS and R statistical analysis software. Bioinformatics was carried out on the shortlisted miRNA of greatest differential expression. This included putative target prediction involvement of these predicted targets in biological processes and finally, pathway analysis.

#### 4.1.1 Chapter Hypothesis:

MicroRNA (miRNA) expression is haemodynamically regulated by cyclic strain and as a result can influence and modulate cell fate decisions and biological functions.

#### 4.1.2 Specific aims and Experimental approach:

The specific aims of this chapter are to show that the miRNA profile in HAoSMCs is altered with cyclic strain at a specific time point. In addition, this study aims to demonstrate that the haemodynamically sensitive miRNA signature plays a role in cell motility. The experimental approach for this chapter was as follows:

- Temporal study of HAoSMC miRNA profile as the cells were exposed to 10% cyclic strain at 1Hz over a time course of 48 hours.

This experiment had a two-fold output:

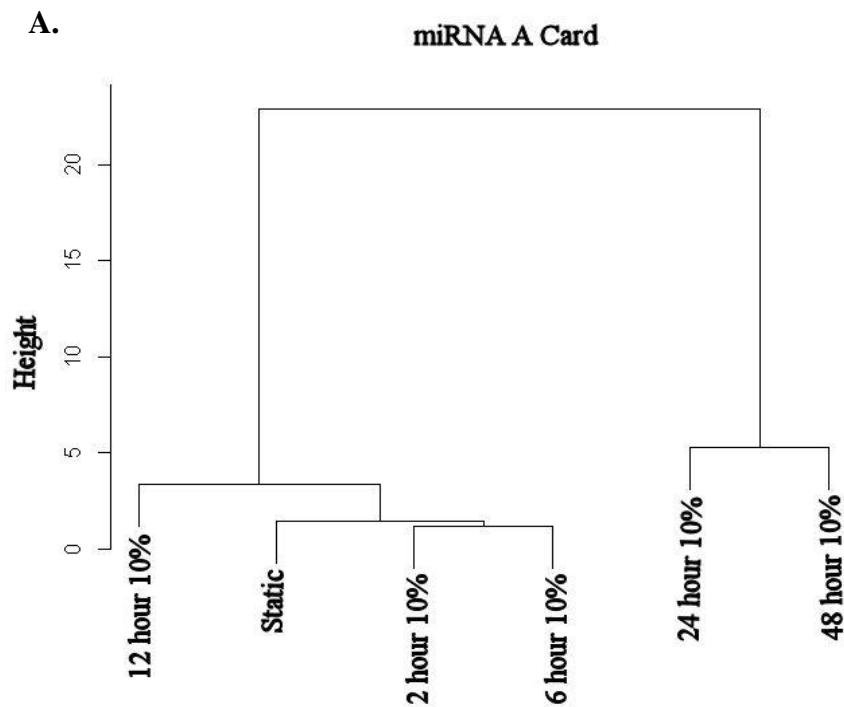
- 1) Elucidate at what time over the 48 hours of cyclic strain the HAoSMC miRNA profile had a significant change.
  - 2) A priority list was also created containing miRNA which showed a linear correlation in expression with respect to time during 10% strain.
- Selection of a time point from the temporal study where a significant shift of the miRNA profile was evident and perform biological replicates of strains at 5%, 10% and static conditions.
  - Establish a shortlist from the biological replicates study of the most differentially expressed miRNA with an adjusted P value  $\leq 0.005$ .
  - Target determination of shortlisted miRNA.
  - Enrichment of Gene Ontology (GO) biological processes using putative conserved targets.
  - KEGG Pathway analysis of putative targets.

## 4.2 Results

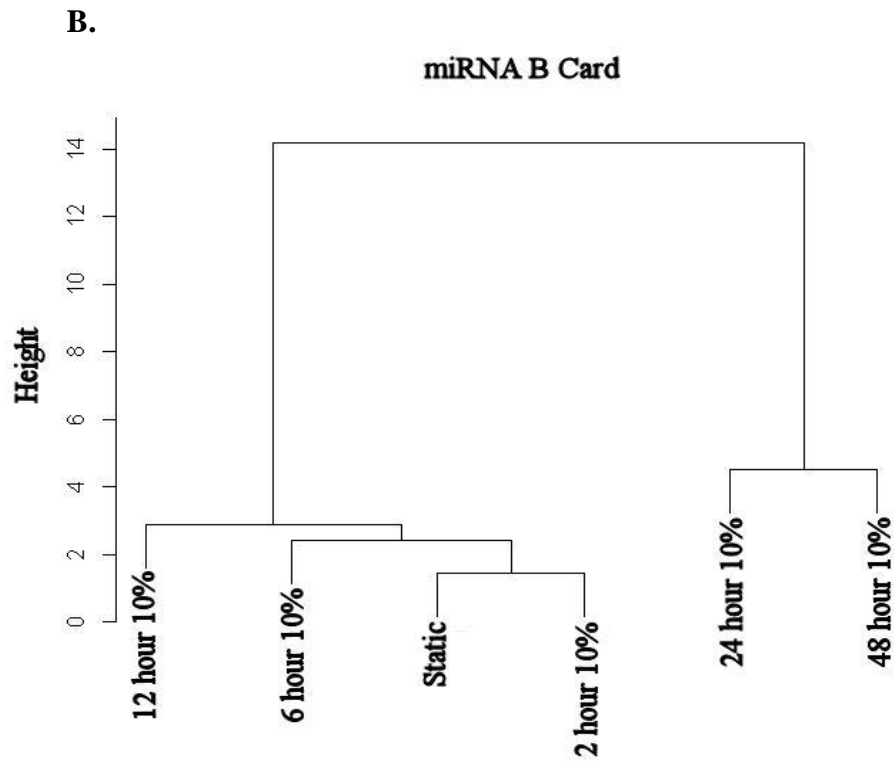
### 4.2.1 Temporal 10% strain study on HAoSMC miRNA profile

#### 4.2.1.1 Hierarchical Cluster Analysis (HCA)

To determine the effect of cyclic strain on the HAoSMC “miRnome”, cells were exposed to 10% cyclic strain over a 48 hour time course. Initial experimental validation was to ensure there was significant separation of samples. This was achieved by hierarchical cluster analysis (HCA) visualised by the use of dendrograms generated from the bioinformatics software as shown in figure 4.1. A dendrogram is a branching diagram used to illustrate the arrangement of clusters produced by hierarchical clustering based on degrees of similarity/number of shared characteristics among samples.



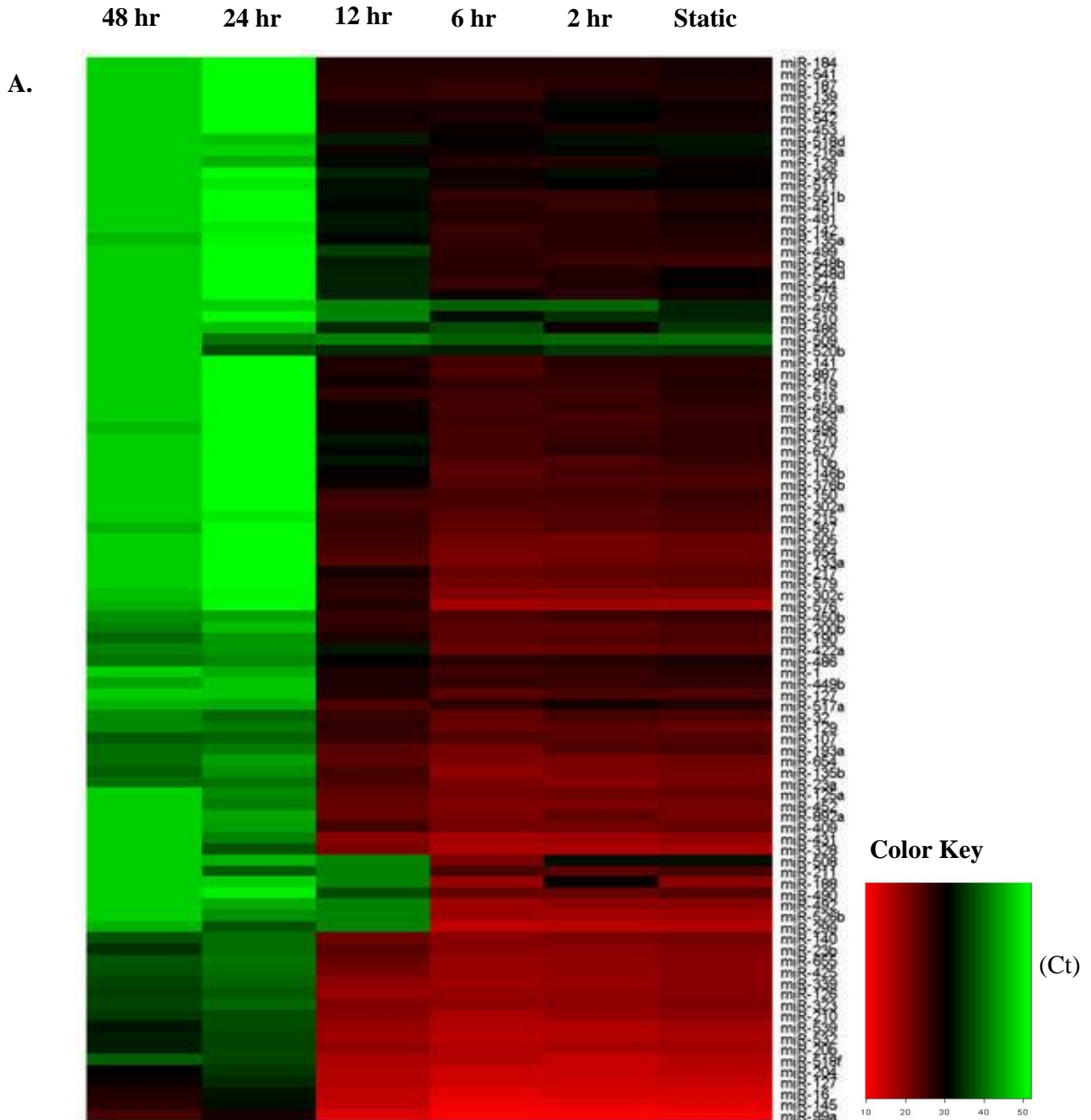




**Figure 4.1 A&B:** Dendrograms of miRNA profiles following temporal strain study. Hierarchical cluster analysis (HCA) of miRNA profiles from HAoSMC. Each cluster represents SMCs exposed to 10% cyclic strain at different time points. A) Human miRNA panel A. B) Human miRNA panel B. All data is mean normalised with a  $PCC \leq \pm 0.9$  and  $P \leq 0.05$ .

4.2.1.2 *Two-way heat map miRNA from priority list*

A two-way heat map comprised of the priority list of miRNA was then constructed for the A and B panel of miRNA. This allowed visualization of the global miRNA expression profiles across the strain time course, as shown in figure 4.2 A & B. A shift in colour from red to green indicates a down regulation of that miRNA detector. Each miRNA detector comprising the heat map is listed on the right hand side. Colour key on the bottom right shows CT value and corresponding colour.



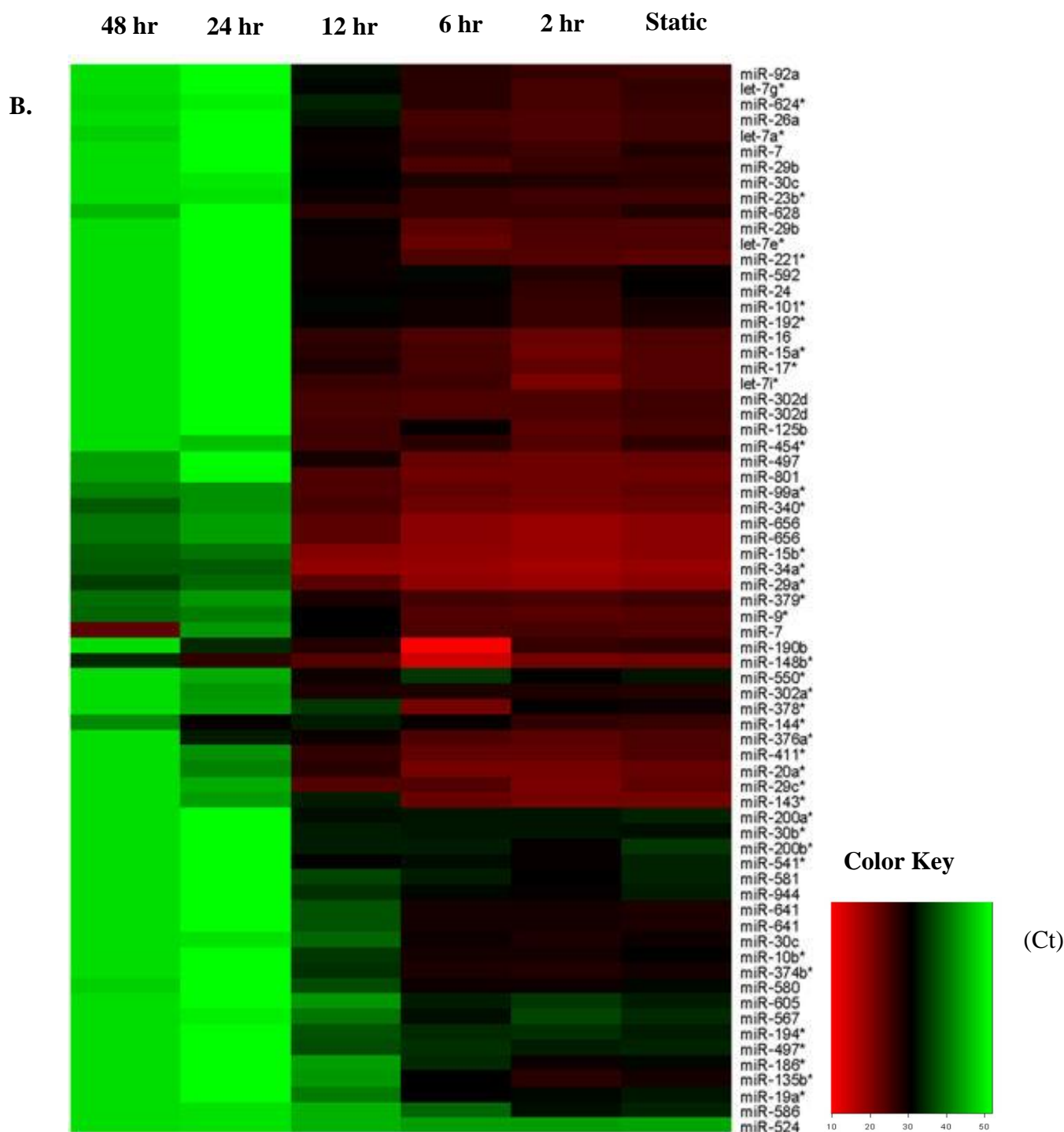


**Figure 4.2 A&B: Two-way heat maps of human miRNA panels A&B** providing a visual representation of miRNA profile of HAoSMCs exposed to 10% cyclic strain. Samples were taken over a time course of 48 hours of cyclic strain and included a static sample and samples at 2hr, 6hr, 12hr, 24hr, and 48hr of strain. Heat-maps were comprised of the priority list of miRNA elucidated following bioinformatics on the HAoSMC miRNA profiles. All data is mean normalized,  $PCC \leq \pm 0.9$ ,  $P \leq 0.05$ .

### 3.2.1.3 Correlated miRNA

To deduce if any miRNA showed a linear relationship of expression between time and 10% cyclic strain, a Pearson Correlation Coefficient (PCC) was generated for each miRNA. From this a priority list, made up solely of miRNA which had a PCC of  $\leq -0.9$  and a P value of  $\leq 0.05$ , was created. miRNA with the strongest correlation were graphically represented. Figure 4.3 (A-C) shows miRNA from the A panel which had a PCC of  $\leq -0.9$  and a  $P \leq 0.05$ .

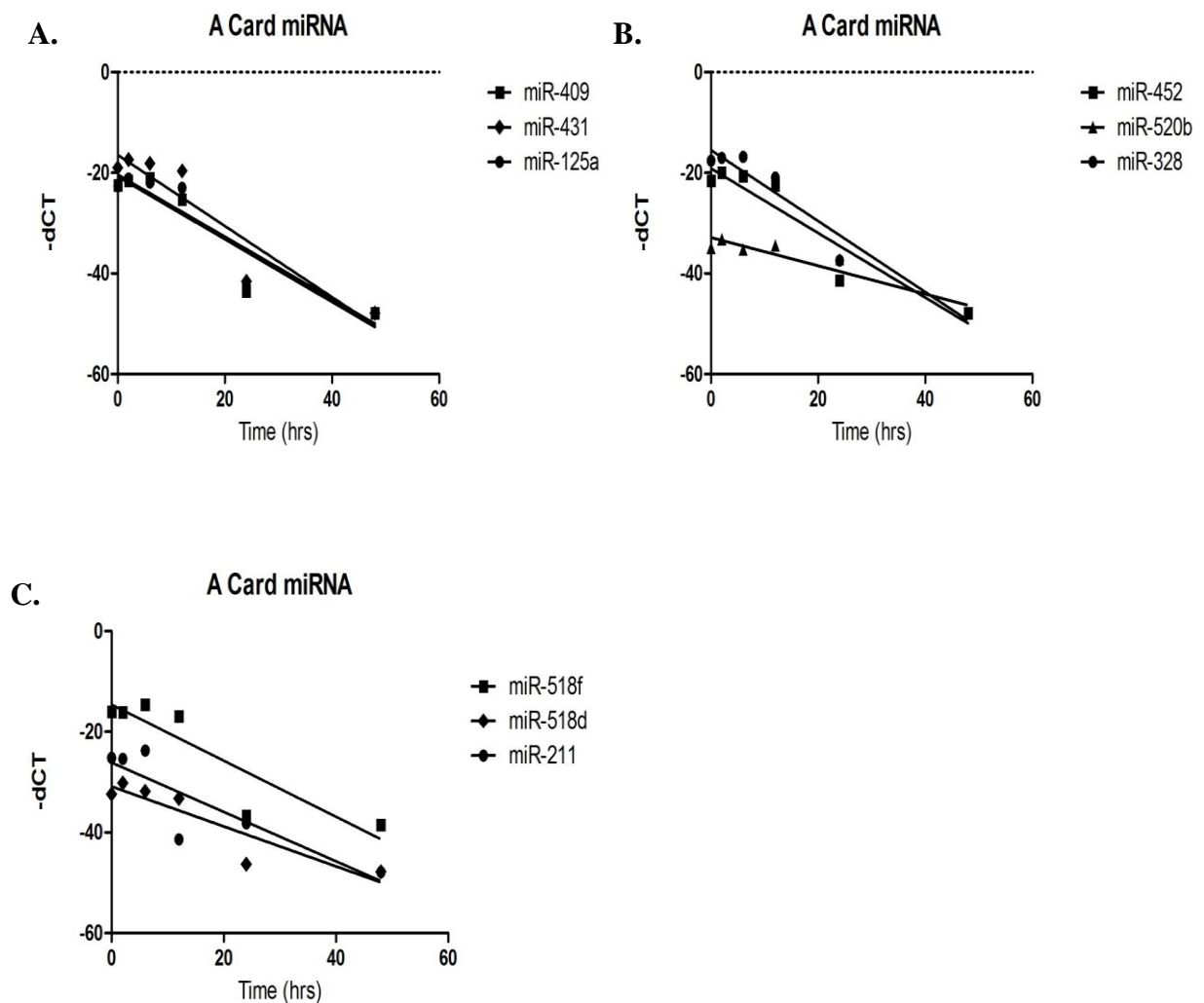


**Figure 4.3 A, B & C: miRNA Down Regulated with 10% cyclic strain.** Shows plotted miRNA from A card panel which showed the strongest linear relationship of expression between time and 10% strain. CT values were multiplied by -1 to ensure decreasing value indicated decreasing expression.  $PCC \geq 0.9$  or  $\leq -0.9$ ,  $P \leq 0.05$ .

miRNA from the B card panel which also made the priority list and showed the strongest PCC (PCC of  $\leq -0.9$  and a P value of  $\leq 0.05$ ) are graphically shown in figure 4.4 A & B.

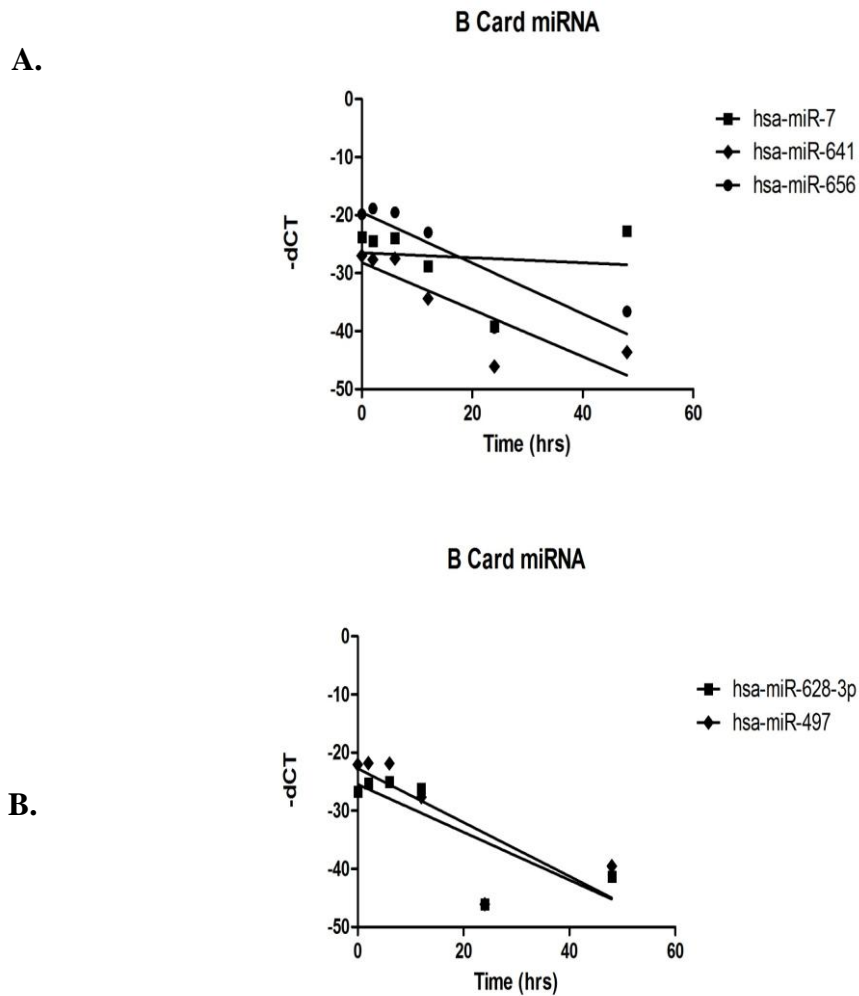


**Figure 4.4 A & B: miRNA Down Regulated with 10% cyclic strain.** Shows miRNA from B card panel which showed the strongest linear relationship of expression between time and 10% strain. CT values were multiplied by -1 to ensure decreasing value indicated decreasing expression.  $PCC \geq 0.9$  or  $\leq -0.9$ ,  $P \leq 0.05$ .

Of all the published miRNA which have been cited to be involved in regulating SMC biology only miR-1 showed a  $PCC \geq 0.9$  or  $\leq -0.9$ ,  $P$  Value  $\leq 0.05$  as shown in figure 4.5 A. However the expression of miRNA clusters miR-143/miR-145 and miR-221/miR-222, which are known to influence SMC differentiation, are also shown in figure 4.5 B & C. These fell outside the criteria for the priority list but as their expression reflects SMC phenotype they have been graphed to evaluate the impact of cyclic strain on phenotypic modulation in the discussion.

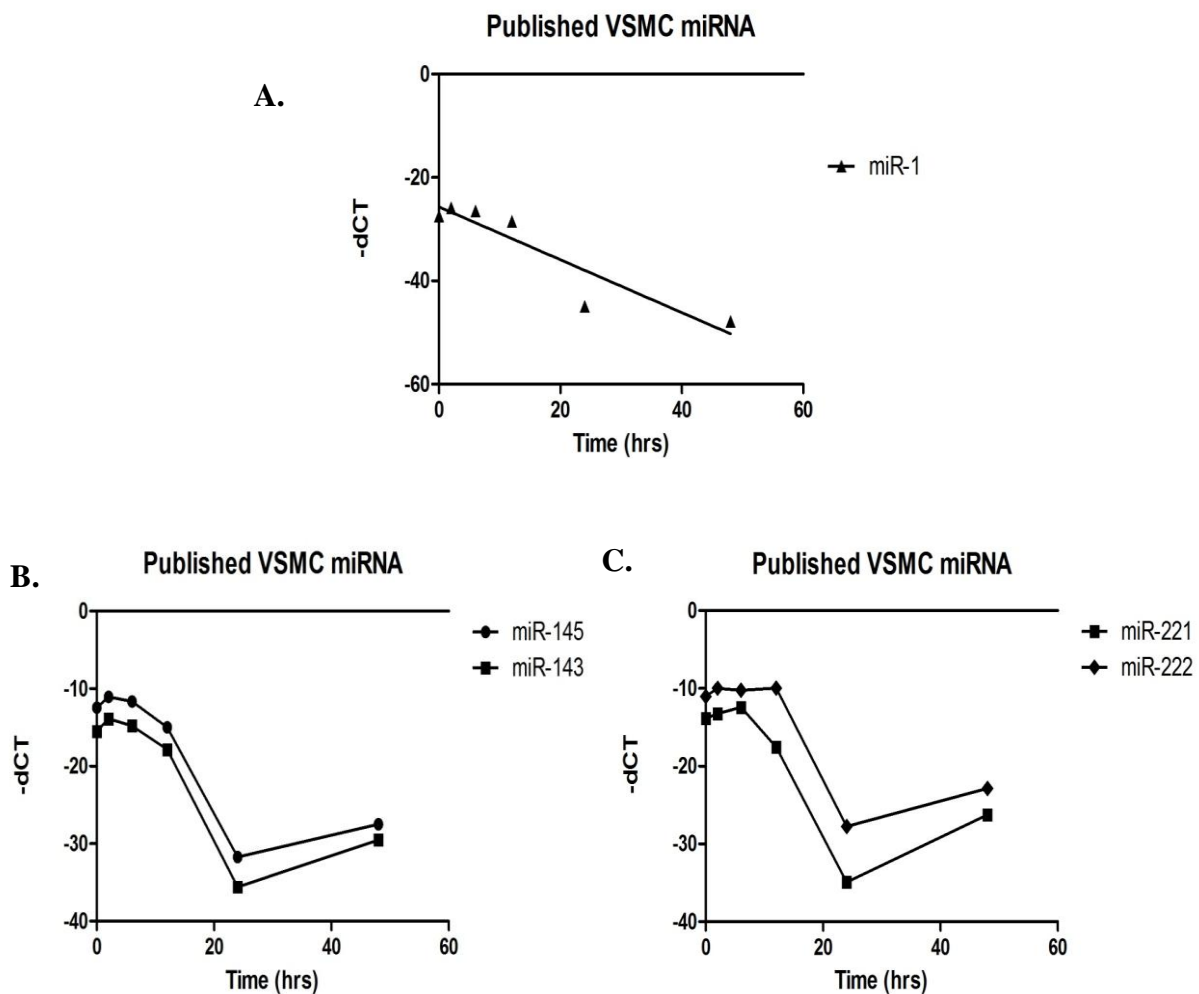


**Figure 4.5 A, B & C: Expression of Published miRNA involved in SMC biology with 10% cyclic strain.** A. Expression plot of miR-1 part of the priority list incorporating a PCC of  $\geq 0.9$  or  $\leq -0.9$ ,  $P$  Value  $\leq 0.05$ . B. Expression of VSMC phenotype marker miR-143/145 cluster C. Expression of miR-221/222 cluster with 10% cyclic strain.

#### 4.2.1.4 Bioinformatic analysis on priority miRNA from temporal 10% strain study

To extrapolate biological meaning from the priority list, bioinformatics was performed on miRNA which showed the strongest PCC. These miRNA were from both the A and B card panel. This involved determination of putative targets using Targetscan. Following this, involvement of these targets in gene ontology (GO) biological processes and pathways of interest from the Kyoto Encyclopedia of Genes and Genomes (KEGG) were analysed using DAVID bioinformatics database. To help visualise the regulatory potential of each short listed miRNA a table was constructed; this illustrates the number of potential genes the miRNA could target, the number of GO biological processes these potential targets were involved in and finally the number of KEGG pathways the predicted targets were part of.

**Table 4.1: Bioinformatics of strain regulated miRNA.** Table composed of miRNA regulated by 10% cyclic strain from A and B panel which have the strongest PCC ( $\geq 0.9$  or  $\leq -0.9$ ) with a P value  $\leq 0.05$ . Table shows the number of *in silico* predicted Conserved Targets of each miRNA along with the number of GO Biological processes and KEGG Pathways these targets are involved in.

Detector	Conserved Targets	Biological Processes	Pathways
<b>Published miRNA involved in VSMC biology</b>			
miR-1	860	333	34
<b>A Card miRNA</b>			
miR-125a	222	102	16
miR-211	669	309	22
miR-328	207	73	6
miR-409	142	59	2
miR-431	166	24	4
miR-452	338	163	14
miR-518d	35	35	1
miR-518f	35	35	1
miR-520b	844	296	29
<b>B Card miRNA</b>			
miR-7	444	182	22
miR-497	1273	454	46
miR-628-3p	112	25	5
miR-641	535	227	18
miR-656	726	341	30

**Table 4.2: Bioinformatics of strain regulated miRNA.** This table shows KEGG pathways which are involved in cell motility and migration. Strain regulated miRNA from the priority list which had *in silico* predicted conserved targets within these pathways are also shown. All miRNA involved hold a PCC of ( $\geq 0.9$  or  $\leq -0.9$ ) with a P Value  $\leq 0.05$ .

<b>MAPK Signalling Pathway</b>	<b>Focal Adhesion</b>	<b>Regulation of Actin Cyto Skeleton</b>
<b>Down Regulated miRNA</b>	<b>Down Regulated miRNA</b>	<b>Published VSMC miRNA</b>
miR-1	miR-1	miR-1
miR-211	miR-211	miR-520b
miR-328	miR-7	miR-7
miR-520b	miR-497	miR-497
miR-	miR-656	
miR-497		
miR-641		
miR-656		
<b>Cell Cycle</b>	<b>Wnt Signalling</b>	<b>Adherens Junction</b>
<b>Down Regulated miRNA</b>	<b>Down Regulated miRNA</b>	<b>DownRegulated miRNA</b>
miR-497	miR-1	miR—1
	miR-211	miR-211
	miR-328	miR-328
	miR-520b	miR-431
	miR-641	miR-497
	miR-656	miR-641
<b>VEGF</b>	<b>p53 Signalling Pathway</b>	miR-656
<b>Down Regulated miRNA</b>	<b>Down Regulated miRNA</b>	
miR-497	miR-497	



## 4.2.2 Investigation of strain amplitude on miRNA profile (biological replicates)

### 4.2.2.1 Hierarchical Cluster Analysis (HCA)

To assess if strain amplitude had any effect on the HAoSMC miRNA profile, cells exposed to 10% and 5% cyclic strain for 24 hours were compared against each other and to the profile of SMCs under static adhesion conditions. Biological triplicates were performed for each of these conditions. Only miRNA which had an adjusted P value of  $\leq 0.05$  were retained to make up the priority lists for each strain comparison. In total there were three priority lists generated for each strain comparison namely 10% vs. 5%, 10% vs. static and 5% vs. static at the 24 hour time point. Initial experiment validation consisted of HCA of the biological replicates and strain conditions schematically shown in figure 4.6.

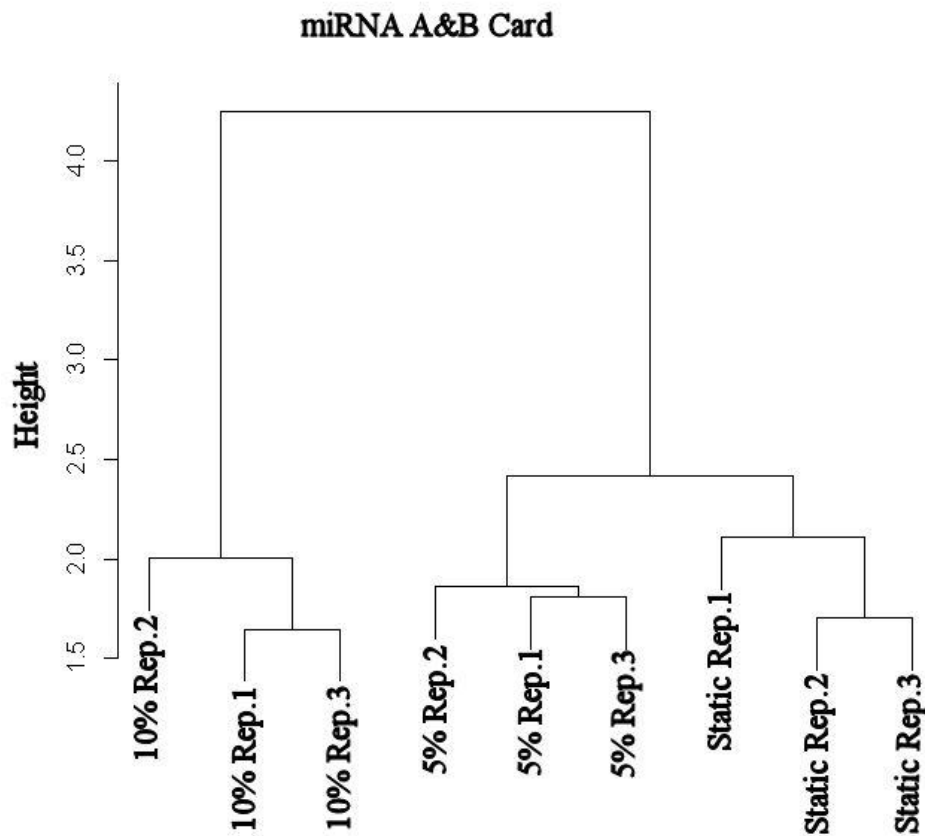


**Figure 4.6: Dendrogram of miRNA profiles from biological replicates.** HCA of biological replicates of SMCs exposed to static, 5% and 10% cyclic strain at a 24 hour time point. Biological replicates are shown to cluster with the highest separation seen between 10% strain and 5% or static adhesion, thus validating the experiment.  $n=3$ , all data has been mean normalized, adjusted  $P \leq 0.05$ .

#### 4.2.2.2 Venn Diagram of commonly expressed miRNA across strain parameters

The number of miRNA which make up the priority list for each strain comparison (10% vs 5%, 10% vs static and 5% vs static), for both the A and B cards were illustrated using venn diagrams. This allowed visualisation of the numbers of miRNA unique to a certain strain comparison as well as those common between strain comparisons. Total numbers of miRNA from the A panel across all strain comparisons are shown in Figure 4.7(A), these are irrespective of direction of expression. While direction of expression of miRNA from the A panel are shown in figure 4.7 (B).

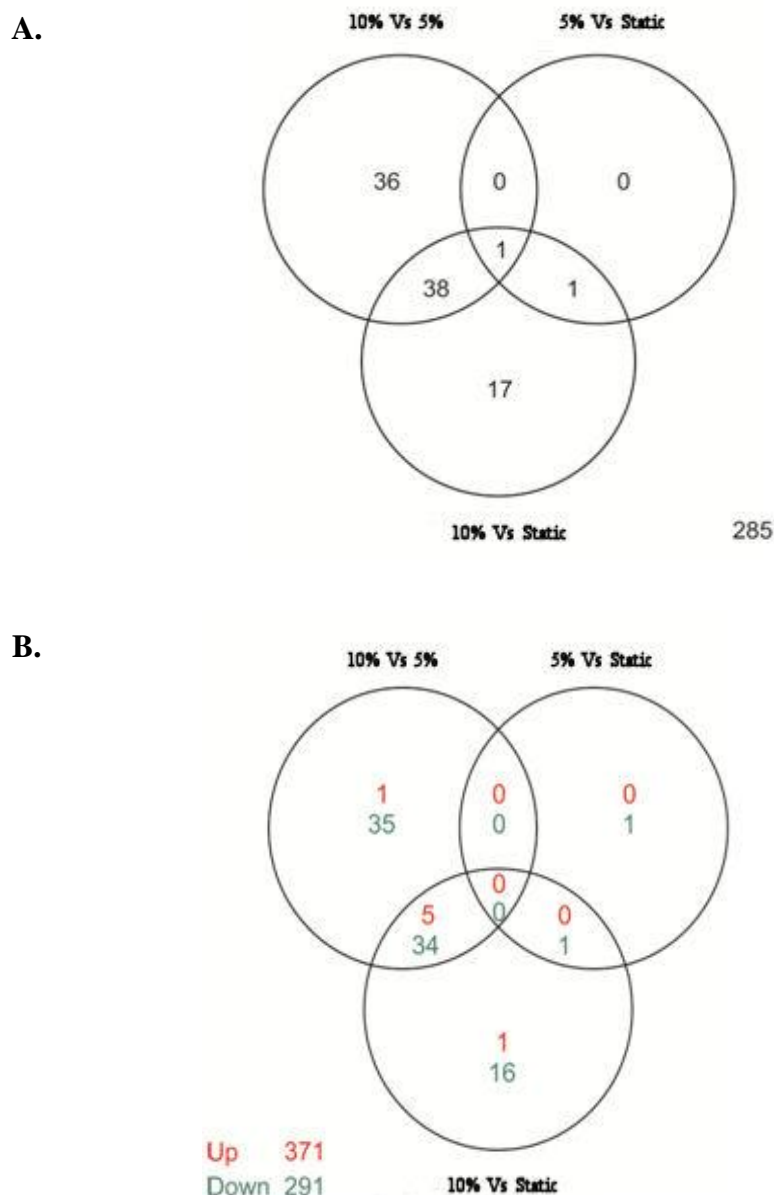


**Figure 4.7: Venn Diagrams of strain sensitive miRNA from A panel. (A)-** Number of unique and common miRNA between strain comparisons with no direction of expression from A card. **(B)-** Shows the number of up (red) and down regulated (green) miRNA expression in each strain comparison priority list as well as showing where they are common across comparisons.

Similarly, figure 4.8 (A & B) show miRNA from the B panel across all strain comparisons without and with direction of expression respectively.

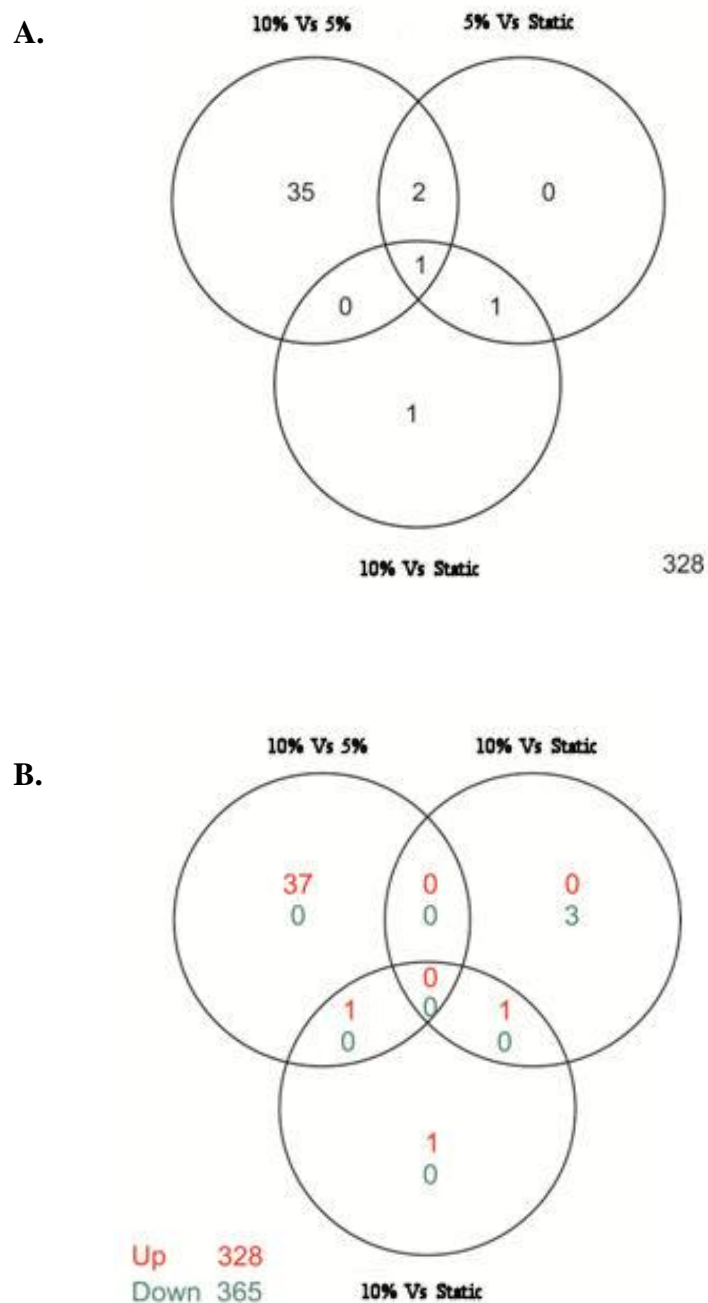


**Figure 4.8: Venn Diagrams of strain sensitive miRNA from B panel. (A)-** Number of unique and common miRNA between strain comparisons with no direction of expression from B card. **(B)-** Shows the number of up (red) and down regulated (green) miRNA expression in each strain comparison priority list as well as showing where they are common across comparisons.

#### *4.2.2.3 Bioinformatic analysis on priority miRNA from strain amplitude investigations*

The next stage of bioinformatics consisted of determining the putative targets of each of the top most differentially expressed miRNA making up the priority lists. As before with the temporal study, these were downloaded using TargetScan. The gene lists generated from TargetScan were then inputted into DAVID online bioinformatics database. From here a full profile of gene ontology (GO) biological processes was retrieved for each gene list. As well as this the involvement of the gene list in cellular pathways was determined using KEGG pathways. A bioinformatics profile for each miRNA was then constructed. This included adjusted P values, fold change, number of conserved targets as well as the number of GO biological processes and the number of KEGG pathways in which the generated gene lists were involved. These were then tabulated for each priority list and separated into miRNA from the A and B panel as well as miRNA which have been published to be involved in SMC biology. These are shown in tables 4.3- 4.5. The priority list generated from this study was used for the remainder of the work in this chapter.

**Table 4.3:** - Short list of most regulated VSMC miRNA in the priority list from the 10% vs. 5% strain comparison. The table is segmented into three sections: Top- miRNA present on A card both up and down regulated, Middle- miRNA present on B card both up and down regulated, Bottom- published VSMC miRNA regulated by strain present on either A or B card. Table shows fold change, adjusted P value and the number of *in silico* predicted Conserved Targets, GO Biological processes and KEGG pathways (n=3, Adjusted  $P \leq 0.05$ ).

<b>miRNA</b>	<b>Adjusted P Value (<math>\leq 0.05</math>)</b>	<b>Fold Change</b>	<b>Conserved Targets</b>	<b>(GO) Biological Processes</b>	<b>(KEGG) Pathways</b>
<b>10% vs. 5% miRNA from A Card</b>					
hsa-miR-618	5.60E-06	185159.4936	189	122	3
hsa-miR-888	9.50E-07	8756.723011	381	107	15
hsa-miR-375	0.000497404	2834.577507	229	130	3
ath-miR159a	0.000209385	826.0306185	—	—	—
hsa-miR-10a	0.014714407	5.124942484	271	124	9
hsa-miR-520e	0.009835236	4.572522715	844	296	29
hsa-miR-210	0.008659358	0.101373098	32	5	0
hsa-miR-148a	0.014714407	0.092054363	698	323	25
hsa-miR-18b	0.01326892	0.091878459	275	145	4
hsa-miR-331-5p	0.026675902	0.087811808	125	39	5
hsa-miR-654-5p	0.009363792	0.047257528	172	21	1
hsa-miR-496	0.008558878	0.02884925	128	60	1
hsa-miR-485-5p	0.031370758	0.016991582	376	82	8
hsa-miR-887	0.014714407	0.015578802	10	0	0
hsa-miR-302a	0.027646841	0.013014899	844	296	29
hsa-miR-501-3p	0.006821052	0.007958486	223	118	17
hsa-miR-518f	0.000209385	1.66E-05	35	35	1

<b>miRNA</b>	<b>Adjusted P Value (≤0.05)</b>	<b>Fold Change</b>	<b>Conserved Targets</b>	<b>(GO) Biological Processes</b>	<b>(KEGG) Pathways</b>
<b>10% vs. 5% miRNA from B Card</b>					
hsa-miR-520c-3p	5.09E-05	150.2434709	844	296	29
hsa-miR-610	0.006143201	121.0558387	265	35	3
hsa-miR-564	0.011041923	118.5591669	25	31	7
hsa-miR-513-3p	0.016115292	45.80254895	—	—	—
hsa-let-7f-2*	0.018066858	40.78959924	—	—	—
hsa-miR-661	0.011917494	39.21246247	319	71	5
hsa-miR-509-3p	0.011917494	31.53671093	143	87	3
hsa-miR-939	0.011917494	26.29849576	178	84	2
hsa-miR-516a-3p	0.011917494	24.26700534	384	175	19
hsa-miR-144*	0.018353118	20.4691761	—	—	—
<b>miRNA</b>	<b>Adjusted P Value (≤0.05)</b>	<b>Fold Change</b>	<b>Conserved Targets</b>	<b>(GO) Biological Processes</b>	<b>(KEGG) Pathways</b>
<b>10% vs. 5% Published miRNA known to be involved in SMC biology</b>					
hsa-miR-29b	0.035749209	0.343665259	1078	207	27
hsa-miR-221	0.046262844	0.296324793	446	243	24
hsa-miR-21	0.023204853	0.270429603	307	230	14
hsa-miR-222	0.032855765	0.259303271	446	243	24
hsa-miR-24	0.042161061	0.243385449	631	127	20
hsa-miR-29a	0.011962396	0.186311116	1078	207	27
hsa-miR-143	0.023204853	0.178962246	404	211	29
hsa-miR-145	0.010960162	0.151332141	731	265	21

**Table 4.4:** Shortlist of most regulated VSMC miRNA in the priority list from the 10% vs. static strain comparison. The table is segmented into three sections: Top- miRNA present on A card both up and down regulated, Middle- miRNA present on B card both up and down regulated, Bottom- published VSMC miRNA regulated by strain present on either A or B card. Table shows fold change, adjusted P value and the number of *in silico* predicted Conserved Targets, GO Biological processes and KEGG pathways (n=3, Adjusted  $P \leq 0.05$ ).

### 10% vs. Static

miRNA	Adjusted P Value ( $\leq 0.05$ )	Fold Change	Conserved Targets	(GO) Biological Processes	(KEGG) Pathways
<b>10% vs. Static miRNA from A Card</b>					
hsa-miR-618	2.68E-05	20297.03377	189	122	3
hsa-miR-375	0.000238093	8387.503833	229	130	3
hsa-miR-888	1.22E-05	703.0431092	381	107	15
hsa-miR-150	0.043245376	140.5210172	275	139	18
ath-miR159a	0.008146783	42.92528172	—	—	—
hsa-miR-520e	0.028916724	3.214904647	844	296	29
hsa-miR-331-5p	0.02176625	0.047716335	125	39	5
hsa-miR-373	0.019658174	0.043471724	844	296	29
hsa-miR-496	0.008761138	0.031264892	128	60	1
hsa-miR-302a	0.043322822	0.021076178	844	296	29
hsa-miR-518b	0.018002544	0.017848513	35	35	1
hsa-miR-198	0.022961614	0.01748052	301	59	5
hsa-miR-520g	0.00097034	0.016112709	579	226	20
<b>10% vs. Static miRNA from B Card</b>					
hsa-miR-23b*	0.014374153	136.408586	—	—	—
hsa-miR-744*	0.024862359	99.59164036	—	—	—
hsa-miR-520c-3p	0.014374153	9.449622002	844	296	—
<b>10% vs. Static Published miRNA known to be involved in SMC biology</b>					
hsa-miR-21	0.033745284	0.313905747	307	230	14
hsa-miR-145	0.037765728	0.273919236	731	265	21
hsa-miR-29b	0.022764928	0.237994414	1078	207	27
hsa-miR-29a	0.022764928	0.213721706	1078	207	27

**Table 4.5:** Shortlist of most regulated VSMC miRNA in the priority list from the 5% vs. static strain comparison. The table is segmented into three sections: Top- miRNA present on A card both up and down regulated, Middle- miRNA present on B card both up and down regulated, Bottom- published VSMC miRNA regulated by strain present on either A or B card. Table shows fold change, adjusted P value and the number of *in silico* predicted Conserved Targets, GO Biological processes and KEGG pathways (Adjusted P. value  $\leq 0.05$ ).

### 5% vs. Static

<b>miRNA</b>	<b>Adjusted P Value (<math>\leq 0.05</math>)</b>	<b>Fold Change</b>	<b>Conserved Targets</b>	<b>(GO) Biological Processes</b>	<b>(KEGG) Pathways</b>
hsa-miR-888	0.008414117	0.080286097	381	107	15
hsa-miR-520g	0.004300767	0.015052375	579	226	20
<b>Strain Regulated miRNA (5% vs. Static B Card)</b>					
hsa-miR-23b*	0.023049829	97.83123344	—	—	—
hsa-miR-596	0.035618543	0.142214688	129	60	5
hsa-miR-520c-3p	0.003873384	0.062895392	844	296	29
hsa-miR-610	0.035618543	0.03407928	165	35	3



#### 4.2.2.4 Cellular pathways analysis

In table 4.6, the miRNA were categorised on the basis of their potential involvement in key cellular pathways involved in cell motility the direction of change in their expression (up regulation or down regulation) is indicated by the arrow.

**Table 4.6:** Table of KEGG pathways of interest which contain *in silico* predicted conserved targets of strain regulated miRNA. Table shows pathway name with the strain condition that regulated the specific miRNA, 10% Vs 3%, 3% Vs Static or 10% Vs static. Arrows show expression change of miRNA with strain, up or down regulated.

<b>Focal Adhesion</b>	<b>Regulation of Actin Cytoskeleton</b>	<b>Vascular Smooth Muscle Contraction</b>
<b>10% vs. 5%</b>	<b>10% vs. 5%</b>	<b>10% vs. 5%</b>
hsa-miR-520e ↑	hsa-miR-520e ↑	hsa-miR-610↑
hsa-miR-148a ↓	hsa-miR-485-5p ↓	has-miR-661↑
hsa-miR-520c-3p ↑	hsa-miR-520c-3p ↑	<b>10% vs. Static</b>
<b>10% vs. Static</b>	hsa-miR-610 ↑	hsa-miR-96 ↓
hsa-miR-373 ↓	<b>10% vs. Static</b>	<b>5% vs. Static</b>
hsa-miR-522 ↓	hsa-miR-373 ↓	hsa-miR-610↓
hsa-miR-96 ↓	hsa-miR-96 ↓	
hsa-miR-520c-3p ↑	hsa-miR-520e ↑	
hsa-miR-520e ↑	hsa-miR-520c-3p ↑	
<b>5% vs. Static</b>	<b>5% vs. Static</b>	
hsa-miR-520c-3p ↓	hsa-miR-610 ↓	
	hsa-miR-520c-3p ↓	
<b>Cell cycle</b>	<b>Adherens Junction</b>	<b>ECM Receptor Interaction</b>
<b>10% vs. 5%</b>	<b>10% vs. 5%</b>	<b>10% vs. 5%</b>
hsa-miR-520e ↑	hsa-miR-10a ↑	hsa-miR-148a ↓
hsa-miR-18b ↓	hsa-miR-485-5p ↓	
hsa-miR-520c-3p ↑	hsa-miR-501-3p ↓	
<b>10% vs. Static</b>	hsa-miR-96 ↓	
hsa-miR-373 ↓	hsa-miR-509-3p ↑	
hsa-miR-520e ↑		
hsa-miR-520c-3p ↑		
<b>5% vs. Static</b>		
hsa-miR-520c-3p ↓		

Maps of key pathways involved in cell motility and migration, figure 4.9 – 4.14, were downloaded from the KEGG database using DAVID. Genes within the pathways which were predicted targets for the short listed miRNA were circled. Gene which were potential targets for multiple miRNA were circled in blue, genes which were targets for a single miRNA were circled in red and genes which were predicted targets for miRNA known to be involved in SMC biology were circled in yellow.

#### 4.2.2.4.1 Focal Adhesion

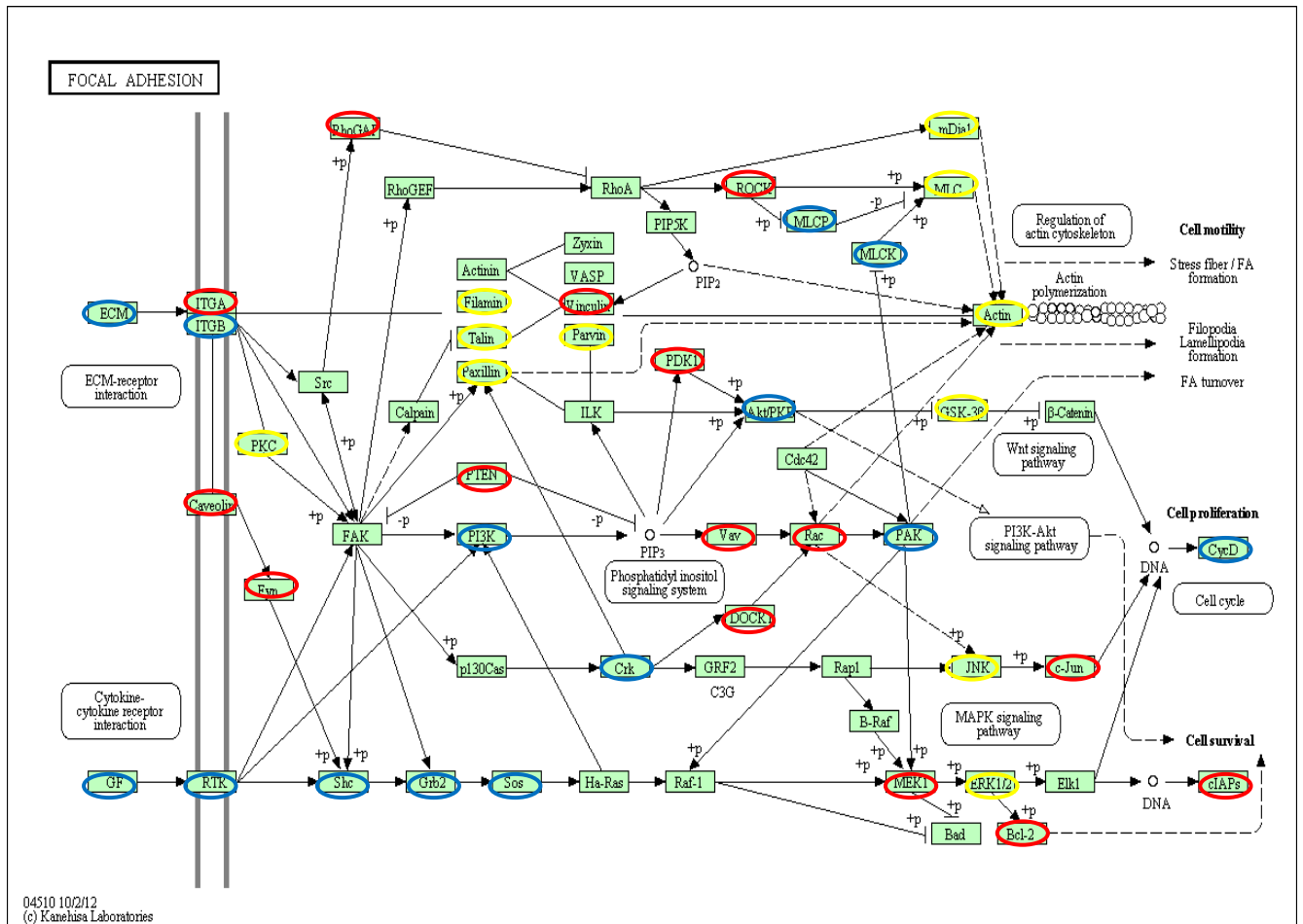


**Figure 4.9:** KEGG map of Focal Adhesion signaling pathway. Genes circled in red are predicted targets for an individual miRNA. Genes circled in blue are predicted targets of multiple miRNA. Genes circled in yellow are predicted targets of published and verified miRNA involved in VSMC function. These may also be predicted targets of multiple novel miRNA along with published miRNA data.

The predicted targets for an individual miRNA, taken from the priority list, involved in each of the key pathways in cell motility were tabulated in tables 4.7-4.12.

**Table 4.7:** Mechano-sensitive miRNA involved in the Focal Adhesion signaling pathway and their predicted targets.

<b>miR-520e</b>	<b>miR-373</b>	<b>miR-96</b>	<b>miR-522</b>	<b>miR-148</b>	<b>miR-520c-3P</b>	<b>miR-221/222</b>	<b>miR-24</b>
ECM	ECM	ECM	Sos	ECM	ECM	ECM	ECM
ITGB	ITGB	PI3K	Cyc D	ITGB	ITGB	ITGA	ITGA
PI3K	PI3K	Sos	MLCP	PI3K	PI3K	ITGB	PKC
GF	GF	Crk	PDK1	GF	GF	PI3K	PI3K
Sos	Sos	Cyc D	c-Jun	Sos	Sos	CrK	Vav
Crk	Crk	PAK	RTK	MLCP	Crk	PAK	PAK
Akt/PKB	Akt/PKB	MLCP	Shc	ITGA	Akt/PKB	JNK	GSK/3 $\beta$
MLCK	MLCK	Vinculin	Grb2	Caveolin	Cyc D	GF	mDial
Cyc D	Cyc D	RAC	Bcl-2	PTEN	PAK	RTK	
PAK	PAK	Fyn		Vav			
		DOCK1					
		RTK					
		Shc					
		Grb2					
		MEK1					
		Ciaps					
		Bcl-2					
<b>miR-143</b>	<b>miR-145</b>	<b>miR-29</b>					
ECM	ITGB	ECM					
ITGA	Caveolin	ITGA					
ITGB	RhoGAP	ITGB					
RTK	Filamin	Vinculin					
Bcl-2	Talin	Akt/PKB					
ERK1/2	Paxillin	GSK/3 $\beta$					
	Parvin	Caveolin					
	ROCK	PI3K					
		CycD					
		JNK					
		GF					
		RTK					

#### 4.2.2.4.2 Regulation of Actin Cytoskeleton

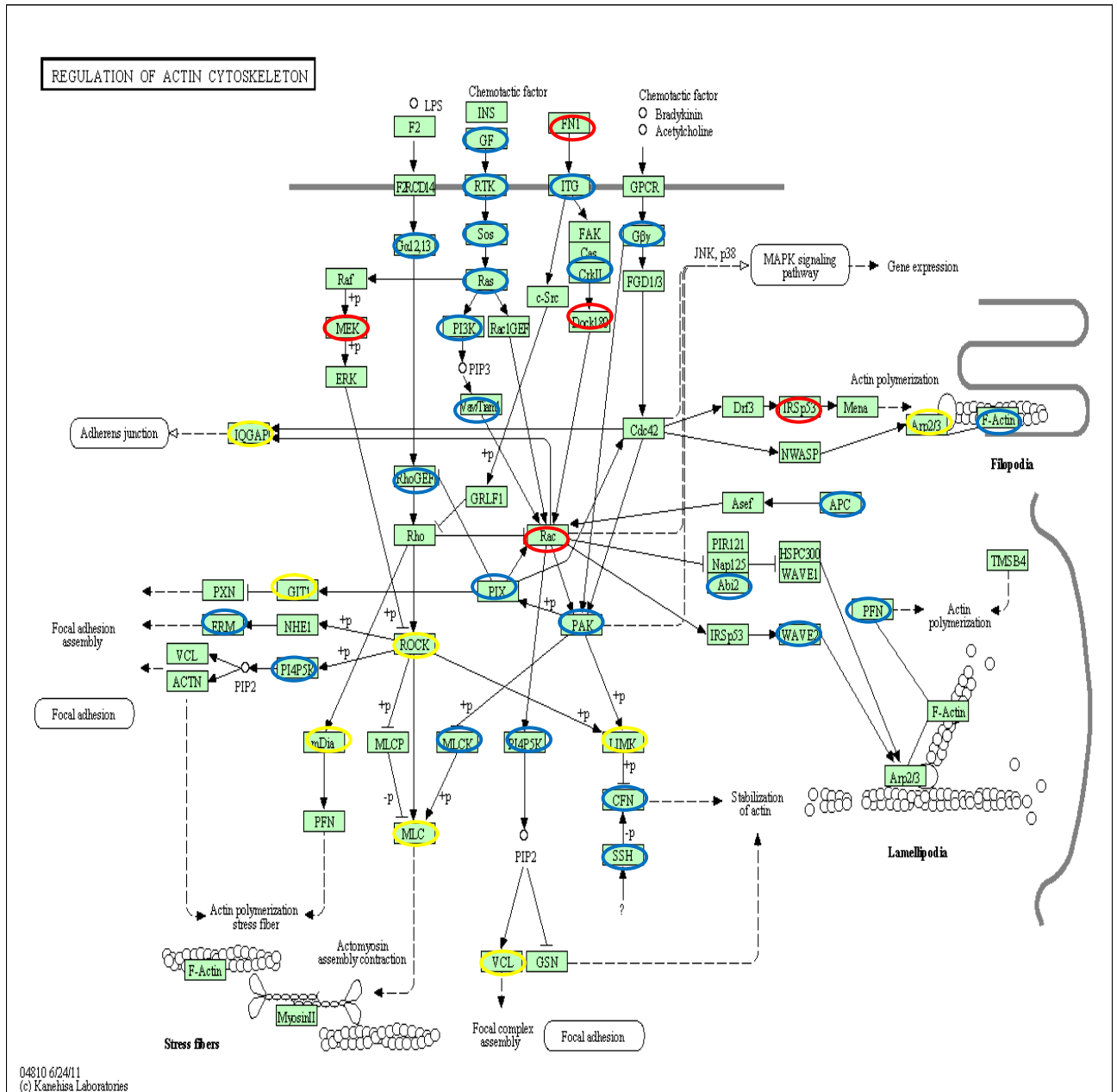


**Figure 4.10:** KEGG map of the Regulation of Actin Cytoskeleton pathway. Genes circled in red are predicted targets for an individual miRNA. Genes circled in blue are predicted targets of multiple miRNA. Genes circled in yellow are predicted targets of published and verified miRNA involved in VSMC function. These may also be predicted targets of multiple novel miRNA along with published miRNA data.

**Table 4.8:** Mechano-sensitive miRNA involved in the Regulation of Actin Cytoskeleton pathway and their predicted targets.

<b>miR-520e</b>	<b>miR-373</b>	<b>miR-485-5p</b>	<b>miR- 520c-3p</b>	<b>miR-96</b>	<b>miR-610</b>	<b>miR-143</b>	<b>miR-222</b>
GF	GF	ITG	GF	GF	GF	GF	GF
ITG	ITG	IRSp53	ITG	RTK	Gα 12, 13	RTK	ITG
Sos	Gβγ	F-Actin	Sos	Sos	WAVE2	ITG	CrkII
Gβγ	Crk II	PAK	Gβγ	RAS	PFN	Ras	PI3K
Crk II	PI3K	PFN	Crk II	Gα 12, 13	MLCK	ERK	PIX
PI3K	Vav/Tiam2	SSH	PI3K	PI3K		RhoGEF	PAK
Vav/Tiam1	APC		Vav/Tiam1	Vav/Tiam2		LIMK	WAVE2
APC	PIX		APC	Dock 180		SSH	
PIX	Abi2		PIX	Crk II			
Abi2	PFN		PAK	Gβγ			
PFN	PAK		PFN	MEK			
PAK	ERM		Abi2	Rho GEF			
ERM	MLCK		ERM	Rac			
MLCK	PI4P5K		MLCK	PIX			
PI4P5K	CFN		PI4P5K	PAK			
CFN			PFN	Abi2			
			CFN	PFN			
				WAVE2			
<b>miR-21</b>	<b>miR-24</b>						
GF	GF						
ITG	ITG						
Gβγ	IQGAP						
PI3K	PI3K						
Vav/Tiam2	LIMK						
RhoGEF	GIT1						
PI4P5K	RTK						
VCL	c-Src						
	Vav/Tiam2						
	PAK						
	mDia						

#### 4.2.2.4.3 Vascular Smooth Muscle Contraction

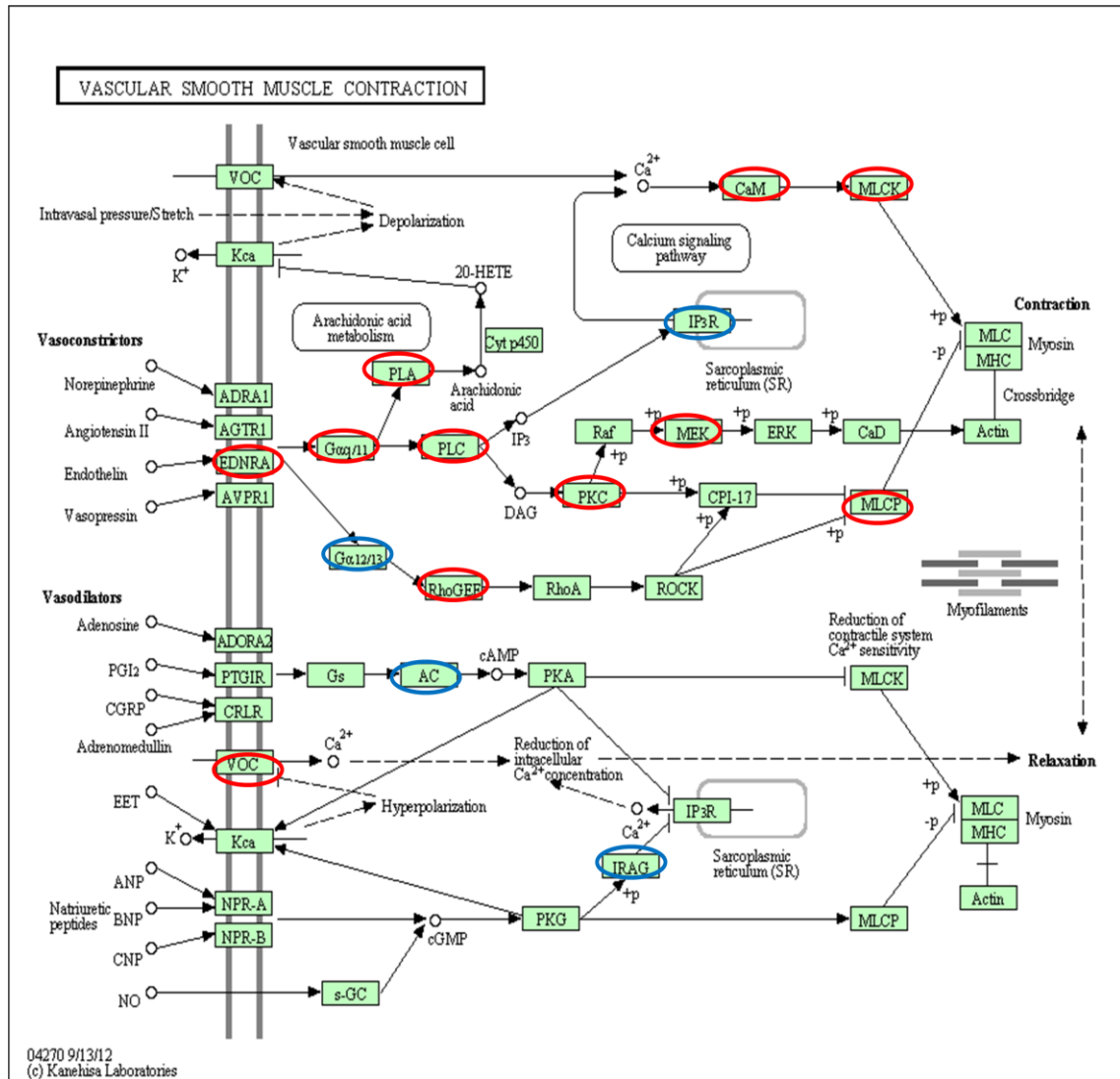


**Figure 4.11:** KEGG map of Vascular Smooth Muscle Cell Contraction pathway. Genes circled in red are predicted targets for an individual miRNA. Genes circled in blue are predicted targets of multiple miRNA.

**Table 4.9:** Mechano-sensitive miRNA involved in the Vascular Smooth Muscle Cell Contraction pathway and their predicted targets.

<b>miR-610</b>	<b>miR-661</b>	<b>miR-96</b>
IP3R	CaM	VOC
Gα12/13	pla	EDNRA
IRAG	IRAG	IP3R
MLCK	AC	Gαq/11
		PLC
		PKC
		MEK
		MLCP
		AC
		Gα12/13
		RhoGEF

#### 4.2.2.4.4 Cell Cycle

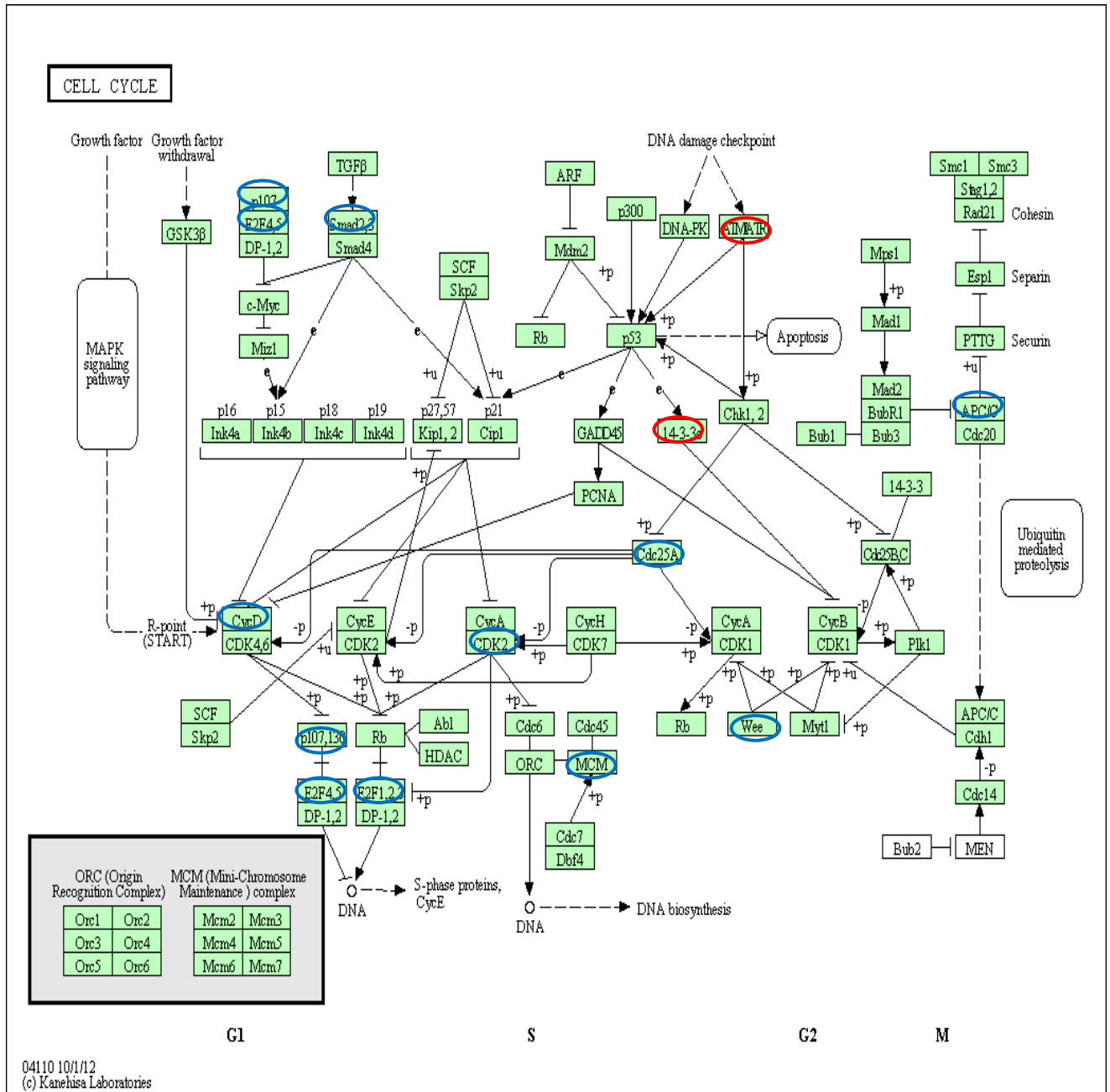


**Figure 4.12:** KEGG map of Cell Cycle pathway. Genes circled in red are predicted targets for an individual miRNA. Genes circled in blue are predicted targets of multiple miRNA. Genes circled in yellow are predicted targets of published and verified miRNA involved in VSMC function. These may also be predicted targets of multiple novel miRNA along with published miRNA data.



**Table 4.10:** Mechano-sensitive miRNA involved in the Cell Cycle pathway and their predicted targets.

<b>miR-520e</b>	<b>miR-18b</b>	<b>miR-373</b>	<b>miR-520c-3p</b>
p107	Smad 2,3	p107	p107
E2F4,5	ATI MATR	E2F4,5	E2F4,5
Smad 2,3	14, 3-3	Smad 2,3	Smacl2,3
APC/C	Cyc-D	APC/C	APC/C
Cdc25A	CDK2	Cdc25A	Cdc25A
CDK2		CycD	CycD
CycD		p107,130	CDK2
P107/130		MCM	p107/130
E2F 1,2,3		Wee	MCM
MCM		CDK2	Wee
Wee			E2F4,5
			E2F1,2,3

#### 4.2.2.4.5 Adherens Junction

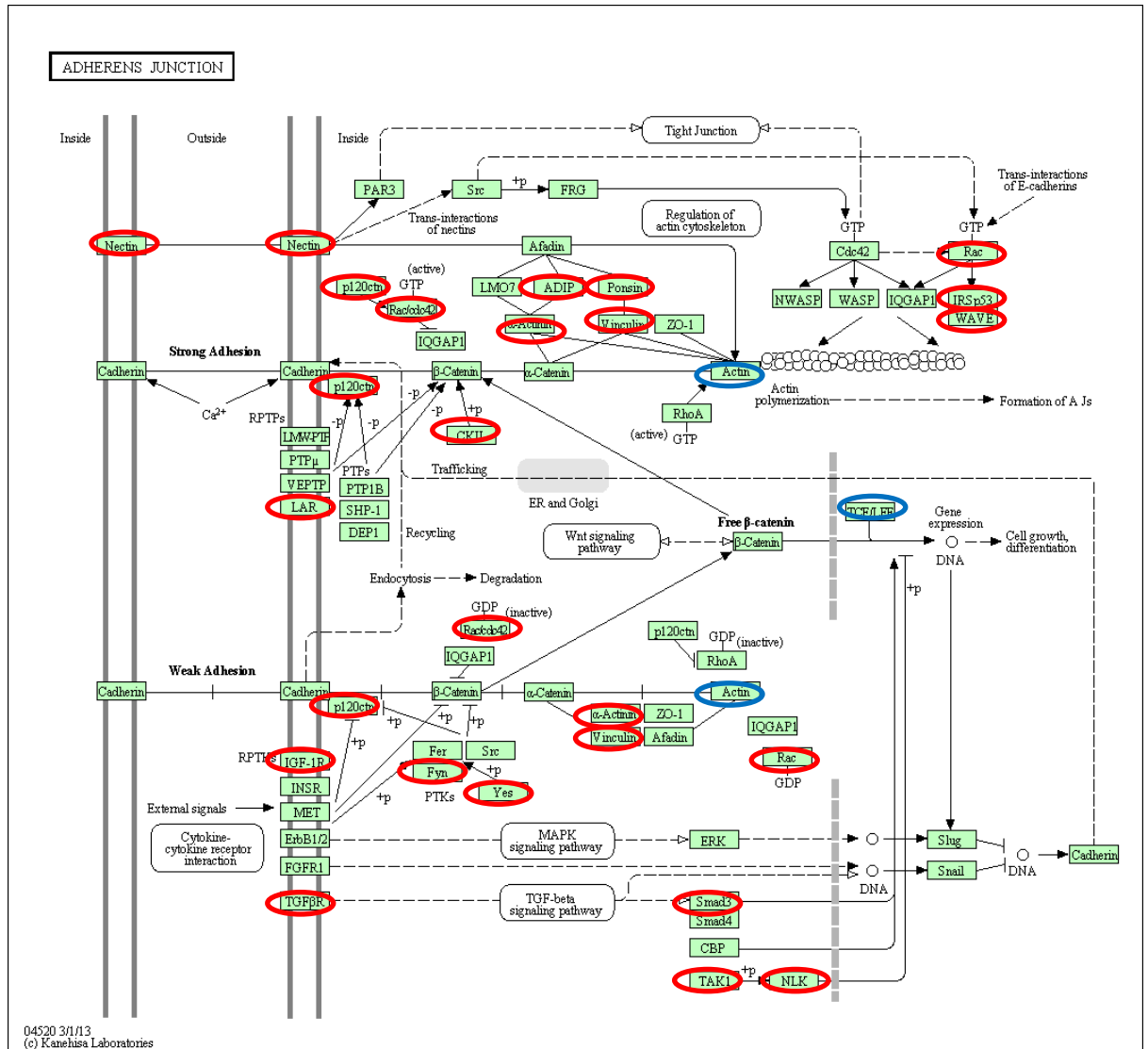


**Figure 4.13:** KEGG map of adherens junction pathway. Genes circled in red are predicted targets for an individual miRNA. Genes circled in blue are predicted targets of multiple miRNA. Genes circled in yellow are predicted targets of published and verified miRNA involved in VSMC function. These may also be predicted targets of multiple novel miRNA along with published miRNA data.

**Table 4.11:** Mechano-sensitive miRNA involved in the Adherens Junction pathway and their predicted targets.

<b>miR-509-3p</b>	<b>miR-501-3p</b>	<b>miR-485-5p</b>	<b>miR-96</b>	<b>miR-10a</b>
Rac/cdc42	Nectin	Ponsin	Nectin	Actin
Rac	$\alpha$ -actinin	CKII	Pl20ctn	ADIP
TCF/LEF	LAR	Actin	Rac/cdc42	Smad3
Smad3		TCF/LEF	Vinculin	
		IRSp53	Wave	
			Rac	
			TCF/LEF	
			IGF-1R	
			Yes	
			Fyn	

#### 4.2.2.4.6 ECM-Receptor Interaction

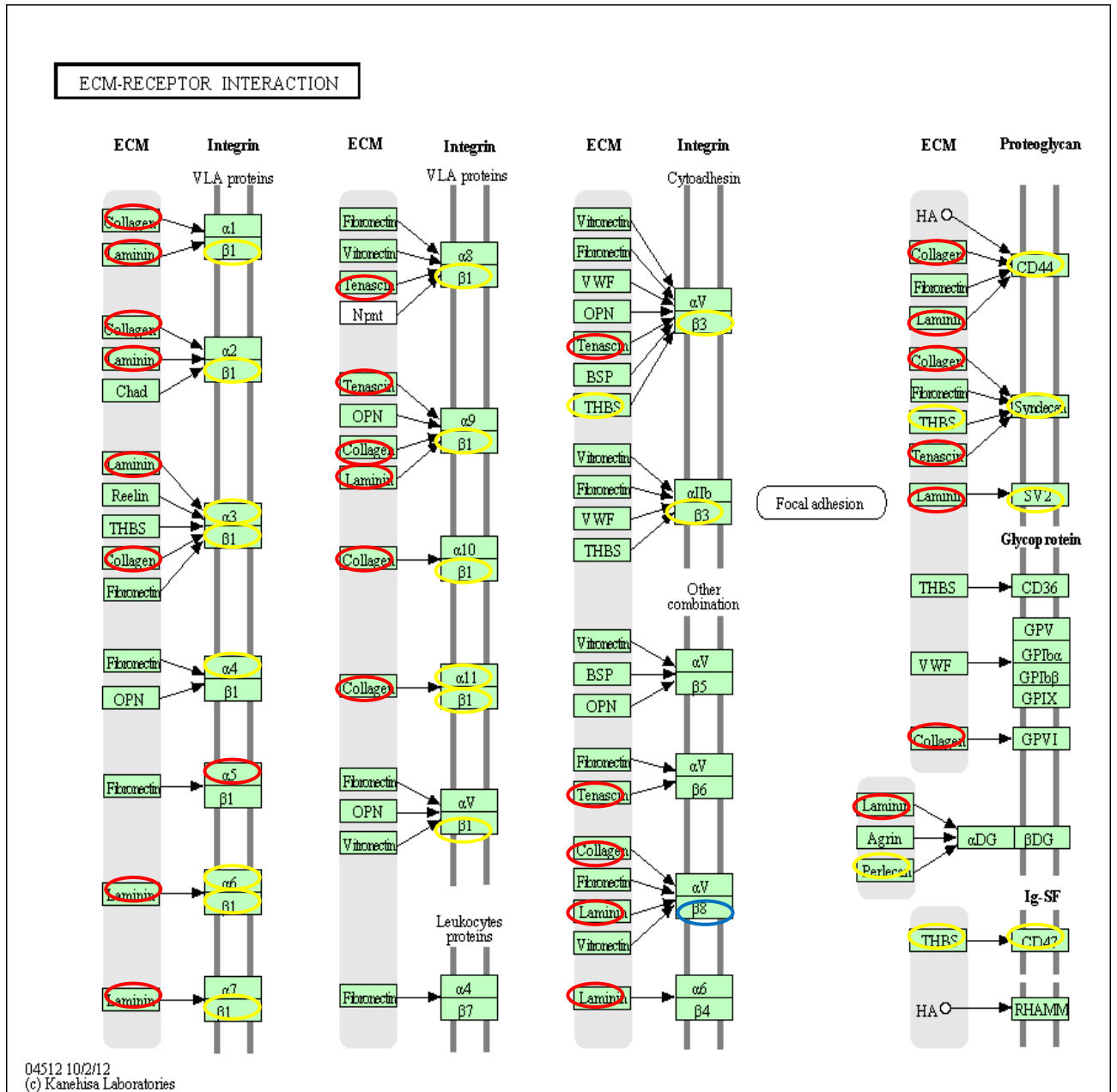


**Figure 4.14:** KEGG map of Extracellular Matrix Receptor Interaction pathway. Genes circled in red are predicted targets for an individual miRNA. Genes circled in blue are predicted targets of multiple miRNA. Genes circled in yellow are predicted targets of published and verified miRNA involved in VSMC function. These may also be predicted targets of multiple novel miRNA along with published miRNA data.

**Table 4.12:** Mechano-sensitive miRNA involved in the ECM-Receptor Interaction signaling pathway and their predicted targets.

<b>miR-143</b>	<b>miR-221/222</b>	<b>miR-29</b>	<b>miR-148a</b>
Collagen	$\beta 8$	Collagen	Collagen
$\alpha 6$	$\beta 3$	Laminin	Laminin
$\beta 8$	CD47	$\beta 1$	Tenascin
CD44	THBS	Perlecan	$\alpha 5$
Syndecam		$\alpha 6$	$\alpha 9$
SV2		$\alpha 11$	$\alpha 11$
			$\beta 8$

### 4.3 Discussion

Since their discovery (R.C. Lee *et al.*, 1993; B Wightman *et al.*, 1993), miRNA have become recognised as one of the key regulators of gene expression during both normal physiological conditions and in disease states. They are short ~22nt non-coding RNA which cause post transcriptional modification by binding to the 3'UTR of their target mRNA. Here, the mRNA either undergoes degradation or translational suppression depending on complementarity between the bases of the miRNA and the gene.

With ~ 30,000 estimated genes encoded by the human genome and only ~ 1,000 miRNA to regulate them, it is clear that one miRNA may regulate hundreds of mRNA. For this reason, miRNA expression signatures can be rich in biological information, especially pertaining to either pathological or disease states. The hundreds of mRNA involved in the fate of cells may only be regulated by a handful of miRNA. These non-coding RNA can also be quantified and qualified with a much greater sensitivity than proteins.

To date, miRNA profiling has been used in developmental biology whereby comparing miRNA profiles at different tissue development stages in organisms can highlight which miRNA are involved in tissue development and cell differentiation (E. Wienholds *et al.*, 2005 Alvarez-Garcia *et al.*, 2005). Their most prevalent use, however, is as biomarkers or bio-indicators for disease. Comparative profiling of miRNA in disease and healthy states can yield certain expression profiles that may be characteristic of disease states and as a result, coined terms such as “angiomiRs” in angiogenesis (S. Wang *et al.*, 2009) and “metastamiRs” for miRNA involved in metastasis (D.R. Hurst., *et al* 2009) have been developed.

The current existing and accepted biological paradigm is that there exists a “miRnome” within a cell, a group of miRNA characteristic to that cell type. The SMC, and in particular the VSMC miRnome has been well characterised. For example, miR- 143 and miR-145 exist as a cluster with their expression being directly related to the phenotype of VSMC by targeting Krupel Like factor 4 (KLF4). Increased expression of this cluster corresponds with a more contractile phenotype, while the opposite is representative of a synthetic SMC (W. Sessa *et al.*, 2010). miR-26a has also shown to be a moderator of VSMC phenotype (N. J. Leeper *et al.*, 2010). The cluster of miR- 221 and miR- 222 has also been implemented in SMC functions such as proliferation (X. Lin *et al.*, 2010) and even SMC calcification (N. Mackenzie *et al.*, 2013).

However, work into the effect of mechanical stimulus such as shear stress or cyclic strain on miRNA is very novel and only a handful have been identified, such as miR-365 (Y.J. Guan *et al.*, 2011) or miR-26a (J. Shaik *et al.*, 2010). Work in this chapter was carried out to identify a panel of mechanically (bio-mechanotransduction) regulated miRNA.

#### 4.3.1 Temporal 10% strain study on HAoSMC miRNA profile

The initial experiment was to try and establish at what time point the miRNA profile of HAoSMC changed most significantly as a result of cyclic strain. Firstly, cells were exposed to a 10% strain at 1Hz over a 48 hour time course. Total RNA was extracted as described in methods chapter 2 section 2.2.5 at time points of 0, 2, 6, 12, 24 and 48 hours. The total RNA was reverse transcribed to cDNA using the miRNA specific primers as described in section 2.2.7. For a full miRNA profile of the cells both A and B human miRNA panels were used for each time point of strain, these utilised qRT-PCR (section. 2.2.7.4).

##### 4.3.1.1 Data Analysis and Normalisation

Initial raw data analysis consisted of extrapolating average delta ( $\Delta$ ) CT values from the profiling and entering them into R statistical analysis software. The data was then mean normalised, which involved removal of all endogenous controls, such as small nuclear RNA. The global measure of miRNA expression was then used as the normalising factor. This method of normalisation is based on the assumption that although specific miRNA may alter expression across samples as a result of experimental condition or stimulus, the overall expression pattern of miRNA is invariable and thus can be used as a normalising factor. This method has been shown to outperform other methods such as use of endogenous small nuclear RNA, in terms of better reduction of technical variance and more accurate appreciation of biological changes (P. Mestdagh *et al.*, 2009; D. Risso *et al.*, 2009; D. Wylie *et al.*, 2011).

The temporal study had a twofold purpose, firstly to establish at what time, if any, the miRNA profile of HAoSMC changed when exposed to 10% cyclic strain at 1Hz, and secondly to see if any miRNA showed a linear relationship between expression and time with 10% strain.

The first stage of experiment validation was to determine if there was a significant separation of the time point samples and this was demonstrated using hierarchical cluster analysis (HCA) on a dendrogram, figure 4.1. This revealed a high degree of similarity between the profiles of static, 2 hour and 6 hour strain samples. A noticeable difference in the miRNA profile expression was not evident until the 12 hour strain time point. However, the later time points of 24 and 48 hours proved to have the highest degree of separation indicating HAoSMCs strained at 10% for these time points had a very different miRNA profile than cells in static culture or cells strained for short periods of time.

Next, the linear expression of miRNA exposed to strain in respect to time was deduced by calculating the Pearson correlation coefficient (PCC). It was also possible to generate a P value for each miRNA using this correlation coefficient. This allowed a priority list to be created made up of miRNA with a strong correlation ( $\geq 0.9$  or  $\leq -0.9$ ) and a P value of  $\leq 0.05$ .

This priority list was then used to formulate two way heat maps for miRNA from the A and B panel (figure 4.2 A and B). This enabled visualisation of the miRNA profile over the time course. A decrease in miRNA expression was represented by a change in color from red to green while similarly an up regulated miRNA is represented by a change from green to red. Similar to the HCA in figure 4.1, the heat map demonstrated that within the first 6 hours of cyclic strain at 10%, the miRNA expression was mostly similar. However, after 12 hours of strain the miRNA expression begins to diverge and by 24 and 48 hours an extensive profile change was observed with the majority of miRNA being down regulated.

As stated in the introduction miRNA have been shown to be heavily involved in supplying robustness to many diverse biological pathways via feed forward and feedback loop mechanisms (M.S. Ebert *et al.*, 2012). It is this level of robustness which allows cells to maintain normal cellular activity during an acute phase of distress or stimulus. This is exemplified by the largely unchanged miRNA profile of HAoSMCs during the initial 12 hours of cyclic strain in this study. Similarly following chronic changes to the cellular environment it is imperative a molecular response is initiated such as the significant miRNA profile expression change seen at the 24 hour stage of cyclic strain.



A selection of correlated miRNA from the heat map which had the strongest PCC was graphed in figures 4.3-4.5. Most of these miRNA are quite novel and only a limited number have been previously characterised and published with even less being associated with vascular biology.

However, one of the novel miRNA, miR-409, was shown to inhibit cell proliferation and vascularization by targeting angiogenin, an angiogenic factor, in a fibrosarcoma HT1080 cell line (C. Weng *et al.*, 2012). Another group showed caveolin-3, a protein responsible for regulating ion channels in the heart, to be a target of miR-328. They found that low expression of this protein coincided with high expression of the miRNA in rat and human tissues with atrial fibrillation, the most common cardiac arrhythmia (Y. J. Lu *et al.*, 2008).

Figure 4.4 A and B show miRNA which had the greatest PCC from the B panel, and again these miRNA are largely unpublished. miR-7 was shown to be differentially expressed in embryonic stem cell differentiation (H. Chen *et al.*, 2010). miR-628 has been associated with both leukemic and normal hematopoiesis (A.J. Favreau *et al.*, 2011). The most published microRNA from the down regulated B panel was miR-497. Down regulation of this miRNA was shown to promote tumor growth and angiogenesis in small lung cancer (W. Zhao *et al.*, 2013).

Figure 4.5 A illustrates miR-1, which is the only microRNA in the priority list known to be involved in VSMCs. Increasing expression of miR-1 was shown in differentiation of embryonic stem cells (ESC) to SMC. A down-regulation of this miRNA in SMCs was also shown to coincide with a reduction in SMC lineage markers (C Xie *et al.*, 2011). Contradictory to this work, however, Y. Jiang *et al.*, (2010) demonstrated myocardin induces miR-1 expression, which represses the expression of contractile proteins and thereby inhibits the contractility of SMCs. This suggested miR-1 plays a role in the negative feedback loop in the regulation of contractility induced by myocardin.

Studies by Jiang *et al.*, (2010) would suggest that the decreased expression of miR-1 found in figure 4.5 (A) dictates a more contractile phenotype in the cells. This correlates to findings in chapter 3 which show that cyclic strain can shift VSMC phenotype to a more contractile state as represented by the increase in expression of the contractile marker mRNA and protein. This has been attributed to myocardin induced expression of miR-1 which in turn inhibits expression of contractile proteins working as a negative feedback loop.

Figures 4.5 (B and C) show graphed expression of two miRNA clusters, namely miR-143/miR-145 and miR-221/miR-222 which both failed to meet the criteria for the priority list. However, their expression was graphed as both of these clusters have been associated with VSMC differentiation. miR-143/miR-145 originate from the same transcriptional unit and are renowned for their crucial role in SMC differentiation and vascular pathogenesis (Elia *et al.*, 2009, W. Sessa *et al.*, 2010).

Both miR-221 and miR-222 are clustered in close proximity on the Xp11.3 chromosome (Altuvia *et al.*, 2005; Calin *et al.*, 2004). In VSMCs, miR-221/222 mediated down-regulation of c-kit reduces the expression level of myocardin which in turn suppresses smooth muscle cell differentiation by inhibition of smooth muscle specific contractile marker gene transcription (Davis *et al.*, 2009). The fact that the expression of this cluster is down regulated over the time course of strain again heightens the fact cyclic strain induces a more contractile state within the cells.

In contrast, the miR- 143/miR-145 cluster was also down regulated with strain which would suggest that the cells were in a more synthetic state. However, due to the limitations in this study, namely the lack of biological replicates, it is impossible to comment with confidence on the expression of any individual miRNA.

To determine which genes may be affected by the down regulated miRNA shown in figures 4.3-4.5, their putative targets were downloaded from Target Scan (Table 4.1). The involvement of these *in silico* predicted genes in cellular processes was then assessed by determining enrichment against Gene Ontology (GO) biological processes. In addition, DAVID bioinformatics software was used to highlight the involvement of predicted targets in pathways of interest from the Kyoto Encyclopedia of Genes and Genomes (KEGG) (Table 4.2).

It is important to note the reason for selecting miRNA which maintained a strong PCC was that the temporal study did not contain replicates. As such, although their expression profile were interesting, it was impossible to have confidence and justify further bioinformatics on miRNA candidates which showed strong expression changes at earlier time points. The primary focus of this temporal study was to elucidate a time point in which the global miRNA expression signature was altered with strain.

#### 4.3.2 Investigation of strain amplitude on miRNA profile (biological replicates)

To ascertain if the strain amplitude had any effect on the SMC miRnome, a second study involving biological replicates was designed. The strain amplitudes chosen were 5%, 10% and static control and these were applied over a time point of 24 hours. They were selected on the basis that in the previous temporal study at 10% cyclic strain, there was minimal change in the miRNA profile over the first 6 hours of strain followed by a slight shift towards global down-regulation of miRNA after 12 hours, while after 24 hours of cyclic strain the profile was significantly altered. Although a greater change was observed after 48 hours, it is possible that some of these changes may be as a result of cross-talk between activation molecules of downstream signaling pathways (e.g. negative and positive feedback loops) and not entirely due to the strain alone.

The average delta CT values were entered into R statistical software where they were mean normalized, as previously described. New priority lists were then created (10% vs. 5%, 5% vs. static and 10% vs. static) comprising of miRNA which had an adjusted P. Value of  $\leq 0.05$ , using the Benjamini-Hochberg approach.

#### 4.3.2.1 Adjusted P Value

The adjusted P value method allows for controlling the rate of false positives. To begin an acceptable false discovery rate is selected, for example 10%. This means 10% of the significant miRNA would be false positives. This is acceptable in a large scale screening experiment, as presented in this chapter, as any false positives would be found in follow-up experiments on short listed miRNA. Next P values of miRNA are placed in order from smallest to largest. The smallest P value has a rank of  $i=1$ , the next has  $i=2$ , etc. Each individual P value is then compared to:

$$(i/m)Q$$

Where  $m$  is the total number being tested and  $Q$  is the chosen false discovery rate. The miRNA which has the largest P value but is  $\leq (i/m)Q$  is significant and all P values smaller than this are also significant (Y. Benjamini., Y. Hochberg *et al.*, 1995).

Using HCA, (figure 4.6) the first stage of experimental validation was to determine if the biological replicates clustered and if there was a reasonable degree of separation between the strain conditions. This validation was shown using a dendrogram (figure 4.6). A substantial difference in the miRNA profile was evident between 10% and 5% cyclic strain, with a more modest change observed between 5% strain and static adhesion.

The Venn diagrams in figures 4.7 and 4.8 have a twofold purpose; to show the numbers of miRNA in the priority lists and to demonstrate whether these miRNA are up-regulated or down-regulated with strain. Figures 4.7 (A) and 4.8 (A) illustrate the number of miRNA, from the A and B panel respectively, which are unique to each strain comparison. In addition to this, they show the numbers of miRNA which are common across strain comparisons. Figures 4.7 (B) and 4.8 (B) show the direction of expression of miRNA in the priority list for each strain comparison. For example in figure 4.7 (A) there are a total of 75 miRNA in the priority list of 10% strain vs. 5%. From the venn diagram we can see 36 of these are unique to 10% vs. 5%, 38 are common between 10% vs. 5% and 10% vs. static and 1 miRNA is common to all three strain comparisons. Figure 4.7 (B) shows the direction of expression of these miRNA. Of the 36 miRNA in 10% vs. 5% 35 are down regulated and 1 is up-regulated. The one

miRNA common to all three strain comparisons is no longer in the centre as its direction of expression is only common in 10% vs. 5% and 10% vs. static.

The majority of miRNA on the A card between the 10% vs 5% and 10% vs. static conditions were down-regulated with strain. The low number of differentially expressed miRNA within the priority list between 5% and static would suggest that the miRnome of HAoSMCs strained at this amplitude is not significantly different to cells in static culture. Interestingly, and in contrast to the A card, the majority of the miRNA on the B card between 10% vs 5% and 10% vs static conditions were up-regulated, this may be explained by the fact the B panel contains many star or passenger strand miRNA which have been shown to be differentially regulated to the leading strand (Kuchenbauer *et al.*, 2011). As with the previous temporal study, putative targets for the priority miRNA were downloaded from Target scan. The involvement of these targets in cellular activity was shown by determining enrichment against GO biological processes. The involvement of the *in silico* predicted targets in pathways of interest were evaluated by downloading KEGG pathway maps from DAVID bioinformatics software. miRNA with the lowest adjusted P value and highest fold change were tabulated in tables 4.3 -4.5, listing miRNA from the 10% vs. 5%, 10% vs. static and 5% vs. static conditions. The adjusted P value, fold change, number of conserved targets, number of biological processes these targets are involved in, and number of pathways the predicted genes are linked to are included in these tables for each miRNA.

Table 4.6 displays the miRNA potentially involved in each of the pathways of interest and whether these specific miRNA were up-regulated or down-regulated with the three strain conditions. Work presented in the literature highlights the involvement of many of these shortlisted miRNA in cell migration, particularly in cancer metastasis. In a study by Zhang *et al.*, (2010), miR-520e was shown to be a novel tumor suppressor, as expression levels in clinical hepatocellular carcinoma tissues were shown to be dramatically decreased. The miR-520e gene is located in 19q13.42 and is reported to be in chromosome 19 miRNA cluster (C19MC), the largest human miRNA gene cluster discovered so far (Bo-an Li *et al.*, 2012). This miRNA is thought to inhibit cell migration through suppression of NIK/p-ERK1/2/NF-κB signaling pathway. In our study, its expression was shown to be increased under conditions of 10% cyclic strain vs 5% strain, and based on the literature, this may represent reduced migration in HAoSMC.

This theory is further strengthened by looking at the expression of miR-373: This miRNA was shown to promote tumour cell invasion and metastasis *in vitro* and *in vivo*. Increased expression was found in human breast cancer samples in which the miRNA was predicted to target CD44 (Q Huang *et al.*, 2008). In our study, expression of miR-373 was shown to be down-regulated under conditions of 10% strain vs static adhesion.

In the same study by Huang *et al.*, (2008), expression of miR-520c-3p showed to be also increased in carcinoma tissues. However, unlike miR-373, in this work its expression was increased between 10% and 5% strain and 10% and static adhesion. Interestingly though expression was decreased between 5% and static adhesion, this would highlight the impact of strain amplitude on the patho-physiological effect of cyclic strain and miRNA expression.

Importance of strain amplitude can also be seen by looking at the expression levels of another novel miRNA, miR-610, which made the priority shortlist. miR-610 has been shown to inhibit the migration and invasion of gastric cancer cells by suppressing the expression of vasodilator-stimulated phosphoprotein (VASP) (Wang *et al.*, 2012). In our study, this miRNA was shown to be increased by greater than 100-fold in the 10% strain vs 5% strain, but is decreased in cells at 5% vs static adhesion. However, as it is possible that a single miRNA can potentially modulate the expression of hundreds of genes and associated pathways, it is probable that miR-610 working as a tumor suppressor in gastric cancer cells may not impact on VSMC migration. With this in mind miRNA specific to VSMC were also investigated.

Levels of the miR-143/miR-145 cluster as discussed previously were shown to be decreased with 10% strain when compared to static adhesion and 5% strain at 24 hours. However, although this cluster fell short of the P value required for the short list in the 5% strain vs static conditions, the expression levels were shown to be increased. This shows a more physiological response of the cells to the lower amplitude strain. The study also yielded potential new miRNA highly involved in VSMC biology these were, miR-610, miR-661 and miR-96. These miRNA were predicted to target several genes in the vascular smooth muscle contraction pathway, as determined by using DAVID software analysis.

The pathway maps downloaded using DAVID from KEGG were used to show the role of predicted targets in pathways of interest. These pathways are shown in figures 4.9 - 4.14 and a list of their associated target genes are shown in tables 4.7 - 4.14. Pathways

were chosen based on their involvement in cell migration and motility. Genes within the pathways of interest targeted by a single miRNA are circled in red, while those potentially targeted by 2 or more miRNA are circled in blue. In addition, genes that were targets of verified and published miRNA involved in VSMC biology are circled in yellow. Selected pathways were based on VSMC functions of interest and included migration, focal adhesion, ECM receptor interaction, VSMC contraction, regulation of actin cytoskeleton and adherens junction and cell cycle.

Cell signaling pathways which also had numerous mechano-sensitive miRNA involved included MAPK (which was shown to be activated by cyclic strain, Wnt and mTOR signalling, p53, VEGF and Calcium signaling pathways. These are highlighted in the appendix. All of these pathways contained copious predicted targets of the mechano-sensitive miRNA which were shortlisted.

#### **4.4 Summary and Conclusion**

Characterisation of an individual cell's "miRnome" is a valuable asset when assessing the patho-physiological impact of a condition, such as cyclic strain. The initial temporal study of the miRNA profile had a two-fold significance. Firstly, it revealed a change in the HAoSMC miRNA profile that was only evident after 12 to 24 hours of strain. This would suggest HAoSMC are not as sensitive to cyclic strain as initially thought. Evidence for this is further shown by the fact that there was such a low number of strain-regulated miRNA differentially expressed between 5% strain and static cells, when compared to the higher strain. Secondly it presented a list of mechanically-sensitive miRNA with expression levels that were linearly correlated with time.

As sample replicates were not performed in this preliminary study reliability of individual miRNA expression is limited, the study was only designed to reveal what time point during strain a global miRNA expression change was evident. A second, more detailed study containing biological triplicates of samples was conducted to look at individual miRNA. This also focused on how strain amplitude was implemented in HAoSMC response to mechanical stimulus. Cells were exposed to 24 hour strain at 10% and 5% and also static conditions.

The priority list of miRNA was generated by retaining only those with an adjusted P value of equal to or less than 0.05 using the Benjamini Hochberg method. This produced a substantial list of miRNA from each of the strain conditions. miRNA with the highest differential expression, either increased or decreased, were presented in tables 4.4-4.5 along with bioinformatic analysis carried out. This included *in silico* prediction of putative targets followed up by assessment of the potential involvement of these targets in cellular process' and pathways.

Of these novel miRNA, some show predicted involvement in SMC biology such as the vascular smooth muscle cell contraction pathway, namely miR-610 and miR-661. Other miRNA selected for bioinformatics, miR-520e, miR- 520c-3p and miR-373, showed promising target predictions involved in pathways concerning cell motility. These included focal adhesion, regulation of actin cytoskeleton, VSMC contraction pathway, cell cycle, adherens junction and ECM receptor interaction pathway. These miRNA are novel and largely unpublished, providing a promising avenue for further investigation. Follow up experiments are also essential as the *in silico* target predictions are just that, predictions. They need to be validated before further research is carried out. Validation can be performed through use of loss and gain of function experiments and luciferase reporter assays.

To conclude, it appears that the use of miRNA expression to identify either VSMC phenotype is ambiguous. For example, miR-1 (figure 4.5) was shown to induce both a contractile and a synthetic phenotype by two different groups. In this thesis, the expressions of both the miR-143/miR-145 and miR-221/miR-222 clusters were decreased compared to that of the static control, at 24 hour 10% strain. In case of the miR-143/miR-145 cluster this would suggest a more synthetic phenotype (Elia *et al.*, 2009; Sessa *et al.*, 2010). Yet reduction in miR-221/miR-222 cluster expression suggests the opposite, a more contractile cell (Altuvia *et al.*, 2005; Calin *et al.*, 2004). In the 5% vs. static condition, however, the miR-143/miR-145 cluster is increased compared with the static control, yet the P value for these two miRNA in this condition did not meet the criteria for the priority list used.



It is obvious from our studies and findings that looking at individual miRNA expression data in isolation, may not give the full biological explanation and rationale to certain events studied and observed, but rather the various permutations and combinations of miRNA expression must be considered. To become fixated with what miRNA expression corresponds to what SMC phenotype is all too easy given the amount of literature. To truly characterise the phenotype of a certain population of SMCs a combination of cell functions, contractile marker expression, cell morphology and the cell miRnome should be utilised. However, work carried out in this chapter was primarily done to establish a shortlisted panel of mechano-sensitive miRNA and not to directly implement these with a specific HAoSMC phenotype.

## **CHAPTER FIVE: Functional Studies on HAoSMCs Exposed to Cyclic Strain**

### **5.1 Introduction**

The primary function of SMCs is to maintain vascular tone and provide vessel resistance to changes in the mechanical environment (Moiseeva *et al.*, 2001). They are able to achieve this through their unique phenotype plasticity. In a healthy vessel, the SMCs are mostly quiescent showing reduced cell functions such as proliferation and migration. All vessels within the body are an environment of constant mechanical strain and stress. This is attributed to the haemodynamic force of blood flow, which is experienced in two forms; shear stress which is a result of the longitudinal force of the blood flow across the endothelial layer and cyclic strain which is produced as a result of the pulsatile nature of blood flow. This is felt by all cells making up the vessel and is perpendicular to the lumen.

Cells within the vessel resist these forces by adhering to the ECM, and by forming cell-cell contacts (Moiseeva *et al.*, 2001). This is achieved through adhesion receptors such as syndecans, cadherins, dystrophin-glycoprotein complex (DGPC) and integrins. Alteration of the normal magnitude of this force (under straining or overstraining) or the initiation and prolonged maintenance of perturbed pathogenic forms (e.g. oscillatory flow) can lead to serious cardiovascular disease such as atherosclerosis. These pathological changes in haemodynamics can be induced in a disease state such as hypertension or following surgical procedures like, balloon angioplasty or coronary artery bypass grafting or stenting (Taylor *et al.*, 2000; Moiseeva *et al.*, 2001). The high levels of cyclic strain as a consequence of these states can result in a pro-migratory, synthetic SMC (Li and Chaikof *et al.*, 2002). Pro-migratory and proliferative SMCs can lead to an array of vascular disorders, including restenosis after stenting and atherosclerosis. In the case of atherosclerosis, the migrating SMCs result in progression of stable plaques, as the cells migrate through the endothelium. This initiates with disengagement of ECM adhesion receptors to allow motility of the cell. Following this, destruction of the basement membrane creates an intracellular space through which the cells can migrate (Hahn and Schwartz *et al.*, 2009).

In contrast to the pathological consequences associated with hypertension or high mechanical loading on the vessel wall, a physiological level of intraluminal pressure is essential for maintenance of homeostasis within the vessel (Birukov *et al.*, 1998). Studies have shown mechanical straining is essential for maintaining levels of contractile markers in SMCs such as SM  $\alpha$ -actin and caldesmon (Tock *et al.*, 2002; Wang *et al.*, 2006; Birukov *et al.*, 1998).

Cyclic strain can also induce expression of SMC specific markers and ultimately differentiation in other cells types (Cevallos *et al.*, 2006).

Attempts to replicate this mechanical environment of blood vessels have been largely successful using several unique *in vitro* models (Brown *et al.*, 2000). However studies have yielded varying results into the functional changes of SMCs in culture exposed to cyclic strain. Qi Ying-Xin *et al.*, (2010) observed an increase in SMC migration and proliferation when exposed to 15% strain at 1.25 Hz for 24 hours in comparison to cells strained at 5%. Similar results were seen in more recent studies which showed cyclic strain at 15% stimulating migration through the PI3K/AKT pathway in SMCs. (Bu-Chun Zhang *et al.*, 2012).

Contradictory to this, Tock *et al.*, (2003) found that cyclic strain of the same amplitude increased VSMC expression of smooth muscle  $\alpha$ -actin pertaining to a more contractile, less proliferative and migratory phenotype. A lot of the conflicting data can probably be attributed to differences in the degree and characteristics of the strain applied as well as the starting phenotype of the cells and passage number (Rensen *et al.*, 2007). Although these opposing results exist in the literature, it is clearly apparent that cyclic strain does indeed regulate SMC function and phenotype. However, to what extent and direction still needs to be fully deduced.

#### 5.1.1 miRNA Regulation of Cell Function

Nearly all biological processes involved in cell growth and survival is now shown in the literature to be regulated to some extent by the still novel moiety, miRNA. As a result numerous institutes are investigating the role of these non-coding RNA in SMC phenotype and function and consequently the VSMC "miRnome" is becoming prominently characterised. W. Sessa's group has shown the miRNA cluster miR-143/miR-145 to be a reliable marker for phenotypic modulation within the cell. A high level of these miRNA within the cell is directly related to a contractile phenotype. In contrast increased expression of other miRNA such as the miR-221/miR-222 cluster and

miR-21 is evident in proliferating synthetic SMCs (Davis *et al.*, 2009; Liu *et al.*, 2009; Cheng *et al.*, 2007)

Manipulation of the cell's miRNA processing machinery, such as knock-out of Dicer or Argonaute-2, is proving to be an advantageous first step in implicating their involvement in a desired cellular mechanism or function. However, this is very much a "blunt instrument" approach. (Suarez *et al.*, 2007; Naoghare *et al.*, 2011) To take true advantage of the regulatory influence of miRNA, individual roles in specific biological processes must be drawn out from profiling experiments. Once a short list panel of miRNA of interest has been established it is possible to elucidate their exact regulatory role in a desired process. This can be achieved by implementing loss and gain of function experiments with individual or combinations of miRNA.

Work in this chapter was based on the theory that miRNA facilitate messaging of external stimulus or environmental cues into a functional response through signaling hubs such as cell-cell and cell-ECM contacts. The external stimulus in this study is mechanical cyclic strain which is predominantly sensed through membrane bound adhesion molecules such as integrins.

### **Chapter Hypothesis:**

This chapter hypothesis was that *cyclic strain alters smooth muscle cell functions such as adhesion, migration and proliferation and that these altered cell fates are controlled by miRNA regulation.*

### **Specific aims and Experimental approach**

To test this hypothesis, experiments in this chapter were designed to characterize:

- **Impact of cyclic strain on HAoSMC migration.**

Cells were exposed to 6, 12, 24, 48 and 72 hours of 10% strain at 1Hz. The rate of migration of the cells was then compared to their static culture counter parts using the xCELLigence impedance based system described in chapter 2.

- **Involvement of miRNA in HAoSMC cell function.**

This was approached by means of an Argonaute 2 (Ago2) knock down using siRNA. Without Ago2 to incorporate mature miRNA into RISC, the effector function of miRNA is lost. To evaluate how this impacted the SMC phenotype expression of the contractile marker,  $\alpha$ -actin was quantified by western blot.

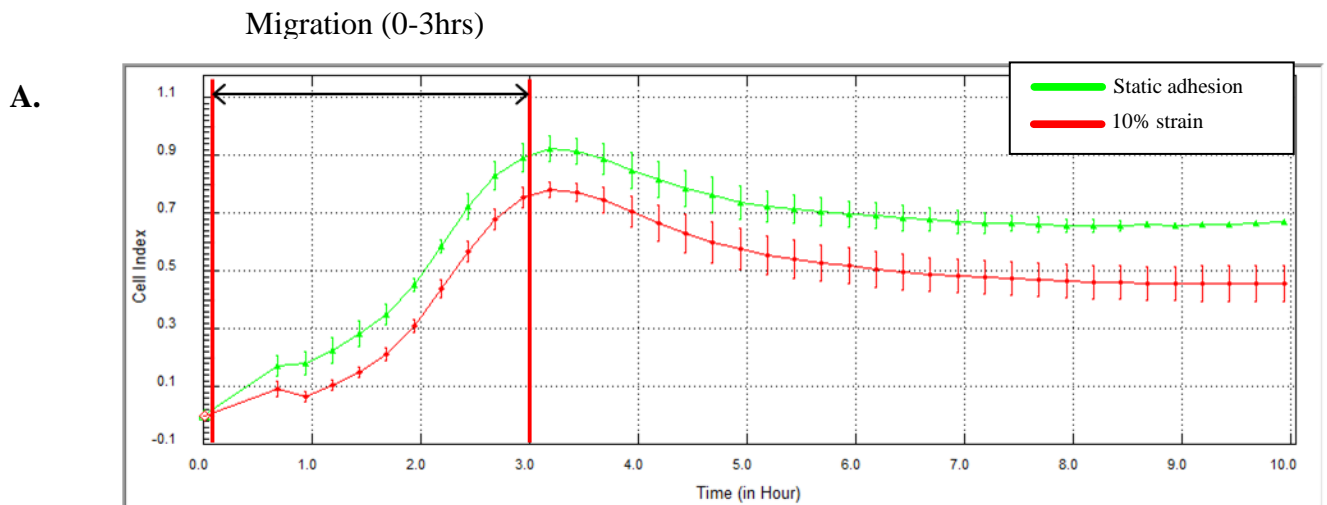
- **Involvement of miRNA on HAoSMC phenotype**

Expression levels of contractile marker  $\alpha$ -actin were determined in Argonaute2 deficient HAoSMCs.

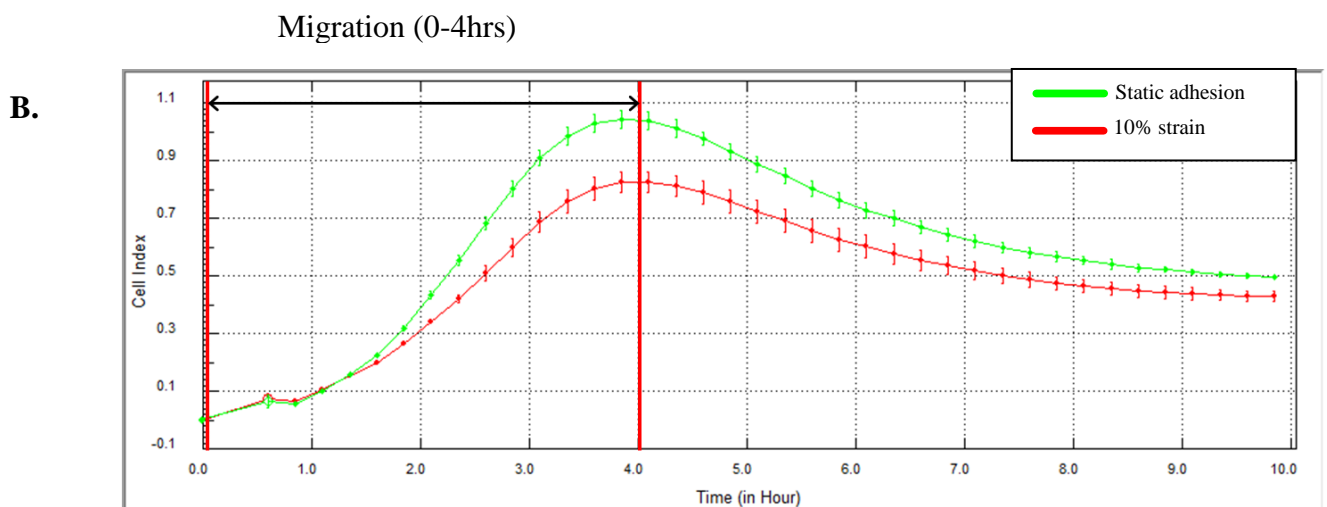
## 5.2 Results

### 5.2.1 Impact of cyclic strain on HAoSMC migration.

HAoSMC migration was monitored using the real time impedance based xCELLigence system. Migration was monitored in SMCs exposed to 10% cyclic over a 72 hour time course, time points included were 6, 12, 24, 48 and 72 hours as shown in figure 5.1 (A-E). Plots shown are migration assays using the xCELLigence “CIM” plate. Rate of migration is quantified off the slope of the graph over the initial time points, typically within the first 5 hours of the experiment.



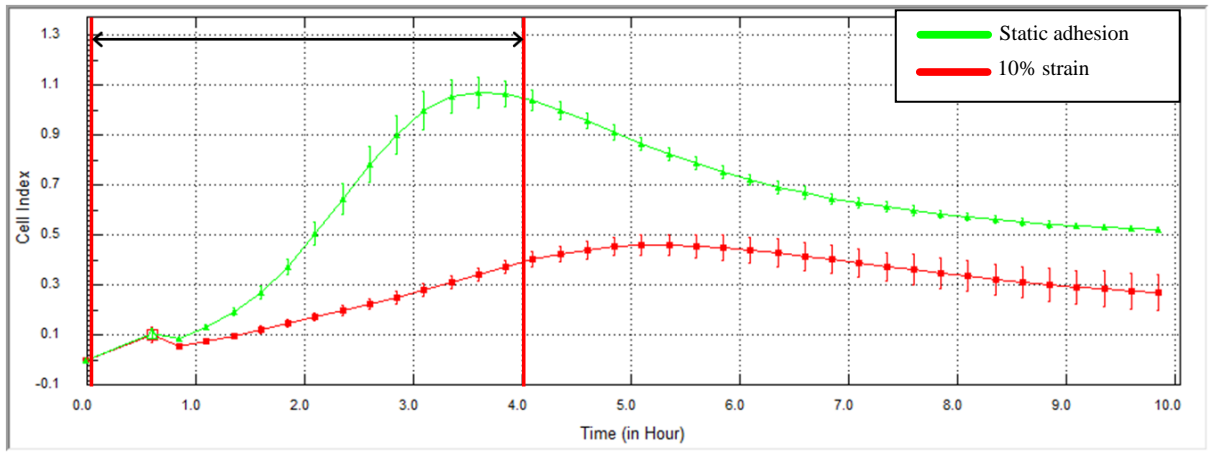
6hr 10% strain vs. static



12hr 10% strain vs. static

Migration (0-4hrs)

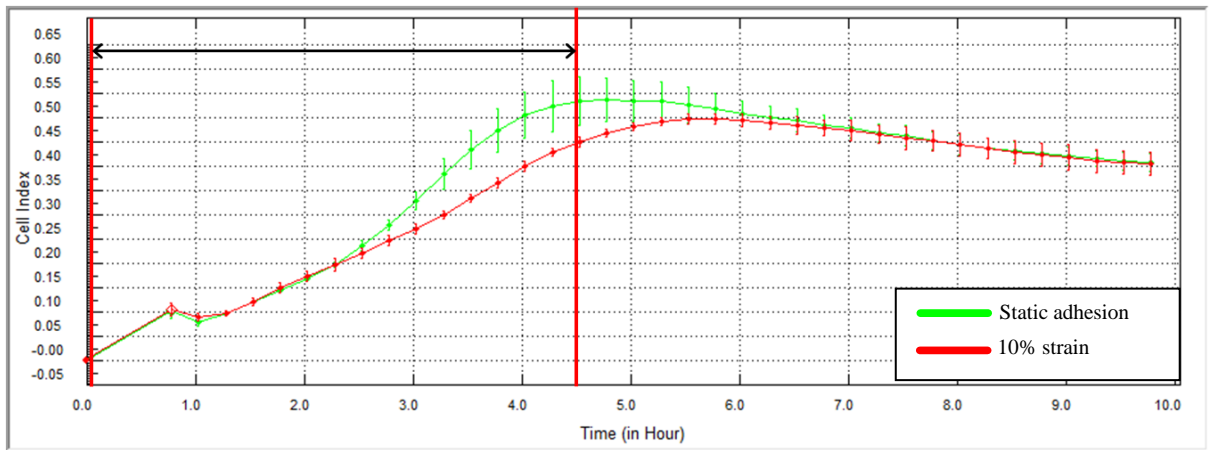
C.



24hr 10% strain vs. static

Migration (0-4hr 30 min)

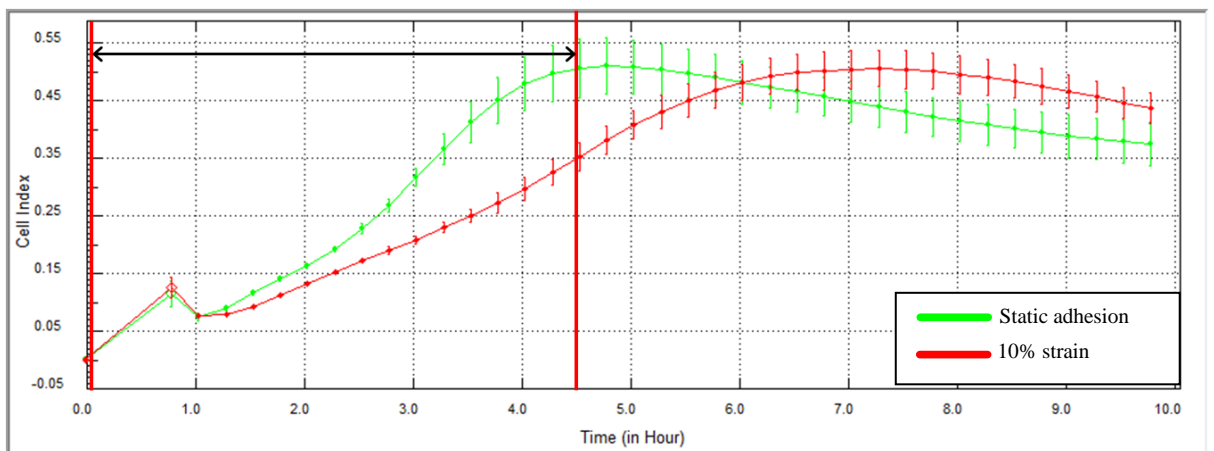
D.



48hr 10% strain vs. static

Migration (0-4hr 30 min)

E.



72hr 10% strain vs. static

F.

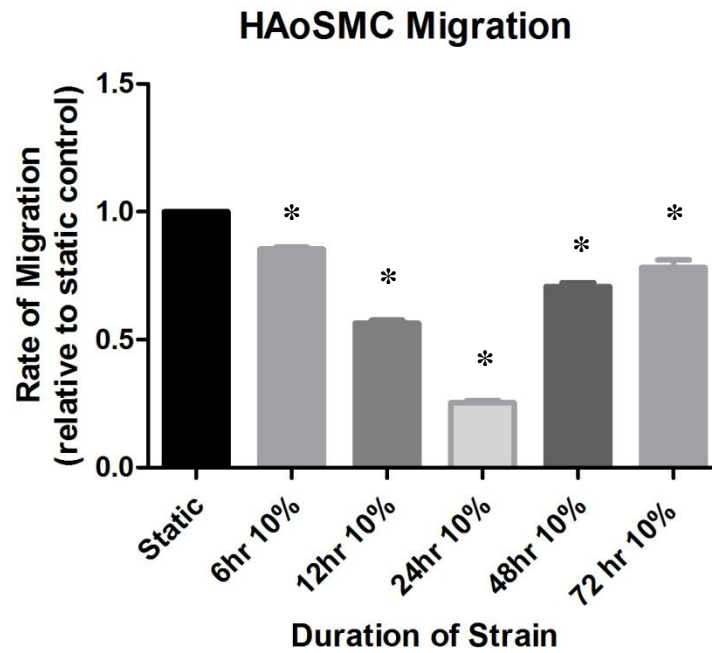


**Figure 5.1 (A-F):** xCELLigence Migration plots of HAoSMCs exposed to 10% cyclic strain. Figure 5.1 (A-F) show plots of migration generated from the xCELLigence instrument. These compare HAoSMCs in static culture to cells exposed to 10% cyclic strain over a 72 hour time course. Time points included were; 6hr 10% vs. static (**A**), 12hr 10% vs. static (**B**), 24hr 10% vs. static (**C**), 48hr 10% vs. static (**D**) and finally 72hr 10% vs. static (**E**). Figure 5.1 **F** shows a quantitative graph of cell migration of strained cells compared against the static control. n=3, \*P $\leq$ 0.05 vs. static adhesion; one-way Anova.



### 5.2.2 Argonaute-2 (Ago2) Knock Down Study.

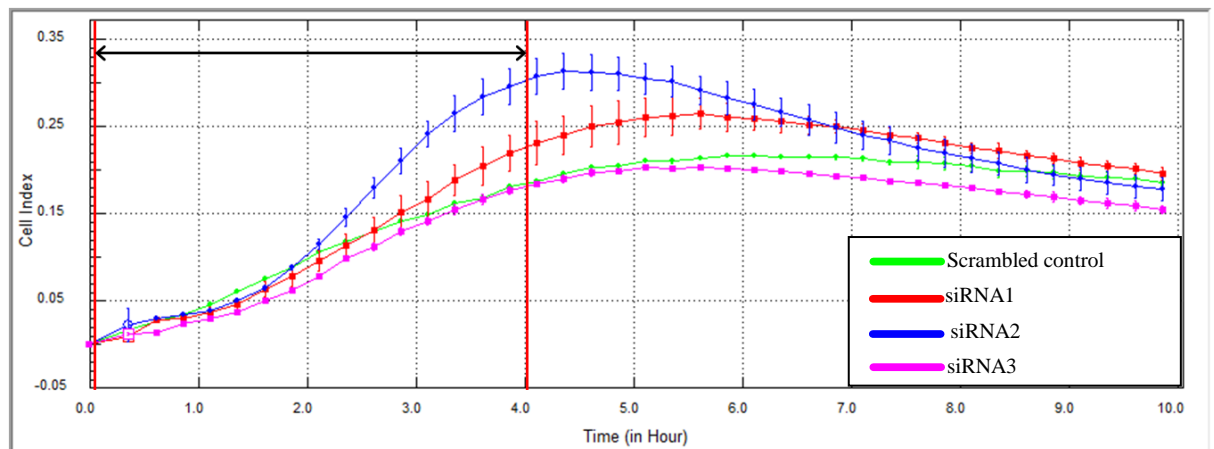
This study was designed to investigate the effect of a diminished miRNA effector function on HAoSMC functions such as migration, adhesion and proliferation. This was achieved by knock down of the Argonaute2 protein which is responsible for incorporating mature miRNA into the RNA Induced Silencing Complex (RISC). Effective knock down was achieved using both a pre validated siRNA from Ambion<sup>®</sup> and a custom synthesised siRNA, sequence taken from the work of Naoghre *et al.*, (2010).

#### 5.2.2.1 Optimisation of siRNA for Ago2

The three pre-designed siRNA supplied by Ambion<sup>®</sup> and the custom synthesised siRNA were tested for their impact on HAoSMC migration using the xCELLigence system as shown in figure 5.3 (A-C). Due to the ease of the assay this was done as an initial screening for the most efficient siRNA prior to quantification of knock down using western blot.

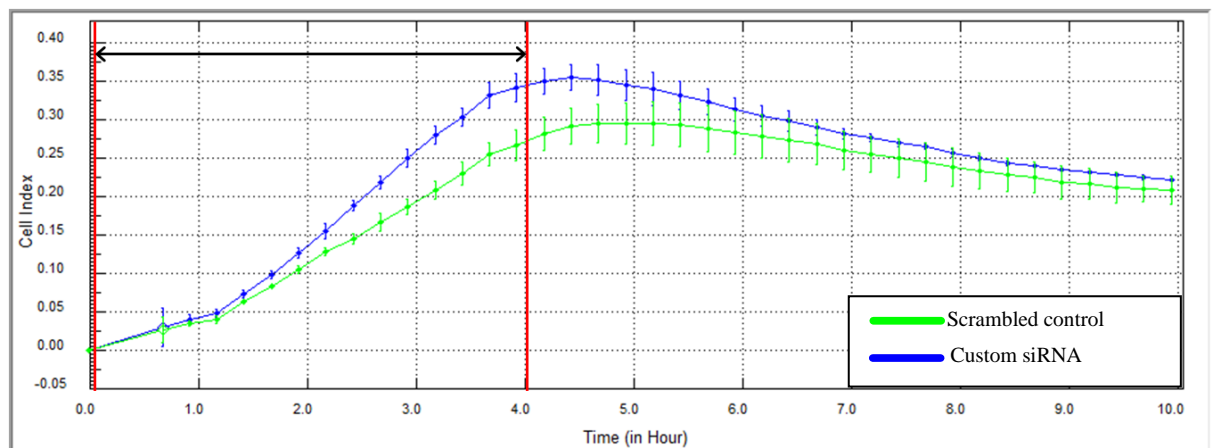
Migration (0-4hrs)

A.



Migration (0-4hrs)

B.



C.

### Ago2 siRNA

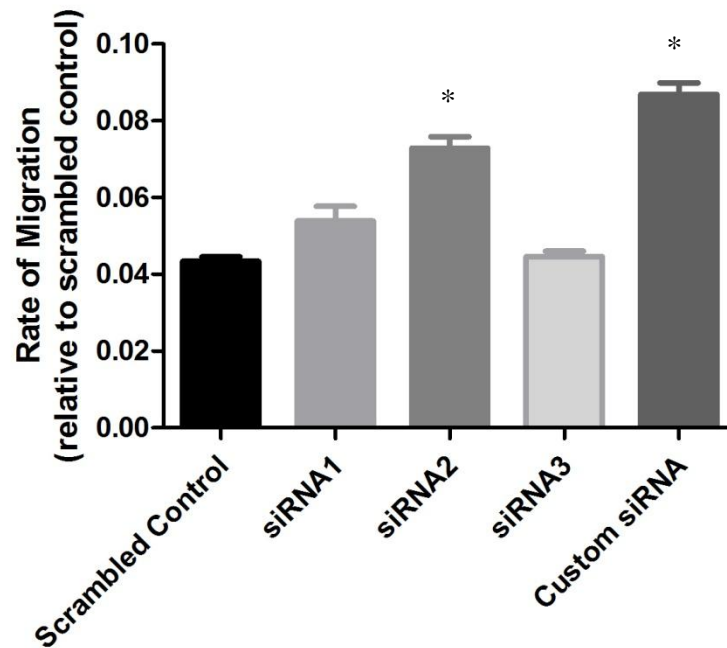


**Figure 5.2 (A-C): Optimisation of siRNA for Ago2.** Figure 5.2 A shows an xCELLigence plot of migration with the three pre designed siRNA and a scrambled siRNA control. **Green plot** – scrambled control, **Pink plot** – siRNA3, **Red plot** – siRNA1, **Blue plot** – siRNA2. Rate of migration was determined over the initial 4 hours. Figure 5.2 B shows an xCELLigence plot of migration with the custom synthesised siRNA and a scrambled control. **Green plot** – scrambled control, **Blue plot** – Custom siRNA. Rate of migration was determined over the initial 4 hours. Figure 5.2 C graph quantifying the rate of migration of HAoSMC transfected with one of the four siRNA compared against the migration of cells transfected with scrambled siRNA. The increased migration of HAoSMCs transfected with siRNA 2 and the custom siRNA was taken as consequence of a reduced miRNA function via the knock down of Ago2. As a result both these siRNA were chosen for quantification of knock down by western blot. n=3, \* $P \leq 0.05$  vs. scrambled control; pairwise t-test.

5.2.2.2 Quantification of Ago2 knock down efficiency with siRNA2 and Custom siRNA.

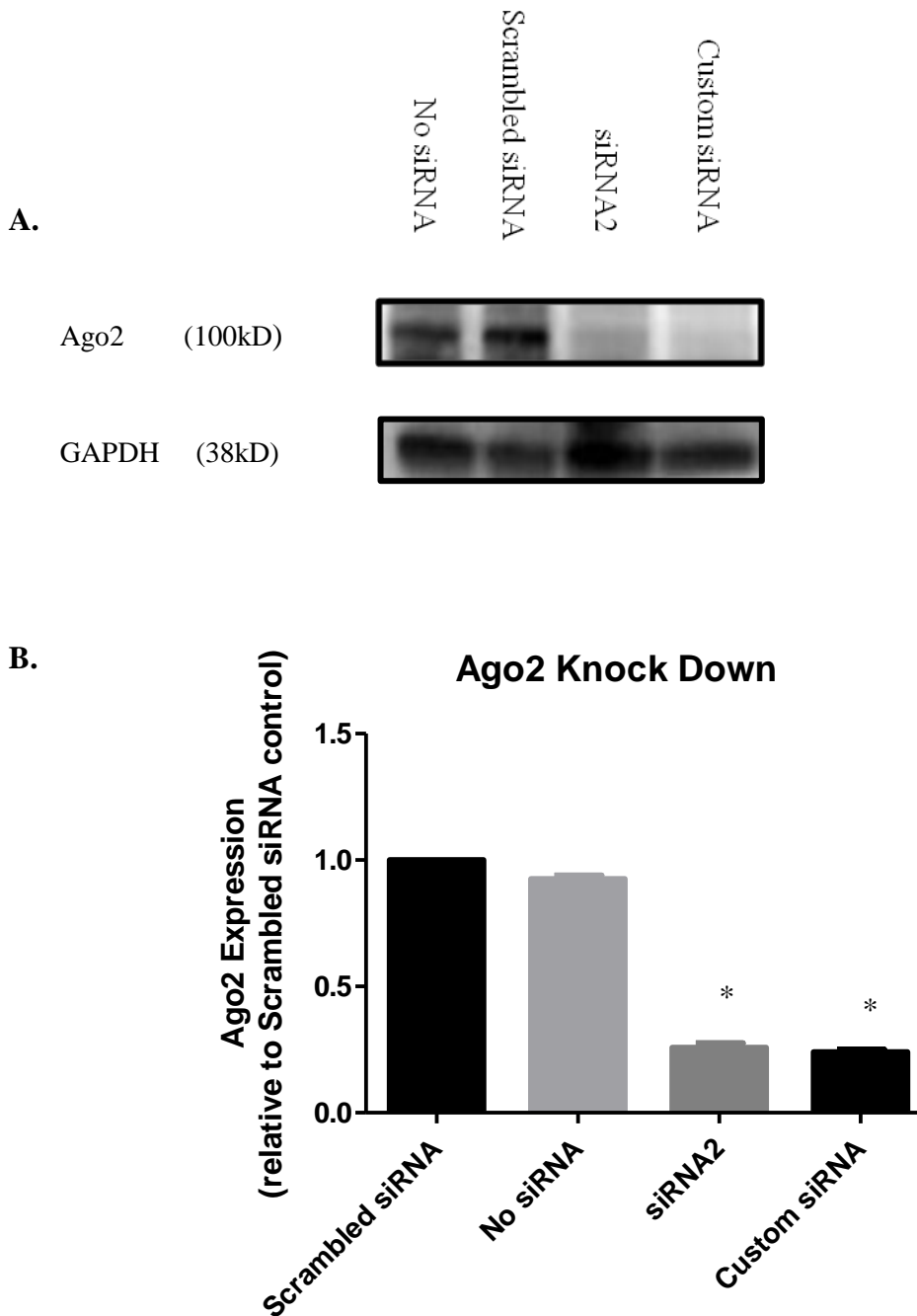


**Figure 5.3 A&B: Quantification of Ago2 Knock Down with siRNA.** Efficiency of siRNA knock down of Ago2 was quantified using western blot (figure 5.3 A). Blot shows expression of Ago2 from four sample lysates; including no siRNA control, scrambled siRNA control, pre-designed siRNA2 and custom synthesised siRNA. Quantification of protein expression was achieved using densitometry analysis on bands with Image J software. n=3, \* $P \leq 0.05$  vs. scrambled control; pairwise t-test.

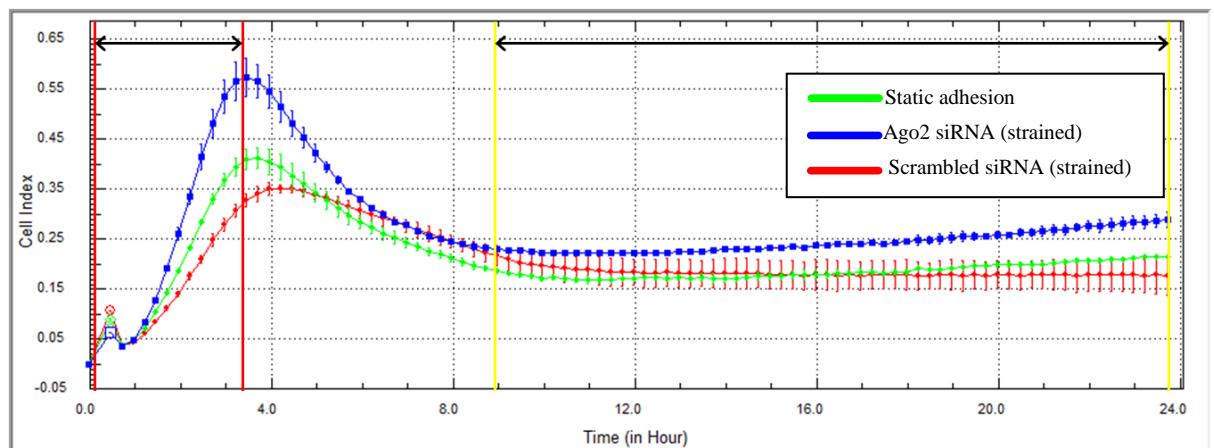
### 5.2.3 Impact of cyclic strain on migration of HAoSMCs with Ago2 knock down

The physiological response of HAoSMCs to 10% cyclic strain at the earlier time points is shown by reduced migration of the cells in figure 5.1 A-C. This correlates to the change in expression of contractile markers, chapter 3, and the change in expression of miRNA in chapter 4. To globally connect miRNA as the regulators of this response, we investigated the implication of knocking down argonaute-2 within the cells. This has the effect of reducing miRNA effector function by inhibiting binding of the mature miRNA to their target mRNA. These Ago2 deficient cells were then exposed to the migration inhibiting 10% cyclic strain as shown in figure 5.1 A-C along with a scrambled control and compared against HAoSMCs which had been in static culture, this is outlined in figure 5.4.

Migration (0-3hr 30min)

Doubling Time (9-24hrs)

A.



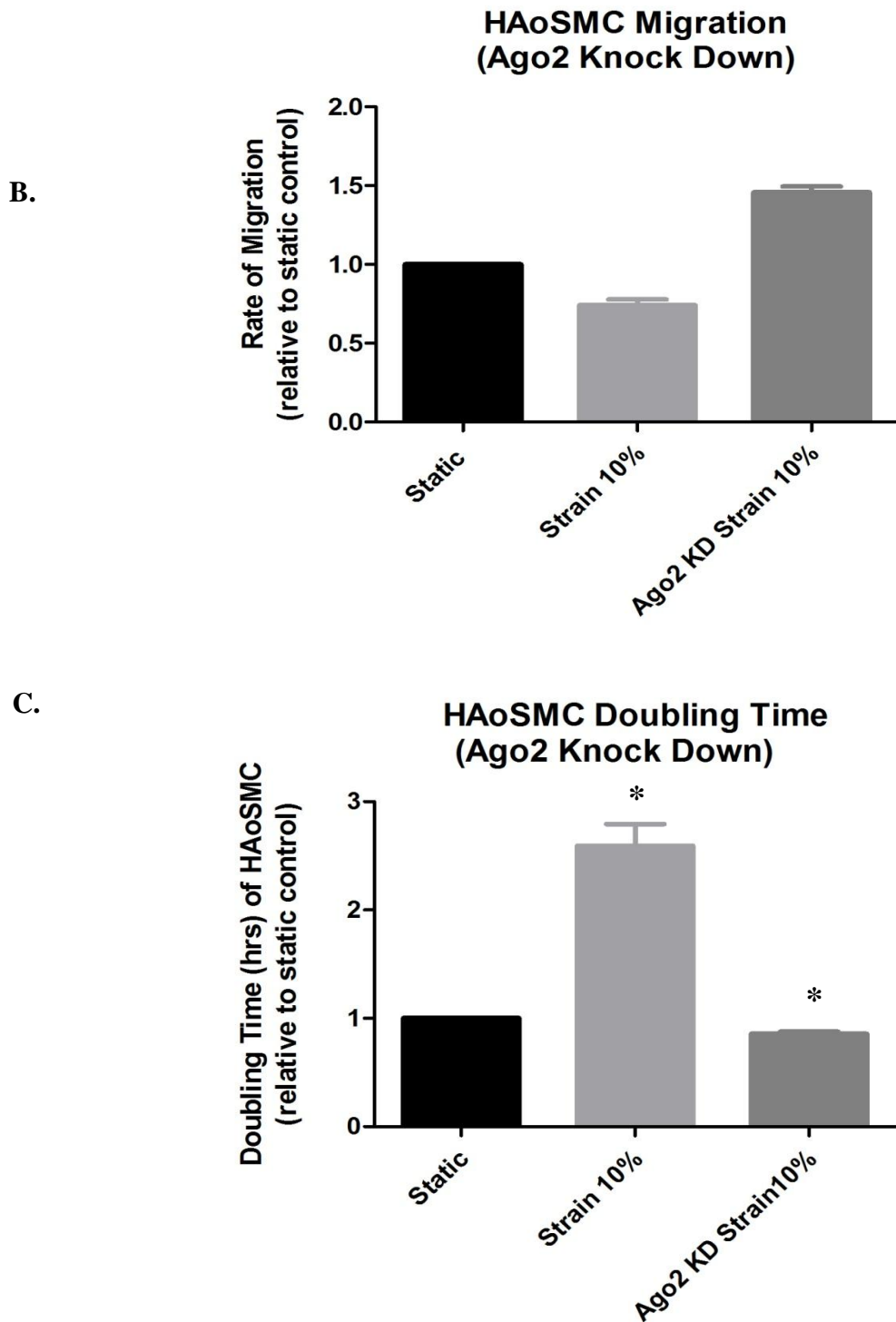
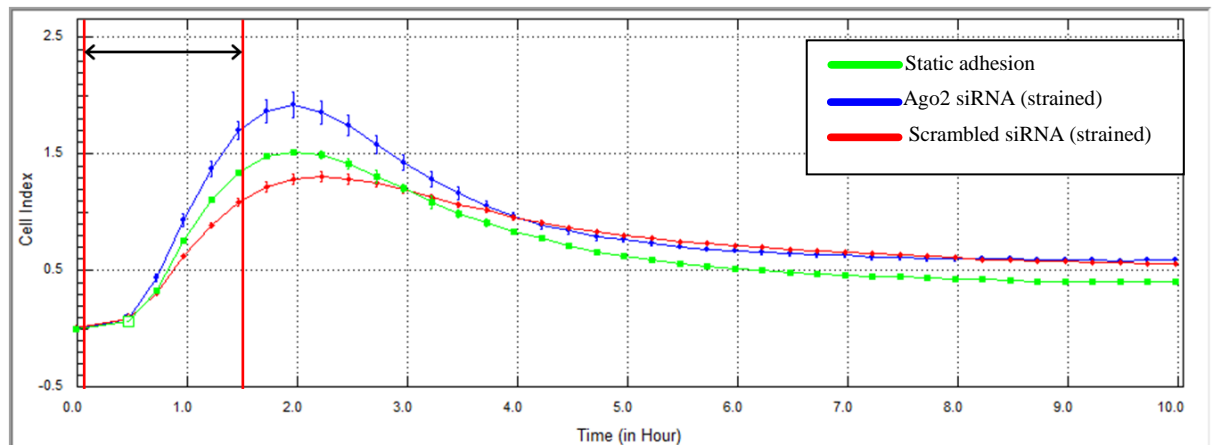


**Figure 5.4 A, B&C: Migration of Ago2 deficient HAoSMCs exposed to cyclic strain.** Figure 5.4 (A) is a migration plot generated from the xCELLigence instrument of strained HAoSMCs vs. static culture. There are two strained plots, one transfected with a scrambled control siRNA and the other transfected with a siRNA for Ago2. **Green** – Static, **Red** - Scrambled siRNA (Strained) and **Blue** – Ago2 siRNA (Strained). (B)- Shows rate of migration for each plot as compared against HAoSMCs in static culture. Migration was measured over the initial 3-4 hours. (C)- Graph of doubling time for each plot shown in figure 5.4 A. n=3, \* $P \leq 0.05$  vs. static adhesion; pairwise t-test.

## 5.2.4 Impact of cyclic strain on adhesion of HAoSMCs with Ago2 knock down

Adhesion (0~2hrs)

A.



B.

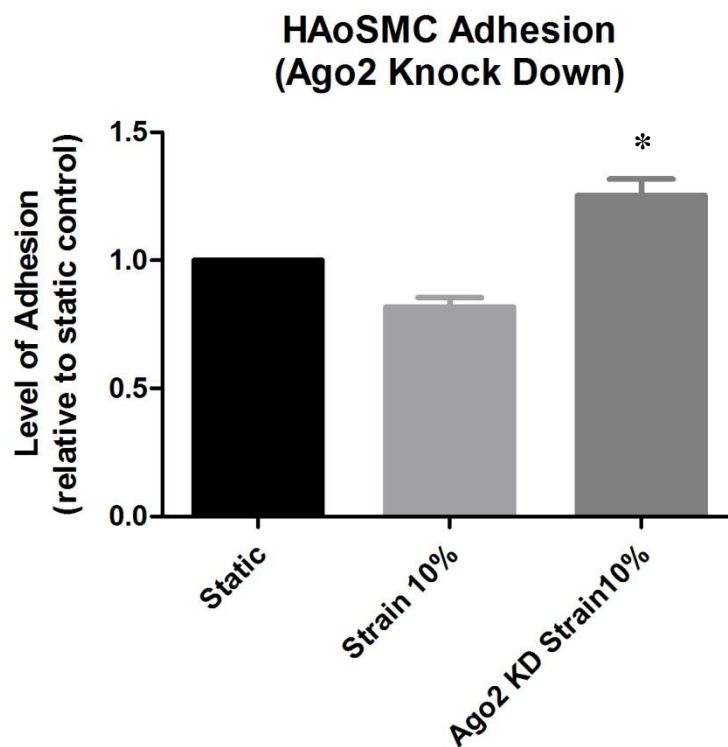


**Figure 5.5 A & B: Adhesion of Ago2 deficient HAoSMCs exposed to cyclic strain.** Figure 5.5A shows an adhesion profile, generated from the xCELLigence instrument, of both strained HAoSMCs and cells in static culture. There are two strained cell plots, one transfected with scrambled siRNA and the other with siRNA for Ago2. **Green – Static**, **Red - Scrambled siRNA (Strained)** and **Blue – Ago2 siRNA (Strained)**. B shows the level of adhesion of each sample of cells as calculated within the initial 1-2 hours of the experiment.

n=3, \* $P \leq 0.05$  vs. static adhesion pairwise t-test.

### 5.2.5 Effect of miRNA deficiency in HAoSMCs on Scratch Wound Closure.

A scratch wound was used as a second migration assay to characterise the implications of Ago2 knock down in HAoSMCs. Monolayer of cells transfected with a scrambled siRNA control and siRNA against Ago2 were scratched using a sterile 10 $\mu$ l tip.

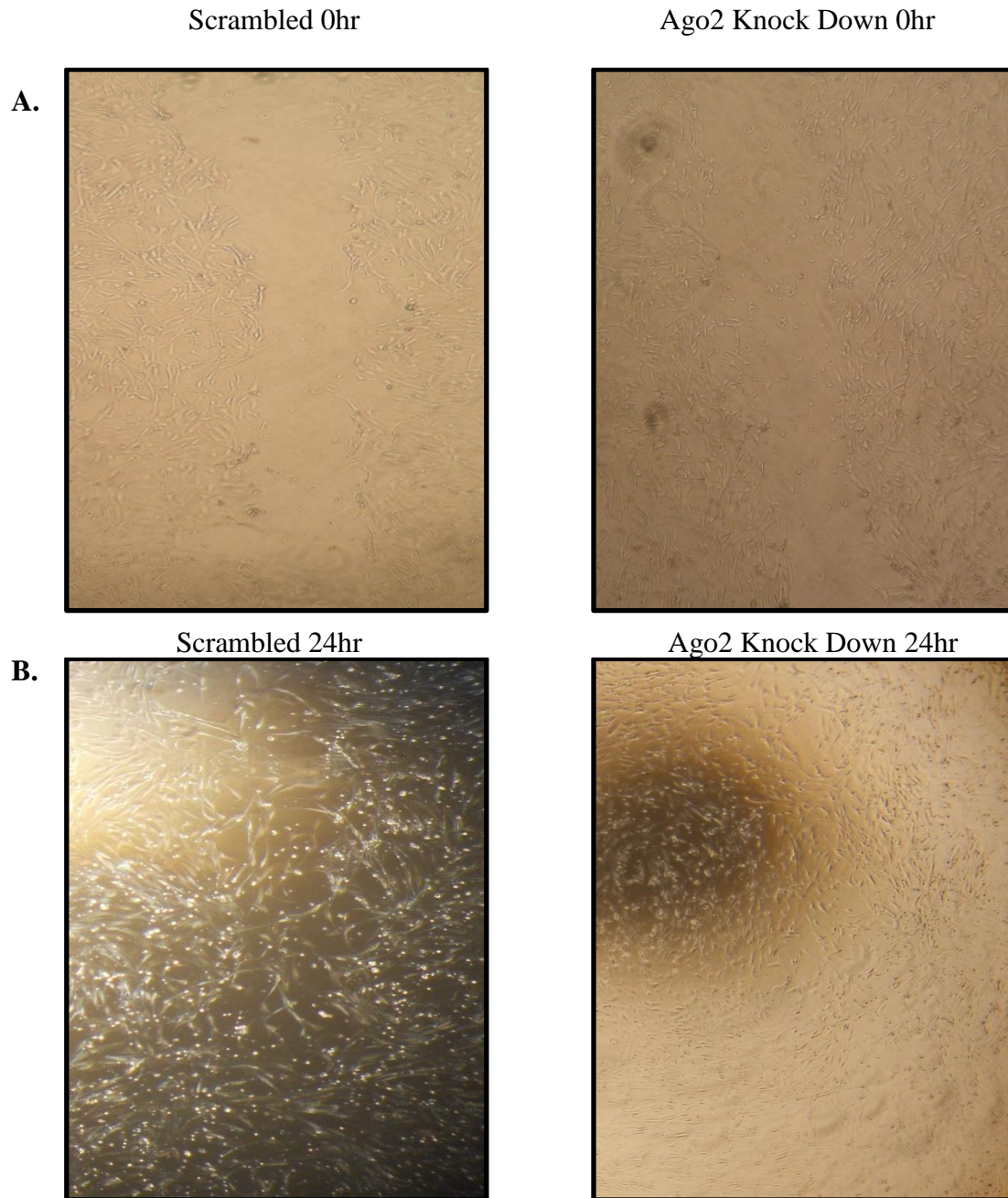


**Figure 5.6 (A-B): Scratch wound closure of Ago2 knock down HAoSMCs.** Shows scratch wound to two monolayers of HAoSMCs. Images of the wounded monolayer were taken at 0 hour (A) and 24 hour (B). Images on the left of each time point are of cells transfected with a scrambled siRNA control, images on the right are of cells transfected with siRNA against Ago2.



### 5.2.6 Impact of Ago2 knockdown in HAoSMCs on contractile phenotype.

Expression of the smooth muscle cell contractile marker,  $\alpha$ -actin, was assessed using western blot as shown in figure 5.7 A & B. This was to elucidate if miRNA deficiency, as a result of the Ago2 knockdown in SMCs had any implication on phenotypic modulation of the cell.

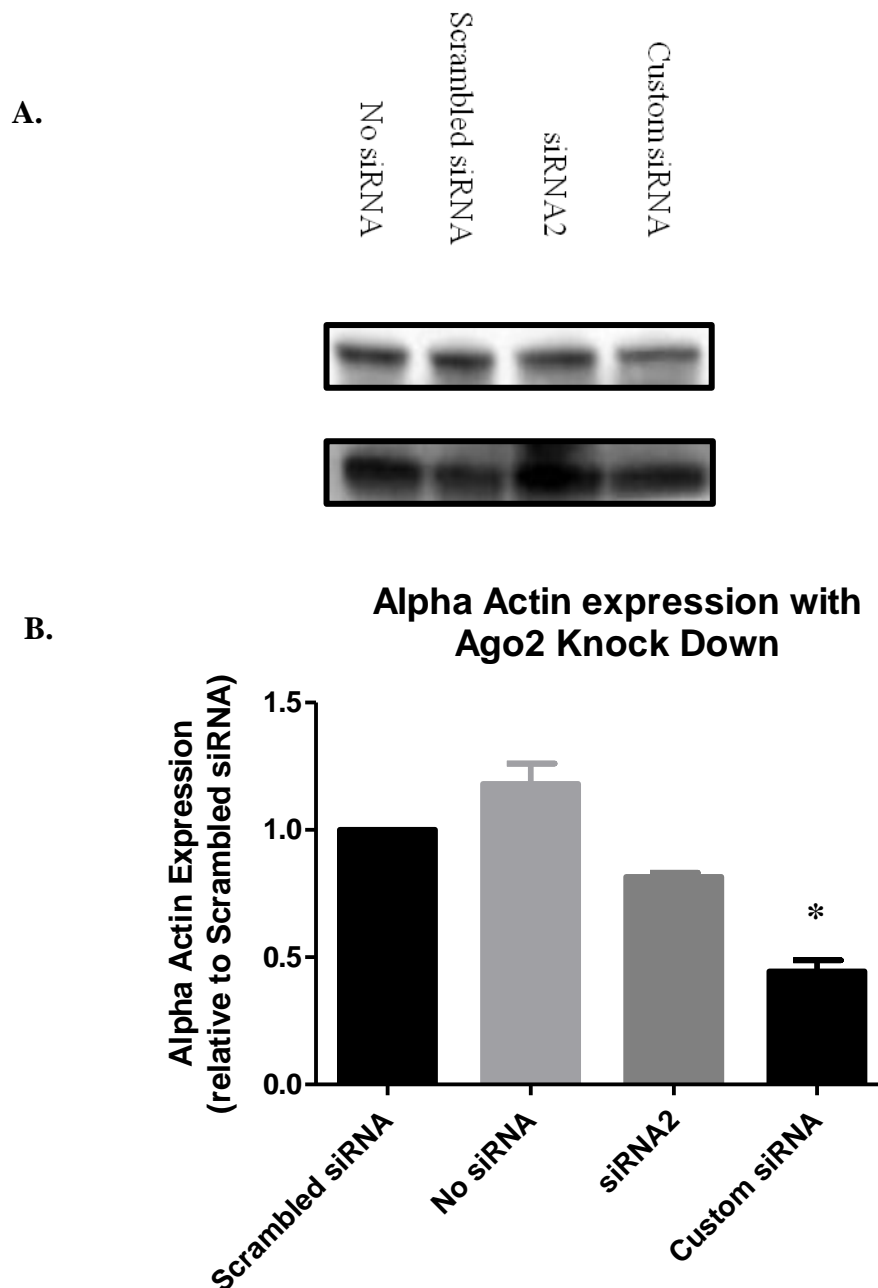


**Figure 5.7 A&B: Quantification of  $\alpha$  – actin expression in miRNA deficient HAoSMCs.** Blot shows expression of  $\alpha$ -actin from four sample lysates; including no siRNA control, scrambled siRNA control, pre designed siRNA2 and custom synthesised siRNA. Quantification of protein expression was achieved using densitometry analysis on bands with Image J software. n=3, \* $P \leq 0.05$  vs. scrambled control pairwise t-test.



### 5.3 Discussion

The focus of this chapter was twofold, firstly to test if haemodynamic force, specifically cyclic strain, altered HAoSMC function, namely migration. Secondly, to elucidate if miRNA were the signaling nexus involved in translating the mechanical stimulus of strain into a cellular process or function.

The following experimental approaches were taken to test the hypothesis that, “*cyclic strain alters smooth muscle cell functions such as adhesion, migration and proliferation and that these altered cell fates are controlled by miRNA regulation.*”

The strain parameters; amplitude, frequency and time points, used in chapters 3 and 4 were applied to HAoSMCs to evaluate cell migration compared with a static culture control using the xCELLigence system. In chapter 4, an altered miRNA signature was revealed in HAoSMCs that were exposed to strain compared to static culture. To identify the role of miRNA effector functions on regulating changes in cell functions following strain, the miRNA regulatory molecule, Argonaute2, was targeted by siRNA. Knock down of this gene interferes with miRNA function within the cell. Ago2 deficient cells were strained along with cells transfected with a scrambled siRNA control. The migration of both these cell populations was compared against a static control using the xCELLigence system. As a secondary migration assay to the xCELLigence, a scratch wound in the cell monolayer was used. Wound closure rate of cells transfected with siRNA targeting Ago2 was compared with HAoSMCs transfected with a scrambled siRNA control. Finally to assess the implication of reduced miRNA function in SMCs on phenotypic modulation, the contractile marker  $\alpha$ -actin was quantified by western blot.

### 5.3.1 Impact of Cyclic Strain on Cell Function

Cyclic stretching of VSMCs is a permanent feature in vessels as a direct result of the constant pulsatile nature of blood flow. Correct intra-luminal pressure is essential for maintaining vessel homeostasis. Mechanical factors also play a positive role in the control of the VSMC differentiated phenotype (Birukov *et al.*, 1998). Alterations in the level of stretch or strain, associated with increased blood pressure or hypertension, however, can lead to a myriad of vascular conditions such as atherosclerosis, pulmonary heart disease, myocardial infarction and aortic aneurysms to name but a few. As stated earlier, vascular smooth muscle cells are responsible for maintaining this vascular tone and vessel resistance to changes in blood pressure. However, smooth muscle cell de-differentiation resulting in a pro-migratory phenotype is the leading cause of stable plaque formation in atherosclerosis.

Cell migration is a complex and highly orchestrated process, which was described in full in chapter 1. In brief, Microfilaments are the main cytoskeletal protein involved in cell migration and are composed of the contractile protein actin. Integrins attach to the actin cytoskeleton, which stimulates the formation of filopodia and lamellipodia. The actin polymerises and presents the membrane to the leading edge of the cell. At this point, a combination of actin treadmilling and integrin mediated attachments such as focal adhesions, provide traction for the cell to pull itself forward. Cell adhesion molecules at the back of the cell also release and contract allowing for cell motility in the direction of migration.

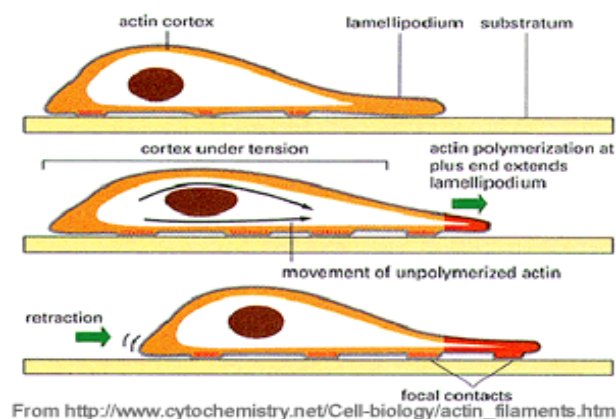


**Figure 5.8: Dynamics of cell migration.** As actin polymerises it extends lamellipodium in the direction of migration. Along with this integrins bind to the polymerised actin and form focal contacts which work as a molecular clutch. These provide an anchorage point from which the cell can gain traction and pull itself forward. Simultaneously to this adhesion points at the rear of the cell disengage and retract to allow cell motility.

### 5.3.1.1 Migration

Work in chapter 3 demonstrated that cyclic strain altered expression of contractile markers such as  $\alpha$ -actin, smoothelin and calponin. Work in this chapter was carried out to ascertain if these changes in contractile marker expression correlate with change in cell function, particularly migration. HAoSMCs for this work were strained as described in chapter 2.2. A 72 hour 10% strain at 1Hz time course was chosen of which 6, 12, 24, 48 and 72 hour time points were selected to monitor cell migration. For each time point, the cells were lifted from flex cell plates using versene, an EDTA derivative, which prevents integrin cleaving. Using trypsin to cleave integrins for detachment would most likely have altered the adhesion and migration profile of the cells on the xCELLigence system. Consequently, their various activation states as a result of the strain would have been negated. Cells were counted twice using the ADAM cell counter and an average was taken. The cell count is crucial for reliability of the system. Cells were then seeded onto the migration “SIM” plate at a density of 8,000 cells per well. For each time point, the migration of strained cells was compared against a static culture of HAoSMCs which were also seeded on to the FlexPlates<sup>®</sup> without being strained. The migration plot for each time point, 6-72 hr, is shown in figure 5.1 (A-E) respectively. The rate of migration for each sample is measured from the initial slope of the plot using the RTCA software. The level of migration for each time point is graphically represented in figure 5.1F, all time points are compared relative to the static control.

The graph reveals that as the cells are strained there is an incremental reduction in the migration of HAoSMCs up until 24hours and at this time point the level of migration is less than 50% that of the static control. This would implicate 10% strain as a physiological stimulus on the cells over the first 24 hours pushing them toward a more contractile, quiescent phenotype. Another theory for the reduced level of migration is due to an increased expression and activation of integrins, stimulated by the strain, facilitating stable adhesions. Deposition of ECM by the cells may also make the substrate more “sticky” reducing migration (O’Callaghan *et al.*, 2000).

At the later time points however, 48hr and 72hr, cell migration rises to ~ 75 % of the static control. This increase in migration would suggest the cells are moving back to a de-differentiated synthetic state as seen in the static culture. This may be facilitated by an increased expression of matrix metalloproteinases (MMP) which degrade the ECM allowing the cells to become more mobile. The trend seen in the migration levels of the strained cells over the 72 hours is similar to the trend seen in the expression of the

contractile markers in chapter 3. That is, 10% cyclic strain at 1Hz of HAoSMCs modulates cell phenotype to a more contractile state. This physiological stimulus is most evident in cells, which have been strained at these parameters for 24 hours. Following this time point the cells shift back on the phenotype spectrum towards the synthetic state. However, the migration level still remains lower than that of the static culture.

This study outlines the wavering effect of strain on HAoSMC migration. Several other groups have also examined the consequences of strain on HAoSMCs, however, these studies typically investigate proliferation and DNA synthesis within the cell (Liu *et al.*, 2007; Kasisis *et al.*, 2005; Qi *et al.*, 2010), and therefore work on SMC migration following strain is far less abundant. Nonetheless, the emphasis of these studies is on the modulating effect strain has on SMC phenotype, showing that both increase and decrease in expression of contractile markers and DNA synthesis is dependent of the strain parameters (Sumpio and Banes *et al.*, 1988; Hipper and Isenberg *et al.*, 2000; Schulze *et al.*, 2003; Wilson *et al.*, 1993).

C. Li *et al.*, (2003) demonstrated an increase in mouse SMC migration when exposed to 5%, 15% and 20% strain, which was mediated mediated by protein kinase C (PKC) $\delta$ . Stretch was also shown to enhance SMC motility through the shedding of heparin sulfate proteoglycan syndecan 4 from the cell surface (Li and Chaikof *et al.*, 2001). Conversely, Zhi-Qiang *et al.*, (2009) showed that application of 10% cyclic strain at 1Hz for 48 hours significantly inhibited SMC migration, suggesting hyperacetylation and deacetylation of histones caused by cyclic strain may play a part in regulating SMC migration. This would suggest an explanation to the modulating effect seen on SMC function by the chronic strain used in experiments in this thesis. The temporal strain may be leading to epigenetic reprogramming of the cell at the later time points, as histone modification is one of the main mechanisms of this. In an attempt to establish both physiological and pathological strain amplitude, Ying-Xin Qi *et al.* (2010) suggested 15% strain causes a marked increase in migration of RAoSMCs compared to cells strained at 5% for 24 hours. This, they believed was regulated via the p38 pathway.

### 5.3.2 Argonaute 2 (Ago2) siRNA

The miRNA signature in all vascular cells is becoming increasingly well characterized. It is likely there will soon be true therapeutic benefit from suppression or over expression of individual or a panel of miRNA implicated in a cardiovascular disorder (Callis *et al.*, 2008; J Yue 2011). Currently, the most significant contribution by miRNA to therapeutics is by way of biomarkers for disease states. These can be found in a multitude of bodily fluids and are a non-invasive method for diagnostic and prognostic assays; this is comprehensively reviewed by Stefano *et al.*, (2011).

However, developing inhibitors or promoters for an extensive panel of miRNA is a time consuming and costly task. This approach can also yield disappointing results as although deeply conserved, many miRNA express only a modest effect on their target mRNA, often less than 2 fold. In fact, miRNA can often be deleted without any obvious impact on phenotype (Bartel *et al.*, 2004). Investigations now highlight the likelihood of several miRNA working together to co-target an mRNA. This is possible as many mRNA 3'UTRs have more than four highly conserved seed sequences. Combined targeting by the miRNA creates enough change on the mRNA to constitute a large physiological effect (Mukherji *et al.*, 2011; Lliopoulos *et al.*, 2009; Friedman *et al.*, 2009; Baek *et al.*, 2008). It is possible for miRNA to also amplify their potency by targeting mRNA contained in pathways (Linsley *et al.*, 2007). In order to elicit a considerable phenotypic change, it may be advantageous to target all members of a seed family (Ebert *et al.*, 2012).

For this reason, a first step approach to implicating miRNA in a cellular process or indeed pathology, often looks at targeting one or more of the of the miRNA biogenesis or effector molecules. These are essential for developing a mature functioning miRNA as described in detail in chapter 1.

Initial evidence that miRNA were involved in endothelial cell function surfaced when Keubacher *et al.*, (2007) silenced Dicer *in vitro* to yield impaired angiogenesis on matrigel formation. This was one of the first investigations into miRNA involvement in endothelial cell function. Later, endothelial cell specific Dicer knockout mice showed leaky vessel membrane and ultimate lethality (Suarez *et al.*, 2008).

However, processing by the biogenesis molecules is not an obligatory step for all miRNA. For example when a miRNA is coded in a small intron it is deemed a "miRton". These small miRNA are able to bypass initial processing by Drosha/DSCR8

and be exported straight to the cytoplasm for maturation. Recent investigations have also revealed that Ago2 is required for the production of mature miRNA but not Dicer (Meister *et al.*, 2010). Argonaute 2 is a crucial element of the RNAi pathway and can direct both short interfering (siRNA) and miRNA-mediated gene regulation (Sonoki *et al.*, 2005).

To command greater control over the effector function of miRNA, work in this chapter was designed to demonstrate that cyclic strain mediated HAoSMC migration was facilitated by miRNA. This was approached through use of siRNA targeting the Argonaute2 complex. By knocking down Ago2, a significantly reduced number of mature miRNA are introduced into the RISC effectively numbing miRNA mediated cell regulation.

Of the eight Argonaute members, only Ago2 can mediate specific endonucleolytic cleavage, leading to mRNA cleavage or translational repression of the target mRNA (Cifuentes *et al.*, 2010). For initial optimization of knock down of the Ago2 protein, four siRNA were implemented. Three pre-designed Silencer Select<sup>®</sup> siRNA were purchased from Ambion<sup>™</sup> and one custom synthesised siRNA also from Ambion<sup>™</sup>, the sequence of which was taken from the work of (Naoghre *et al.*, 2010). This number of siRNA targeting the one gene increased the likelihood of achieving an effective level of knockdown. Cells were transfected with siRNA as described in chapter 2.2.

As an initial means of selecting the most efficient siRNA, transfected cells were seeded onto an xCELLigence “CIM-Plate”, figure 5.2 A & B, in order to assess the direct effect of siRNA for Ago2 on cell migration. This was a less time consuming method than western blotting for knock down which would be carried out regardless on selected siRNA from this experiment.

Rate of migration for cells transfected with each siRNA and the scrambled control were quantified and shown in figure 5.2 C. From this it was evident migration was increased in each sample transfected with the siRNA however siRNA2, from the pre-designed siRNA, and the custom siRNA sequence showed a marked increase in migration over the scrambled control.

These two siRNA were selected out for quantification of percentage knock down of Ago2 in the cells, this was achieved using western blot, figure 5.3 A. Both siRNA appeared to suppress functional levels of Ago2 in the cell by over 75% compared with

cells transfected with a scrambled siRNA control; figure 5.3 B. Quantification was achieved using densitometry software on the protein bands. A stronger knock down was evident in cells transfected with the custom sequence siRNA resulting in this siRNA being the one of choice for the remainder of the study.

To investigate if the reduced migration seen in HAoSMCs strained for 24hours, (figure 5.1 C) was mediated by miRNA regulation, cells transfected with siRNA for Ago2 and cells transfected with a scrambled siRNA control were strained under the same conditions. Migration of these two cell populations was compared against cells in static culture as shown in figure 5.4. Cells transfected with scrambled siRNA which were strained for 24 hours showed reduced migration compared with the static culture as seen before in figure 5.1 C. However, Ago2 knock down cells, which were strained under the same conditions show over a 50% increase in migration compared with the static control. The migrated cells also demonstrate a significantly reduced doubling time compared with both the static culture and the scrambled siRNA strained control as seen in figure 5.4C. The reduced expression of Ago2, pertaining to reduced functioning of miRNA within the cell, shows to negate the physiological effect of the strain. It would suggest that without miRNA silencing, cells are transformed into an un-regulated pro-migratory phenotype.

It must be noted that static controls of HAoSMCs transfected with Ago2 and scrambled siRNA were not included in this study and the strained cell populations were compared against a wildtype static population to determine migration levels. This makes a finite conclusion that the Ago2 knock down alone caused the noted increase in migration. Only with a redesign of the experiment to include these controls and an expected result of increased migration of the static cell population transfected with Ago2 siRNA compared to that of the scrambled controls would verify this result. That said the secondary migration assay, a static scratch wound in figure 5.7, shows HAoSMCs transfected with Ago2 siRNA close the wound at an earlier time point to the scrambled control. This strengthens the theory that Ago2 deficient HAoSMCs migrate at a higher rate to a scrambled siRNA or wild type control.

The impact of reduced miRNA function on cell adhesion was also assessed in figure 5.6. Here, the adhesion is strongest in cells transfected with siRNA Ago2. This is indicative of activated adhesion molecules such as syndecans, cadherins, dystrophin-

glycoprotein complex (DGPC) and integrins, which are essential to allow cell motility and traction.

A second migration assay in the form of a monolayer scratch wound was utilized to confirm results seen in figure 5.4. For this, HAoSMCs transfected with siRNA for Ago2 and a scrambled control were seeded to confluence on a 6 well plate. The cell monolayer was wounded with a sterile 10 $\mu$ l pipette tip. Images of the wound were subsequently taken at 0 hours and 24 hours post wound, figure 5.6 (A&B). At 24 hours the wound in Ago2 deficient cells has closed while the scrambled control still shows areas of intracellular space and is not fully closed. This strengthens the work done in figure 5.4 on the xCELLigence, showing increased migration in Ago2 deficient HAoSMCs.

The reduced effector function of miRNA in Ago2 deficient HAoSMCs was correlated back to the priority list for the 10% strain vs. static comparison in table 4.4, chapter 4. Within this shortlist two miRNA presented as promising candidates for further investigation, miR-520e and miR-520C-3p. Both are upregulated in the strained HAoSMCs where migration is reduced compared to that of the static control. In recent work by (Zhang *et al.*, 2011) published in *Oncogene* levels of miR-520e were shown to be dramatically decreased in hepatoma cell lines and in clinical hepatocellular carcinoma (HCC) tissues. Suggesting miR-520e may be a novel tumor suppressor through targeting of NF- $\kappa$ B-inducing kinase (NIK). Silencing of NIK was able to inhibit the growth of hepatoma cells. Within the bioinformatics performed in this thesis miR-520e was also shown to have multiple predicted targets in pathways concerning with cell motility such as; focal adhesion, regulation of actin cytoskeleton and cell cycle.

However, similar to the implications of cyclic strain on cell function, studies which examine the consequences of depleting the mature miRNA pool in a cell are also ambiguous. Genetic silencing of Dicer and Drosha in endothelial cells using siRNA demonstrated a significant reduction in capillary sprouting and tube formation. Migration was also reduced in dicer siRNA transfected cell but interestingly not in drosha siRNA transfected cells (Kuehbachner *et al.*, 2007). Angiogenesis and wound healing was also reported to be impaired in Dicer diminished endothelial cells (Suarez *et al.*, 2008). VSMC proliferation was also significantly inhibited in Dicer knockout mice (Pan *et al.*, 2011). Conversely, siRNA mediated knock down of Dicer and Drosha



in coronary SMCs significantly augmented both growth factor secretion and cell functions such as proliferation, cell cycle and migration

The ambiguity to the effects of miRNA biogenesis molecule depletion can be attributed to the fact that; a global diminishment of miRNA in a cell will lead to suppression of miRNA which are pro migratory; miR-24, miR- 26a, and miRNA which inhibit migration; miR-221/miR-222, miR-143/miR-145.

To implicate miRNA regulation in phenotypic modulation of HAoSMCs, the contractile marker  $\alpha$ -actin was quantified in Ago2 deficient cells using western blot, figure 5.7. Levels of  $\alpha$ -actin were decreased in the Ago2 deficient cells in comparison to the scrambled control. The reduced expression of contractile markers is synonymous with a pro migratory synthetic phenotype, which is what was shown in figures 5.4 & 5.6. This highlights the role miRNA play in regulating and maintaining VSMC phenotype and homeostasis. The expression of VSMC marker genes were also shown to be significantly down regulated in Dicer knockout mice (Pan *et al.*, 2011).

The conclusion from this study is that altered expression of the key miRNA processing molecule, Argonaute 2, seems to regulate HAoSMC function.

### 5.3.3 Summary and Conclusion

This chapter looked at the implication cyclic strain has on SMC function, namely migration. The migration of cells exposed to 10% cyclic strain over 72 hours was monitored over several time points and compared to that of a static culture. This revealed cyclic strain reduced cell migration, the effect of which was most evident at 24 hours where migration of the cells was less than half that of the static culture. However, cell migration increased at the 48 and 72 hour time points yet still remained less than that of the static culture, ~75%.

This study showed the modulating effect mechanical force can have on SMC biology; the strain is clearly orchestrating the cells into a more contractile, anti migratory phenotype. However, this stimulus does not appear to be sustainable as the strain becomes more chronic and migration levels increase, perhaps highlighting the limitations of the *in vitro* model

To implicate miRNA as key coordinators in the reduced cell migration observed after cyclic strain, siRNA were targeted against an essential miRNA biogenesis molecule, Argonaute2 (Ago2). This resulted in a numbing of function of mature miRNA within the cell. This had a significant effect on cell migration, whereas cells exposed to cyclic strain responded with reduced cell migration. Cells transfected with siRNA for Ago2 exposed to the same strain negated the physiological stimulus and had a marked increase in migration even over the static control. This would be indicative of a dedifferentiated SMC which was confirmed by protein analysis of the contractile marker  $\alpha$ -actin. This protein was shown to be reduced in ago2 deficient cells.

To conclude, cyclic strain, as suggested from results in chapters 3 and 4, has a direct impact on HAoSMC function particularly migration. Works in this chapter show 10% cyclic strain at 1Hz inhibits migration when compared to static cultured cells. This physiological stimulus is most likely transduced into the cytoplasm via membrane bound adhesion molecules such as integrins; some preliminary work carried out, appendix, shows inhibition of  $\alpha$ V $\beta$ 3 has a profound effect on HAoSMC adhesion. It would seem that this entire process is also regulated by the miRNA profile within the cell. Studies in this chapter demonstrated that reduced function of these miRNA through knock down of Ago2 resulted to negate the physiological stimulus of strain and send the cells into a migratory phenotype. Therefore, miRNA regulation is essential for HAoSMC response to stimulus.

## Overall Summary and Conclusion

All work carried out in this thesis was performed on Human Aortic Smooth Muscle Cells (HAoSMCs) taken from the thoracic aorta of a 19 year old Caucasian male.

The overall hypothesis for this thesis was “*cyclic mechanical strain, mediated by miRNA regulation, modulates vascular smooth muscle phenotype and ultimately function*”.

Experimental work designed to test this hypothesis was divided across three chapters:

Chapter 3 looked at the affect of cyclic strain on HAoSMC health and phenotype. This was approached by quantification of injury markers FGF-2 and TM and the contractile markers  $\alpha$ -actin, calponin and smoothelin.

Chapter 4 was concerned with miRNA profiling of HAoSMCs under static and strained conditions. The aim of this chapter was to develop a short list of “mechano sensitive” miRNA and perform bioinformatics on the individual miRNA. This included target prediction and involvement of these targets in biological processes and pathways of interest.

Chapter 5 was designed to correlate any change in expression of contractile markers seen in chapter 3, as a result of strain, to an altered cell function. Cell migration was the predominant function of interest. This chapter also looked to implement miRNA as the facilitators of any altered phenotype or function resulting from strain. This was approached by knocking down one of the major miRNA biogenesis molecules, Argonaute 2 (Ago2). As a result this is a first principles experiment as it was designed to inhibit miRNA regulation globally as opposed to manipulating the shortlisted mechano sensitive miRNA from chapter 4.

Vascular smooth muscle cells making up the *tunica media* of the vessel wall are responsible for controlling vascular tone and blood pressure within the circulatory system. They achieve this by a unique plasticity in which they can modulate their phenotype between a synthetic and contractile state (Owens *et al.*, 2004). Characteristics of the contractile state are a quiescent cell with an elongated morphology and increased expression of contractile markers. The synthetic cell boasts essentially the opposite features with increased migration, proliferation a rhomboid morphology and reduced expression of contractile markers. Due to the environment they are found VSMCs are constantly exposed to mechanical force resulting from the pulsatile nature of blood flow. This can be divided into two forms, shear stress and cyclic strain.

Primary studies for this thesis looked at the impact cyclic strain had on expression of contractile markers. After quantifying the mRNA and protein expression levels, it is clear cyclic strain increases the abundance of phenotype markers  $\alpha$ -actin, smoothelin and calponin. This holds for both 5% and 10% levels of cyclic strain amplitude. This would suggest cyclic strain is modulating the phenotype of the cells towards a contractile state. However, the higher strain, although encouraging a more physiological state initially, appears to create a higher degree of cell injury. This is evidenced through release of the injury markers FGF-2 and TM.

To investigate if the miRNA signature or “miRnome” of HAoSMCs was being altered by cyclic strain profiling experiments were performed. A temporal study of strain over 48hours at 10% showed the miRNA profile of the cells undergoes a significant shift in expression at ~ 24hours. To validate this, a second profiling study was carried out performing biological replicates at this time point as well as looking at how different strain amplitudes impacted miRNA expression, these were static culture, 5% strain and 10% strain. This study generated three priority lists of differentially expressed miRNA from comparisons of profiles of 5% vs. static, 10% vs. 5% and 10% vs. static. Bioinformatics was performed on the most differentially expressed miRNA in the mechano sensitive short lists. This included downloading of *in silico* predicted targets of each miRNA from the online algorithm Targetscan. These putative targets were then inputted to DAVID bioinformatics database which mapped their involvement in cellular processes pathways of interest.

Of these novel shortlisted miRNA, some show predicted involvement in SMC biology, such as the vascular smooth muscle cell contraction pathway, namely miR-610 and miR-661. Other miRNA selected for bioinformatics, miR-520e, miR-520c-3p and miR-373, showed promising target predictions involved in pathways concerning cell motility. These included focal adhesion, regulation of actin cytoskeleton, VSMC contraction pathway, cell cycle, adherens junction and ECM receptor interaction pathway. These miRNA are novel and largely unpublished, therefore providing a promising avenue for further investigation.

It was hoped that in line with generating a short list of mechano sensitive miRNA, the profiling experiment would reveal expression of specific miRNA from the literature which corresponded to a certain phenotype. However, it appears that the use of miRNA expression to identify a VSMC phenotype is ambiguous. For example, miR-1 was shown to induce both a contractile and a synthetic phenotype by two different groups. A down-regulation of this miRNA in SMCs was shown to coincide with a reduction in SMC lineage markers (Xie *et al.*, 2011). Contradictory to this work Jiang *et al.*, (2010) demonstrated myocardin induces miR-1 expression, which represses the expression of contractile proteins and thereby inhibits the contractility of SMCs. This suggested miR-1 plays a role in the negative feedback loop in the regulation of contractility induced by myocardin.

In this thesis, the expressions of both the miR-143/miR-145 and miR-221/miR-222 clusters were decreased compared to that of the static control, at 24 hour 10% strain. In case of the miR-143/miR-145 cluster this would suggest a more synthetic phenotype (Elia *et al.*, 2009; Sessa *et al.*, 2010). Yet work by Altuvia *et al.*, (2005) and Calin *et al.*, (2004) shows that reduction in miR-221/miR-222 cluster expression coincides with a more contractile cell. It is apparent from these studies that a “one miRNA one function” paradigm is not the case, particularly when assessing SMC phenotype. Instead to truly characterise the phenotype of a certain population of SMCs a combination of contractile marker expression, cell morphology, the cell miRnome and cell functions should be utilised.

As a result the implication of cyclic strain on SMC function, namely migration was investigated. The migration of cells exposed to 10% cyclic strain over 72 hours was monitored over several time points and compared to that of a static culture. This

revealed cyclic strain reduced cell migration, the effect of which was most evident at 24 hours where migration of the cells was less than half that of the static culture.

The increase in contractile marker expression with strain and this reduced migration would correspond to a more differentiated phenotype. Another possible explanation for the reduced level of migration is strain stimulated deposition of ECM by the cells (O'Callaghan *et al.*, 2000). This would have the effect of making the substrate more "sticky" reducing migration, especially if there is an increased expression and activation of integrins facilitating stable adhesions.

As the strain reached chronic time points of 48 and 72 hours, cell migration was seen to increase, although still remained less than (~75%) that of the static culture. This increase in migration would suggest the cells are moving back to a de-differentiated synthetic state as seen in the static culture. This may be facilitated by an increased expression of matrix metalloproteinases (MMP) which degrade the ECM allowing the cells to become more mobile

This study showed the modulating effect mechanical force can have on SMC biology; the strain is clearly orchestrating the cells into a more contractile, anti migratory phenotype. However, this stimulus does not appear to be sustainable as the strain becomes more chronic and migration levels increase, perhaps highlighting the limitations of the *in vitro* model.

To implicate miRNA as key coordinators of the reduced cell migration observed after cyclic strain, siRNA were targeted against an essential miRNA biogenesis molecule, Argonaute2 (Ago2). This resulted in a numbing of function of mature miRNA within the cell. This had a significant effect on cell migration, whereas cells exposed to cyclic strain responded with reduced cell migration. Cells transfected with siRNA for Ago2 exposed to the same strain negated the physiological stimulus and had a marked increase in migration even over the static control. This would be indicative of a dedifferentiated SMC which was confirmed by protein analysis of the contractile marker  $\alpha$ -actin. This protein was shown to be reduced in ago2 deficient cells.

To conclude, cyclic strain has a direct influence on HAoSMC biology. Works from the three chapters of this thesis have shown how this haemodynamic force alters a myriad of cellular processes from cell injury to phenotypic switching to cell function, specifically migration. Loss of function studies using siRNA against Ago2 has shown these changes in SMC fate are facilitated and monitored by the novel moiety of miRNA.

### **Future Work**

Studies in this thesis looked at amplitude and duration of strain only whereas to take this project further the frequency of the strain is most certainly a key contributor, this is demonstrated in works by Cheng *et al* (1997). Greater strain amplitude than 10% is also most likely needed to represent a pathological hypertensive model as although cell injury was evident through use of TM, the contractile markers still remained elevated in cells exposed to 10%. A higher, more pathological 15% was attempted using the *in vitro* model discussed here but resulted in cell rounding and detachment. Follow up experiments are also essential as the *in silico* target predictions are just that, predictions. They need to be validated before further research is carried out. Validation can be performed through use of loss and gain of function experiments and luciferase reporter assays. Targeting of other biogenesis molecules such as drosha, exportin 5 and dicer could show the difference between inhibition of miRNA function as seen with the Ago2 knock down and reduced expression of mature miRNA.

### ***Concluding Thoughts***

It would seem the complexity of the molecular mechanisms and stimuli governing smooth muscle differentiation gives rise to both conflicting and compounding results from several groups. To fully elucidate the phenotype of a particular population of SMCs, a battery of tests on contractile marker expression, synthetic marker expression, cell morphology, the cell miRnome and functional studies are required. Armed even with this data, a subpopulation of cells within a culture may exist where the phenotype is at a different stage along the phenotypic spectrum to the remaining population. However, work carried out in this chapter was primarily done to establish a shortlisted panel of mechano-sensitive miRNA and not to directly implement these with a specific HAoSMC phenotype. These mechanically regulated, small, non-coding RNAs may be the key to response and adaption of the vessel to altered haemodynamic force.



## Bibliography

**Albinsson S, Sessa WC.**

2010. Can microRNAs control vascular smooth muscle phenotypic modulation and the response to injury? *Physiol Genomics*, 43(10):529-33.

**Altuvia Y, Landgraf P, Lithwick G, Elefant N, Pfeffer S, Aravin A, Brownstein MJ, Tuschl T, Margalit H.** 2005. Clustering and conservation patterns of human microRNAs. *Nucleic Acids Res*, 33(8):2697-706.

**Alvarez-Garcia I, Miska EA.** 2005.

MicroRNA functions in animal development and human disease. *Development*, 132(21):4653-62.

**Ambros V, Bartel B, Tuschl T,** A uniform system for microRNA annotation. *RNA*, 9 (3) 277-279

**Archer E, Blair SN.** 2011. Physical Activity and the Prevention of Cardiovascular Disease: From Evolution to Epidemiology. *Progress in Cardiovascular Diseases*, 53(6): 387-396.

**Arnaout MA, Mahalingam B, Xiong JP.** 2005. Integrin structure, allostery, and bidirectional signalling. *Annu Rev Cell Dev Biol*, 21:381-410.

**Bader AG.** 2012. miR-34 - a microRNA replacement therapy is headed to the clinic. *Front Genet*, 3:120.

**Baek D, Villén J, Shin C, Camargo FD, Gygi SP, Bartel DP.** 2008. The impact of microRNAs on protein output. *Nature*, 455(7209):64-71.

**Banno A, Ginsberg MH.** 2008. Integrin activation. *Biochem Soc Trans*, 36(2):229-34.

**Barbee KA, Macarak EJ, Thibault LE.** 1994.

Strain measurements in cultured vascular smooth muscle cells subjected to mechanical deformation. *Ann Biomed Eng*, 22(1):14-22.

**Barker, K.** 2005 *At the Bench, A Laboratory Navigator..* Cold Spring Harbour Laboratory Press. New York. Chapter 12. DNA, RNA and Protein.

**Barresi R, Di Blasi C, Negri T, Brugnoli R, Vitali A, Felisari G, Salandi A, Daniel S, Cornelio F, Morandi L, Mora M.** 2000. Disruption of heart sarcoglycan complex

and severe cardiomyopathy caused by beta sarcoglycan mutations. *J Med Genet*, 37(2):102-7.

**Barron N, Sanchez N, Kelly P, Clynes M.** 2011.

MicroRNAs: tiny targets for engineering CHO cell phenotypes? *Biotechnol Lett*, 33(1):11-21.

**Bartel DP.**2004. MicroRNAs: genomics, biogenesis, mechanism, and function. *Cell*, 116(2):281-97.

**Bartlett, J. M. S.; Stirling, D.** (2003). "A Short History of the Polymerase Chain Reaction". *PCR Protocols* 226. pp. 3–6.doi:10.1385/1-59259-384-4:3. ISBN 1-59259-384-4.

**Bashkin P, Doctrow S, Klagsbrun M, Svahn CM, Folkman J, Vlodavsky I.** 1989. Basic fibroblast growth factor binds to subendothelial extracellular matrix and is released by heparitinase and heparin-like molecules. *Biochemistry*, 28(4):1737-43.

**Benjamini & Hochberg.** 1995. Controlling the false discovery rate — a practical and powerful approach to multiple testing. *Journal of the Royal Statistical Society Series B-Methodological*, 57: 289–300

**Bhadriraju K, Yang M, Alom Ruiz S, Pirone D, Tan J, Chen CS.** 2007. Activation of ROCK by RhoA is regulated by cell adhesion, shape, and cytoskeletal tension. *Exp Cell Res*, 313(16):3616-23.

**Bharyana MK, Calinb GA, Lai LY.** 2012. Functional relevance of miRNA sequences in human disease. *Mutation Research*, 731: 14– 19.

**Bielenberg W, Prock A, Tillmanns H, Sedding D.** 2009. Proliferation, Remodeling, Extracellular Matrix I: The regulating role of MicroRNAs for smooth muscle cell function. *Circulation*, 120:1083.

**Bilato C, Curto KA, Monticone RE, Pauly RR, White AJ, Crow MT.** 1997. The inhibition of vascular smooth muscle cell migration by peptide and antibody antagonists of the alphavbeta3 integrin complex is reversed by activated calcium/calmodulin-dependent protein kinase II. *J Clin Invest*, 100(3):693-704.

**Birukov KG, Shirinsky VP, Stepanova OV.** 1995. Stretch affects phenotype and proliferation of vascular smooth muscle cells. *Mol Cell Biochem*, 144: 131-9.

- Birukov KG, Bardy N, Lehoux S, Merval R, Shirinsky VP, Tedgui A.** 1998. Intraluminal pressure is essential for the maintenance of smooth muscle caldesmon and filamin content in aortic organ.
- Birukov KG.** 2009. Cyclic stretch, reactive oxygen species, and vascular remodeling. *Antioxid Redox Signal*, 11(7):1651-67.
- Blume-Jensen P, Jiang G, Hyman R, Lee KF, O'Gorman S, Hunter T.** 2000. Kit/stem cell factor receptor-induced activation of phosphatidylinositol 3'-kinase is essential for male fertility. *Nat Genet*, 24(2):157-62.
- Bo-an Li.** 2012. A novel tumor suppressor miRNA miR-520e contributes to suppression of hepatoma. *Acta Pharmacologica Sinica*, 33: 3–4.
- Bochaton-Piallat ML, Ropraz P, Gabbiani F, Gabbiani G.**1996. Phenotypic heterogeneity of rat arterial smooth muscle cell clones. Implications for the development of experimental intimal thickening. *Arterioscler Thromb Vasc Biol*, 16(6):815-20.
- Boehme MW, Galle P, Stremmel W.** 2002. Kinetics of thrombomodulin release and endothelial cell injury by neutrophil-derived proteases and oxygen radicals. *Immunology*, 107(3):340-9.
- Bohnsack MT, Czaplinski K, Gorlich D.** 2004. Exportin 5 is a RanGTP-dependent dsRNA-binding protein that mediates nuclear export of pre-miRNAs. *RNA*, 10(2):185-91.
- Borysenko M, Beringer T.** 1984. Functional histology, Little, Brown and Company, Boston pp. 195–208
- Bretscher, A.** 1999. Regulation of cortical structure by the ezrin-radixin-moesin protein family. *Current Opinion in Cell Biology*, 11(1): 109-116.
- Brown TD.** 2000. Techniques for mechanical stimulation of cells in vitro: a review. *J Biomech*, 33(1):3-14.
- Burnette WN:** Western blotting: Remembrance of Things Past. (2009) *Protein Blotting and Detection: Methods and Protocols*, Biji T Kurien and R Hal Scofield (eds.) Methods in Molecular Biology. 536:5-8. Humana Press/Springer, New York, NY.

**Burrige K, Chrzanowska-Wodnicka M. 1996.** Focal adhesions, contractility, and signaling. *Annu Rev Cell Dev Biol*, 12:463-518.

**Calin GA, Sevignani C, Dumitru CD, Hyslop T, Noch E, Yendamuri S, Shimizu M, Rattan S, Bullrich F, Negrini M, Croce CM. 2004.** Human microRNA genes are frequently located at fragile sites and genomic regions involved in cancers. *Proc Natl Acad Sci*, 101(9):2999-3004.

**Callis TE, Wang D. 2008.** Taking microRNAs to heart. *Trends in Molecular Medicine*, 14(6): 254-260.

**Campbell JH, Campbell GR (Eds.)** Vascular Smooth Muscle in Culture. 1987:131-43.

**Campbell JH, Campbell GR.** Endothelial Cell Influences on Vascular Smooth Muscle Phenotype. *Annual Review of Physiology*, 48: 295-306.

**Cantley LG, Cantley LC. 1995.** Signal transduction by the hepatocyte growth factor receptor, c-met. Activation of the phosphatidylinositol 3-kinase. *J Am Soc Nephrol*, 5(11):1872-81.

**Caporali A, Emanuelli C. 2011.** MicroRNA regulation in angiogenesis. *Vascular Pharmacology*, 55(4): 79-86.

**Castellot JJ JR., Cochran DL, Karnovsky JM** Effect of heparin on vascular smooth muscle cells. 1985. *Journal of Cellular Physiology, Cell metabolism*, 124(1): 21–28.

**Cevallos M, Riha GM, Wang X, Yang H, Yan S, Li M, Chai H, Yao Q, Chen C. 2006.**

Cyclic strain induces expression of specific smooth muscle cell markers in human endothelial cells. *Differentiation*, 74(9-10):552-61.

**Chan AC. 2004.** Syk Family of Protein Tyrosine Kinases *IN*: William J. Lennarz and M. Daniel Lane (eds.) *Encyclopedia of Biological Chemistry*. New York Elsevier, pp.139-145.

**Chaurasia P, Aguirre-Ghiso JA, Liang OD, Gardsvoll H, Ploug M, Ossowski L. 2006.** A region in urokinase plasminogen receptor domain III controlling a functional association with alpha5beta1 integrin and tumor growth. *J Biol Chem*, 281(21):14852-63.

**Chen C, Ridzon DA, Broomer AJ, Zhou Z, Lee DH, Nguyen JT, Barbisin M, Xu NL, Mahuvakar VR, Andersen MR, Lao KQ, Livak KJ, Guegler KJ.** 2005. Real-time quantification of microRNAs by stem-loop RT-PCR. *Nucleic Acids Res*, 33(20): 179.

**Chen CS.** 2008. Mechanotransduction - a field pulling together? *J Cell Sci*, 121(20): 3285-92.

**Chen H, Shalom-Feuerstein R, Riley J, Zhang SD, Tucci P, Agostini M, Aberdam D, Knight RA, Genchi G, Nicotera P, Melino G, Vasa-Nicotera M.** 2010. miR-7 and miR-214 are specifically expressed during neuroblastoma differentiation, cortical development and embryonic stem cells differentiation, and control neurite outgrowth in vitro. *Biochem Biophys Res Commun*, 394(4):921-7.

**Chen J, Wang D.** 2012. MicroRNAs in cardiovascular development. *Journal of Molecular and Cellular Cardiology*, 52(5): 949-957.

**Chen K, Hank Juo S.** MicroRNAs in atherosclerosis. 2012. *The Kaohsiung Journal of Medical Sciences*, (12):631-40.

**Chen K, Fan W, Wang X, Ke X, Wu G, Hu C.** 2012. MicroRNA-101 mediates the suppressive effect of laminar shear stress on mTOR expression in vascular endothelial cells. *Biochem Biophys Res Commun*, 427(1):138-42.

**Chen W, Yin K, Zhao G, Fu Y, Tang C.** 2012. The magic and mystery of MicroRNA-27 in atherosclerosis. *Atherosclerosis*, 222(2): 314-323.

**Cheng GC, Briggs WH, Gerson DS, Libby P, Grodzinsky AJ, Gray ML, Lee RT.** Mechanical strain tightly controls fibroblast growth factor-2 release from cultured human vascular smooth muscle cells. *Circ Res*, 80(1):28-36.

**Chiu JJ, Wang DL, Chien S, Skalak R, Usami S.** 1998. Effects of disturbed flow on endothelial cells. *J Biomech Eng*, 120(1):2-8.

**Christen T, Bochaton-Piallat ML, Neuville P, Rensen S, Redard M, van Eys G, Gabbiani G.** 1999. Cultured porcine coronary artery smooth muscle cells. A new model with advanced differentiation. *Circ Res*, 85(1):99-107.

**Chomczynski, P. Sacchi, N. 2006** The single-step method of RNA isolation by acid guanidinium thiocyanate–phenol–chloroform extraction: twenty-something years on

*Nature Protocols* 1, 581 - 585

**Cifuentes D, Xue H, Taylor DW, Patnode H, Mishima Y, Cheloufi S, Ma E, Mane S, Hannon GJ, Lawson ND, Wolfe SA, Giraldez AJ. 2010.** A novel miRNA processing pathway independent of Dicer requires Argonaute2 catalytic activity. *Science*, 328(5986):1694-8.

**Cines DB, Pollak ES, Buck CA, Loscalzo J, Zimmerman GA, McEver RP, Pober JS, Wick TM, Konkle BA, Schwartz BS, Barnathan ES, McCrae KR, Hug BA, Schmidt AM, Stern DM. 1998.** Endothelial cells in physiology and in the pathophysiology of vascular disorders. *Blood*, 91(10):3527-61.

**Clark MSF, Caldwell RW, Chiao H, Miyake K, McNeil PL. 1995.** Contraction-induced cell wounding and release of fibroblast growth factor in an autocrine manner. *Circ Res*, 76:927- 934.

**Clark MSF, Khakee R, McNeil PL. 1993.** Loss of cytoplasmic basic fibroblast growth factor from physiologically wounded myofibers of normal and dystrophic muscle. *J Cell Sci*, 106:121-133.

**Clifford RL, Singer CA, John AE. 2013.**

Epigenetics and miRNA emerge as key regulators of smooth muscle cell phenotype and function. *Pulm Pharmacol Ther*, 26(1):75-85.

**Clowes AW, Reidy MA, Clowes MM. 1983. Mechanisms of stenosis after arterial injury.** *Lab Invest*, 49:208–215.

**Clyman RI, McDonald KA, Kramer RH. 1990.** Integrin receptors on aortic smooth muscle cells mediate adhesion to fibronectin, laminin, and collagen. *Circ Res*. 67(1):175-86.

**Colgan OC, Ferguson G, Collins NT, Murphy RP, Meade G, Cahill PA, Cummins PM. 2007.**

Regulation of bovine brain microvascular endothelial tight junction assembly and barrier function by laminar shear stress. *Am J Physiol Heart Circ Physiol*, 292(6):3190-7.

**Collins T, Pober JS , Gimbrone MA, r Hammacher A, Betsholtz C, Westermarck B, Heldin CH. 1987.** Cultured human endothelial cells express platelet-derived growth factor A chain. *Am J Pathol*, 126(1): 7–12.

**Coopman PJ, Mueller SC. 2006.** The Syk tyrosine kinase: A new negative regulator in tumor growth and progression. *Cancer Letters*, 241(2): 159-173.

**Cordes KR, Sheehy NT, White MP, Berry EC, Morton SU, Muth AN, Lee TH, Miano JM, Ivey KN, Srivastava D. 2009.** miR-145 and miR-143 regulate smooth muscle cell fate and plasticity. *Nature*, 460(7256):705-10.

**Crowley ST, Ray CJ, Nawaz D, Majack RA, Horwitz LD. 1995.** Multiple growth factors are released from mechanically injured vascular smooth muscle cells. *Am J Physiol*, 269(5 Pt 2):1641-7.

**Da Silva, F.P., Aloulou, M., Benhamou, M. and Monteiro, R.C. 2008.** Inhibitory ITAMs: a matter of life and death. *Trends in Immunology*, 29(8): 366-373.

**Daubman S. 2010.** MicroRNAs in angiogenesis and vascular smooth muscle cell function. *Circ Res*, 106(3):423-5.

**Davis BN, Hilyard AC, Nguyen PH, Lagna G, Hata A. 2009.** Induction of microRNA-221 by platelet-derived growth factor signaling is critical for modulation of vascular smooth muscle phenotype. *J Biol Chem*, 284(6):3728-38.

**Davis MJ, Donovitz JA, Hood JD. 1992.** Stretch-activated single-channel and whole cell currents in vascular smooth muscle cells. *Am J Physiol*, 262(1):1083-8.

**De Planell-Saguer M, Rodicio MC. 2011.** Analytical aspects of microRNA in diagnostics: a review. *Anal Chim Acta*, 699(2):134-52.

**Delon J, Kaibuchi K, Germain RN. 2001.** Exclusion of CD43 from the Immunological Synapse Is Mediated by Phosphorylation-Regulated Relocation of the Cytoskeletal Adaptor Moesin. *Immunity*, 15(5): 691-701.

**Desai A, Mitchison TJ. 1997.** Microtubule Polymerization Dynamics. *Annual Review of Cell and Developmental Biology*, 13: 83-117.

- Desmoulière A, Rubbia-Brandt L, Gabbiani G.** 1991. Modulation of actin isoform expression in cultured arterial smooth muscle cells by heparin and culture conditions. *Arterioscler Thromb*, 11(2):244-53.
- Di Stefano V, Zaccagnini G, Capogrossi MC, Martelli F.** 2011. MicroRNAs as peripheral blood biomarkers of cardiovascular disease. *Vascul Pharmacol*, 55(4):111-8.
- Dimmeler S, Hermann C, Zeiher AM.** 1998. Apoptosis of endothelial cells. Contribution to the pathophysiology of atherosclerosis? *Eur Cytokine Netw*, 9(4):697-8.
- Dong DL, Yang BF.** 2011. Role of microRNAs in cardiac hypertrophy, myocardial fibrosis and heart failure de -li dong. *Acta pharmaceutica Sinica B*, (1) 1-7.
- Dorn II GW.** 2011. MicroRNAs in cardiac disease. *Translational Research*, 157(4): 226-235.
- Dueck A, Meister G.** 2010. MicroRNA processing without Dicer. *Genome Biol*, 11(6):123.
- Easow G, Teleman AA, Cohen SM.** 2007. Isolation of microRNA targets by miRNP immunopurification *RNA*, 13(8):1198-1204.
- Ebert M, Sharp P.** 2012. Roles for MicroRNAs in Conferring Robustness to Biological Processes. *Cell*, 149(3): 515-524.
- Elia L, Quintavalle M, Zhang J, Contu R, Cossu L, Latronico MV, Peterson KL, Indolfi C, Catalucci D, Chen J, Courtneidge SA, Condorelli G.** 2009. The knockout of miR-143 and 145 alters smooth muscle cell maintenance and vascular homeostasis in mice: correlates with human disease. *Cell Death Differ*, 16(12):1590-8.
- Etheridge A, Lee I, Hood L, Galas D, Wang K. 2011. **Extracellular microRNA: a new source of biomarkers.** *Mutat Res*, 717(1-2):85-90.
- Evanko SP, Angello JC, Wight TN.** 1999. Formation of hyaluronan- and versican-rich pericellular matrix is required for proliferation and migration of vascular smooth muscle cells. *Arterioscler Thromb Vasc Biol*, 19(4):1004-13.



- Fager G, Hansson GK, Gown AM, Larson DM, Skalli O, Bondjers G.** 1989. Human arterial smooth muscle cells in culture: inverse relationship between proliferation and expression of contractile proteins. *In Vitro Cell Dev Biol*, 25(6):511-20.
- Fang JH, Zhou HC, Zeng C, Yang J, Liu Y, Huang X, Zhang JP, Guan XY, Zhuang SM.** 2011. MicroRNA-29b suppresses tumor angiogenesis, invasion, and metastasis by regulating matrix metalloproteinase 2 expression. *Hepatology*, 54(5):1729-40.
- Fang Y, Shi C, Manduchi E, Civelek M, Davies PF.** 2010. MicroRNA-10a regulation of proinflammatory phenotype in atherosusceptible endothelium in vivo and in vitro. *Proc Natl Acad Sci*, 107: 13450-5.
- Fatigati V, Murphy RA.** 1984. Actin and tropomyosin variants in smooth muscles. Dependence on tissue type. *J Biol Chem*, 259(23):14383-8.
- Favreau AJ, Sathyanarayana P.** 2012. miR-590-5p, miR-219-5p, miR-15b and miR-628-5p are commonly regulated by IL-3, GM-CSF and G-CSF in acute myeloid leukemia. *Leuk Res*, 36(3):334-41.
- Fehon RG, McClatchey AI, Bretscher A.** 2010. Organizing the cell cortex: the role of ERM proteins. *Nat Rev Mol Cell Bio*, 11(4):276-87.
- Feng Y, Yang JH, Huang H, Kennedy SP, Turi TG, Thompson JF, Libby P, Lee RT.** 1999. Transcriptional profile of mechanically induced genes in human vascular smooth muscle cells. *Circ Res*, 85(12):1118-23.
- Fiedler J, Gupta SK, Thum T.** 2011. Identification of cardiovascular microRNA targetomes. *J Mol Cell Cardiol*, 51(5):674-81.
- Fiedler J, Park D, Thum T.** MicroRNA and disease models: focus on cardiac fibrosis. *Drug Discovery Today: Disease Models*,
- Fiévet B, Louvard D, Arpin M.** 2007. ERM proteins in epithelial cell organization and functions. *Biochimica Et Biophysica Acta (BBA) - Molecular Cell Research*, 1773(5): 653-660.

- Finnerty JR, Wang W, Hébert SS, Wilfred BR, Mao G, Nelson PT.** 2010. The miR-15/107 Group of MicroRNA Genes: Evolutionary Biology, Cellular Functions, and Roles in Human Diseases. *Journal of Molecular Biology*, 402(3): 491-509.
- Fish JE, Santoro MM, Morton SU, Yu S, Yeh RF, Wythe JD, Ivey KN, Bruneau BG, Stainier DY, Srivastava D.** 2008. miR-126 regulates angiogenic signaling and vascular integrity. *Dev Cell*, 15(2):272-84.
- Fish JE.** 2012. A Primer on the Role of MicroRNAs in Endothelial Biology and Vascular Disease. *Seminars in Nephrology*, 32(2): 167-175.
- Fodor S, Jakus Z, Mócsai A.** 2006. ITAM-based signaling beyond the adaptive immune response. *Immunology Letters*, 104(1-2): 29-37.
- Folkow B.** 1993. Early structural changes in hypertension: pathophysiology and clinical consequences. *J Cardiovasc Pharmacol*, 1:1-6.
- Fox CS.** 2010. Cardiovascular Disease Risk Factors, Type 2 Diabetes Mellitus, and the Framingham Heart Study. *Trends in Cardiovascular Medicine*, 20(3): 90-95.
- Fox SB, Gasparini G, Harris AL.** 2001. Angiogenesis: pathological, prognostic, and growth-factor pathways and their link to trial design and anticancer drugs. *The Lancet Oncology*, 2(5): 278-289.
- R. Ian Freshney Wiley-Blackwell, 2011** (Culture of Animal Cells - A Manual of basic technique and specialized applications. sixth edition) Science
- Frid MG, Aldashev AA, Dempsey EC, Stenmark KR.** 1997. Smooth muscle cells isolated from discrete compartments of the mature vascular media exhibit unique phenotypes and distinct growth capabilities. *Circ Res*, 81(6):940-52.
- Friedman RC, Farh KK, Burge CB, Bartel DP.** Most mammalian mRNAs are conserved targets of microRNAs. *Genome Res*, 19(1):92-105.
- Fütterer K, Wong J, Gruzza RA, Chan AC Waksman G.** 1998. Structural basis for syk tyrosine kinase ubiquity in signal transduction pathways revealed by the crystal structure of its regulatory SH2 domains bound to a dually phosphorylated ITAM peptide. *Journal of Mol Biol*, 281(3): 523-537.

- Fulwyler, M. J.** (1965). "Electronic separation of biological cells by volume". *Science* **150**(698): 910–911. doi:10.1126/science.150.3698.910. PMID 5891056
- Gajdusek CM, Schwartz SM.** 1984. Comparison of intracellular and extracellular mitogenic activity. *J Cell Physiol*, 121(2):316-22.
- Gajdusek CM.** 1984. Release of endothelial cell-derived growth factor (ECDGF) by heparin. *J Cell Physiol*, 121(1):13-21.
- Galbraith CG, Yamada KM, Sheetz MP.** 2002. The relationship between force and focal complex development. *J Cell Biol*, 159(4):695-705.
- Garzon MC, Huang JT, Enjolras O, Frieden IJ.** 2007. Vascular malformations: Part I. *Journal of the American Academy of Dermatology*, 56(3): 353-370.
- Gautreau A, Louvard D, Arpin M.** 2002. ERM proteins and NF2 tumor suppressor: the Yin and Yang of cortical actin organization and cell growth signaling. *Current Opinion in Cell Biology*, 14(1): 104-109.
- Geiger B, Bershadsky A.** 2001. Assembly and mechanosensory function of focal contacts. *Curr Opin Cell Biol*, 13(5):584-92.
- Geng YJ, Libby P.** 2002. Progression of atheroma: a struggle between death and procreation. *Arterioscler Thromb Vasc Biol*, 22(9):1370-80.
- Gianfagna F, Cugino D, Santimone I, Iacoviello L.** 2012. From candidate gene to genome-wide association studies in cardiovascular disease. *Thromb Res*, 129(3): 320-324.
- Gilad S, Meiri E, Yogev Y, Benjamin S, Lebanony D, Yerushalmi N, Benjamin H, Kushnir M, Cholakh H, Melamed N, Bentwich Z, Hod M, Goren Y.** 2008. Serum microRNAs are promising novel biomarkers. *PLoS One*, 3(9):3148.
- Gimbrone MA Jr, Alexander RW.** Vasoactive hormone receptor expression in cultured vascular smooth muscle cells.
- Gimbrone MA Jr.** 1987. Vascular endothelium: nature's blood-compatible container. *Ann N Y Acad Sci*, 516:5-11.

**Gladka MM, Da Costa Martins PA, De Windt LJ.** 2012. Small changes can make a big difference — MicroRNA regulation of cardiac hypertrophy. *Journal of Molecular and Cellular Cardiology*, 52(1): 74-82.

**Glucksmann A.** 1939. Studies on bone mechanics in vitro: II, The role of tension and pressure in chondrogenesis. *Anatomical Record*, 73: 39-56

**Goettsch C, Rauner M, Pacyna N, Hempel U, Bornstein SR, Hofbauer LC.** 2011. miR-125b Regulates Calcification of Vascular Smooth Muscle Cells. *The American Journal of Pathology*, 179(4):1594-1600.

**Goldman RD, Chou YH, Prahlad V, Yoon M.** 1999.

Intermediate filaments: dynamic processes regulating their assembly, motility, and interactions with other cytoskeletal systems. *FASEB J*, 13 (2):261-5.

**Goldstein JL, Anderson RG, Buja LM, Basu SK, Brown MS.** 1977.

Overloading human aortic smooth muscle cells with low density lipoprotein-cholesteryl esters reproduces features of atherosclerosis in vitro. *J Clin Invest*, 59(6):1196-202.

**Gottardo F, Liu CG, Ferracin M, Calin GA, Fassan M, Bassi P, Sevignani C, Byrne D, Negrini M, Pagano F, Gomella LG, Croce CM, Baffa R.** 2007. Micro-RNA profiling in kidney and bladder cancers. *Urol Oncol*, (5):387-92.

**Grant DS, Tashiro K, Segui-Real B, Yamada Y, Martin GR, Kleinman HK.** 1989. Two different laminin domains mediate the differentiation of human endothelial cells into capillary-like structures in vitro. *Cell*, 58(5):933-43.

**Gray DS, Liu WF, Shen CJ, Bhadriraju K, Nelson CM, Chen CS.** 2008. Engineering amount of cell-cell contact demonstrates biphasic proliferative regulation through RhoA and the actin cytoskeleton. *Exp Cell Res*, 314(15):2846-54.

**Griffiths-Jones S, Grocock RJ, van Dongen S, Bateman A, Enright AJ.** 2006. miRBase: microRNA sequences, targets and gene nomenclature. *Nucleic Acids Res*, 1(34):140-4.

**Grinnell F.** 1984. Fibronectin and wound healing. *J Cell Biochem* 26 (2): 107–116.

**Grinnell BW, Berg DT.** 1996.

Surface thrombomodulin modulates thrombin receptor responses on vascular smooth muscle cells. *Am J Physiol*, 270(2):603-9.

**Grönholm, M., Teesalu, T., Tyynelä, J., Piltti, K., Böhling, T., Wartiovaara, K., Vaheri, A. and Carpén, O.** 2005. Characterization of the NF2 protein merlin and the ERM protein ezrin in human, rat, and mouse central nervous system. *Molecular and Cellular Neuroscience*, 28(4): 683-693.

**Grosshans H, Slack FJ.** 2002. Micro-RNAs: small is plentiful. *J Cell Biol*, 156(1):17-21.

**Grover-Paez F, Zavalza-Gomez AB.** 2009. Endothelial dysfunction and cardiovascular risk factors. *Diabetes Res Clin Pract*, 84: 1-10.

**Guan JL, Trevithick JE, Hynes RO.** 1991.

Fibronectin/integrin interaction induces tyrosine phosphorylation of a 120-kDa protein *Cell Regul.* 2(11):951-64.

**Guan JL.** 1997. Role of focal adhesion kinase in integrin signalling. *Int J Biochem Cell Biol.* (8-9):1085-96.

**Guan YJ, Yang X, Wei L, Chen Q.** 2011. MiR-365:

a mechanosensitive microRNA stimulates chondrocyte differentiation through targeting histone deacetylase 4. *FASEB J*, 25(12):4457-66.

**Gumbiner BM.** 1996. Cell adhesion: the molecular basis of tissue architecture and morphogenesis. *Cell*, 84(3):345-57.

**Guo H, Ingolia NT, Weissman JS, Bartel DP.** 2010.

Mammalian microRNAs predominantly act to decrease target mRNA levels. *Nature*, 466(7308):835-40.

**Haga JH, Li YS, Chien S.** 2007. Molecular basis of the effects of mechanical stretch on vascular smooth muscle cells. *J Biomech*, 40(5):947-60.

**Hahn C, Schwartz MA.** 2009. Mechanotransduction in vascular physiology and atherogenesis. *Nat Rev Mol Cell Biol*, 10(1):53-62.

- Hamm A, Krott N, Breibach I, Blindt R, Bosserhoff AK.** (2002) Efficient transfection method for primary cells. *Tissue Eng*, 8(2):235-45.
- Hannan RL, Kourembanas S, Flanders KC, Rogelj SJ, Roberts AB, Faller DV, Klagsbrun M.** 1988. Endothelial cells synthesize basic fibroblast growth factor and transforming growth factor beta. *Growth Factors*, 1(1):7-17.
- Hans FP, Moser M, Bode C, Grundmann S.** 2010. MicroRNA Regulation of Angiogenesis and Arteriogenesis. *Trends in Cardiovascular Medicine*, 20(8): 253-262.
- Hanson EK, Lubenow H, Ballantyne J.** 2009. Identification of forensically relevant body fluids using a panel of differentially expressed microRNAs. *Anal Biochem*, 387:303-314.
- Hao H, Ropraz P, Verin V, Camenzind E, Geinoz A, Pepper MS, Gabbiani G, Bochaton-Piallat ML.** 2002. Heterogeneity of smooth muscle cell populations cultured from pig coronary artery. *Arterioscler Thromb Vasc Biol*, 22(7):1093-9.
- Harris TA, Yamakuchi M, Ferlito M, Mendell JT, Lowenstein CJ.** 2008. MicroRNA-126 regulates endothelial expression of vascular cell adhesion molecule 1. *Proc Natl Acad Sci*, 105: 1516-21.
- Hartmann D, Thum T.** 2011. MicroRNAs and vascular (dys)function. *Vascul Pharmacol*, 55(4):92-105.
- Harvey NL, Oliver G.** 2004. Choose your fate: artery, vein or lymphatic vessel? *Current Opinion in Genetics & Development*, 14(5):499-505.
- Hautmann MB, Madsen CS, Owens GK.** 1997. A transforming growth factor beta (TGFbeta) control element drives TGFbeta-induced stimulation of smooth muscle alpha-actin gene expression in concert with two CArG elements. *J Biol Chem*, 272(16):10948-56.
- Haver VG, Slart RHJA, Zeebregts CJ, Peppelenbosch MP, Tio R.A.** 2010. Rupture of Vulnerable Atherosclerotic Plaques: MicroRNAs Conducting the Orchestra? *Trends in Cardiovascular Medicine*, 20(2): 65-71.
- Hedin U, Holm J, and Hansson GK.** 1991. Induction of tenascin in rat arterial injury. Relationship to altered smooth muscle cell phenotype. *Am J Pathol*, 139(3): 649-656.

- Heimberg AM, Sempere LF, Moy VN, Donoghue PC, Peterson KJ.** 2008. MicroRNAs and the advent of vertebrate morphological complexity. *Proc Natl Acad Sci*, 105(8):2946-50.
- Hellstrom, M, Kalen, M, Lindahl P.** 1999. Role of PDGF-B and PDGFR-beta in recruitment of vascular smooth muscle cells and pericytes during embryonic blood vessel formation in the mouse. *Development*, 126(14) 3047-55.
- Higgs HN, Pollard TD.** 2001. Regulation of actin filament network formation through ARP2/3 complex: activation by a diverse array of proteins. *Annu Rev Biochem*, 70:649-76.
- Hipper A, Isenberg G.** 2000. Cyclic mechanical strain decreases the DNA synthesis of vascular smooth muscle cells. *Pflugers Arch*, 440(1):19-27.
- Hirasawa M, Cho A, Sreenath T, Sauer B, Julien J, Kulkarni AB.** 2001. Neuron-specific expression of Cre recombinase during the late phase of brain development. *Neuroscience Research*, 40(2):125-132.
- Hirschi KK, D'Amore PP.** 1996. Pericytes in the microvasculature. *Cardiovasc Res*, 687-698
- Horace L.**1928. *Statics: Including Hydrostatics and the Elements of the Theory of Elasticity*. Cambridge University Press.
- Houbaviy HB, Murray MF, Sharp PA.** 2003. Embryonic stem cell-specific MicroRNAs. *Dev Cell*, 5(2):351-8.
- Hsu HJ, Lee CF, Locke A, Vanderzyl SQ, Kaunas R.** (2010). Stretch-induced stress fibre remodelling and the activations of JNK and ERK depend on mechanical strain rate, but not FAK.
- Huang DW, Sherman BT, Lempicki RA.** (2009). Bioinformatics enrichment tools: paths toward the comprehensive functional analysis of large gene lists. *Nucleic Acids Res*, 37(1):1-13.
- Huang DW, Sherman BT, Lempicki RA.** 2009. Systematic and integrative analysis of large gene lists using DAVID Bioinformatics Resources. *Nature Protoc*, 4(1):44-57.

- Hughes SC, Fehon RG.** 2007. Understanding ERM proteins – the awesome power of genetics finally brought to bear. *Current Opinion in Cell Biology*, 19(1): 51-56.
- Humphries JD, Byron A, Humphries MJ.** 2006. Integrin ligands at a glance. *J Cell Sci*, 119 (19):3901-3.
- Hungerford JE, Owens GK, Argraves WS, Little CD.** 1996. Development of the aortic vessel wall as defined by vascular smooth muscle and extracellular matrix markers. *Dev Biol*, 178(2):375-92.
- Hurst DR, Edmonds MD, Welch DR.** 2009. Metastamir: the field of metastasis-regulatory microRNA is spreading. *Cancer Res*, 69(19):7495-8.
- Hynes RO.** 2002. Integrins: bidirectional, allosteric signaling machines. *Cell*, 110:673–687
- Inatome R, Yanagi S, Takano T, Yamamura H.** 2001. A Critical Role for Syk in Endothelial Cell Proliferation and Migration. *Biochemical and Biophysical Research Communications*, 286(1): 195-199.
- Iwasaki H, Eguchi S, Ueno H, Marumo F, Hirata Y.** 2000. Mechanical stretch stimulates growth of vascular smooth muscle cells via epidermal growth factor receptor. *Am J Physiol Heart Circ Physiol*, 278(2): 21-9.
- Jalali S, Li YS, Sotoudeh M, Yuan S, Li S, Chien S, Shyy J Y.** 1998. Shear stress activates p60src-Ras-MAPK signalling pathways in vascular endothelial cells. *Arterioscler. Thromb Vasc Biol*, 18:227–234.
- Janmey PA, Weitz DA.** 2004. Dealing with mechanics: mechanisms of force transduction in cells. *Trends Biochem Sci*, 29(7):364-70.
- Ji R, Cheng Y, Yue J, Yang J, Liu X, Chen H, Dean DB, Zhang C.** 2007. MicroRNA expression signature and antisense-mediated depletion reveal an essential role of MicroRNA in vascular neointimal lesion formation. *Circ Res*, 100(11):1579-88.
- Jiang Y, Yin H, Zheng XL.** 2010. MicroRNA-1 inhibits myocardium-induced contractility of human vascular smooth muscle cells. *J Cell Physiol*, 225(2):506-11.



- Joshi R, Jan S, Wu Y, MacMahon S.** 2008. Global inequalities in access to cardiovascular health care: our greatest challenge. *J Am Coll Cardiol*, 52(23):1817-25.
- Kakisis JD, Pradhan S, Cordova A, Liapis CD, Sumpio BE.** 2005. The role of STAT-3 in the mediation of smooth muscle cell response to cyclic strain. *Int J Biochem Cell Biol*, 37(7):1396-406.
- Kanehisa M, Goto S.** 2000. KEGG: kyoto encyclopedia of genes and genomes. *Nucleic Acids Res*, 28(1):27-30.
- Kanehisa M.** 1997. A database for post-genome analysis. *Trends Genet*, 13(9):375-6.
- Kapsimalis F, Basta M, Varouchakis G, Gourgoulianis K, Vgontza A, Kryger M.** 2008. Cytokines and pathological sleep. *Sleep Medicine*, 9(6): 603-614.
- Karginov FV, Conaco C, Xuan Z, Schmidt BH, Parker JS, Mandel G, Hannon, GJ.** 2007. A biochemical approach to identifying microRNA targets *Proceedings of the National Academy of Sciences of the United States of America*, 104(49): 19291-19296.
- Katsumi K, Orr W, Tzima E, Schwartz MA.** 2004. Integrins in Mechanotransduction. *J Biol Chem*, 279(13):12001-4.
- Kaunas R, Nguyen P, Usami S, Chien S.** 2005. Cooperative effects of Rho and mechanical stretch on stress fiber organization. *Proc Natl Acad Sci*, 102(44):15895-900.
- Kaunas R, Usami S, Chien S.** 2006. Regulation of stretch-induced JNK activation by stress fiber orientation. *Cell Signal*, 18(11):1924-31
- Ke N, Wang X, Xu X, Abassi YA** 2011. The xCELLigence system for real-time and label-free monitoring of cell viability. *Methods Mol Biol*; **740**: 33–43.
- Kengne AP, Turnbull F, MacMahon S.** 2010. The Framingham Study, diabetes mellitus and cardiovascular disease: turning back the clock. *Prog Cardiovasc Dis*, 53(1):45-51.
- Kim BS, Nikolovski J, Bonadio J, Mooney DJ.** 1999. Cyclic mechanical strain regulates the development of engineered smooth muscle tissue. *Nat Biotechnol*, 17(10):979-83.

**Kiosses WB, Shattil SJ, Pampori N, Schwartz MA.** 2001. Rac recruits high-affinity integrin  $\alpha v \beta 3$  to lamellipodia in endothelial cell migration. *Nat Cell Biol.* 3(3):316-20.

**Kitano H.** 2004. Biological robustness. *Nat Rev Genet*, 5: 826–837

**Kluiver J, Gibcus JH, Hettinga C, Adema A, Richter MK, Halsema N, Slezak-Prochazka I, Ding Y, Kroesen BJ, van den Berg A.** 2012. Rapid generation of microRNA sponges for microRNA inhibition. *PLoS One*, 7(1)

**Ko YS, Yeh HI, Haw M, Dupont E, Kaba R, Plenz G, Robenek H, Severs NJ.** 1999. Differential expression of connexin43 and desmin defines two subpopulations of medial smooth muscle cells in the human internal mammary artery. 19(7):1669-80.

**Kosaka N, Iguchi H, Ochiya T.** 2010. Circulating microRNA in body fluid: a new potential biomarker for cancer diagnosis and prognosis. *Cancer Sci.* 101(10):2087-92.

**Kotani, M, Fukuda N, Ando H.** 2003. Chimeric DNA-RNA hammerhead ribozyme targeting PDGF A-chain mRNA specifically inhibits neointima formation in rat carotid artery after balloon injury. *Cardiovasc Res*, 57, 265-76.

**Koyama N, Seki J, Vergel S, Mattsson EJ, Yednock T, Kovach NL, Harlan JM, Clowes AW.** 1996. Regulation and function of an activation-dependent epitope of the beta 1 integrins in vascular cells after balloon injury in baboon arteries and in vitro. *Am J Pathol*, 148(3): 749–761.

**Kozak M.**

2008. Faulty old ideas about translational regulation paved the way for current confusion about how microRNAs function. *Gene*, 423(2):108-15.

**Kratsios P, Catela C, Salimova E, Huth M, Berno V, Rosenthal N, Mourkioti F.** 2010. Distinct roles for cell-autonomous Notch signaling in cardiomyocytes of the embryonic and adult heart. *Circ Res*, 106(3):559-72.

**Kuchenbauer F, Mah SM, Heuser M, McPherson A, Rüschemann J, Rouhi A, Berg T, Bullinger L, Argiropoulos B, Morin RD, Lai D, Starczynowski DT, Karsan A, Eaves CJ, Watahiki A, Wang Y, Aparicio SA, Ganser A, Krauter J, Döhner H, Döhner K, Marra MA, Camargo FD, Palmqvist L, Buske C, Humphries RK.**

2011. Comprehensive analysis of mammalian miRNA\* species and their role in myeloid cells. *Blood*, 118(12):3350-8.

**Kuehbacher A, Urbich C, Zeiher AM, Dimmeler S.** 2007.

Role of Dicer and Drosha for endothelial microRNA expression and angiogenesis. *Circ Res*, 101(1):59-68.

**Kuhn AR, Schlauch K, Lao R, Halayko AJ, Gerthoffer WT, Singer CA.** 2009.

MicroRNA expression in human airway smooth muscle cells: role of miR-25 in regulation of airway smooth muscle phenotype. *Am J Respir Cell Mol Biol*, 42(4):506-13.

**Kyttaris VC, Tsokos GC.** 2007. Syk kinase as a treatment target for therapy in autoimmune diseases. *Clinical Immunology*, 124(3): 235-237.

**Lal H, Verma SK, Smith M, Guleria RS, Lu G, Foster DM, Dostal DE.** (2007).

Stretch-induced MAP kinase activation in cardiac myocytes: differential regulation through beta1-integrin and focal adhesion kinase. *J Mol Cell Cardiol*. 43(2):137-4.

**Lanier LL.** 2006. Viral immunoreceptor tyrosine-based activation motif (ITAM)-mediated signaling in cell transformation and cancer. *Trends in Cell Biology*, 16(8): 388-390.

**Laplace E.** 1899. A New Forceps for Intestinal Anastomosis. *Ann Surg*, 29, 297- 305.

**Lau NC, Lim LP, Weinstein EG, Bartel DP.** 2001.

An abundant class of tiny RNAs with probable regulatory roles in *Caenorhabditis elegans*. *Science*, 294(5543):858-62.

**Lawler J, Weinstein R, Hynes RO.** 1988. Cell attachment to thrombospondin:

the role of ARG-GLY-ASP, calcium, and integrin receptors. *J Cell Biol*, 107(1):2351-61.

**Lee RC, Feinbaum RL, Ambros V.** 1993. The *C. elegans* heterochronic gene *lin-*

*4* encodes small RNAs with antisense complementarity to *lin-14*. *Cell*, 75: 843–854.

**Lee TY, Gotlieb AI.** 2003.

Microfilaments and microtubules maintain endothelial integrity. *Microsc Res Tech*, 60(1):115-27.

**Lee YG, Chain BM, Cho JY.** 2009. Distinct role of spleen tyrosine kinase in the early phosphorylation of inhibitor of  $\kappa$ B $\alpha$  via activation of the phosphoinositide-3-kinase and Akt pathways. *The International Journal of Biochemistry & Cell Biology*, In Press, Corrected Proof

**Leeper NJ, Raiesdana A, Kojima Y, Chun HJ, Azuma J, Maegdefessel L, Kundu RK, Quertermous T, Tsao PS, Spin JM.** 2011. MicroRNA-26a is a novel regulator of vascular smooth muscle cell function. *J Cell Physiol*, 226(4):1035-43.

**Lehoux S, Tedgui A.** 1998. Signal transduction of mechanical stresses in the vascular wall. *Hypertension*, 32(2):338-45.

**Lema C, Cunningham MJ.** 2010. MicroRNAs and their implications in toxicological research. *Toxicology Letters*, 198(2): 100-105.

**Levesque MJ, Nerem RM, Sprague EA.** 1990. Vascular endothelial cell proliferation in culture and the influence of flow. *Biomaterials*, 11(9):702-7.

**Li C, Pei F, Zhu X, Duan DD, Zeng C.** 2012. Circulating microRNAs as novel and sensitive biomarkers of acute myocardial Infarction. *Clinical Biochemistry*, 45(10–11): 727-732.

**Li C, Hu Y, Sturm G, Wick G, Xu Q.** 2000. Ras/Rac-Dependent activation of p38 mitogen-activated protein kinases in smooth muscle cells stimulated by cyclic strain stress. *Arterioscler Thromb Vasc Biol*, 20(3): 1-9.

**Li C, Wernig F, Leitges M, Hu Y, Xu Q.** 2003. Mechanical stress-activated PKC $\delta$  regulates smooth muscle cell migration. *FASEB J*, 17(14):2106-8.

**Li F, Guo WY, Li WJ, Zhang DX, Lv AL, Luan RH, Liu B, Wang HC.** 2009. Cyclic stretch upregulates SDF-1 $\alpha$ /CXCR4 axis in human saphenous vein smooth muscle cells. *Biochem Biophys Res Commun*. 386(1):247-51.

**Li JP, Fu YN, Chen YR, Tan TH.** (2010). JNK pathway associated phosphatase dephosphorylates focal adhesion kinase and suppresses cell migration. *J Biol Chem*. 285(8):5472-8.

**Li L, Chaikof EL.** 2002. Mechanical stress regulates syndecan-4 expression and redistribution in vascular smooth muscle cells. *Arterioscler Thromb Vasc Biol*, 22(1):61-8.

**Li M, Luraghi P, Amour A, Qian X, Carter PS, Clark CJ, Deakin A, Denyer J, Hobbs CI, Surby M, Patel VK, Schaefer EM.** 2009. Kinetic assay for characterization of spleen tyrosine kinase activity and inhibition with recombinant kinase and crude cell lysates. *Analytical Biochemistry*, 384(1): 56-67.

**Li S, Fan YS, Chow LH, Van Den Diepstraten C, van Der Veer E, Sims SM, Pickering JG.**

2001. Innate diversity of adult human arterial smooth muscle cells: cloning of distinct subtypes from the intrathoracic artery. *Circ Res*, 89(6):517-25.

**Li T, Cao H, Zhuang J, Wan J, Guan M, Yu B, Li X, Zhang W.** 2011. Identification of miR-130a, miR-27b and miR-210 as serum biomarkers for atherosclerosis obliterans. *Clinica Chimica Acta*, 412(1-2): 66-70.

**Lim SS, Noakes M, Keogh JB, Clifton PM.** 2010. Long-term effects of a low carbohydrate, low fat or high unsaturated fat diet compared to a no-intervention control. *Nutr Metab Cardiovasc Dis*, 20(8):599-607.

**Lindner V, Reidy MA.** 1993. Expression of basic fibroblast growth factor and its receptor by smooth muscle cells and endothelium in injured rat arteries. An en face study. *Circ Res*, 73(3):589-95.

**Linsley PS, Schelter J, Burchard J, Kibukawa M, Martin MM, Bartz SR, Johnson JM, Cummins JM, Raymond CK, Dai H, Chau N, Cleary M, Jackson AL, Carleton M, Lim L.** 2007. Transcripts targeted by the microRNA-16 family cooperatively regulate cell cycle progression. *Mol Cell Biol*, 27(6):2240-52.

**Liu WF, Nelson CM, Tan JL, Chen CS.** 2007. Cadherins, RhoA, and Rac1 are differentially required for stretch-mediated proliferation in endothelial versus smooth muscle cells. *Circ Res*, 101(5): 44-52.

**Liu, M, Jiang, S, Lu, Z, Li, Y, Young, KH.** 2010. Physiological and Pathological Functions of Mammalian MicroRNAs *IN*: (ed.) McQueen, CA *Comprehensive Toxicology*. (Second Edition). Oxford Elsevier, pp. 427-446.

**Liu, N. and Olson, E.N.** 2010. MicroRNA Regulatory Networks in Cardiovascular Development. *Dev Cell*, 18(4): 510-525.

**Lo, SH.** 2006. Focal adhesions: What's new inside. *Dev Biol*, 294(2):280-91.

- Louvet-Vallée, S.** 2000. ERM proteins: From cellular architecture to cell signaling. *Biology of the Cell*, 92(5): 305-316.
- Lovallo, W.R.** 2005. Cardiovascular reactivity: Mechanisms and pathways to cardiovascular disease. *International Journal of Psychophysiology*, 58(2–3): 119-132.
- Lu YJ, Zhang Y, Wang N, Pan ZW, Yang BF.** 2008. The role MiR-328 in atrial fibrillation via repressing caveolin-3 expression. *J Mol Cell Cardiol*, 44:736.
- Luque A, Gómez M, Puzon W, Takada Y, Sánchez-Madrid F, Cabañas C.** (1996). Activated conformations of very late activation integrins detected by a group of antibodies (HUTS) specific for a novel regulatory region (355-425) of the common beta 1 chain. *J Biol Chem*. 271(19):11067-75.
- Lusis, AJ, Mar, R and Pajukanta, P.** 2004. Genetics of atherosclerosis. *Annual review of Genomics and Human Genetics*, 5: 189-218
- Mackenzie N, Zhu D, Genever P, MacRae V.** 2013. The miR-221/222 family regulates vascular smooth muscle cell calcification. *Bone Abstracts*, 1: 496
- Mangeat P, Roy C, Martin M.** 1999. ERM proteins in cell adhesion and membrane dynamics. *Trends in Cell Biology*, 9(5): 187-192.
- Martinac B.** 2004. Mechanosensitive ion channels: molecules of mechanotransduction. *J Cell Sci*, 117(12):2449-60.
- Mason IJ.** 1994. The ins and outs of fibroblast growth factors. *Cell*, 78:547–552.
- Matsumoto T, Hwang PM.** 2007. Resizing the genomic regulation of restenosis. *Circ Res*, 100(11):1537-9.
- Mayr, M.** 2012. Integration of miRNA and proteomic screening for cardiovascular disease. *Vascular Pharmacology*, 56(5–6): 343.
- Mazuc E, Villoutreix BO, Malbec O, Roumier T, Fleury S, Leonetti J, Dombrowicz D, Daëron M, Martineau P, Dariavach P.** 2008. A novel druglike spleen tyrosine kinase binder prevents anaphylactic shock when administered orally. *Journal of Allergy and Clinical Immunology*, 122(1): 188-194.

**Mendis, S.** 2010. The Contribution of the Framingham Heart Study to the Prevention of Cardiovascular Disease: A Global Perspective. *Progress in Cardiovascular Diseases*, 53(1): 10-14.

**Menghini R, Casagrande V, Cardellini M, Martelli E, Terrinoni A, Amati F .**2009. MicroRNA 217 modulates endothelial cell senescence via silent information regulator 1. *Circulation*,210: 1524-32.

**Mestdagh P, Van Vlierberghe P, De Weer A, Muth D, Westermann F, Speleman F, Vandesompele J.** 2009. A novel and universal method for microRNA RT-qPCR data normalization. *Genome Biol*, 10(6): 64

**J A Meyers, D Sanchez, L P Elwell, and S Falkow.** 1976. Simple agarose gel electrophoretic method for the identification and characterization of plasmid deoxyribonucleic acid. *J Bacteriol.* 1976 September; 127(3): 1529–1537.

**Miano JM, Cserjesi P, Ligon KL, Periasamy M, Olson EN.** 1994. Smooth muscle myosin heavy chain exclusively marks the smooth muscle lineage during mouse embryogenesis. *Circ Res*, 75(5):803-12.

**Milburn Jessup, J.** 1998. Tumor markers – prognostic and therapeutic implications for colorectal carcinoma. *Surgical Oncology*, 7(3-4): 139-151.

**Mitchell JJ, Reynolds SE, Leslie KO, Low RB, Woodcock-Mitchell J.** 1990. Smooth muscle cell markers in developing rat lung. *Am J Respir Cell Mol Biol*, 3(6):515-23.

**Mitchell PS, Parkin, RK, Kroh, EM, Fritz BR, Wyman SK, Pogossova-Agadjanyan, EL, Peterson A, Noteboom J O'Briant KC, Allen A, Lin DW, Urban N, Nelson PS, Drescher CW, Knudsen BS, Stirewalt DL, Gentleman R, Vessella RL, Martin DB, Tewari M,** 2008. Circulating microRNAs as stable blood-based markers for cancer detection. *Proc Natl Acad Sci*, 105(30): 10513–8.

**Miyauchi A, Alvarez J, Greenfield EM, Teti A, Grano M, Colucci S, Zambonin-Zallone A, Ross FP, Teitelbaum SL, Cheresch D.** 1991. Recognition of osteopontin and related peptides by an alpha v beta 3 integrin stimulates immediate cell signals in osteoclasts. *J Biol Chem*, 266(30):20369-74.

**Mócsai, A., Zhou, M., Meng, F., Tybulewicz, V.L. and Lowell, C.A.** 2002. Syk Is Required for Integrin Signaling in Neutrophils. *Immunity*, 16(4): 547-558.

**Mogford JE, Davis GE, Platts SH, Meininger GA.** (1996). Vascular smooth muscle alpha v beta 3 integrin mediates arteriolar vasodilation in response to RGD peptides. *Circ Res.* 79(4):821-6.

**Mohamed JS, Lopez MA, Boriek AM.** 2010. Mechanical stretch up-regulates microRNA-26a and induces human airway smooth muscle hypertrophy by suppressing glycogen synthase kinase-3 $\beta$ . *J Biol Chem*, 285(38):29336-47.

**Mohanty MJ, Li X.** 2002. Stretch-induced Ca(2+) release via an IP(3)-insensitive Ca(2+) channel. *Am J Physiol Cell Physiol*, 283(2):C456-62.

**Moiseeva EP.** 2001. Adhesion receptors of vascular smooth muscle cells and their functions. *Cardiovasc Res*, 52(3):372-86.

**Morla AO, Mogford JE.** 2000. Control of smooth muscle cell proliferation and phenotype by integrin signaling through focal adhesion kinase. *Biochem Biophys Res Commun*, 272(1):298-302.

**Morrow D, Scheller A, Birney YA, Sweeney C, Guha S, Cummins PM, Murphy R, Walls D, Redmond EM, Cahill PA.** 2005. Notch-mediated CBF-1/RBP-J {kappa}-dependent regulation of human vascular smooth muscle cell phenotype invitro. *Am J Physiol Cell Physiol*, 289(5): 1188-96.

**Morrow D, Sweeney C, Birney YA, Guha S, Collins N, Cummins PM, Murphy R, Walls D, Redmond EM, Cahill PA.** 2007. Biomechanical regulation of hedgehog signaling in vascular smooth muscle cells in vitro and in vivo. *Am J Physiol Cell Physiol*. 292(1):C488-96.

**Mukherji S, Ebert MS, Zheng GX, Tsang JS, Sharp PA, van Oudenaarden A.** 2011. MicroRNAs can generate thresholds in target gene expression. *Nat Genet* 43:854–859.

**Multhaupt HA, Yoneda A, Whiteford JR., Oh ES., Lee W. & Couchman JR.** Syndecan signalling: when, where and why? 2009. *J Physiol Pharmacol*, 4:31-8.



- Muniategui A, Pey J, Planes FJ, Rubio A.** 2013. Joint analysis of miRNA and mRNA expression data. *Brief Bioinform*, 14(3):263-78.
- Naoghare PK, Tak YK, Kim MJ, Han E, Song JM.** 2011. Knock-down of argonaute 2 (AGO2) induces apoptosis in myeloid leukaemia cells and inhibits siRNA-mediated silencing of transfected oncogenes in HEK-293 cells. *Basic Clin Pharmacol Toxicol*, (4): 274-82.
- Ndiaye NC, Azimi Nehzad M, El Shamieh S, Stathopoulou MG, Visvikis-Siest S.** 2011. Cardiovascular diseases and genome-wide association studies. *Clin Chim Acta*, 412(19-20):1697-701.
- Neppl RL, Wang D.** 2009. Smooth(ing) Muscle Differentiation by MicroRNAs. *Cell Stem Cell*, 5(2): 130-132.
- Ng G, Sharma K, Ward SM, Desrosiers MD, Stephens LA, Schoel WM, Li T, Lowell CA, Ling C, Amrein MW, Shi Y.** 2008. Receptor-Independent, Direct Membrane Binding Leads to Cell-Surface Lipid Sorting and Syk Kinase Activation in Dendritic Cells. *Immunity*, 29(5): 807-818.
- Nieves-Cintrón M, Amberg GC, Navedo MF, Molkenin JD, Santana LF.** 2008. The control of Ca<sup>2+</sup> influx and NFATc3 signaling in arterial smooth muscle during hypertension. *Proc Natl Acad Sci*, 105(40):15623-8.
- Nikolovski J, Kim BS, Mooney DJ.** 2003. Cyclic strain inhibits switching of smooth muscle cells to an osteoblast-like phenotype. *Faseb J*, 17(3):455-7.
- Nishikawa KC, Millis AJ.** 2003. gp38k (CHI3L1) is a novel adhesion and migration factor for vascular cells. *Exp Cell Res*, 287(1):79-87.
- O'Callaghan CJ, Williams B.** 2000. Mechanical strain-induced extracellular matrix production by human vascular smooth muscle cells: role of TGF-beta(1). *Hypertension*, 36(3):319-24.
- Olivieri F, Antonicelli R, Lorenzi M, D'Alessandra Y, Lazzarini R, Santini G, Spazzafumo L, Lisa R, La Sala L, Galeazzi R, Recchioni R, Testa R, Pompilio G, Capogrossi MC, Procopio AD.** Diagnostic potential of circulating miR-499-5p in elderly patients with acute non ST-elevation myocardial infarction. *International Journal of Cardiology*, 167(2):531-6.

**Oppenheimer GM.** 2010. Framingham Heart Study: The First 20 Years. *Progress in Cardiovascular Diseases*, 53(1): 55-61.

**Orom UA, Lund AH.** 2007. Isolation of microRNA targets using biotinylated synthetic microRNAs. *Methods*, 43(2):162-5.

**Orr AW, Ginsberg MH, Shattil SJ, Deckmyn H, Schwartz MA.** (2006). Matrix-specific suppression of integrin activation in shear stress signaling. *Mol Biol Cell*. 17(11):4686-97.

**Orr AW, Lee MY, Lemmon JA, Yurdagul A Jr, Gomez MF, Bortz PD, Wamhoff BR.** Molecular mechanisms of collagen isotype-specific modulation of smooth muscle cell phenotype. *Arterioscler Thromb Vasc Biol*, 29(2):225-31.

**Osol G.** 1995. Mechanotransduction by vascular smooth muscle. *J Vasc Res*, 32(5):275-92.

**Oui Carp6n, Peter Pallai, Donald E. Staunton, Timothy A.** Springer Association of Intercellular Adhesion Moleculeq (ICAM-1) with Actin-containing Cytoskeleton and -actinin

**Owens GK, Loeb A, Gordon D, Thompson MM.** 1986. Expression of smooth muscle-specific alpha-isoactin in cultured vascular smooth muscle cells: relationship between growth and cytodifferentiation. *J Cell Biol*, 102(2):343-52.

**Owens GK.** 1995. Regulation of differentiation of vascular smooth muscle cells. *Physiol Rev*, (3):487-517.

**Pan Y, Balazs L, Tigyi G, Yue J.** 2011.

Conditional deletion of Dicer in vascular smooth muscle cells leads to the developmental delay and embryonic mortality. *Biochem Biophys Res Commun*, 408(3):369-74.

**Pantaloni D, Le Clainche C, Carlier MF.** 2001. Mechanism of actin-based motility. *Science*, 292(5521): 1502-1506

**Parsons JT, Martin KH, Slack JK, Taylor JM, Weed SA.** 2000. Focal adhesion kinase: a regulator of focal adhesion dynamics and cell movement. *Oncogene*, 19(49):5606-13.

- Parsons, JT.** 2003. Focal adhesion kinase: the first ten years. *J Cell Sci.* 15;116 (8):1409-16.
- Passerini AG, Polacek DC, Shi C, Francesco NM, Manduchi E, Grant ER.** 2004. Coexisting proinflammatory and antioxidative endothelial transcription profiles in a disturbed flow region of the adult porcine aorta. *Proc Natl Acad Sci*, 101: 2484-7.
- Pawson, T., Gish, G.D. and Nash, P.** 2001. SH2 domains, interaction modules and cellular wiring. *Trends in Cell Biology*, 11(12): 504-511.
- Peltier HJ, Latham GJ.** 2008. Normalization of microRNA expression levels in quantitative RT-PCR assays: identification of suitable reference RNA targets in normal and cancerous human solid tissues. *RNA*, 14: 844–852.
- Petrof BJ.** 2002. Molecular pathophysiology of myofiber injury in deficiencies of the dystrophin-glycoprotein complex. *Am J Phys Med Rehabil*, 81(11):162-74.
- Pierschbacher MD, Ruoslahti E.** 1984. Cell attachment activity of fibronectin can be duplicated by small synthetic fragments of the molecule. *Nature*. 309. 30-33
- Pine PR, Chang B, Schoettler N, Banquerigo ML, Wang S, Lau A, Zhao F, Grossbard EB, Payan DG, Brahn E.** 2007. Inflammation and bone erosion are suppressed in models of rheumatoid arthritis following treatment with a novel Syk inhibitor. *Clinical Immunology*, 124(3): 244-257.
- Pintucci G, Yu PJ, Sharony R, Baumann FG, Saponara F, Frasca A, Galloway AC, Moscatelli D, Mignatti P.** 2003. Induction of stromelysin-1 (MMP-3) by fibroblast growth factor-2 (FGF-2) in FGF-2<sup>-/-</sup> microvascular endothelial cells requires prolonged activation of extracellular signal-regulated kinases-1 and -2 (ERK-1/2).
- Platts SH, Mogford JE, Davis MJ, Meininger GA.** 1998. Role of K<sup>+</sup> channels in arteriolar vasodilation mediated by integrin interaction with RGD-containing peptide. *Am J Physiol*, 275(2):1449-54.
- Plow EF, Haas TA, Zhang L, Loftus J, Smith JW.** 2000. Ligand binding to integrins. *J Biol Chem*, 275:21785–21788.

- Polesello, C. and Payre, F.** 2004. Small is beautiful: what flies tell us about ERM protein function in development. *Trends in Cell Biology*, 14(6): 294-302.
- Presta M, Maier JA, Rusnati M, Ragnotti G.** 1989. Basic fibroblast growth factor is released from endothelial extracellular matrix in a biologically active form. *J Cell Physiol*, 140(1):68-74.
- Pritchard CC, Cheng HH, Tewari M.** 2012. MicroRNA profiling: approaches and considerations. *Nat Rev Genet*, 13(5):358-69.
- Pugsley MK, Tabrizchi R.** 2000. The vascular system. An overview of structure and function. *J Pharmacol Toxicol Methods*, 44(2):333-40.
- Pulikkan JA, Peramangalam PS, Dengler V, Ho PA, Preudhomme C, Meshinchi S, Christopheit M, Nibourel O, Müller-Tidow C, Bohlander SK, Tenen DG, Behre G.** 2010. C/EBP $\alpha$  regulated microRNA-34a targets E2F3 during granulopoiesis and is down-regulated in AML with CEBPA mutations. *Blood*, 116(25):5638-49.
- Pytela R, Pierschbacher MD, Argraves S, Suzuki S, Ruoslahti E.** 1987. Arginine-glycine-aspartic acid adhesion receptors. *Methods Enzymol*, 144:475-89.
- Qi YX, Qu MJ, Yan ZQ, Zhao D, Jiang XH, Shen BR, Jiang ZL.** 2010. Cyclic strain modulates migration and proliferation of vascular smooth muscle cells via Rho-GDI $\alpha$ , Rac1, and p38 pathway. *J Cell Biochem*, 109(5): 906-14.
- Qiao, Y, Ma, N, Wang, X., Hui, Y, Li, F., Xiang, Y., Zhou, J., Zou, C., Jin, J., Lv, G., Jin, H. and Gao, X.** 2011. MiR-483-5p controls angiogenesis in vitro and targets serum response factor. *FEBS Letters*, 585(19): 3095-3100.
- Quintavalle C, Garofalo, M, Croce, C.M. and Condorelli, G.** 2011. "ApoptomiRs" in vascular cells: Their role in physiological and pathological angiogenesis. *Vascular Pharmacology*, 55(4): 87-91.
- Quintavalle, M., Condorelli, G. and Elia, L.** 2011. Arterial remodeling and atherosclerosis: miRNAs involvement. *Vascular Pharmacology*, 55(4): 106-110.
- Raines EW, Koyama H, Carragher NO.** 2000. The extracellular matrix dynamically regulates smooth muscle cell responsiveness to PDGF. *Ann N Y Acad Sci*, 902:39-52.

**Raitoharju E, Lyytikäinen L, Levula M, Oksala N, Mennander A, Tarkka M, Klopp N, Illig T, Kähönen M, Karhunen PJ, Laaksonen R, Lehtimäki, T.** 2011. miR-21, miR-210, miR-34a, and miR-146a/b are up-regulated in human atherosclerotic plaques in the Tampere Vascular Study. *Atherosclerosis*, 219(1): 211-217.

**Rapraeger AC, Ott VL.** 1998. Molecular interactions of the syndecan core proteins. *Curr Opin Cell Biol*, 10(5):620-8.

**Reddy K, Satija A.** 2010. The Framingham Heart Study: Impact on the Prevention and Control of Cardiovascular Diseases in India. *Progress in Cardiovascular Diseases*, 53(1): 21-27.

**Redis RS, Calin S, Yang, Y., You, M.J, Calin, G.A.** Cell-to-cell miRNA transfer: From body homeostasis to therapy. *Pharmacology & Therapeutics*, 136(2):169-74

**Redmond EM, Lally C, Cahill PA.** 2012. Hemodynamic Control of Vascular Smooth Muscle Function *IN: Hill, J (ed.) Muscle*. Boston/Waltham Content Repository Only. Pp.1231-1242.

**Reidy MA, Fingerle J, Lindner V.** 1992. Factors controlling the development of arterial lesions after injury. *Circulation*, 86(6):43-6.

**Reidy MA.** 1992. Factors controlling smooth-muscle cell proliferation. *Arch Pathol Lab Med*, 116(12):1276-80.

**Rena G, Houslay MD.**

1998. A simple method for sequencing small DNAs by introducing precise overlapping ends into restriction digestion fragments. *Nucleic Acids Res*, 26(16):3867-8.

**Renko M, Quarto N, Morimoto T, Rifkin DB.** 1990. Nuclear and cytoplasmic localization of different basic fibroblast growth factor species. *J Cell Physiol*, 144(1):108-14.

**Rensen SS, Doevendans PA, Van Eys GJ.** 2007.

Regulation and characteristics of vascular smooth muscle cell phenotypic diversity. *Neth Heart J*, 15(3):100-8.

**Rensen SS, Niessen PM, Long X, Doevendans PA, Miano JM, van Eys GJ.** 2006. Contribution of serum response factor and myocardin to transcriptional regulation of smoothelin. *Cardiovasc Res*, 70(1):136-45.

**Reusch HP, Chan G, Ives HE, Nemenoff RA.** 1997.

Activation of JNK/SAPK and ERK by mechanical strain in vascular smooth muscle cell depends on extracellularmatrix composition. *Biochem Biophys Res Commun*, 237(2):239-44.

**Rhaitoharju E, Lyytikainen LP, Levula M, Oksala N, Mennander A, Tarkka M.**

2011. miR-21, miR-21-, miR-34a, miR-146a/b are up-regulated in human atherosclerotic plaques in the Tampere Vascular study. *Atherosclerosis*, 219: 211-7.

**Riha GM, Wang X, Wang H, Chai H, Mu H, Lin PH, Lumsden AB, Yao Q, Chen C.** 2007.

Cyclic strain induces vascular smooth muscle cell differentiation from murine embryonic mesenchymal progenitorcells. *Surgery*, 141(3):394-402.

**Rippe C, Blimline M, Magerko KA, Lawson BR, LaRocca TJ, Donato AJ, Seals DR.** 2012.

MicroRNA changes in human arterial endothelial cells with senescence: relation to apoptosis, eNOS andinflammation. *Exp Gerontol*, 47(1):45-51.

**Risso D, Massa MS, Chiogna M, Romualdi C.** 2009. A modified LOESS normalization applied to microRNA arrays: a comparative evaluation. *Bioinformatics*, 25(20):2685-91.

**Robinson DR, Wu YM, Lin SF.** 2000. The protein tyrosine kinase family of the human genome. *Oncogene*, 19(49):5548-57.

**Roca-Cusachs P, Gauthier NC, Del Rio A, Sheetz MP.**2009. Clustering of alpha(5)beta(1) integrins determines adhesion strength whereas alpha(v)beta(3) and talin enable mechanotransduction. *Proc Natl Acad Sci*, 106(38):16245-50.

**Rossant, J. and Hirashima, M.** 2003. Vascular development and patterning: making the right choices. *Current Opinion in Genetics & Development*, 13(4): 408-412.

**Ruoslahti E, Pierschbacher MD.** 1987.

New perspectives in cell adhesion: RGD and integrins. *Science*, 238(4826):491-7.

**Ruoslahti, E.** 2003. RGD story: a personal account. A Landmark Essay. *Matrix Biology*, 22(6):459-65.

- Sadler JE.** 1997. Thrombomodulin structure and function. *Thromb Haemost*, 78(1):392-5.
- Sadoshima J, Izumo S.** 1997. The cellular and molecular response of cardiac myocytes to mechanical stress. *Annu Rev Physiol*, 59:551-71.
- Sadoshima J, Xu Y, Slayter HS, Izumo S.** 1993. *Cell*, Autocrine release of angiotensin II mediates stretch-induced hypertrophy of cardiac myocytes in vitro. 75(5):977-84.
- Samal E, Srivastava D.** Role of microRNAs in Cardiovascular Biology *IN: Anonymous Advances in Developmental Biology*. Elsevier, pp.167-178.
- Sambrook and Russell** (2001). *Molecular Cloning: A Laboratory Manual* (3rd ed.). Cold Spring Harbor Laboratory Press. ISBN 978-0-87969-577-4.
- San Martín A, Lee MY, Williams HC, Mizuno K, Lassègue B, Griendling KK.** 2008. Dual regulation of cofilin activity by LIM kinase and Slingshot-1L phosphatase controls platelet-derived growth factor-induced migration of human aortic smooth muscle cells. *Circ Res*, 102(4):432-8.
- Santovito D, Mezzetti A, Cipollone F.** MicroRNAs and atherosclerosis: New actors for an old movie. *Nutrition, Metabolism and Cardiovascular Diseases*, 22(11):937-43.
- Sarkar D, Parkin R, Wyman S, Bendoraite A, Sather C, Delrow J, Godwin AK, Drescher C, Huber W, Gentleman R, Tewari M.** 2009. Quality assessment and data analysis for microRNA expression arrays. 37(2):e17
- Sarnow P, Jopling CL, Norman KL, Schütz S, Wehner KA.** 2006. MicroRNAs: expression, avoidance and subversion by vertebrate viruses. *Nat Rev Microbiol*, 4(9):651-9.
- Sayers RL, Sundberg-Smith LJ, Rojas M, Hayasaka H, Parsons JT, Mack CP, Taylor JM.** (2008). FRNK expression promotes smooth muscle cell maturation during vascular development and after vascular injury. *Arterioscler Thromb Vasc Biol.* (12):2115-22.
- Scalbert E, Bril A.** 2008. Implication of microRNAs in the cardiovascular system. *Current Opinion in Pharmacology*, 8(2): 181-188.

- Schattemann GC, Loushin C, Li T, et al.** 1996. PDGF-A is required for normal murine cardiovascular development. *Dev Biol*, 176:133-42.
- Schlaepfer DD, Hauck Cr Sieg, DJ.** 1999. Signaling through focal adhesion kinase. *Biophysics and molecular biology*. 71 435-478.
- Schor AM, Canfield PAE, Sutton AB, Arciniegas E Allen TD .** 1995. Pericyte differentiation. *Current orthopaedic practice*.
- Schwartz MA.** 2009. Cell biology. The force is with us. *Science*, 323(5914):588-9.
- Schwartz SM, Campbell GR, Campbell JH.** 1986. Replication of smooth muscle cells in vascular disease. *Circ Res*, 58(4):427-44.
- Schwartz SM, Reidy MA.** 1987. Common mechanisms of proliferation of smooth muscle in atherosclerosis and hypertension. *Hum Pathol*, 18(3):240-7.
- Scott Nowell C, Richie E, Ruth Manley N, Blackburn C.** 2007. Thymus and parathyroid organogenesis *IN: Robert Lanza, Robert Langer and Joseph Vacanti (eds.) Principles of Tissue Engineering (Third Edition)*. Burlington Academic Press, pp.647-662.
- Sebzda E, Hibbard C, Abtahian F, Tybulewicz V, Koretzky GA, Kahn ML.** 2004. Blood-Lymphatic vessel integrity requires syk tyrosine kinase signaling withing the endothelial cell compartment. *Cardiovascular Pathology*, 13(3, Supplement 1), pp.21-21.
- Sebzda, E, Hibbard, C, Sweeney, S, Abtahian, F, Bezman, N, Clemens, G, Maltzman, JS, Cheng, L, Liu, F, Turner, M, Tybulewicz, V, Koretzky, GA, anKahn, ML.** 2006. Syk and Slp-76 Mutant Mice Reveal a Cell-Autonomous Hematopoietic Cell Contribution to Vascular Development. *Developmental Cell*, 11(3): 349-361.
- Seki J, Koyama N, Kovach NL, Yednock T, Clowes AW, Harlan JM.** 1996. Regulation of beta1 integrin function in cultured human vascular smooth muscle cells. *Circ Res*, 78(4):596-605.
- Serrels, B, Serrels A, Brunton VG, Holt M, McLean GW, Gray CH, Jones GE, Frame MC.** 2007. Focal adhesion kinase controls actin assembly via a FERM-mediated interaction with the Arp2/3 complex. *Nat Cell Biol*, 9(9):1046-56.



- Sessa WC.** 2011. MicroRNA regulation of cardiovascular functions. *Arterioscler Thromb Vasc Biol*, 31(11):2369.
- Shah NM, Groves, AK, Anderson, DJ.** 1996. Alternative neural crest cell fates are instructively promoted by TGFbeta superfamily members. *Cell*, 85: 331-43.
- Shara, NM.** 2010. Cardiovascular disease in Middle Eastern women. *Nutr Metab Cardiovasc Dis*, (6):412-8.
- Shattil SJ, Kim C, Ginsberg MH.** 2010. The final steps of integrin activation: the end game. *Nat Rev Mol Cell Biol*, 11(4):288-300
- Shen E, Diao X, Wei C, Wu Z, Zhang L, Hu B.** 2010. MicroRNAs target gene and signaling pathway by bioinformatics analysis in the cardiac hypertrophy. *Biochemical and Biophysical Research Communications*, 397(3): 380-385.
- Shi ZD, Tarbell JM.** 2011. Fluid flow mechanotransduction in vascular smooth muscle cells and fibroblasts. *Ann Biomed Eng*, 39(6):1608-19.
- Silva R, D'Amico G, Kairbaan M. Hodivala-Dilke, Reynolds EL.** 2008. Integrins: The Keys to Unlocking Angiogenesis. *Arterioscler Thromb Vasc Biol*, 28:1703-1713;
- Sims DE.** 1986. The pericyte--a review. *Tissue Cell*, 18(2):153-74.
- Singh R, Masuda ES.** 2007. Spleen Tyrosine Kinase (Syk) Biology, Inhibitors and Therapeutic Applications *IN: Macor, J.E. (ed.) Annual Reports in Medicinal Chemistry.* Academic Press, pp.379-391.
- Small JV, Stradal T, Vignal E, Rottner K.** 2002. The lamellipodium: where motility begins. *Trends Cell Biol*, 12(3):112-20.
- Smalley SE, Wittler RR, Oliverson RH.** 2004. Adolescent assessment of cardiovascular heart disease risk factor attitudes and habits. *Journal of Adolescent Health*, 35(5): 374-379.
- Smith, P.K.,** (1985). Measurement of protein using bicinchoninic acid. *Anal. Biochem.* **150** (1): 76–85. doi:10.1016/0003-2697(85)90442-7
- Soff GA, Jackman RW, Rosenberg RD.** 1991. Expression of thrombomodulin by smooth muscle cells in culture: different effects of tu

mor necrosis factor and cyclic adenosine monophosphate on thrombomodulin expression by endothelial cells and smooth muscle cells in culture. *Blood*, 77(3):515-8.

**Somel M, Guo S, Fu N, Yan Z, Hu HY, Xu Y, Yuan Y, Ning Z, Hu Y, Menzel C, Hu H, Lachmann M, Zeng R, Chen W, Khaitovich P.** 2010. MicroRNA, mRNA, and protein expression link development and aging in human and macaque brain. *Genome Res*, 20(9):1207-18.

**Sonoki T, Iwanaga E, Mitsuya H, Asou N.** 2005. Insertion of microRNA-125b-1, a human homologue of lin-4, into a rearranged immunoglobulin heavy chain gene locus in a patient with precursor B-cell acute lymphoblastic leukemia. *Leukemia*, 19:2009–10

**Sotoudeh M, Jalali S, Usami S, Shyy JY, Chien S.** 1998.

A strain device imposing dynamic and uniform equi-biaxial strain to cultured cells. *Ann Biomed Eng*, 26(2):181-9.

**Stark A, Brennecke J, Bushati N, Russell RB, Cohen SM.** 2005. Animal MicroRNAs Confer Robustness to Gene Expression and Have a Significant Impact on 3'UTR Evolution. *Cell*, 123(6):1133-46.

**Stegemann JP, Nerem RM.** 2003.

Phenotype modulation in vascular tissue engineering using biochemical and mechanical stimulation. *Ann Biomed Eng*, 31(4):391-402

**Stijn van Dongen, Cei Abreu-Goodger, Anton J Enright** 2008. Detecting microRNA binding and siRNA off-target effects from expression data. *Nat Methods*, 5(12): 1023–1025.

**Suárez Y, Fernández-Hernando C, Pober JS, Sessa WC.** 2007.

Dicer dependent microRNAs regulate gene expression and functions in human endothelial cells. *Circ Res*, 100(8):1164-73.

**Suárez Y, Fernández-Hernando C, Yu J, Gerber SA, Harrison KD, Pober JS, Iruela-Arispe ML, Merkenschlager M, Sessa WC.** 2008. Dicer-dependent endothelial microRNAs are necessary for postnatal angiogenesis. *Proc Natl Acad Sci*, 105(37):14082-7.

**Suárez, Y, Fernández-Hernando, C.** 2012. New insights into microRNA-29 regulation: A new key player in cardiovascular disease. *Journal of Molecular and Cellular Cardiology*, 52(3): 584-586.

**Sukkar MB, Stanley AJ, Blake AE, Hodgkin PD, Johnson PR, Armour CL, Hughes JM.** 2004. 'Proliferative' and 'synthetic' airway smooth muscle cells are overlapping populations. *Immunol Cell Biol.* 82 (5):471-8

**Sumpio BE, Banes AJ. 1988.**

Response of porcine aortic smooth muscle cells to cyclic tensional deformation in culture. *J Surg Res*, 44(6):696-701.

**Taniyama Y, Griendling KK. 2003.** Reactive oxygen species in the vasculature: molecular and cellular mechanisms. *Hypertension*, 42(6):1075-81.

**Tatsuguchi M, Seok HY, Callis TE, Thomson JM, Chen J, Newman M, Rojas M, Hammond SM, Wang D.** 2007. Expression of microRNAs is dynamically regulated during cardiomyocyte hypertrophy. *Journal of Molecular and Cellular Cardiology*, 42(6): 1137-1141.

**Taylor JM, Mack CP, Nolan K, Regan CP, Owens GK, Parsons JT.** 2001. Selective expression of an endogenous inhibitor of FAK regulates proliferation and migration of vascular smooth muscle cells. *Mol Cell Bio*, 21(5):1565-72.

**Tennyson CN, Klamut HJ, Worton RG.** 1995.

The human dystrophin gene requires 16 hours to be transcribed and is cotranscriptionally spliced. *Nat Genet*, 9(2):184-90.

**Thum T, Mayr M.** 2012. Review focus on the role of microRNA in cardiovascular biology and disease. *Cardiovasc Res*, 93(4):543-4

**Timmins LH, Miller MW, Clubb FJ Jr, Moore JE Jr.** 2011. Increased artery wall stress post-stenting leads to greater intimal thickening. *Lab Invest*, 91(6):955-67.

**Tock J, Van Putten V, Stenmark KR, Nemenoff RA.** 2003. Induction of SM-alpha-actin expression by mechanical strain in adult vascular smooth muscle cells is mediated

through activation of JNK and p38 MAP kinase. *Biochem Biophys Res Commun*, 301(4):1116-21.

**Towbin H, Staehelin T, Gordon J.** 1979. Electrophoretic transfer of proteins from polyacrylamide gels to nitrocellulose sheets: procedure and some applications. *Proceedings of the National Academy of Sciences USA* **76** (9): 4350–54.

**Towbin JA.** 1998. The role of cytoskeletal proteins in cardiomyopathies. *Curr Opin Cell Biol*, 10(1):131-9.

**Toyama T, Iwase H, Yamashita H, Hara Y, Omoto Y, Sugiura H, Zhang Z, Fujii Y.** 2003. Reduced expression of the Syk gene is correlated with poor prognosis in human breast cancer. *Cancer Letters*, 189(1): 97-102.

**Traub O, Berk BC.** 1998. Laminar shear stress: mechanisms by which endothelial cells transduce an atheroprotective force. *Arterioscler Thromb Vasc Biol*, 18(5):677-85.

**Tristano AG.** 2009. Tyrosine kinases as targets in rheumatoid arthritis. *Int Immunopharmacol*, 9(1):1-9.

**Tsang J, Zhu J, van Oudenaarden A.** 2007. MicroRNA-Mediated Feedback and Feedforward Loops Are Recurrent Network Motifs in Mammals. *Molecular Cell*, 26(5): 753-767.

**Turnbull F, Kengne AP, MacMahon S.** 2010.

Blood pressure and cardiovascular disease: tracing the steps from Framingham. *Prog Cardiovasc Dis*, 3(1):39-44.

**Turner M, Schweighoffer E, Colucci F, Di Santo JP, Tybulewicz VL.** 2000. Tyrosine kinase SYK: essential functions for immunoreceptor signalling. *Immunology Today*, 21(3): 148-154.

**Udali S, Guarini P, Moruzzi S, Choi S, Friso S.** Cardiovascular epigenetics: From DNA methylation to microRNAs. *Molecular Aspects of Medicine*, 34(4):883-901.

**Underhill DM, Goodridge HS.** 2007. The many faces of ITAMs. *Trends in Immunology*, 28(2): 66-73.

**Van der Flier A, Sonnenberg A.** 2001. Function and interactions of integrins. *Cell Tissue Res*, 305(3):285-98.

**van Engeland M, Ramaekers FC, Schutte B, Reutelingsperger CP.** 1996. A novel assay to measure loss of plasma membrane asymmetry during apoptosis of adherent cells in culture. *Cytometry*,24(2):131-9.

**Van Eys GJ, Niessen PM, Rensen SS.** 2007. Smoothelin in vascular smooth muscle cells. *Trends Cardiovasc Med*, 17(1):26-30.

**Van Rooij E, Olson EN.** 2007. MicroRNAs: powerful new regulators of heart disease and provocative therapeutic targets. *J Clin Invest*, 117(9):2369-76.

**Vandekerckhove J, Weber K.**

1979. The complete amino acid sequence of actins from bovine aorta, bovine heart, bovine fast skeletal muscle, and rabbit slow skeletal muscle. A protein-chemical analysis of muscle actin differentiation. *Differentiation* 14, 123

**Vasudevan S, Tong Y, Steitz JA.** 2007.

Switching from repression to activation: microRNAs can up-regulate translation. *Science*, 318(5858):1931-4.

**Vicente-Manzanares M, Choi CK, Horwitz AR.** 2009. Integrins in cell migration--the actin connection. *J Cell Sci.* 122(Pt 2):199-206.

**Villar AV, García R, Merino D, Llano M, Cobo M, Montalvo C, Martín-Durán R, Hurlé MA, Nistal JF.** Myocardial and circulating levels of microRNA-21 reflect left ventricular fibrosis in aortic stenosis patients. *International Journal of Cardiology*, 1-7.

**Vines CM, Potter JW, Xu Y, Geahlen RL, Costello PS, Tybulewicz, VL, Lowell CA, Chang PW, Gresham HD, Willman CL.** 2001. Inhibition of  $\beta$ 2 Integrin Receptor and Syk Kinase Signaling in Monocytes by the Src Family Kinase Fgr. *Immunity*, 15(4): 507-519.

**Vita JA, Keaney JF Jr.** 2002. Endothelial function:

a barometer for cardiovascular risk? *Circulation*, 106(6):640-2.

**Vogel C, Marcotte EM.** 2012. Insights into the regulation of protein abundance from proteomic and transcriptomic analyses. *Nat Rev Genet*, 13(4):227-32.

**Von Brandenstein M, Richter C, Fries JWU.** MicroRNAs: Small but amazing, and their association with endothelin. *Life Sciences*, 91(13-14):475-89.

**Von Wichert G, Jiang G, Kostic A, De Vos K, Sap J, Sheetz MP.** (2003). RPTP-alpha acts as a transducer of mechanical force on alpha5/beta3-integrin-cytoskeleton linkages. *J Cell Bio*, 161(1):143-53.

**Wang J, Zohar R, McCulloch CA.** 2006. Multiple roles of alpha-smooth muscle actin in mechanotransduction. *Exp Cell Res*, 312(3):205-14.

**Wang S, Aurora AB, Johnson BA, Qi X, McAnally J, Hill JA, Richardson JA, Bassel-Duby R, Olson EN.** 2008. The endothelial-specific microRNA miR-126 governs vascular integrity and angiogenesis. *Dev Cell*, 15(2):261-71.

**Wang WX, Wilfred BR, Hu Y, Stromberg AJ, Nelson PT.** 2010. Anti-Argonaute RIP-Chip shows that miRNA transfections alter global patterns of mRNA recruitment to microRNA-protein complexes. *RNA*, 16(2):394-404.

**Weber M, Baker MB, Moore JP, Searles CD.** 2010. MiR-21 is induced in endothelial cells by shear stress and modulates apoptosis and eNOS activity. *Biochem Biophys Res Commun*, 393(4):643-8.

**Wehrle-Haller B, Imhof BA.** 2003. Actin, microtubules and focal adhesion dynamics during cell migration. *Int J Biochem Cell Biol*, 35(1):39-50.

**Weinholds E, Kloosterman WP, Miska E, Alvarez-Saavedra E, Berezikov E, de Bruijn E, Horvitz HR, Kauppinen S, Plasterk RHA.** 2005. MicroRNA expression in zebrafish embryonic development. *Science* 309: 310–311.

**Weng C, Dong H, Chen G, Zhai Y, Bai R, Hu H, Lu L, Xu Z.** 2012. miR-409-3p inhibits HT1080 cell proliferation, vascularization and metastasis by targeting angiogenin. *Cancer Lett*, 323(2):171-9.

**Wernig F, Mayr M, Xu Q.** 2003. Mechanical stretch-induced apoptosis in smooth muscle cells is mediated by beta1-integrin signaling pathways. *Hypertension*, 41(4):903-11.

**Wide L, Porath J.** 1966. Radioimmunoassay of proteins with the use of sephadex coupled antibodies. *Biochem Biophys Acta*

**Wightman B, Ha I, Ruvkun G.** Posttranscriptional regulation of the heterochronic gene *lin-14* by *lin-4* mediates temporal pattern formation in *C. elegans*. *Cell*, 75(5):855-62.

**Wilfred BR, Wang W, Nelson PT.** 2007. Energizing miRNA research: A review of the role of miRNAs in lipid metabolism, with a prediction that miR-103/107 regulates human metabolic pathways. *Molecular Genetics and Metabolism*, 91(3): 209-217.

**Wilson E, Mai Q, Sudhir K, Weiss, RH, Ives HE.** 1993. Mechanical strain induces growth of vascular smooth muscle cells via autocrine action of PDGF. *Journal Cell Bio*, 123: 741-747.

**Wilson E, Sudhir K, Ives HE.** 1995.

Mechanical strain of rat vascular smooth muscle cells is sensed by specific extracellular matrix/integrin interactions. *J Clin Invest*, 96(5):2364-72.

**Winder SJ, Allen BG, Clément-Chomienne O, Walsh MP.**1998. Regulation of smooth muscle actin-myosin interaction and force by calponin. *Acta Physiol Scand*, 164(4):415-26.

**Woodcock-Mitchell J, Mitchell JJ, Low RB, Kiency J, Sengel P, Rubbia L, Skalli O, Jackson B, Gabbiani G.** 1988. Alpha-smooth muscle actin is transiently expressed in embryonic rat cardiac and skeletal muscles. *Differentiation*, 39: 161-166

**Woodside DG, Oberfell A, Leng L, Wilsbacher JL, Miranti CK, Brugge JS, Shattil SJ, Ginsberg MH.** 2001. Activation of Syk protein tyrosine kinase through interaction with integrin  $\beta$  cytoplasmic domains. *Current Biology*, 11(22):1799-1804.

**Wright CE, O'Donnell K, Brydon L, Wardle J, Steptoe A.** 2007. Family history of cardiovascular disease is associated with cardiovascular responses to stress in healthy youngmen and women. *Int J Psychophysiol*, 63(3):275-82.

**Wu MH, Ustinova E, Granger HJ.** 2001.

Integrin binding to fibronectin and vitronectin maintains the barrier function of isolated porcine coronary venules. *J Physiol*, 532 (3):785-91.

**Wylie D, Shelton J, Choudhary A, Adai AT.** 2011. A novel mean-centering method for normalizing microRNA expression from high-throughput RT-qPCR data. *BMC Res Notes*, 21;4:555.

- Xie C, Huang H, Sun X, Guo Y, Hamblin M, Ritchie RP, Garcia-Barrio MT, Zhang J, Chen YE.** 2011. MicroRNA-1 regulates smooth muscle cell differentiation by repressing Kruppel-like factor 4. *Stem Cells Dev*, 20(2):205-10.
- Yamaguchi S, Yamahara K, Homma K, Suzuki S, Fujii S, Morizane R, Monkawa T, Matsuzaki Y, Kangawa K, Itoh H.** 2011. The role of microRNA-145 in human embryonic stem cell differentiation into vascular cells. *Atherosclerosis*, 219(2):468-74.
- Yan ZQ, Yao QP, Zhang ML, Qi YX, Guo ZY, Shen BR, Jiang ZL.** 2009. Histone deacetylases modulate vascular smooth muscle cell migration induced by cyclic mechanical strain. *J Biomech*, 42(7):945-8.
- Yanagawa B, Lovren F, Pan Y, Garg V, Quan, A Tang, G Singh, KK Shukla, PC, Kalra, NP, Peterson, MD, Verma, S.** 2012. miRNA-141 is a novel regulator of BMP-2-mediated calcification in aortic stenosis. *The Journal of Thoracic and Cardiovascular Surgery*, 144(1): 256-262.
- Yanagi, S, Inatome, R, Takano, T, Yamamura, H.** 2001. Syk Expression and Novel Function in a Wide Variety of Tissues. *Biochemical and Biophysical Research Communications*, 288(3): 495-498.
- Yang KC, Ku YC, Lovett M, Nerbonne JM.** 2012. Combined deep microRNA and mRNA sequencing identifies protective transcriptomal signature of enhanced PI3K $\alpha$  signaling in cardiac hypertrophy. *J Mol Cell Cardiol*, 53(1):101-12
- Yelian FD, Edgeworth NA, Dong LJ, Chung AE and Armant DR.** 1993. Recombinant entactin promotes mouse primary trophoblast cell adhesion and migration through the Arg-Gly-Asp(RGD) recognition sequence. *J Cell Biol*. 121(4):923-9.
- Younger ST, Pertsemlidis A, Corey DR.** 2009. Predicting potential miRNA target sites within gene promoters. *Bioorg Med Chem Lett*, 19(14):3791-4.
- Yue J.** 2011. miRNA and vascular cell movement. *Advanced Drug Delivery Reviews*, 63(8): 616-622.



**Yusuf S, Anand S.** 2010. Deciphering the Causes of Cardiovascular and Other Complex Diseases in Populations: Achievements, Challenges, Opportunities, and Approaches. *Progress in Cardiovascular Diseases*, 53(1): 62-67.

**Zampetaki A, Willeit P, Tilling L, Drozdov I, Prokopi M, Renard J, Mayr A, Weger S, Schett G, Shah A, Boulanger CM, Willeit J, Chowienczyk PJ, Kiechl S, Mayr M.** 2012. Prospective Study on Circulating MicroRNAs and Risk of Myocardial Infarction. *Journal of the American College of Cardiology*, 60(4): 290-299.

**Zhang BC, Li WM, Guo R, Xu YW.** 2012. Salidroside decreases atherosclerotic plaque formation in low-density lipoprotein receptor-deficient mice. *Evid Based Complement Alternat Med*,

**Zhang, B, et al.** (2003). *Mol. Cell. Biol.* **23**: 5716-5725

**Zhang L, Zhou Y, Zhu J, Xu, Q.** 2012. An updated view on stem cell differentiation into smooth muscle cells. *Vascular Pharmacology*, 56(5–6): 280-287.

**Zhang Q, Lu M, Shi L, Rui W, Zhu X, Chen G, Shang T, Tang J.** 2004. Cardio: a web-based knowledge resource of genes and proteins related to cardiovascular disease. *Int J Cardio*, 97(2) 245-9.

**Zhang Y, He Y, Bharadwaj S, Hammam N, Carnagey K, Myers R, Atala A, Van Dyke M.** 2009. Tissue-specific extracellular matrix coatings for the promotion of cell proliferation and maintenance of cell phenotype. *Biomaterials*, 30(23-24):4021-8.

**Zhang, C.** 2009. MicroRNA and vascular smooth muscle cell phenotype: new therapy for atherosclerosis? *Genome Medicine*, 1(9):85.

**Zhang S, Shan C, Kong G, Du Y, Ye L, Zhang X.** 2011 MicroRNA-520e suppresses growth of hepatoma cells by targeting the NF- $\kappa$ B-inducing kinase (NIK).

**Zhao WY, Wang Y, An ZJ, Shi CG, Zhu GA, Wang B, Lu MY, Pan CK, Chen P.** 2013. Downregulation of miR-497 promotes tumor growth and angiogenesis by targeting HDGF in non-small cell lung cancer. *Biochem Biophys Res Commun*, 435(3):466-71.

**Zheng L, Xu CC, Chen WD, Shen WL, Ruan CC, Zhu LM, Zhu DL and Gao PJ.** 2010. MicroRNA-155 regulates angiotensin II type 1 receptor expression and

phenotypic differentiation in vascular adventitial fibroblasts. *Biochem Biophys Res Comm*, 400 (4) 483-8.

**Zhiqiang Gao, Yuan Hong Yu.** 2007. A microRNA biosensor based on direct chemical ligation and electrochemically amplified detection. *Sensors and Actuators B: Chemical*, 121 (2): 552–559.

**Zhou J, Wang KC, Wu W, Subramaniam S, Shyy JY, Chiu JJ Li JY, Chien S.** 2010. MicroRNA-21 targets peroxisome proliferators activated receptor-alpha in an autoregulatory loop to modulate flow-induced endothelial inflammation. *Proc Natl Acad Sci*, 108: 10355-60.

## Appendix

This appendix is composed of additional and or preliminary data for each of the results chapters. This data was not essential to test the thesis hypothesis but is rather included in the appendix to demonstrate the breadth of the studies performed and potential avenues for future work.

### Chapter 3

#### ECM Adhesion study

Initial experiments in chapter 3 were designed to establish the ECM or coating factor which provided the longest duration of adhesion for HAoSMCs. The downstream objective of this was to allow extended strain studies on the difficult to adhere Flexcell plates. Only 12 hour time points of the study was included in chapter 3 for purpose of illustration. Figure A1 and A2 show adhesion data over full 72 hour and 60 hour time courses respectively.

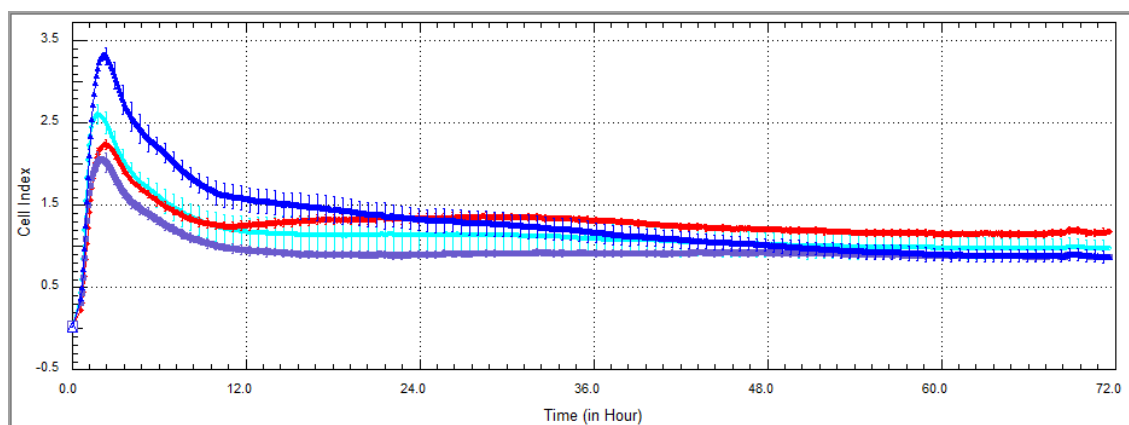


**Figure A1 – xCELLigence plot of HAoSMC adhesion.** Plot shows full 72hour time course of HAoSMC adhesion profile on several ECM and coating factors. Figure 3.3 shows a 12 hour time point of this plot.

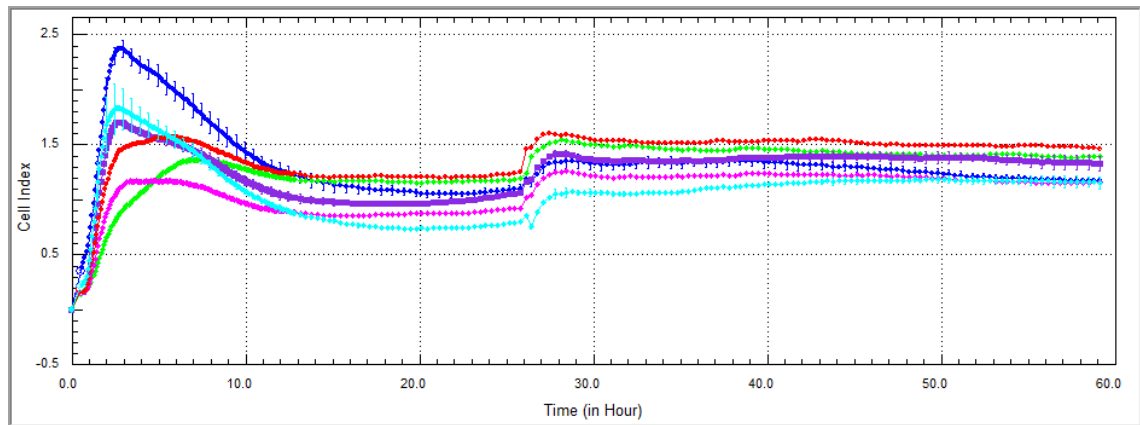


**Figure A2 – xCELLigence plot of HAoSMC adhesion.** Plot shows full 60hour time course of HAoSMC adhesion profile on several ECM and coating factors. Figure 3.4 shows a 12 hour time point of this plot.

The extended time scale reveals that fibronectin in figure A1, although initially demonstrates the highest adhesion, results in reduced overall adhesion and cell lifting as discussed in chapter 3.

## Chapter 4

Complete priority list of miRNA

Tables A1.1-A1.6 contains the complete shortlist of priority miRNA from each strain comparison in the biological replicate study.

**Table A1.1 – 5% vs. Static A Card:** Shows entire list of miRNA from A card in 5% vs. Static strain comparison which met statistical criteria.

<b>miRNA Detector</b>	<b>adjusted P. Value <math>\leq</math> 0.05</b>	<b>Fold Change</b>
hsa-miR-888-4395323	0.008414117	0.080286097
hsa-miR-520g-4373257	0.004300767	0.015052375

**Table A1.2 – 10% vs. Static A Card:** Shows entire list of miRNA in 10% vs. static strain comparison which met statistical criteria.

<b>miRNA Detector</b>	<b>adjusted P. Value <math>\leq</math> 0.05</b>	<b>Fold Change</b>
hsa-miR-618-4380996	2.68E-05	20297.03377
hsa-miR-375-4373027	0.000238093	8387.503833
hsa-miR-888-4395323	1.22E-05	703.0431092
hsa-miR-150-4373127	0.043245376	140.5210172
ath-miR159a-4373390	0.008146783	42.92528172
hsa-miR-520e-4373255	0.028916724	3.214904647
hsa-miR-18a-4395533	0.043322822	0.330272467
hsa-miR-181a-4373117	0.033745284	0.326129307
hsa-miR-193a-5p-4395	0.031908623	0.314401817
hsa-miR-21-4373090	0.033745284	0.313905747
hsa-miR-199a-5p-4373	0.031908623	0.308976666
hsa-miR-15b-4373122	0.043322822	0.281042855
hsa-miR-539-4378103	0.043971755	0.277327145
hsa-miR-145-4395389	0.037765728	0.273919236
hsa-miR-654-3p-43953	0.037336656	0.263102902
hsa-miR-195-4373105	0.027303825	0.261544894
hsa-miR-379-4373349	0.031908623	0.260681665
hsa-miR-328-4373049	0.031908623	0.256410548
hsa-miR-494-4395476	0.031908623	0.251668602
hsa-miR-29b-4373288	0.022764928	0.237994414
hsa-miR-655-4381015	0.028916724	0.23725058
hsa-miR-590-5p-43951	0.037336656	0.237074744
hsa-miR-370-4395386	0.025294605	0.236803981
hsa-miR-106b-4373155	0.024259351	0.233680731

hsa-miR-652-4395463	0.029629166	0.230784151
hsa-miR-95-4373011	0.028916724	0.227393249
hsa-miR-337-5p-43952	0.029368191	0.226991211
hsa-miR-485-3p-43780	0.031908623	0.225763221
hsa-miR-340-4395369	0.043322822	0.222515846
hsa-miR-362-3p-43952	0.016602628	0.222334519
hsa-miR-29a-4395223	0.022764928	0.213721706
hsa-miR-744-4395435	0.025294605	0.209701215
hsa-miR-324-5p-43730	0.025294605	0.199731887
hsa-miR-210-4373089	0.025294605	0.183793294
hsa-miR-135b-4395372	0.031908623	0.169398667
hsa-miR-18b-4395328	0.033745284	0.163665866
hsa-miR-365-4373194	0.022280611	0.158534193
hsa-miR-363-4378090	0.031908623	0.12363679
hsa-miR-148a-4373130	0.027303825	0.116038646
hsa-miR-671-3p-43954	0.022280611	0.113894188
hsa-miR-487a-4378097	0.029629166	0.107133045
hsa-miR-335-4373045	0.005651196	0.087815556
hsa-miR-654-5p-43810	0.022764928	0.08151309
hsa-miR-141-4373137	0.029629166	0.056619752
hsa-miR-518e-4395506	0.043322822	0.055024481
hsa-miR-501-3p-43955	0.029629166	0.054037801
hsa-miR-331-5p-43953	0.02176625	0.047716335
hsa-miR-373-4378073	0.019658174	0.043471724
hsa-miR-496-4386771	0.008761138	0.031264892
hsa-miR-302a-4378070	0.043322822	0.021076178
hsa-miR-518b-4373246	0.018002544	0.017848513
hsa-miR-198-4395384	0.022961614	0.01748052
hsa-miR-520g-4373257	0.00097034	0.016112709
hsa-miR-522-4395524	0.018002544	0.007116154
hsa-miR-96-4373372	0.029629166	0.007069915
hsa-miR-188-3p-4395	0.029629166	0.000808063
hsa-miR-518f-4395499	9.71E-05	5.16E-06

**Table A1.3 – 10% vs. 5% A Card:** Shows entire list of miRNA in 10% vs. 5% strain comparison which met statistical criteria.

<b>miRNA Detector</b>	<b>adjusted P. Value <math>\leq</math> 0.05</b>	<b>Fold Change</b>
hsa-miR-618-4380996	5.60E-06	185159.4936
hsa-miR-888-4395323	9.50E-07	8756.723011
hsa-miR-375-4373027	0.000497404	2834.577507
ath-miR159a-4373390	0.000209385	826.0306185
hsa-miR-10a-4373153	0.014714407	5.124942484
hsa-miR-520e-4373255	0.009835236	4.572522715
hsa-miR-125b-4373148	0.045960477	0.380575603

hsa-miR-29b-4373288	0.035749209	0.343665259
hsa-miR-181a-4373117	0.032226054	0.335929589
hsa-miR-185-4395382	0.040540634	0.31811133
hsa-miR-221-4373077	0.046262844	0.296324793
hsa-miR-199a-5p-4373	0.025504795	0.293806519
hsa-miR-218-4373081	0.046262844	0.292541285
hsa-miR-18a-4395533	0.026675902	0.282266187
hsa-miR-127-3p-43731	0.03499719	0.274832422
hsa-miR-21-4373090	0.023204853	0.270429603
hsa-miR-30b-4373290	0.04337885	0.267201123
hsa-miR-654-3p-43953	0.032855765	0.266857404
hsa-miR-222-4395387	0.032855765	0.259303271
hsa-miR-132-4373143	0.036514563	0.253359622
hsa-miR-34a-4395168	0.031393735	0.25244189
hsa-miR-425-4380926	0.046262844	0.251272338
hsa-miR-532-3p-43954	0.031370758	0.251187398
hsa-miR-539-4378103	0.031370758	0.250215153
hsa-miR-660-4380925	0.031370758	0.247791282
hsa-miR-30c-4373060	0.046262844	0.245782325
hsa-miR-106b-4373155	0.01984699	0.245192746
hsa-miR-24-4373072	0.042161061	0.243385449
hsa-miR-339-5p-43953	0.048740009	0.241009509
hsa-miR-15b-4373122	0.025504795	0.226552645
hsa-miR-379-4373349	0.023204853	0.224338225
hsa-miR-532-5p-43809	0.038783717	0.223864316
hsa-miR-27b-4373068	0.025504795	0.220299035
hsa-miR-345-4395297	0.031370758	0.211611885
hsa-miR-31-4395390	0.027646841	0.207058012
hsa-miR-502-3p-43951	0.031370758	0.206717722
hsa-miR-320-4395388	0.023204853	0.203653053
hsa-miR-328-4373049	0.018138949	0.202729906
hsa-miR-193b-4395478	0.023512644	0.201967448
hsa-miR-369-5p-43731	0.036514563	0.200681508
hsa-miR-148b-4373129	0.044407914	0.199480743
hsa-miR-491-5p-43810	0.023559619	0.194605618
hsa-miR-22-4373079	0.028188765	0.19444535
hsa-miR-362-3p-43952	0.008659358	0.190551476
hsa-miR-193a-5p-4395	0.009735756	0.188492077
hsa-miR-29a-4395223	0.011962396	0.186311116
hsa-miR-331-3p-43730	0.038946676	0.179829353
hsa-miR-143-4395360	0.023204853	0.178962246
hsa-miR-135b-4395372	0.030971428	0.175604322
hsa-miR-485-3p-43780	0.019810904	0.175067263
hsa-miR-337-5p-43952	0.013232672	0.166817015
hsa-miR-758-4395180	0.027646841	0.166572425
hsa-miR-214-4395417	0.031370758	0.162686725
hsa-miR-27a-4373287	0.027646841	0.160153861
hsa-miR-370-4395386	0.009363792	0.159302501

hsa-miR-652-4395463	0.011069733	0.154853909
hsa-miR-145-4395389	0.010960162	0.151332141
hsa-miR-335-4373045	0.010695184	0.149802573
hsa-miR-431-4395173	0.019810904	0.142104332
hsa-miR-484-4381032	0.023559619	0.136397434
hsa-miR-744-4395435	0.009363792	0.135230052
hsa-miR-324-5p-43730	0.009363792	0.129227222
hsa-miR-671-3p-43954	0.014714407	0.115784606
hsa-miR-365-4373194	0.008659358	0.102125242
hsa-miR-210-4373089	0.008659358	0.101373098
hsa-miR-148a-4373130	0.014714407	0.092054363
hsa-miR-18b-4395328	0.01326892	0.091878459
hsa-miR-331-5p-43953	0.026675902	0.087811808
hsa-miR-654-5p-43810	0.009363792	0.047257528
hsa-miR-496-4386771	0.008558878	0.02884925
hsa-miR-485-5p-43732	0.031370758	0.016991582
hsa-miR-887-4395485	0.014714407	0.015578802
hsa-miR-302a-4378070	0.027646841	0.013014899
hsa-miR-501-3p-43955	0.006821052	0.007958486
hsa-miR-518f-4395499	0.000209385	1.66E-05

**Table A1.4 – 10% vs. 5% B Card:** Shows entire list of miRNA in 10% vs. 5% strain comparison which met statistical criteria.

<b>miRNA Detector</b>	<b>adjusted P. Value <math>\leq</math> 0.05</b>	<b>Fold Change</b>
hsa-miR-520c-3p-4395	5.09E-05	150.2434709
hsa-miR-610-4380980	0.006143201	121.0558387
hsa-miR-564-4380941	0.011041923	118.5591669
hsa-miR-513-3p-43952	0.016115292	45.80254895
hsa-let-7f-2*-4395529	0.018066858	40.78959924
hsa-miR-661-4381009	0.011917494	39.21246247
hsa-miR-509-3p-43953	0.011917494	31.53671093
hsa-miR-939-4395293	0.011917494	26.29849576
hsa-miR-516a-3p-4373	0.011917494	24.26700534
hsa-miR-144*-4395259	0.018353118	20.4691761
hsa-miR-572-4381017	0.018365096	20.31884701
hsa-miR-545*-4395377	0.036850905	18.60895461
hsa-miR-138-1*-43952	0.015455901	17.74196611
hsa-miR-206-4373092	0.040814343	17.04761764
hsa-miR-151-3p-43953	0.011917494	15.64595355
hsa-miR-519b-3p-4395	0.018365096	13.28558305
hsa-miR-596-4380959	0.008351598	12.62643834
hsa-miR-126*-4373269	0.044738036	11.37051654
hsa-miR-942-4395298	0.011917494	9.12576064



hsa-miR-596-4380959	0.016115292	8.545503826
hsa-miR-923-4395264	0.033495659	7.820606073
hsa-miR-149*-4395275	0.028856462	7.81541337
hsa-miR-34a*-4395427	0.013388298	7.470314506
hsa-miR-638-4380986	0.033495659	7.000752196
hsa-miR-135a*-43953	0.011041923	6.834243052
hsa-miR-630-4380970	0.024683849	6.73051846
hsa-miR-650-4381006	0.016115292	5.605555798
hsa-miR-656-4380920	0.027355236	5.444960195
hsa-miR-30e-4395334	0.027355236	4.943176599
hsa-miR-892b-4395325	0.048914058	4.887532435
RNU43-4373375	0.027355236	4.813549178
hsa-miR-100*-4395253	0.048914058	4.452552809
hsa-miR-337-3p-43952	0.016115292	4.424628581
hsa-miR-432-4373280	0.044738036	4.140888708
hsa-miR-340*-4395370	0.044738036	4.071414566
hsa-miR-136*-4395211	0.048914058	4.008121018
hsa-miR-877-4395402	0.041743228	3.845314394
hsa-miR-497-4373222	0.045803482	3.540074856
hsa-miR-378-4395354	0.048914058	3.235326996

**Table A1.5 – 10% vs. Static B Card:** Shows entire list of miRNA in 5% vs. Static strain comparison which met statistical criteria.

<b>miRNA Detector</b>	<b>adjusted P. Value <math>\leq</math> 0.05</b>	<b>Fold Change</b>
hsa-miR-23b*-4395237	0.014374153	136.408586
hsa-miR-744*-4395436	0.024862359	99.59164036
hsa-miR-520c-3p-43955	0.014374153	9.449622002

**Table A1.6 – 5% vs. Static B Card:** Shows entire list of miRNA in 5% vs. Static strain comparison which met statistical criteria.

<b>miRNA Detector</b>	<b>adjusted P. Value <math>\leq</math> 0.05</b>	<b>Fold Change</b>
hsa-miR-23b*-4395237	0.023049829	97.83123344
hsa-miR-596-4380959	0.035618543	0.142214688
hsa-miR-520c-3p-43955	0.003873384	0.062895392
hsa-miR-610-4380980	0.035618543	0.03407928

## Chapter 5

Works in chapter 5 were designed to test the implication cyclic strain had on HAoSMC function and if found to be altered were miRNA working as molecular switches facilitating these changes.

In addition several exploratory studies, not included in chapter 5, were performed in efforts to characterize:

- **Effect of cyclic strain on HAoSMC apoptosis.**

Levels of surface Annexin V were quantified along with the nuclear stain Propidium Iodide (PI) to assess levels of apoptosis in cells exposed to 48 hours of 10% cyclic strain and cells in static culture.

- **Integrins which are most abundantly activated on the SMC surface.**

Initial investigation into adhesion molecules responsible for transducing the mechanical stimulation of the cyclic strain into a cellular response looked at integrins, specifically integrins which primarily bind the RGD sequence motif. This was approached using synthetic RGD peptides. These were incorporated while seeding SMCs on to xCELLigence adhesion plates. A substantially reduced adhesion profile of cells incorporated with the peptides would correspond to RGD binding integrins being highly expressed on the cell surface.

- **Impact of over expressing FAK and FRNK in SMCs.**

Experiments were also designed to investigate the consequence of over expression of focal adhesion kinase (FAK) and its endogenous negative regulator Focal Adhesion Non Receptor Kinase (FRNK). Vectors containing FAK and its endogenous inhibitor FRNK were transfected into HAoSMCs to evaluate the impact on cell adhesion and proliferation. As this study is still in its infancy it has not been included in this chapter but preliminary work can be found in the appendix.

## Apoptosis Study

To determine if strain regulated apoptosis signaling within the cell, levels of annexin V and the nuclear stain Propidium Iodide were quantified using flow cytometry in both a static and strained population of cells. Cells were strained at 10% 1Hz for 48 hours. This time was chosen to assess if the increase in migration seen in figure 5.1 corresponded with compromised cell health and death often observed in synthetic cells.

Levels of apoptotic cells were measured with an Annexin V staining kit as described in chapter 2.2. In normal live cells, phosphatidylserine (PS) is located on the cytoplasmic surface of the cell membrane. However in apoptotic cells, PS is translocated from the inner to the outer leaflet of the plasma membrane, thus exposing PS to the external cellular environment. The human anticoagulant, Annexin V, is a 35-36kDa  $\text{Ca}^{2+}$  dependent phospholipid-binding protein that has a high affinity for PS. Thus, Annexin V labelled with a flurophore can identify apoptotic cells by binding to the exposed PS on the outer membrane.

The assay also incorporated a nuclear dye to measure cell death, red-fluorescent propidium iodide (PI). PI is impermeable to live or apoptotic cells. Therefore, after staining a cell population with Alexafluor®488 Annexin V and PI, dead cells will show red and green fluorescence, apoptotic cells will show green only and live healthy cells should show little or no fluorescence.

Figure A3 shows scatter plots of Annexin V apoptosis study of HAoSMCs in both static and strained culture.

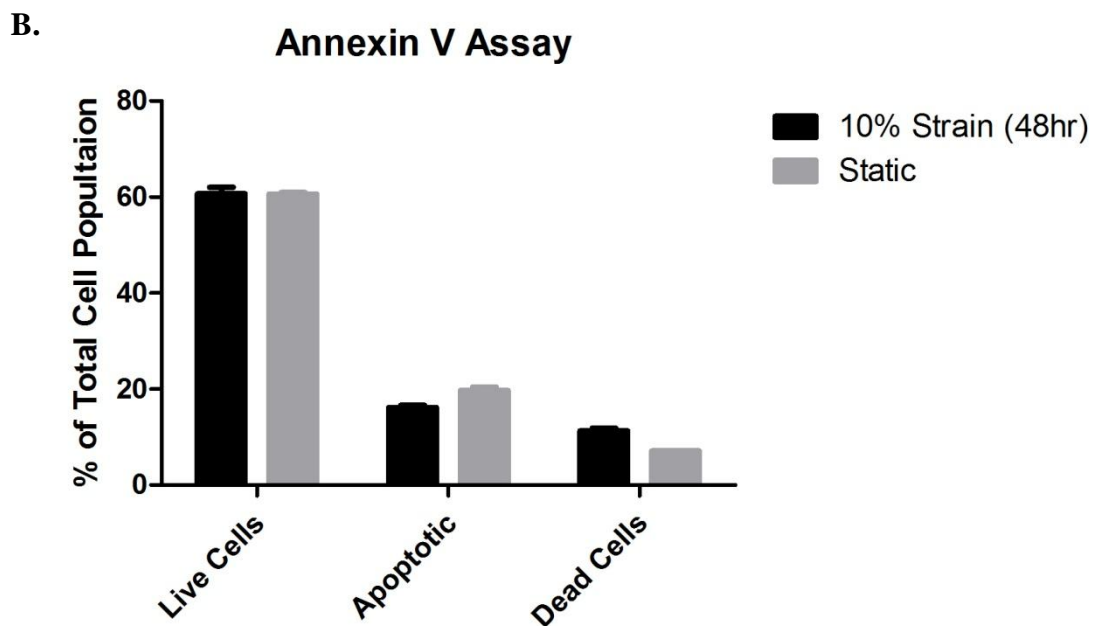
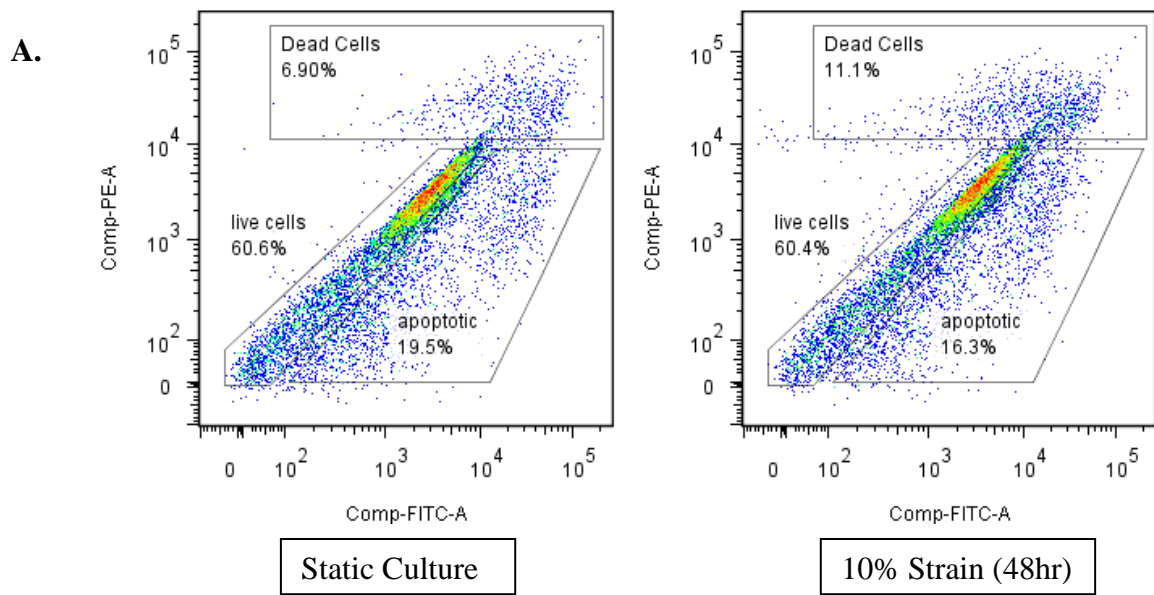


**Figure A3 A&B: Apoptosis assay on static vs. strained HAoSMCs.** (A)- Flow cytometry analysis of the presence of Annexin V and nuclear stain PI in static (left) and 10% strained (right) HAoSMC cultures. Cells were strained for 48hours. Three populations were gated; healthy cells, apoptotic cells and dead cells. (B)- shows graphed percentage of total cell population for each population identified, healthy, apoptotic and dead cells, for both strained and static culture. n=3, no statistical significance between strain and static.

### *Discussion*

With nearly an identical level of live cell population, figure A, between the strained and static culture and only a slight increase in the apoptotic cells in static, it was concluded that strain was not inducing apoptosis. Similar results were seen by Hipper *et al.*, (2000) only 0.2% difference in apoptosis and an identical release of lactate dehydrogenase (LDH) in VSMC in static culture and those exposed to 5% strain at 0.5Hz for 48 hours. This excluded the possibility of necrosis and influence of apoptosis by the strain. Contrary to this however, cyclic strain was reported to increase apoptosis in smooth muscle cells coated on collagen type I matrix (Wernig *et al.*, 2003). This highlights and goes somewhat to explain varying results reported by different groups, in that assessing cell fate and function in response to cyclic strain, or indeed, any other biomechanical force, is dependent on its microenvironment, in particular the ECM composition.

## Integrin Study

Integrins and ion channels are the membrane molecules predominantly involved in “mechano-sensing” by the cells to their environment. Integrins are transmembrane molecules consisting of an intracellular and extra cellular domain. They are made up of both an alpha and beta glycoprotein subunits which are non-covalently bonded. To date there are 18 alpha and 8 beta subunits allowing for a total of 24 different integrin compositions. (Plow *et al.*, 2000; Van der Flier & Sonnenberg 2001; Hynes 2002). They facilitate ‘inside-out’ and ‘outside-in’ cell signaling and are responsible, in part, for integrating the cell with its microenvironment. This can be accomplished through engaging with ECM macromolecules or with counter receptors on adjacent cell surfaces (Humphries *et al.*, 2006).

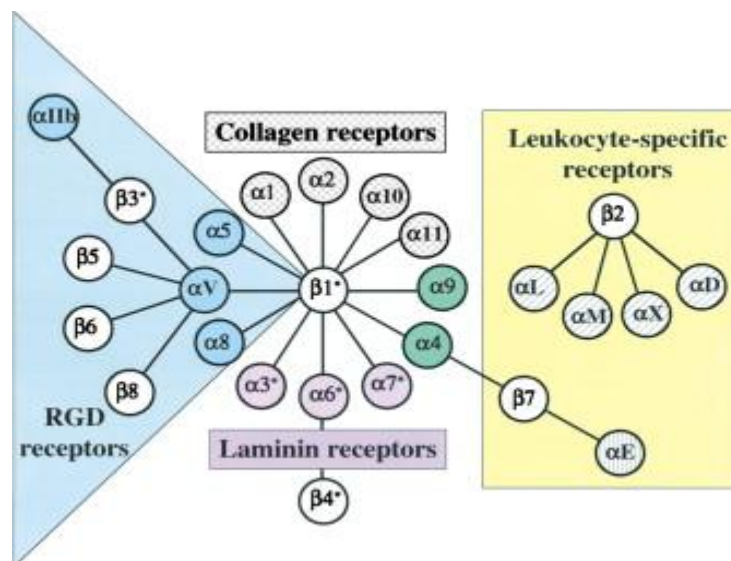


**Figure A4:** Integrin receptors are  $\alpha\beta$  heterodimers; each subunit crosses the cell membrane, with the majority of the polypeptide (>1600 amino acids in total) in the extracellular space and two short cytoplasmic domains (20–50 amino acids). This schematic depicts the mammalian subunits and their  $\alpha\beta$  associations; 8  $\beta$  subunits can assort with 18  $\alpha$  subunits to form 24 distinct integrins. (Hynes *et al.*, 2002).

Activation of the integrin families is mediated by contact with ECM components such as fibronectin and collagen which leads to the formation of focal adhesion structures. These focal adhesions contain anchorage points for the cell where the cytoplasmic tail of the integrin is physically tethered to the actin fibres of the cytoskeleton (A. Katsumi & W. Orr *et al.*, 2004; C. Galbraith *et al.*, 2002; Schwartz *et al.*, 2000). They also bind with signaling molecules, such talin and paxillin, which become activated in an adhesion dependent manner (Burrige *et al.*, 1996). Recruitment of the protein tyrosine kinase, FAK, to the integrin rich sites also appears to be central to focal adhesion formation. This is paramount to downstream signaling controlling cell migration and proliferation. This FAK mediated signaling is modulated by expression of an endogenous FAK inhibitor termed FRNK (FAK Related Non Kinase). This is expressed as an independent protein and is essentially the carboxyl-terminal noncatalytic domain of FAK (Taylor *et al.*, 2001).

Following strain and Ago2 knock-down experiments, the focus of investigation turned to the underlying mechanisms by which “mechano-sensing” is orchestrated by HAoSMCs in response to cyclic strain. As this is attributed to membrane bound adhesion molecules, preliminary experiments looked at integrin mediated signaling. Initial studies used synthetic RGD peptides, which bind a sub group of integrins (shown in diagram below). These were seeded in solution with HAoSMCs onto xCELLigence adhesion plates to assess their impact on adhesion of the cell.

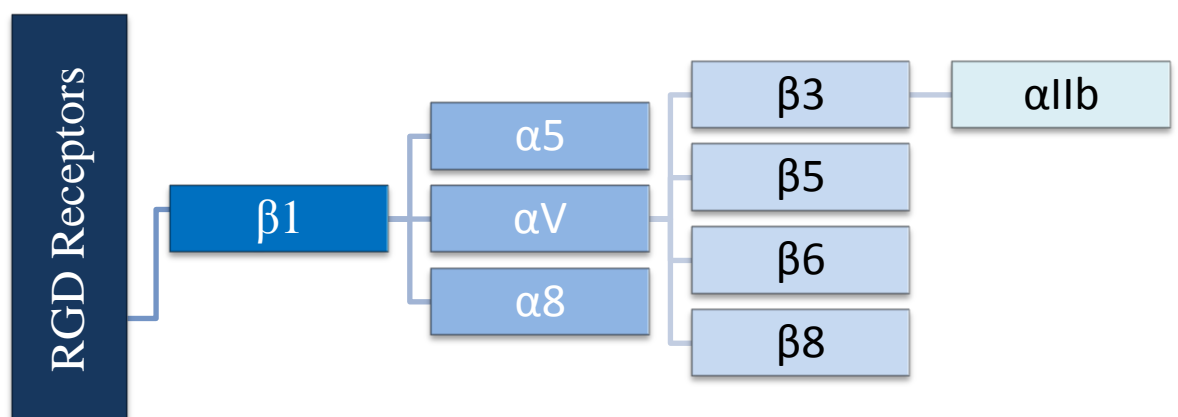
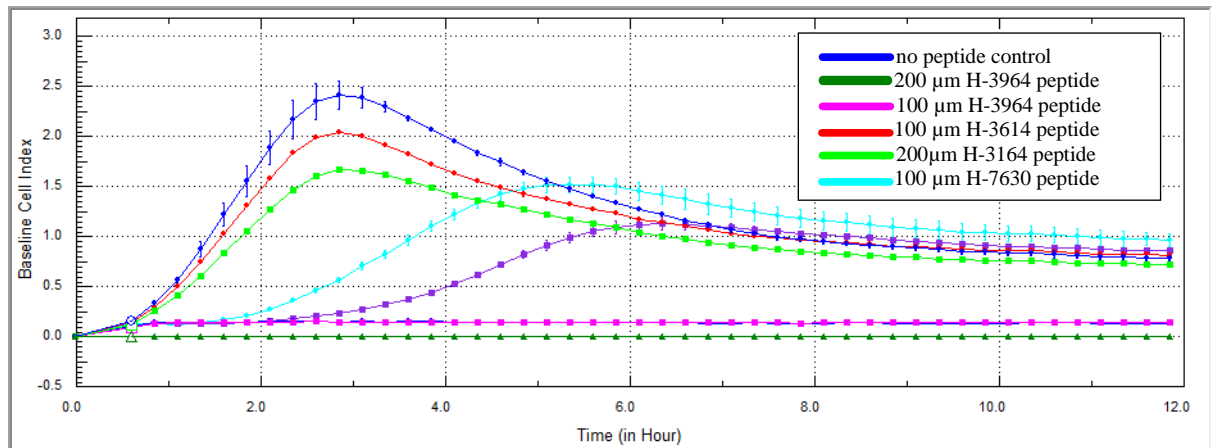


**Figure A5: RGD Receptors.** Schematic showing the combinations of  $\alpha\beta$  subunits which make up RGD binding integrins (8 in total).

Effect of RGD peptides (100µM & 200µM concentrations) on HAoSMC adhesion.

A.



B.

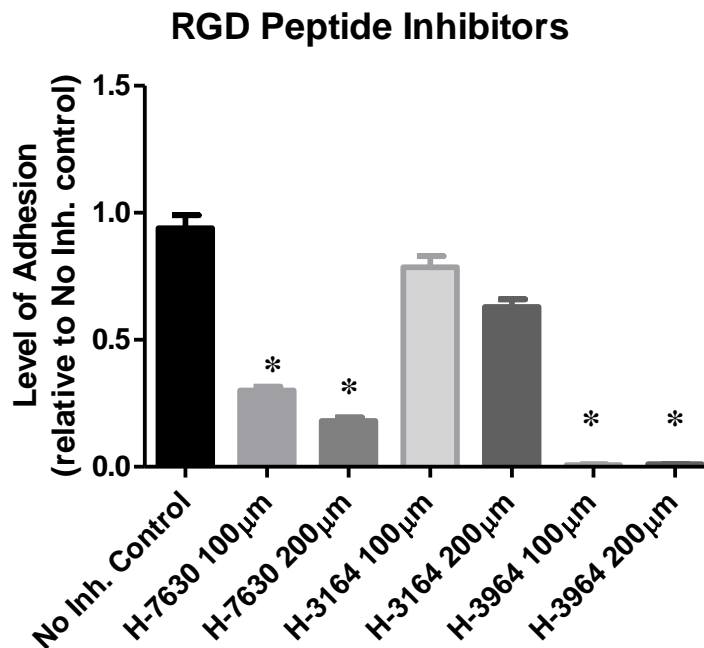
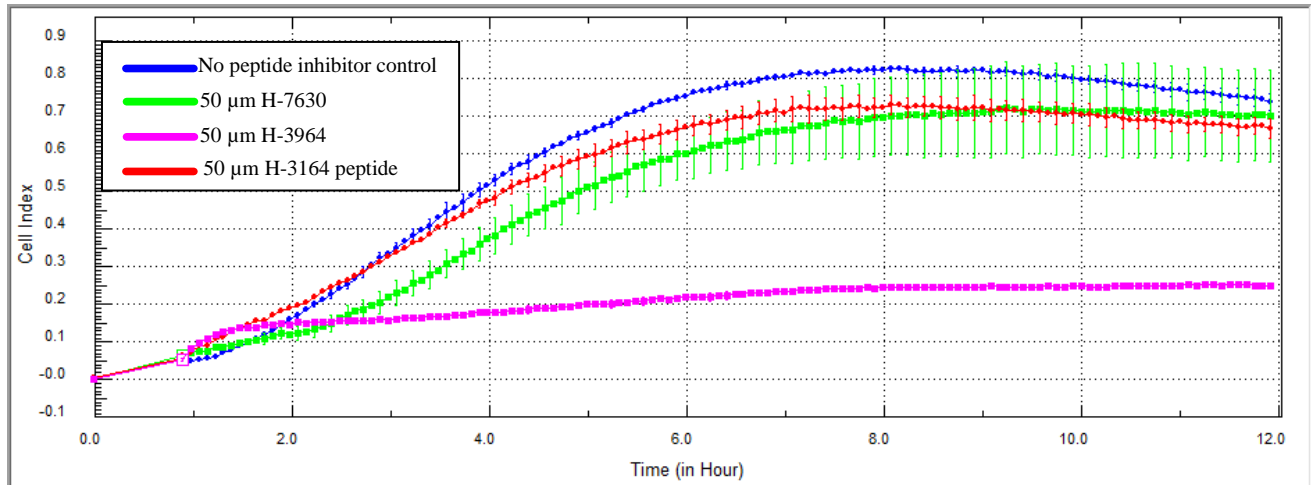


**Figure A6 A, B & C: Adhesion profile of HAoSMCs seeded with RGD peptides.** Figure A6 A shows adhesion profile of HAoSMC incorporated with RGD synthetic peptides. Blue plot – No peptide control, Red & Green plot –100µM & 200µM of H-3164 peptide respectively, Light Blue & Purple plot 100µM & 200µM of H-7630 peptide respectively, Pink & Dark green plot –100µM & 200µM of H-3964 peptide. Figure A6 B graph showing level of adhesion of each sample compared to the no peptide control. n=3, \* $P \leq 0.05$  vs. no inhibitor one way anova.



Effect of RGD peptides (50 $\mu$ M concentration) on HAoSMC adhesion.

A.



B.

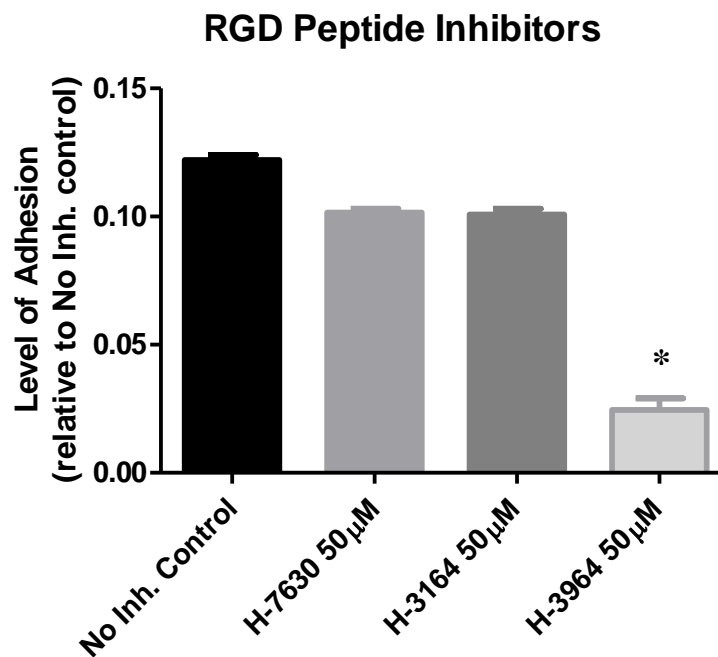


**Figure A7 A&B: Adhesion profile of HAoSMCs seeded with RGD peptides.** Figure A7 A shows the adhesion profile, generated from xCELLigence instrument, of HAoSMCs seeded with RGD peptides at 50 $\mu$ M concentration. **Blue plot** – No peptide inhibitor control, **Red plot** – 50 $\mu$ M H-3164 peptide, **Green plot** - 50 $\mu$ M H-7630 peptide, **Pink plot** - 50 $\mu$ M H-3964 peptide. Figure 5.10B shows graphical representations for the level of HAoSMC adhesion seeded with each of the peptides. . n=3, \* $P \leq 0.05$  vs. no inhibitor one way anova.

The adhesion experiment in figure A7 (A) was continued over a 96 hour time course to evaluate impact of the RGD peptides on the proliferation of HAoSMCs and to evaluate the performance of the peptides at longer time points.

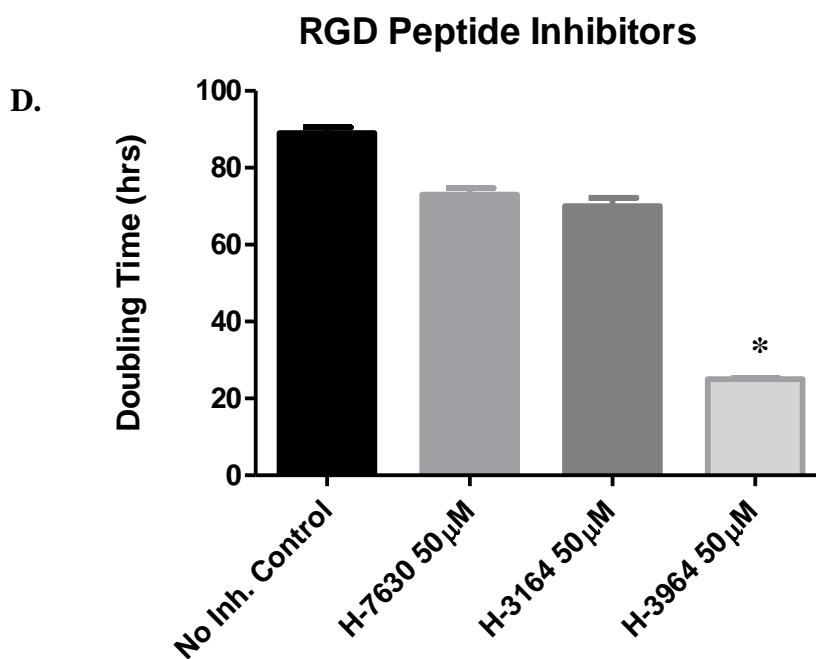
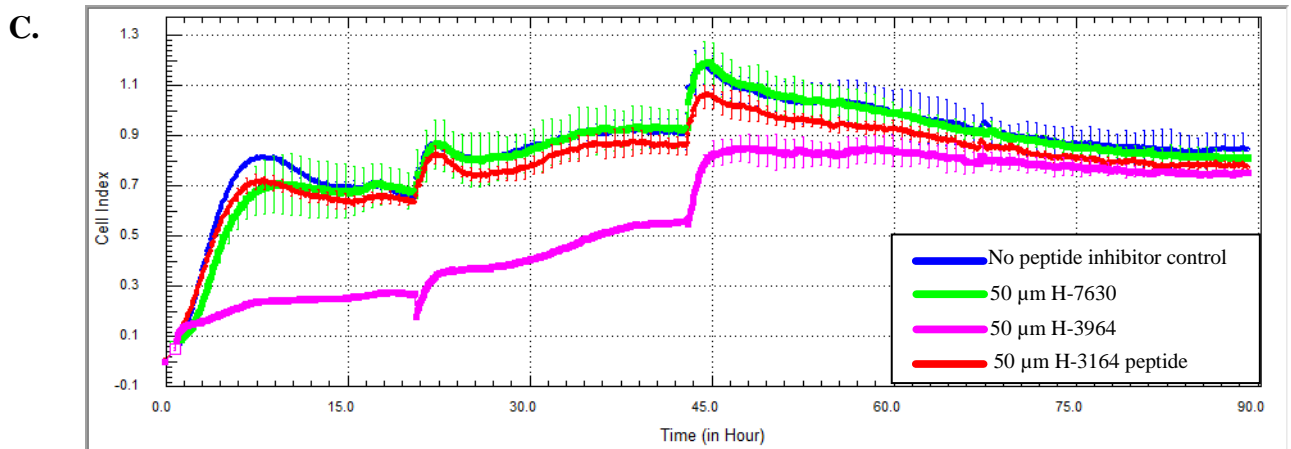


**Figure A7 C&D: Proliferation profile of HAoSMCs seeded with RGD peptides.** Figure A7 C- shows the adhesion and proliferation of HAoSMCs seeded with RGD peptides at 50µM concentration over 96 hours, plot generated from xCELLigence system. **Blue plot** – No peptide inhibitor control, **Red plot** –50µM H-3164 peptide, **Green plot** - 50µM H-7630 peptide, **Pink plot** - 50µM H-3964 peptide. Figure A7 D graph showing the doubling time of each cell sample, including the no inhibitor control and the three RGD peptides. n=3, \* $P \leq 0.05$  vs. no inhibitor one way anova.

### *Discussion.*

Cells making up the vasculature are equipped with an array of receptors and adhesion molecules which allow them to detect and respond to the mechanical forces generated by pulsatile blood flow (Lehoux *et al.*, 2006). These mechanical stresses are transmitted through cell contacts with the substrate; this inherently implicates integrins in mechanotransduction (Katsumi *et al.*, 2004). These forces stimulate conformational activation of vascular smooth muscle cell integrins, resulting in increased cell binding to the ECM (Jalali *et al.*, 2001). Binding of ECM protein ligands by integrins is required for intracellular signal transduction induced by mechanical force. RGD binding integrins are one of the four major classes of integrin families. They are the most promiscuous of the receptors, finding ligands with a multitude of ECM proteins. As the name suggest they recognise the arginine-glycine-aspartic acid (RGD) sequence within their ligands. Consequently to their prevalence and large array of ligands these adhesion molecules were investigated in this thesis to establish their involvement in SMC adhesion.

This was approached through use of synthetic RGD (Arginine, Glycine, Aspartic Acid) binding peptides, these compete with substrate ECM for docking sites on RGD integrins. Studies have shown it is possible to block alterations in cellular functions induced by strain by use of these peptides (Wernig *et al.*, 2003). All five  $\alpha$ V integrins, two  $\beta$ 1 integrins ( $\alpha$ 5,  $\alpha$ 8) and  $\alpha$ IIb $\beta$ 3 share the ability to recognise ligands containing the RGD sequence motif (Humphries *et al.*, 2006). In this chapter RGD peptides were incorporated while seeding HAoSMCs to investigate which integrin is predominantly expressed on SMC surface.

The adhesion and proliferation assays in figures A6 & A7 show HAoSMCs, which have been seeded with three soluble RGD peptides.

Peptides used were purchased from Bachem under their product names of;

H-7630 – competes against integrins for the RGD fibronectin binding domain.

H-3164 - competes for fibronectin binding but not vitronectin.

H-3964 – An RGD peptide which predominantly competes for the  $\alpha$ V $\beta$ 3 integrin.

Concentrations used in Figure A6 were 100 and 200  $\mu$ M for each peptide. H-3164 showed the least change in SMC adhesion and proliferation dynamics compared with

the no peptide control. This is likely due to it not competing for the Vitronectin binding domain and selectively fibronectin. H-7630, which is not solely binding fibronectin shows a higher impact on cell adhesion, however the most notable is H-3964. At these concentrations H-3964 inhibits all cell attachment.

H-3964 competes against integrin  $\alpha V\beta 3$ , which finds ligands on multiple ECM such as Fibronectin, Osteopontin, PECAM1, Fibrinogen, Fibrillin, VWF & Thrombospondin is highly expressed on SMC surface. Cyclic strain induced cell cycle is thought to be mediated through this integrin by release of platelet derived growth factor (Wilson *et al.*, 1995).

A similar study to the one shown in figure A6 is shown in figure A7, this time incorporating a lowered peptide concentration of 50 $\mu$ M. At this concentration it was possible to achieve cell attachment with the H-3964 peptide, thus allowing investigation into the altered cellular dynamics over an extended time course.

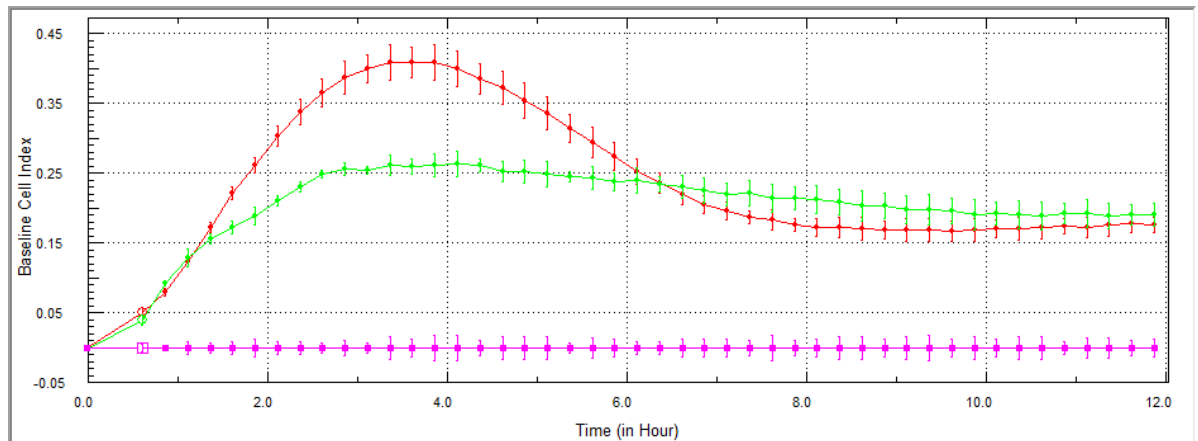
It is evident from both figure A6 & A7 the peptides are effective during the cell attachment phase in blocking integrin binding to the culture plate surface. However, as the experiment progresses past 48 hours the cell index begins to return to that of the no peptide control. Naturally, this can be attributed to cell proliferation, however along with proliferation new integrins are most likely being synthesised by the original cell population, thus negating the effect of the peptides in conjunction with laying down additional ECM, further diluting the impact of the peptides.

This preliminary study emphasizes the importance of  $\alpha V\beta 3$  in HAoSMC adhesion and suggests a promising avenue into exploring which cell surface molecules are responsible for "mechanosensing" strain.

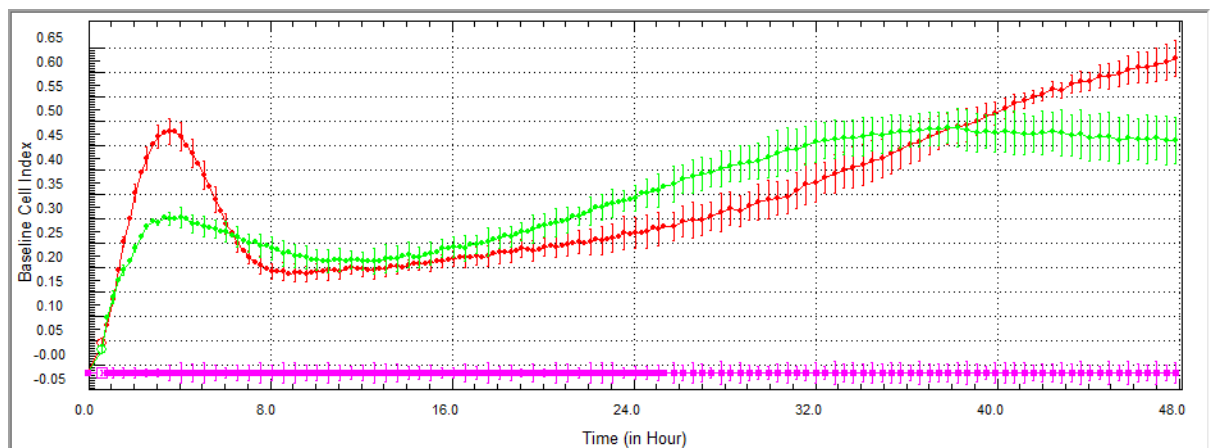
## Over expression of FAK and FRNK plasmids in HAoSMCs

Early stage experimentation into focal adhesion sites as signaling hubs for mechano transduction consisted of transfecting plasmids containing the signaling molecules FAK and FRNK into the cells using the microporator transfection system described in chapter 2.2. This allowed assessment of over expression of these proteins on the impact on cell adhesion and proliferation.

**A.**



**B.**



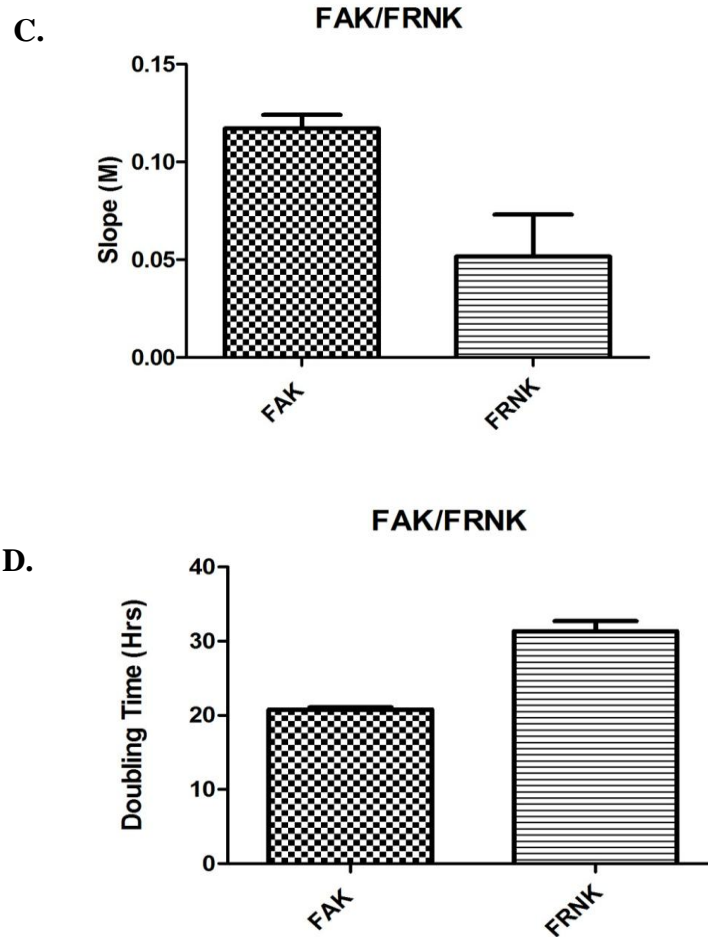
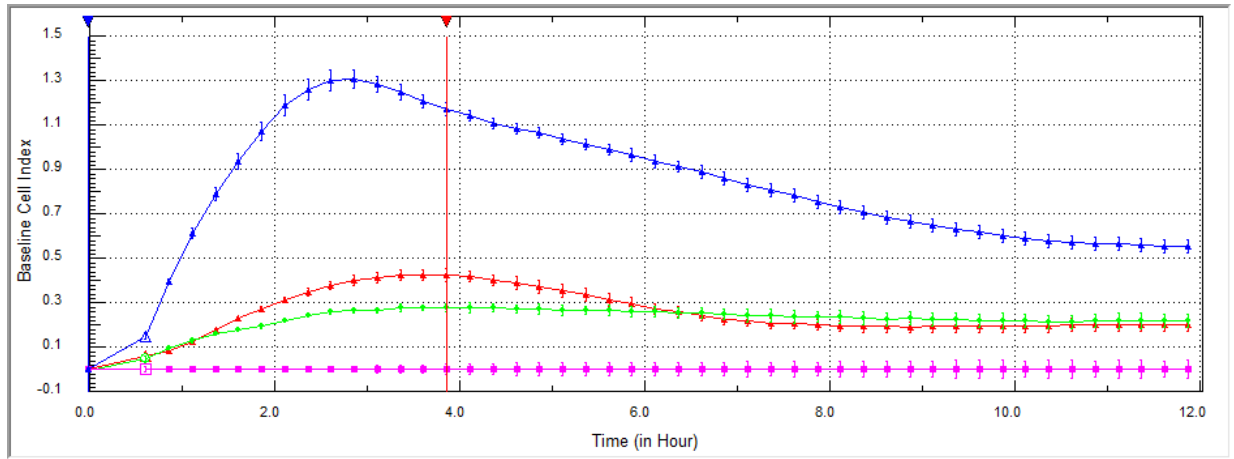
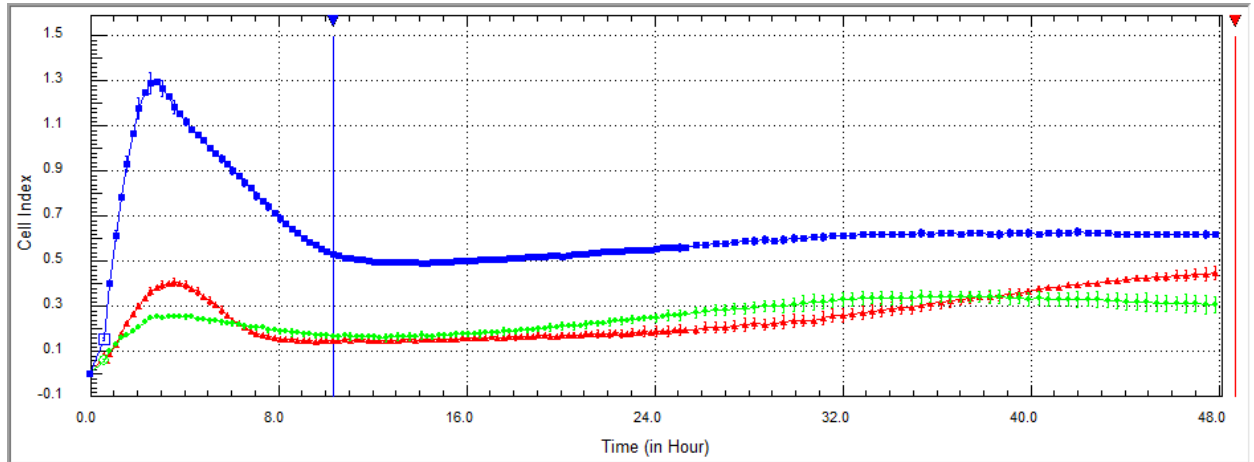


**Figure A8** - Plots A&B show 12 and 48 hour time points for adhesion and proliferation assay on HAoSMC transfected with FAK and FRNK plasmids. Red plot – HAoSMC transfected with FAK plasmid, Green plot – HAoSMC transfected with FRNK. Rate of adhesion is increased in HAoSMC transfected with FAK as shown in C compared with FRNK transfected cells. Doubling time of FAK transfected cells is reduced when compared with FRNK transfected cells (D). n=3.

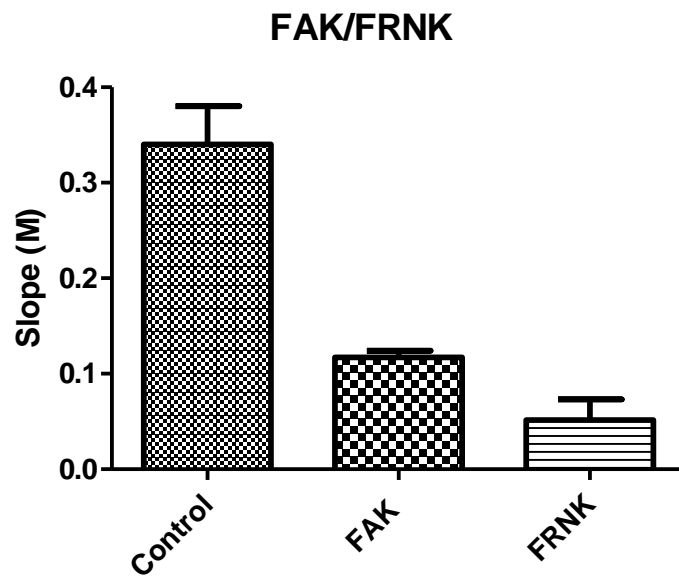
**A.**



**B.**



**C.**



D.

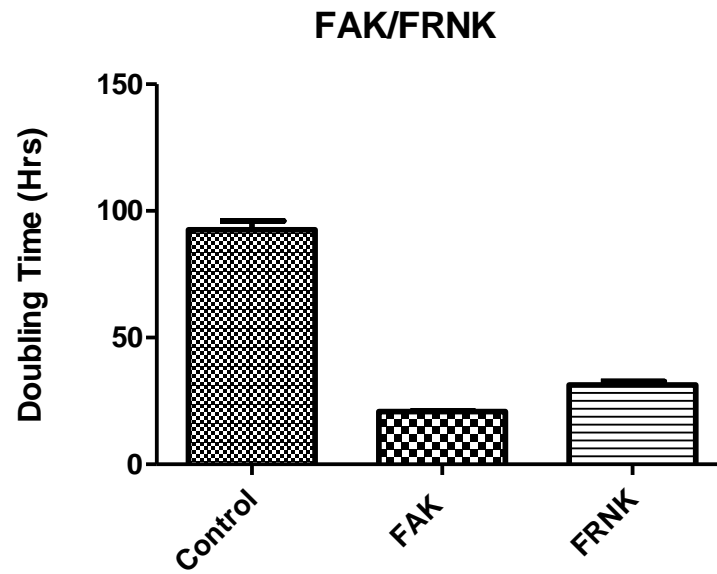
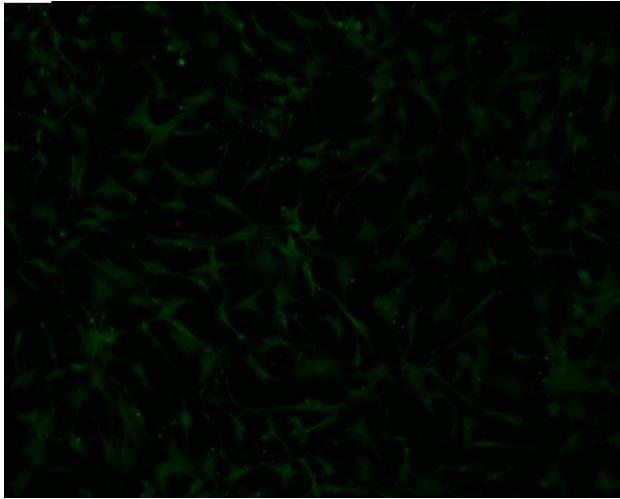


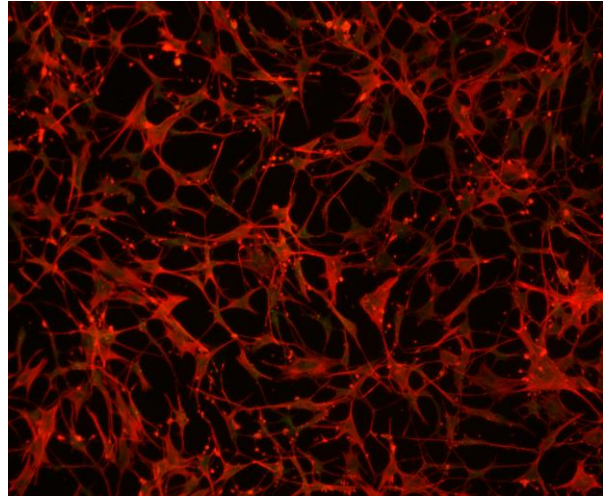
**Figure A9** - Plots A&B show 12 and 48 hour time points for adhesion and proliferation assay on HAoSMC transfected with FAK and FRNK plasmids and wild type control. Red plot – HAoSMC transfected with FAK plasmid, Green plot – HAoSMC transfected with FRNK, Blue plot – Wild type control. Rate of adhesion is significantly decreased in both plasmid transfected cells when compared with wild type control. Adhesion is stronger in HAoSMC transfected with FAK as shown in C compared with FRNK transfected cells. Doubling time of FAK and FRNK transfected cells is reduced when compared with wild type control (D). n=3



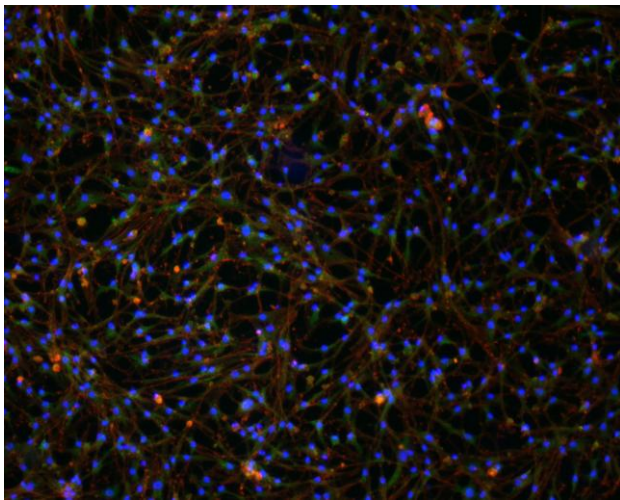
A.



B.



C.



D.

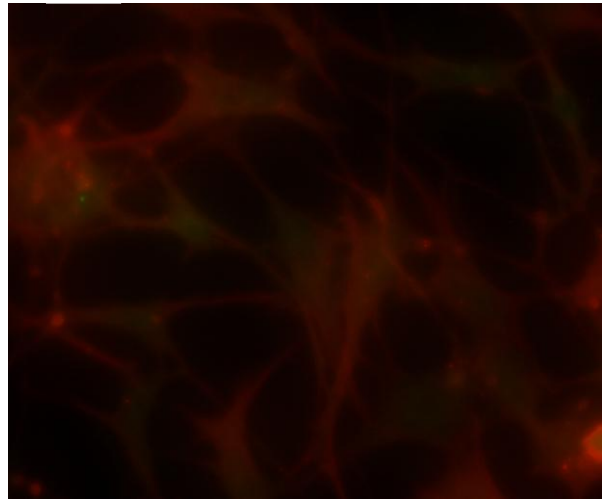


**Figure A10** – A; HAoSMC stained with FAK Ab conjugated with FITC 2° (10X), B; HAoSMC stained for FAK aswell as cell actin fibres stained red with Phalloidin (10X), C & D; HAoSMC stained with FAK, Phalloidin and nucleus stained blue with DAPI (10X, 20X respectively).

### *Discussion*

The focus of this study initially was to optimize transfection of the two plasmids into HAoSMCs. This was particularly challenging due to large plasmid size of FAK (>8kb) and the difficult to transfect nature of HAoSMCs. Using the Invitrogen® Microporator® a transfection efficiency of ~ 80% was finally reached, figure A10.

Preliminary over expression experiments showed an increase in adhesion of HAoSMCs transfected with FAK compared to those transfected with FRNK, figure A8. This was expected as more adhesion molecules within the cell become activated due to the abundance of this kinase, leading to an increase in focal contacts and adhesions. However when comparing the adhesion of HAoSMCs transfected with either the FAK or FRNK plasmid to a vector only control, figure A9, they are both significantly reduced. This is potentially due to a damaging effect on the cell health or membrane integrity of HAoSMCs transfected with the plasmids highlighting the need for further optimization and investigative studies into cell toxicity associated with plasmid transfection.